

Intracellular delivery of therapeutic antibodies

By Gavin S. Hackett, BSc (Hons)

Thesis submitted to the University of Nottingham for the degree
of Doctor of Philosophy

October 2011

Abstract

Therapeutic antibodies are highly versatile macromolecules that can be engineered to bind and inhibit a target with high specificity. Unfortunately, the cell membrane is impenetrable to antibody reagents, thus limiting their use almost entirely to extracellular targets. Expanding the application of therapeutic antibodies to intracellular targets is an exciting concept that could have a huge impact on how intracellular protein-protein interactions involved in diseases can be modulated. The modification of therapeutic antibodies with Cell Penetrating Peptides (CPPs) can enable cellular penetration, however, no general approach to modifying antibodies with CPPs has been developed that allows for systematic optimisation of both the *in vivo* and cell penetrating properties.

In this study, neutralising single-chain variable fragment antibodies (scFvs) have been isolated from naïve scFv libraries using antibody phage display that are specific to the model intracellular targets Bcl-2 and Bcl-xL. Lead scFvs showed potent inhibition of these proteins in an *in vitro* assay with IC₅₀ values of <10 nM being calculated, which is superior to the small molecule Bcl-2/xL inhibitor ABT-737. The lead anti-Bcl-xL scFv was conjugated to the CPPs octa-arginine, HIV Tat₄₉₋₅₇ or Antp₅₂₋₅₈. These peptides were synthesised to possess either an *N*-isobutyryl cysteinyl or *N*-maleimidopropionyl moiety and a *C*-terminal lysine residue, allowing for site-specific conjugation to an unpaired cysteine residue introduced to the scFv construct and regioselective introduction of 5-carboxyfluorescein to the CPP, respectively. Live-cell confocal microscopy showed that the scFv-octa-arginine conjugate possessed superior cell entry capabilities compared to the scFv-Tat₄₉₋₅₇ and scFv-Antp₅₂₋₅₈ conjugates. Further studies using a panel of cancer cell lines are required to determine if the anti-Bcl-xL scFv-octa-arginine conjugate can induce apoptosis through inhibition of cellular Bcl-xL.

Additionally, a novel approach to controlling the cell penetrating properties of the CPP octa-arginine has been developed. It was demonstrated that carbamate protection of octa-arginine's guanidine functionality effectively inhibited its cell entry capabilities. Moreover, esterase-labile acyloxymethyl carbonyl (AM) protecting groups were

utilised to protect the guanidine functionality of octa-arginine, inhibiting its cell entry capabilities. In a HPLC based assay it was demonstrated that the AM protected octa-arginine was deprotected by pig liver esterase, suggesting that *in vivo* deprotection could be achieved by serum esterases. The controlled unmasking of octa-arginine is predicted to increase its circulation time and reduce non-specific tissue uptake *in vivo*, potentially making this CPP more suitable for *in vivo* applications.

The methodologies utilised for the preparation of scFv-CPP conjugates and developed for the controlled unmasking of octa-arginine in this study will allow for optimisation of the cell penetrating and *in vivo* properties of this promising class of macromolecular therapeutic, thus providing a gate-way to unlocking the immense potential of therapeutic intracellular antibodies.

Acknowledgments

I would like to thank my supervisors Peter Fischer, Weng Chan and Ron Jackson for their continued support, encouragement and guidance throughout my PhD studies. I would also like to acknowledge the EPSRC, AstraZeneca and MedImmune for funding the PhD.

I am especially grateful to all of the present and past members of the chemistry corridor in CBS for their friendship and for providing an enjoyable working atmosphere. I particularly want to thank Cillian Byrne, Chris Gordon, Charlie Mathews and Chou-Hsiung Chen for their invaluable suggestions and help. I also want to thank Chris for his encouragement while I was writing-up and for proof-reading my thesis.

I am extremely grateful for all of the help and invaluable advice from so many people at MedImmune in Cambridge, in particular Monica Papworth, Peter Ravn, Siobhan O'Brien, Jeff Revell, Anna-Lena Schinke, Des O'Shea and Sara Carmen for both advice with my work and also friendship, making the time that I spent in Cambridge an enjoyable and invaluable experience.

I would also like to express my thanks to all of the technical staff in CBS, in particular Lee Hibbett and Graham Coxhill for help with the HPLC, MS and many other lab related things.

I must also thank my two past house-mates Asa Bluck and Graham Mullard for always being ready for a beer (or two...) after work. Finally, I thank my parents, brothers, sister, and grandparents for supporting me when things were difficult. I am also very grateful to Jessica Chu for her support throughout the final year of my PhD studies .

This thesis is dedicated to my parents

Abbreviations

ACPP	Activatable cell penetrating peptide
Alpha screen	Amplified luminescent proximity homogeneous assay
AM	Acyloxymethyl carbonyl
AMI	Acute myocardial infarction
Antp	Penetratin
AO	Acyloxy carbonyl
ATTEMPTS	Antibody targeted, [protamine] triggered, electrically modified pro-drug strategy
BH 1- 4	Bcl-2 homology domain 1-4
CDR	Complementarity determining region
CHO	Chinese hamster ovary
CPP	Cell penetrating peptide
EC ₅₀	50% maximal effective concentration
ELISA	Enzyme linked immunosorbant assay
Fab	Fragment antigen binding region
FBS	Fetal bovine serum
Fc region	Fragment crystalline
Fv	Variable domain
HIV	Human immunodeficiency virus
HPLC	High-performance liquid chromatography

HRMS	High resolution mass mass spectrometry
HRP	Horse radish peroxidase
HSPG	Heperan sulfate proteoglycans
HTS	High throughput screening
IACT	Intracellular antibody capture technology
IC ₅₀	50% maximal inhibitory concentration
%ID/g	% Injected dose per gram of target tissue
K _d	Dissociation constant
K _i	Inhibition constant
MALDI-TOF	Matrix-assisted laser desorption/ionization time-of-flight
MMP	Matrix metalloproteinase
MS	Mass spectrometry
naCPP	Non-amphipathic cell penetrating peptide
NK1R	Neurokinin-1 receptor
NMR	Nuclear magnetic resonance
paCPP	Primary amphipathic cell penetrating peptide
PD	Pharmacodynamic
PLE	Pig liver esterase
PK	Pharmacokinetic
PPI	Protein-protein interaction
R _f	Retention factor
RISC	RNA-induced silencing complex
RNAi	RNA interference

rt	Room tempertaure
SA	Streptavidin
saCPP	Secondary amphipathic cell penetrating peptide
ScFv	Single chain variable fragments
SMoC	Small molecule carrier
SPPS	Solid-phase peptide synthesis
Tat	HIV Transactivator of Transcription
TNF	Tumour necrosis factor
TOF	Time-of-flight

Contents

1 Introduction.....	1
1.1 Inhibiting protein-protein interactions.....	1
1.2 Therapeutic antibodies.....	4
1.2.1 Antibody Engineering.....	5
1.3 Targeting intracellular protein-protein interactions with antibodies.....	9
1.3.1 Intrabodies	11
1.3.2 Transbodies.....	13
1.4 Cell penetrating peptides	16
1.4.1 Mechanism of CPP internalisation.....	19
1.4.2 The application of CPPs <i>in vivo</i>	22
1.4.3 Modulation of CPP <i>in vivo</i> properties.....	25
1.5 Making Transbodies	30
1.5.1 Chemical conjugation of CPPs to antibodies	31
1.6 Research aims and objectives	39
2 Isolation of neutralising single chain antibodies specific to Bcl-2.....	42
2.1 Bcl-2 - The model target	42
2.2 Isolation of anti-Bcl-2 and Bcl-xL scFv using antibody phage display	46
2.2.1 Selection of anti-Bcl-2 and anti-Bcl-xL scFvs.....	49
2.3 Identification of scFv neutralising towards Bcl-2 and Bcl-xL	54
2.3.1 Profiling of positive hits	59
2.3.2 Binding of scFv in reducing environment.....	62
2.4 Conclusions.....	64
2.5 Materials and Methods.....	66
2.5.1 Biotinylation of Bcl-2 and Bcl-xL	66
2.5.2 Direct binding ELISA	67
2.5.3 Phage selection protocol	68
2.5.4 Phage rescue for subsequent selection rounds	70
2.5.5 Analysis of selected phage.....	70
2.5.6 Phage ELISA	71
2.5.7 High-throughput screening	72
2.5.8 Alpha Screen profiling of His-tag affinity purified scFv.	74
2.5.9 scFv binding ELISA in the presence of reduced glutathione.....	74
3 Preparation and characterisation of scFv-CPP conjugates.....	76
3.1 Synthetic approaches for scFv-CPP conjugation.....	77
3.2 Expression of scFv-Cys	78

3.2.1	Mammalian expression of scFv-Cys.....	82
3.3	Fmoc solid-phase peptide synthesis of CPPs.....	87
3.3.1	Synthetic strategies for CPP derivatives	89
3.3.2	Penetratin derivatives.....	92
3.3.3	Octa-arginine derivatives	98
3.3.4	HIV Tat ₄₉₋₅₇ derivatives.....	100
3.3.5	Pro ₁₄ derivatives.....	102
3.3.6	Summary of CPP derivative synthesis	104
3.4	Preparation of scFv-CPP conjugates	105
3.4.1	Thioether conjugation	105
3.4.2	Disulfide conjugation.....	107
3.4.3	Summary of scFv-CPP conjugate preparation.....	111
3.5	Cellular delivery of scFv-CPP(FAM) conjugates.....	114
3.5.1	Fluorescence microscopy.....	114
3.5.2	Confocal Laser Scanning Microscopy (CLSM).....	116
3.5.3	Summary of scFv-CPP cell internalisation	121
3.6	Biological activity of scFv-CPP conjugates	122
3.6.1	The effect of scFv-CPP constructs on Rat basophilic leukaemia cell (RBL-2H3) viability	124
3.7	Conclusions	126
3.8	Materials and Methods	129
3.8.1	SDS-PAGE and western blot analysis	129
3.8.2	General sub-cloning procedure	130
3.8.3	Expression of scFv-Cys in <i>E. coli</i> with pUC119MCH vector	132
3.8.4	Expression of scFv-Cys in <i>E. coli</i> with p10HISCYS vector.....	133
3.8.5	Transient expression of scFv-Cys in Cep6 cells with pEOMCH vector	135
3.8.6	Preparation of scFv-CPP conjugates.....	137
3.8.7	General cell culture protocol.....	139
3.8.8	Fluorescence microscopy.....	140
3.8.9	Confocal scanning laser microscopy.....	140
3.8.10	Biological activity of scFv-CPP conjugates - Cell Titre Glo assay®	141
4	Isolation of neutralising single chain antibodies specific to Bcl-2.....	143
4.1	Proof-of-concept: Inhibition of CPP cell internalisation by carbamate protection of the guanidine moieties.....	146
4.1.1	Cell internalisation of protected octa-arginine derivatives	157
4.2	Protection of arginine side-chain with hydrolytic and esterase-labile protecting groups	161
4.2.1	Synthesis of protected isothioureas.....	164
4.2.2	The stability of acyloxycarbonyl and acyloxymethoxy carbonyl protected arginine..	169
4.2.3	Synthesis of an acyloxymethyl carbonyl protected octa-arginine derivative	184

4.1	Conclusions	192
4.2	Materials and methods.....	195
4.2.1	Hydrolytic stability assay.....	195
4.2.2	Esterase assay	195
4.2.3	Confocal scanning laser microscopy.....	196
5	Conclusions and future directions	197
6	Experimental	210
6.1	Materials and Instrumentation	210
6.1.1	General method for Fmoc solid-phase peptide synthesis of CPPs.....	211
6.2	Experimental for Chapter 3	213
6.3	Experimental for Chapter 4	224
7	References.....	243
	Appendix I-III.....	263

1

Introduction

Antibodies are extremely versatile molecules that can be engineered to be highly specific for a particular target. These properties have made them one of the most successful classes of macromolecular drugs. Unfortunately, the large size of antibodies restricts their application to extracellular targets. Thus, expanding the application of therapeutic antibodies to target intracellular protein-protein interactions (PPIs) is undoubtedly an exciting concept.

The major goal of this project is to obtain insight into how antibodies can be modified to possess cell entry capabilities whilst possessing therapeutically suitable *in vivo* properties. These are two essential criteria for the successful application of therapeutic antibodies to target intracellular PPIs. In this chapter, the different approaches currently available for inhibiting intracellular protein interactions will be discussed, with particular emphasis on the application of therapeutic antibodies to achieve this goal.

1.1 Inhibiting protein-protein interactions

PPIs are pivotal in almost every biological process, the deregulation or disruption of a protein interaction is often the underlying cause in a variety of diseases, including many cancers.¹ Some well characterised pathways, for example, the intrinsic apoptotic pathway and p53-regulated apoptosis are known to be deregulated through aberrant protein interactions, resulting in cancer formation.²⁻³ Viruses also rely on protein interactions with host proteins for viral infectivity and replication.⁴ For

example, members of the papillomavirus and herpesvirus family are able to deregulate the cell cycle through virus-host protein interactions, which often results in benign growths, but can also lead to cancer formation.⁴ It therefore comes as no surprise that PPIs are of huge interest to the medicinal chemist. The inhibition of a PPI can be achieved using a range of different molecules, for example, small organic molecules, peptides, peptidomimetics and protein therapeutics.

The surfaces involved in a PPI are generally large (1500-3000 Å²) and hydrophobic in nature.⁵ This makes the design of selective small molecule inhibitors a challenging task. Furthermore, this often means that potent small molecule inhibitors are also hydrophobic, which can cause significant solubility and aggregation problems.⁶ With the development of high-throughput screening (HTS), *in silico* screening and molecular modelling, it is now possible to rationally design molecules to selectively inhibit a PPI. Nevertheless, this is still a time consuming and challenging process due to the nature of the protein surfaces involved.⁷

Two different alternatives to small molecule inhibitors are therapeutic proteins and peptides and the exploitation of RNA interference (RNAi). Both methods work at different cellular levels. RNAi can be artificially induced to specifically ‘knock-out’ a protein’s function by activating RNA-induced silencing complex (RISC) mediated degradation of the target cellular mRNA.⁸ In contrast, therapeutic macromolecules can be used to inhibit a target protein at the post-translational level (Figure 1-1).⁹

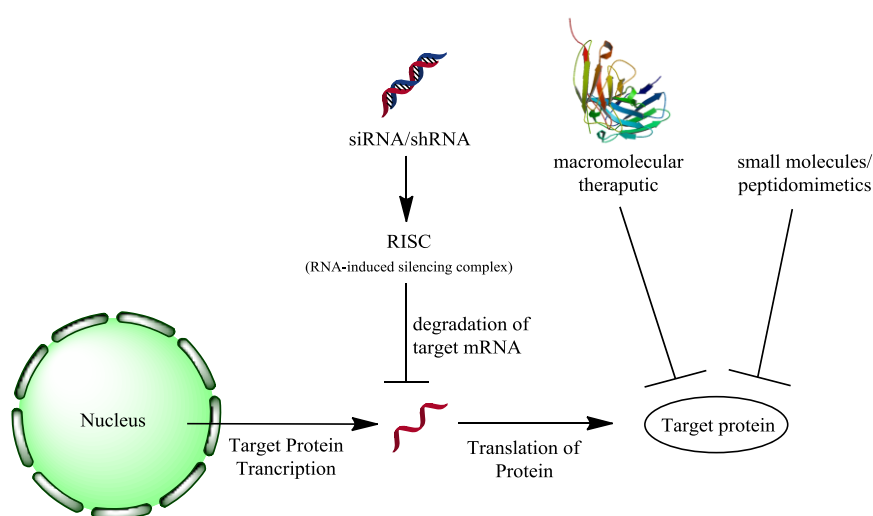


Figure 1-1: The inhibition of a target protein using RNAi, macromolecular therapeutics or small molecules. RNAi using siRNA inhibits a protein’s function by activating RISC mediated mRNA degradation of the target protein mRNA resulting in a complete functional ‘knock-out’. In contrast, small molecule and macromolecular inhibitors act at the protein level.

The inhibition of protein expression using RNAi can be achieved using short-interfering RNA (siRNA)⁸ or short hairpin RNA (shRNA).¹⁰ The use of siRNA to transiently knockout the expression of a target protein has proven a very effective tool in functional genomics.¹¹ Furthermore, siRNA has shown potential as a therapeutic entity when administered locally for the treatment of eye and lung diseases.¹²

Recently, safety concerns have been raised over the therapeutic application of RNAi regarding innate immune responses, and off-target non-specific interactions.¹³ Moreover, the major obstacle associated with siRNA is intracellular delivery, due to the hydrophilic and anionic nature of RNA making the cell membrane impenetrable.¹⁴ It should be noted that intracellular delivery is also a problem associated with many protein based therapeutics. Extensive research in this area offers promise in overcoming some of these problems.

Macromolecules, such as proteins and peptides can also be used to inhibit intracellular targets. The size and complexity of a macromolecule allows for the design of inhibitors that closely resemble the native protein interaction and occupy large areas of an active-site.¹⁵ Effective inhibitors can be designed by firstly identifying the region of a protein that is involved in the interaction of interest, based on this region, it is then possible to design highly selective peptides and peptidomimetics.¹⁵

The application of antibodies and other recombinant proteins to target cell surface receptors and other extracellular targets has been very successful.¹⁶ By either ‘evolutionary’ or rational methods, antibodies can be engineered to be highly selective for a chosen target. It is also possible to engineer antibodies that are specific to particular protein conformations¹⁷⁻¹⁸ and post-translational modifications.¹⁹ Using antibody reagents to modulate a PPI would allow for highly specific and transient modulation of a target, which is in contrast to the functional knock-out achieved using RNAi.⁹

However, the non-trivial challenge associated with using antibodies to inhibit an intracellular target is intracellular delivery. The cell membrane is highly regulated and effectively impenetrable to large polar molecules, such as proteins and DNA. Thus, the application of therapeutic antibodies is almost exclusively restricted to extracellular targets. The development of effective methods to address such molecules to intracellular targets *in vitro* and *in vivo* is an area of intense research.

1.2 Therapeutic antibodies

Antibodies are part of the vertebrate immune system and are structurally related proteins that bind with high specificity to foreign molecules (antigens) marking them for destruction.²⁰

It is possible to isolate antibodies possessing high selectivity to a particular molecule. The simplest approach to achieve this is by immunisation of an animal with the molecule of interest invoking an immune response. Antibodies can then be isolated from the host's blood plasma.²⁰ This method allows for the isolation of a mixture of antibodies i.e. polyclonal antibodies, which recognise different regions (epitopes) of the antigen.²⁰ Polyclonal antibodies are extremely useful for diagnostic purposes, for example, in western blotting or HTS. However, they are limited in their use as therapeutic agents because of the inherent variability between immunisation batches thus making them difficult to standardise.²¹ The therapeutic potential of antibodies was only realised following the development of technology for the isolation of a single antibody species, specific for one epitope, referred to as a monoclonal antibody (mAb).

The versatility and function of an antibody is derived from its molecular structure. There are five different classes of antibody isotypes, defined by their heavy chain. These are: IgA, IgD, IgE, IgG and IgM, the most abundant isoform in humans being the IgG.²² The IgG is composed of two heavy chains (50 kDa) and two light chains (25 kDa) giving a molecule of 150 kDa.

In 1959, Porter *et al.* showed that the digestion of an IgG with the plant protease papain resulted in three distinct antibody fragments.²³ One fragment is the fragment crystalline (Fc) region, which is responsible for the initiation of the complement system and antibody-dependant cell-mediated cytotoxicity²⁴, and the other two identical fragments are responsible for antigen binding, referred to as the Fragment Antigen Binding (Fab) region. The Fab region can be further deconstructed into the variable domain (Fv domain), which is the minimum required fragment for antigen recognition (Figure 1-2).²²

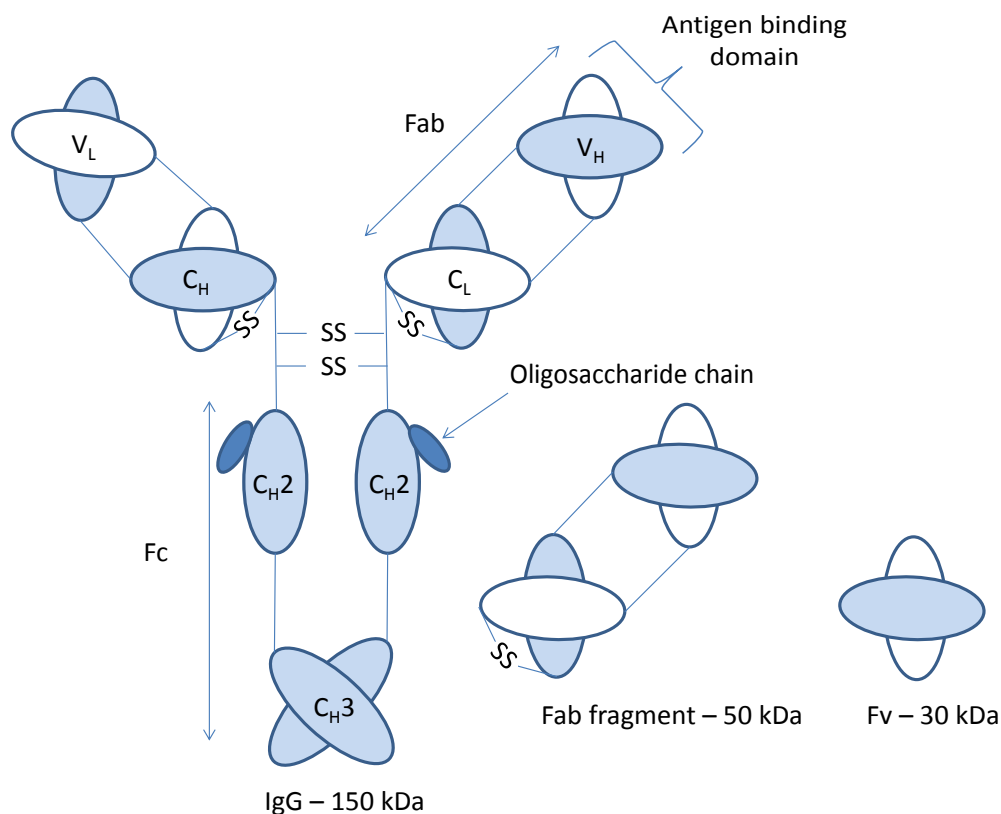


Figure 1-2: Antibody structure; the antibody isotype IgG is a 150 kDa protein comprised of constant (C) and variable (V) regions. These regions are divided up into variable heavy (V_H), constant heavy (C_H, C_{H2} and C_{H3}), variable light (V_L) and constant light (C_L) chains. The Fab fragment is composed of a constant light (C_L), constant heavy (C_H), variable (V_L) and a variable heavy (V_H) chain. The Fv fragment is composed of one V_H and V_L region are responsible for antigen recognition.

The two heavy chains of an IgG are linked to each other and also to a light chain by interdomain disulfide bonds. The two heavy and light chains are also further divided into constant (C) and variable (V) regions. Each heavy chain is folded to form four distinct domains (V_H, C_H, C_{H2} and C_{H3}) and the light chain folds to form two domains (C_L and V_L). The variable regions (V_H and V_L) are further divided into three hyper-variable regions, commonly referred to as complementarity determining regions (CDRs), which are inter-dispersed with framework regions. The six CDRs are responsible for the antigen specificity of an antibody.²²

1.2.1 Antibody Engineering

In 1975, Kohler and Milstein reported the development of a technique capable of producing cell lines that secrete mAbs.²⁵ This technique, referred to as hybridoma

technology involves the fusion of immunised spleen cells with mouse myeloma cells, resulting in an immortalised cell line secreting antibodies of a defined specificity.²⁵

Mouse mAbs found limited use as therapeutic agents due to an immunogenic response in humans, resulting in human anti-mouse antibodies (HAMA response).²⁶ In an attempt to reduce immunogenicity, mouse variable domains were introduced to a human constant region to produce a chimaeric antibody.²⁷ A further improvement was achieved by grafting mouse CDR regions, selected by hybridoma technology, to an antibody variable fragment framework of human origin affording a humanised antibody fragment.²⁸

In 1990, Winter's group described the application of filamentous M13 phage for the *in vitro* presentation and selection of 'fully' human antibodies.²⁹ Antibody libraries of naïve or immune origin (ideally containing 10^9 - 10^{11} clones) can be cloned into the phage genome next to a phage coat protein gene. As a result, the antibody is displayed on the surface of the phage particle as a fusion with the coat protein.³⁰ This links the antibody genotype with the phenotype allowing for the selection and recovery of antigen specific antibodies. Subsequent infection of *E. coli* amplifies the selected phage, generating a new library containing antigen specific antibodies. Finally, screening of enriched libraries can allow for the isolation of human mAbs of high affinity and specificity for an antigen.²⁹⁻³¹ Subsequently, other *in vitro* display techniques, such as ribosome display and yeast surface display have also proven to be effective tools for antibody engineering.³²

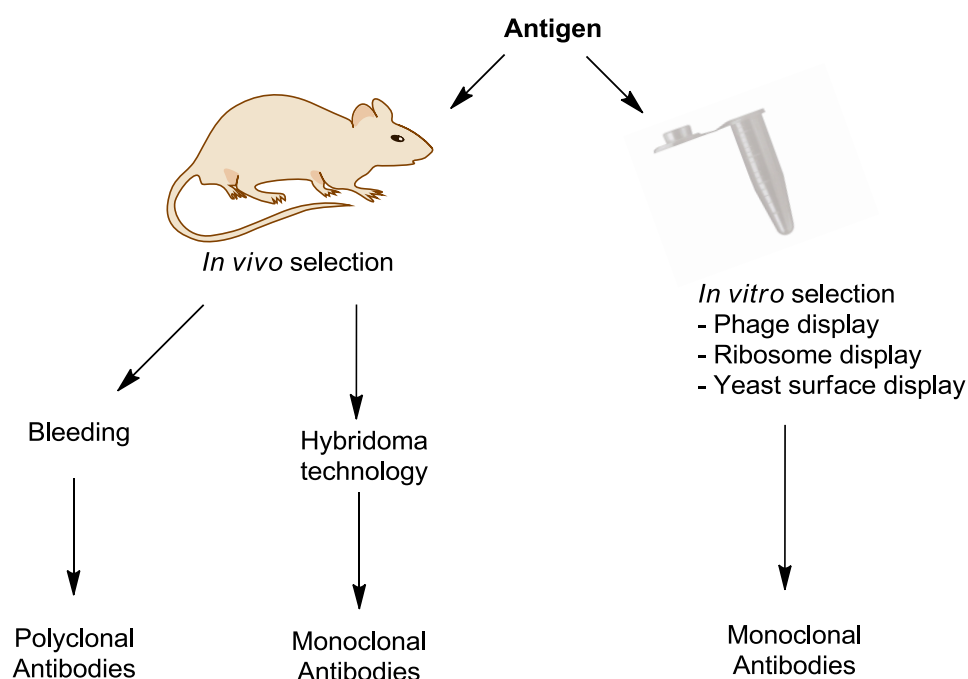


Figure 1-3: *In vitro* and *in vivo* selection of antibodies.

The development of *in vitro* display technologies has made it possible to rapidly isolate antibodies of therapeutic potential to almost any target. Additionally, *in vitro* display allows greater control over selection conditions, such as antigen concentration, pH, salt concentration and temperature.³² Alteration of these parameters can allow identification of antibodies that are specific to certain antigen conformation, or particular epitopes that would not be accessible using *in vivo* selection.³² The selection of antibodies specific to non-immunogenic molecules and post-translational protein modifications is also possible.¹⁹

The ease of obtaining the antibody-encoding DNA after *in vitro* selection has made it possible to engineer new recombinant antibody formats with new properties. The most notable modification to an antibody fragment is the engineering of the single chain variable fragment (scFv). The isolated Fv domain is relatively unstable, but can be stabilised by linking the V_H and V_L domains with a 10-15 amino acid polypeptide, generally (Gly₄-Ser)₃.³³ This stabilised Fv fragment is commonly referred to as a scFv.

The scFv can be further modified by altering the length of the polypeptide linker. Reducing the linker length to approximately five amino acids can result in the two domains being too close to pair. Consequently, the V_L and V_H domains pair with

another scFv to form a dimer, which is often referred to as a diabody.³⁴ Further reduction of the polypeptide linker to less than five residues results in the formation of triabodies³⁵ and even tetrabodies³⁶ (Figure 1-4).

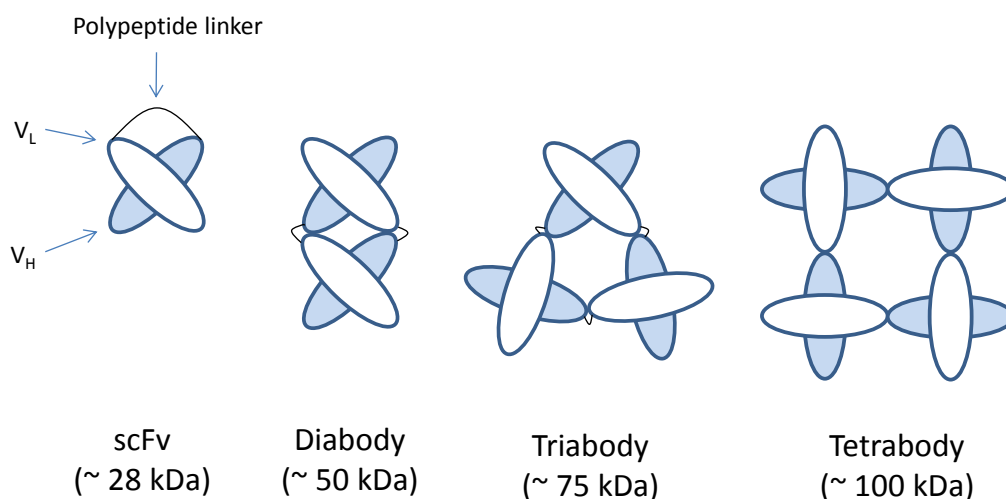


Figure 1-4: The different antibody formats formed by reducing the polypeptide linker between the V_H and V_L domain. The smallest is the scFv (~ 28 kDa). Reduction of the polypeptide linker to 5 amino acids results in the formation of a diabody (~ 50 kDa). Further reduction to < 5 amino acids results in triabody (~ 75 kDa) and tetrabody (~ 100 kDa) formation.

These multivalent fragments possess greater avidity for an antigen over the scFv.³⁷ There has been a wide variety of antibody formats developed, both multivalent and multispecific, based on the Fv and Fab domains. Unfortunately, the detailed discussion of the many antibody formats is outside the scope of this chapter (see review by Holliger *et al.* (2005)³⁸).

The *in vivo* distribution of an antibody and fragments thereof vary with size and antigen affinity. For example, the larger IgG and Fab fragments are retained in tumour tissue to a greater extent than the smaller fragments. However, with decreasing antibody fragment size the tumour penetration increases and the retention is more specific.³⁹ Thus, the intermediate-sized antibody formats, such as diabodies and triabodies, possess the most desirable *in vivo* properties.³⁹⁻⁴⁰

In addition to the different antibody formats, *in vitro* selection techniques also allow for engineering of antibodies that possess significantly greater affinity for an antigen than is possible to select using *in vivo* selection. This can be achieved by generating a new library based on an antibody previously selected against an antigen by

randomised mutagenesis of the CDR regions. From this synthetic library it is then possible to select new scFv with higher affinity for the antigen. Using this approach, antibodies with affinities in the pM range have been developed.⁴¹ Notably, Boder *et al.* (2000) reported the selection of an anti-fluorescein scFv with a K_d of 48 fM.⁴² This was achieved by screening a synthetic scFv yeast surface display library of 10^5 - 10^7 scFv based on an anti-fluorescein scFv with a K_d of 310 pM.⁴²

The unique molecular structure and the techniques available for the isolation and engineering of antibodies make them extremely versatile molecules. *In vitro* selection makes it possible to isolate antibodies with the desired specificity within weeks.³⁰ Additionally, further modifications can afford antibodies of remarkable affinity with properties tailored for the specific application. Consequently, expanding the application of antibodies to intracellular targets is unsurprisingly of huge interest.

1.3 Targeting intracellular protein-protein interactions with antibodies

The plasma membrane of a eukaryotic cell tightly regulates the influx and efflux of bioactive molecules. Large hydrophobic molecules are unable to efficiently enter cells through passive diffusion, thus requiring alternative means of entry. For this reason, antibodies that are specific for intracellular antigens require delivery across the cell membrane.

There are two distinct approaches to address antibodies to intracellular targets. One method is the intracellular delivery of DNA encoding for an antibody fragment, followed by protein expression using the host's cellular machinery.⁴³ The alternative approach is the delivery of an antibody fragment across the cell membrane and into the cytoplasm using delivery vectors.⁴³ Figure 1-5 illustrates the different approaches for the cytoplasmic delivery of an antibody reagent.

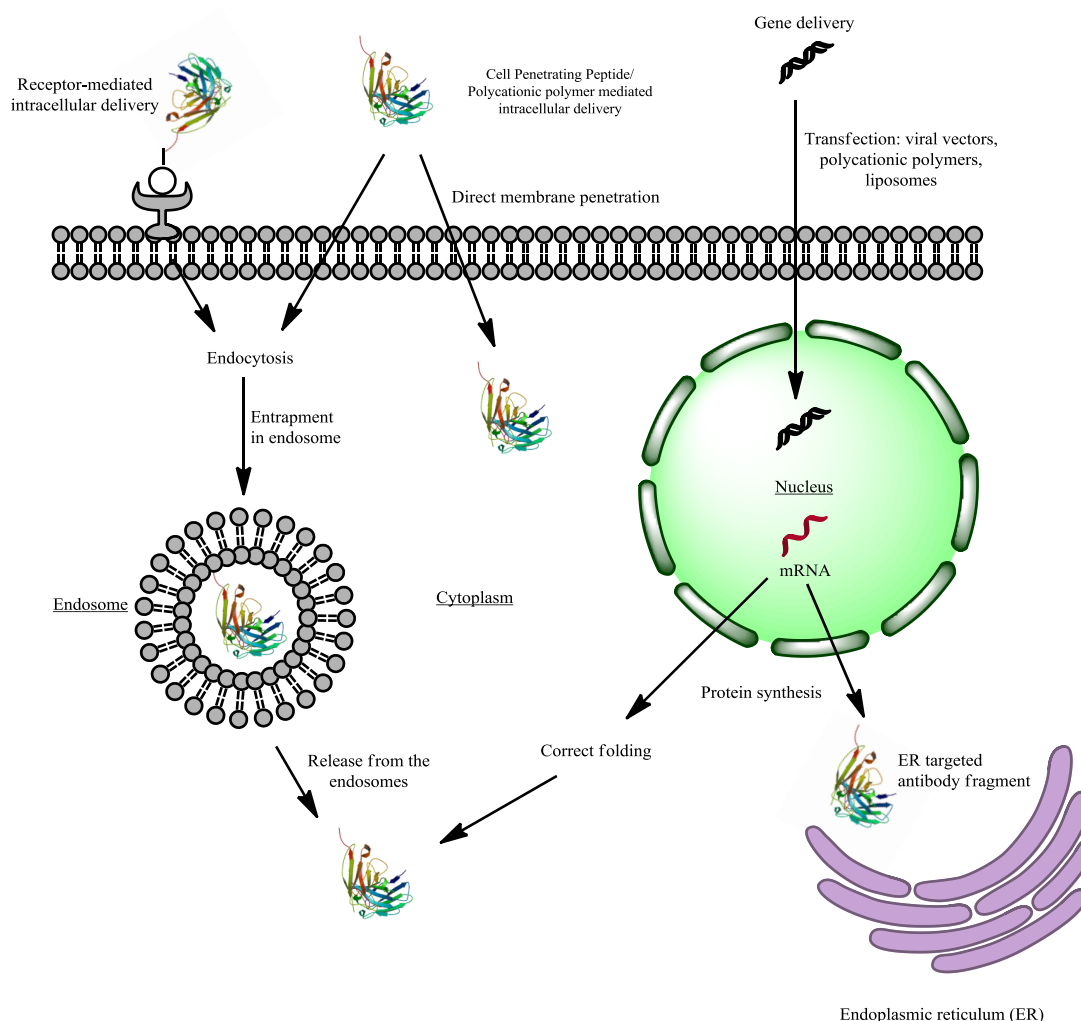


Figure 1-5: The different approaches to target antibody fragments to intracellular compartments. There are two distinct methods, one is the delivery of DNA encoding for an antibody fragment into the cell. Once inside the cell, the DNA is transcribed and translated by the cellular machinery either in the cytoplasm or in the endoplasmic reticulum. The second approach is by intracellular delivery of an antibody molecule to the cytoplasm either *via* direct cellular penetration or endocytosis, of which the former often results in entrapment in cellular vesicles. This can be achieved by using delivery vectors such as, Cell Penetrating Peptides (CPPs), cationic polymers or by receptor-mediated endocytosis.

Intracellularly expressed recombinant antibody molecules are often referred to as ‘Intrabodies’ whereas an intracellularly delivered antibody molecule is referred to as a ‘Transbody’.⁴³ The aim of both approaches is to efficiently target an antibody molecule to the correct cellular compartment for binding to the target antigen.

Many interesting therapeutic targets for intracellular antibodies are located in the cytoplasm. However, antibody internalisation mediated by delivery vectors such as, cell penetrating peptides (CPPs), cationic polymers or by receptor-mediated endocytosis often result in entrapment of the antibody molecule in the endosomal

compartment.⁷⁴ The antibody molecule is then destined for degradation in the lysosome unless it is released into the cytoplasm by rupturing of the endosome.

Antibody fragments targeted to the cytoplasm *via* gene delivery are presented by equally challenging obstacles such as, protein expression levels and correct folding in the reducing cytoplasmic environment.⁴³ Without correct folding the antibody fragment is unlikely to bind the target antigen.

Methods for addressing antibody reagents to intracellular compartments employing the intrabody and transbody approaches, together with techniques to overcome some of the many obstacles involved with these approaches are discussed in more detail below.

1.3.1 Intrabodies

In 1988, Carlson and co-workers reported the first example of an intrabody by expressing an antibody specific for alcohol dehydrogenase I (ADH I) in *Saccharomyces cerevisiae*. This approach successfully inhibited ADH I activity.⁴⁴

Marasco *et al.* (1993) were the first to utilise intrabodies in mammalian cells by expressing a monoclonal antibody specific for the CD4 binding region of the human immunodeficiency virus type 1 (HIV-1) envelope protein in the endoplasmic reticulum of COS cells.⁴⁵ Research has since continued to explore intrabodies for both therapeutic and diagnostic application.

Although the concept of intrabodies seems simple, there are many challenges presented by the cellular barriers and the reducing intracellular milieu. Many antibodies rely on intrachain disulfide bond for correct folding and activity.⁴⁶ Intrabodies that are targeted to the endoplasmic reticulum have the benefit of molecular chaperones and a favourable redox environment for correct folding.⁴⁷ However, cytosolic intrabodies offer the greatest potential for the inhibition of intracellular PPIs. Unfortunately, the reducing cellular environment can cause antibody insolubility, instability and folding issues.⁴⁷

Recent studies have focused on engineering antibody fragments so that intrachain disulfides are not required for correct folding.⁴⁸ Intracellular selection techniques have

also been developed that allow identification of scFv that can fold correctly in the reducing cellular environment. The most notable example of this approach is Intracellular Antibody Capture Technology (IACT).⁴⁹ This method is based on the yeast-two hybrid system and allows for selection based on successful scFv expression, folding and antigen binding in the intracellular environment of yeast. The successful formation of the scFv/antigen complex results in the activation of a reporter gene and subsequent identification of the functional scFv.⁴⁹⁻⁵⁰

IACT has proven effective in identifying intrabodies when used as a secondary screening technique for scFv libraries selected using antibody phage display.⁵⁰ Further development of IACT focussed on screening naïve single domain antibody (Dab) libraries. Unfortunately, this was limited by the low transformation efficiency of yeast, hence only small library sizes could be accessed.⁵¹ Third generation IACT (ICA³) circumvents this problem by repeated cycles of library screening and CDR randomisation to generate new sub-libraries.⁵² Thus, ICA³ may prove to be a powerful tool for the selection of high affinity functional intrabodies.

Another recent development in the area of intrabodies is the design of an intrabody phage display library. Philibert *et al.* (2007) created a scFv library based on a scFv scaffold developed for cytoplasmic expression.⁵³ Using this library they were able to isolate scFv specific for the papilloma virus protein E6. Impressively, these scFvs were expressed in the cytoplasm of *E. coli* in yields of ~0.5 g/L. The transfection of HeLa cells with an expression plasmid containing the scFv-GFP construct afforded soluble expression of the scFv-GFP fusion in the cytoplasm of HeLa cells.⁵³ This approach holds great promise for the selection and application of functional scFvs able to inhibit intracellular PPIs.

However, even with an antibody that is intracellularly stable, the significant challenge of efficiently and specifically delivering recombinant DNA to target cells *in vivo* still remains. There have been a variety of non-viral and viral based DNA delivery systems described.⁵⁴ Unfortunately, many of the current non-viral vectors are relatively inefficient at delivering DNA to target cells and in several clinical studies viral vectors have been reported to induce immune responses and have been linked to the development of a leukaemia-like syndrome.⁵⁵⁻⁵⁷

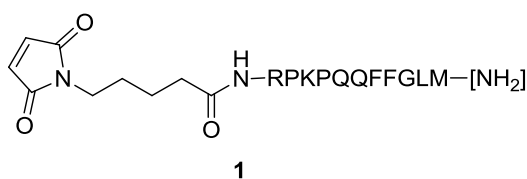
1.3.2 Transbodies

A possible solution to the stability and delivery problems associated with intrabodies is the intracellular delivery of antibody fragments. Heng *et al.* (2005) coined the phrase ‘Transbodies’ for an antibody that is modified to enable cellular internalisation.⁴³

Transbodies are expressed and purified using standard protein expression systems, such as *Escherichia coli* (*E. coli*) allowing for correct folding and characterisation of the protein before administration. Furthermore, the intradomain disulfide bonds in the folded V_H and V_L domains of the Fv domain provide stability and are often essential for antigen-binding⁴⁶, once folded these disulfide bonds are buried and unsolvated making them relatively stable to reducing agents.⁵⁸ This circumvents the protein stability and folding problems that are associated with intrabodies.⁴³

The major benefit of transbodies is that no genetic modification to the target cells is required, avoiding the problems associated with gene delivery. Additionally, transbodies would possess a limited half-life, unlike gene therapy. The major obstacle however, is the intracellular delivery of antibodies.

Recently, receptor-mediated delivery of an antibody fragment has been demonstrated. Rizk *et al.* (2009) described the cellular internalisation of an anti-actin Fab fragment mediated by the neurokinin-1 receptor (NK1R). This receptor is not only overexpressed in some aggressive brain tumours, but also breast and colon carcinomas.⁵⁹ An unpaired cysteine residue introduced to the Fab fragment allowed for the conjugation of the NK1R ligand substance P **1** by a thioether bond. The conjugated Fab was internalised by cells expressing the NK1R receptor, subsequently enabling the Fab to bind to actin.⁶⁰



Although, receptor-mediated endocytosis shows great potential for the intracellular delivery of macromolecules it is limited to cells that overexpress a particular receptor. The amount of protein delivered into the cell is also limited by the number of receptors available.

An alternative and extensively investigated method for intracellular delivery of macromolecules is offered by a class of peptide often referred to as ‘Cell Penetrating Peptides’ (CPPs). The use of CPPs has showed great promise for the delivery of macromolecules, including antibody reagents into cells. By conjugation of a CPP to a protein or the expression of a CPP fusion protein, it is possible to internalise a protein that otherwise would not be able to traverse the cellular membrane.⁶¹ Table 1-1 shows a selection of studies that have reported the successful intracellular delivery of antibody fragments using CPPs.

Table 1-1: Examples of Transbodies

Antibody-CPP construct	CPP sequence	Description	Reference
scFv-Tat ₄₄₋₅₇ conjugate	CGISYGRKKRRQRRR	<i>In vivo</i> study. Anti-ED-B scFv – a marker for tumour neovasculature.	Niesner <i>et al.</i> (2002) ⁶²
scFv-Tat ₄₇₋₅₇ fusion	YGRKKRRQRRR	<i>In vitro</i> study. Intracellular delivery of anti-Bcl-2 scFv. The inhibition of Bcl-2 induces apoptosis in cancer cell lines relying on Bcl-2 overexpression for survival.	Cohen-Saidon <i>et al.</i> (2003) ⁶³
scFv-Tat ₄₇₋₅₇ fusion	YGRKKRRQRRR	Anti-morphine scFv. <i>In vivo</i> study assessing the delivery of scFv-Tat across blood brain barrier	Nakajima <i>et al.</i> (2004) ⁶⁴
scFv-Antp ₄₁₋₅₈ fusion	FIRQIKIWFQNRMMKWKK	Intracellular delivery of an anti-myc scFv – mutated c-myc is implicit in some cancers. Inhibition induces apoptosis in some cell lines.	Avignolo <i>et al.</i> (2008) ⁶⁵
scFv-Antp ₄₃₋₅₈ fusion	QIKIWFQNRMMKWKK	<i>In vitro</i> study. scFv specific for Matrix Protein (M1) of Influenza A	Poungpair <i>et al.</i> (2010) ⁶⁶
scFv-MTS fusion	KGEGAAVLLPVLLAAPG	<i>In vitro</i> study. Anti-Akt kinase scFv – Akt is involved in cell survival and proliferation	Shin <i>et al.</i> (2005) ⁶⁷
scFv-MTS conjugate	KGEGAAVLLPVLLAAPG	<i>In vitro</i> study. anti-Ricin A-chain scFv – intracellular delivery neutralised the ricin toxin	Wu <i>et al.</i> (2010) ⁶⁸
Fab-Tat ₄₈₋₆₀ , HIV-1 REV ₃₄₋₅₀ and Antp ₄₃₋₅₈ conjugate	HIV-1 Rev ₃₄₋₅₀ : RQARRNRRRRWRERQR	Non-specific Fab – <i>in vivo</i> study comparing the biodistribution of Fab-CPP fragments in rats	Kamayama <i>et al.</i> (2006) ⁶⁹
F(ab') ₂ -Tat ₃₇₋₇₂ conjugate	³⁷ CFITKALGISYGRKKRRQ-RRRPPQGSQTHQVSLSKQ ⁷²	<i>In vitro</i> study. Anti-Tetanus toxin antibody fragment, intracellular delivery neutralising the toxin in chromaffin cells.	Stein <i>et al.</i> (1999) ⁷⁰
IgG-Polyarginine conjugate	R ₆₈	<i>In vitro</i> study. Anti-cyclin D mAb. Intracellular delivery inhibited cell cycle progression	Chen <i>et al.</i> (2006) ⁷¹
IgG-Tat ₄₄₋₆₀ conjugate	GRKKRRQRRRPPQGYG	<i>In vitro</i> and <i>in vivo</i> study. Radio- labelled anti-p21 ^{WAF/CIP-2} mAb labelled with Tat. Intracellular delivery inhibited G1-S phase cell cycle arrest by EGF	Hu <i>et al.</i> (2007) ⁷²

Table 1-1 shows some promising examples of transbodies, antibodies have been delivered into a number of cell lines using CPPs for a variety of different targets. For example, an anti-tetanus toxin F(ab')₂ fragment was successfully delivered into

chromaffin cells neutralising the toxin.⁷⁰ There are also examples of transbodies being used to inhibit protein interactions implicated in cancer formation. The anti-apoptotic protein Bcl-2 that is overexpressed in a number of cancer cells was successfully inhibited using a neutralising anti-Bcl-2 scFv Tat fusion protein.⁶³

However, there are still relatively few examples of antibodies being used for intracellular targets. Additionally, the reported use of transbodies is largely focused on *in vitro* delivery, with very few studies utilising transbodies *in vivo*. Unfortunately, the current examples of transbodies, in general, apply different approaches to achieve intracellular delivery, making it difficult to determine the specific requirement for effective intracellular delivery of an antibody reagent. There are a large number of variables that should be considered when designing a transbody, such as the size of the antibody fragment, the CPP and the nature of the antibody construct (i.e. fusion protein or conjugate).^{70,73} Thus, a general and systematic approach for the construction and application of transbodies is required.⁷⁴

1.4 Cell penetrating peptides

The discovery and subsequent application of the many CPPs was sparked by two major discoveries. The first was in 1988 when Frankel *et al.* (1988) reported that the protein HIV transactivator of transcription (Tat) was able to directly penetrate cells, activating its target gene involved in HIV infectivity.⁷⁵ In a later study, Joliot *et al.* (1991) demonstrated that the 60 amino acid homeodomain of the Antennapedia protein of *Drosophila* was also able to translocate across cell membranes.⁷⁶ Detailed studies into these two proteins resulted in the discovery of the minimum peptide sequences responsible for cell penetration, referred to as Tat⁷⁷ and Penetratin (Antp)⁷⁸⁻⁷⁹, respectively.

However, the most significant finding was the ability of these peptides to internalise an attached cargo that otherwise was unable to penetrate cells.⁶¹ Peptides possessing these properties are now commonly referred to as CPPs. This led to extensive research focusing on the potential applications of CPPs and other peptides that may possess similar properties.

To date, there are >100 reported peptides with cell penetrating capabilities.⁸⁰ Almost all CPPs are cationic, adopt amphipathic structures and are rich in lysine and arginine residues.⁸¹ CPPs are usually <30 amino acids and possess a net positive charge at physiological pH.⁸²

CPPs can be divided into three groups based on the primary structure, these are primary amphipathic (paCPPs), secondary amphipathic (saCPPs) and non-amphipathic (naCPPs).⁸³ A selection of CPPs is shown in Table 1-2.

Table 1-2: A selection of cell penetrating peptides

#	Name*	Amino acid sequence	Reference
<u>paCPPs</u>			
2	Transportan	GWTLNSAGYLLGKINLKALAALAKKIL	Pooga <i>et al.</i> (1998) ⁸⁴
3	Pep-1	KETWWETWWTEWSQPKKKRKV	Morris <i>et al.</i> (2001) ⁸⁵
4	MPG	GALFLGFLGAAGSTMGAWSQPKSKRKV	Morris <i>et al.</i> (1999) ⁸⁶
<u>saCPPs</u>			
5	Antp ₄₃₋₅₈	RQIKIWFQNRRMKWKK	Derossi <i>et al.</i> (1996) ⁷⁹
6	KLAL	KLALKLALKALKAAALKLA	Oehlke <i>et al.</i> (1998) ⁸⁷
7	pVEC	LLILRRRIRKQAHASK	Elmqvist <i>et al.</i> (2001) ⁸⁸
<u>naCPPs</u>			
8	Octa-Arginine	RRRRRRRR	Wender <i>et al.</i> (2000) ⁸⁹
9	HIV Tat ₄₇₋₅₇	YGRKKRRQRRR	Vives <i>et al.</i> (1994) ⁷⁷
10	HIV Tat ₄₉₋₅₇	RKKRRQRRR	Vives <i>et al.</i> (1997) ⁹⁰

*Divided into groups based on primary structure; primary amphipathic (paCPPs), secondary amphipathic (saCPPs) and non-amphipathic (naCPPs).

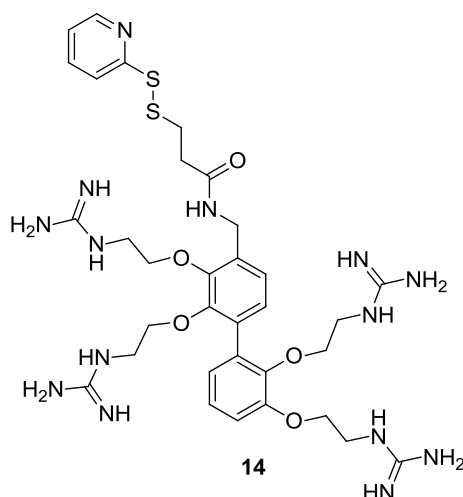
The paCPPs are generally >20 amino acids and are composed of sequential hydrophobic and hydrophilic amino acids.⁸² Peptide internalisation occurs by both endocytosis and direct translocation across the membrane.⁸³

The saCPPs are commonly used for the delivery of proteins and are generally shorter than the paCPPs. Again, these peptides possess amphipathicity but are predicted to only form this secondary structure when interacting with the phospholipid bilayer.⁹¹ The naCPPs are generally the shortest CPPs and are able to penetrate cells solely based on their cationic features.⁹²⁻⁹³

Amphipathicity is an important property of peptides that possess cell penetrating capabilities. Amphipathicity is often presented in α -helical or β -structures by spatial separation of hydrophobic and hydrophilic amino acid residues for example tryptophan and arginine, respectively.⁸² The strong amphipathicity of phospholipid membranes explains this important requirement of CPPs to favourably interact with cell membranes.⁸¹ Several mechanisms have been described such as the pore formation, inverted micelle and carpet-like models.⁸¹⁻⁸² Common to all of these models is the requirement for amphipathicity, which allows for the interaction of the hydrophobic residues of a peptide with the lipid components of a membrane and the hydrophilic residues with the charged components.⁸¹⁻⁸² This interaction may then disrupt the integrity of the membrane allowing for the peptide to directly penetrate into the cell in an energy independent process.

There have been a number of examples of peptides that internalise into cells but possess properties different to the majority of CPPs. A recent example is the non-cationic peptide p18 (⁵⁰LSTAADMQGVVTDGMASG⁶⁷) **11**. This peptide is derived from the protein Azurin.⁹⁴ Similarly, Crespo *et al.* (2003) reported that the non-cationic peptide FAM-(Pro)₁₄-OH **12** was able to internalise into cells.⁹⁵ Unfortunately, there are no further examples of these two peptides being used as CPPs. The use of a non-cationic CPP could potentially avoid some of the problems associated with using a polycationic peptide *in vivo*. Further studies into these two peptides may shed light on their ability to deliver attached cargo into cells. In complete contrast to the cationic CPPs, Martin *et al.* (2011) recently reported the design of an anionic CPP called SAP(E) (VELPPP)₃ **13**.⁹⁶ This peptide showed internalisation into a number of cell lines, however, with less efficiency than Tat and Antp.⁹⁶ Nonetheless, this peptide still offers an interesting alternative to the cationic CPPs.

An alternative to using peptides for intracellular delivery is the use of small molecule mimics of CPPs. Okuyama *et al.* (2007) describe the use of a biphenyl scaffold for the display of guanidine moieties in an attempt to mimic the cationic α -helix of many CPPs. This molecule was named 'small-molecule carrier' (SMoC) **14**.⁹⁷



The SMoC **14** when conjugated to the 25 kDa protein geminin enabled the internalisation of the protein into a variety of cell lines. SMoCs offer a simple and protease resistant alternative to CPPs.⁹⁷⁻⁹⁸ However, a study comparing the efficiency of SMoCs with commonly used CPPs, together with the use of different sized cargos has yet to be reported.

1.4.1 Mechanism of CPP internalisation

Many early studies using fixed cells demonstrate CPP internalisation at 4 °C suggesting internalisation *via* an energy independent route.^{79,90,93} However, Richard *et al.* (2003) suggested that fixing cells actually perturbs the cell membrane resulting in artifactual results and overestimation of peptide internalisation.⁹⁹ More recent studies using live cells show minimal, if any, uptake at 4 °C but uptake principally at 37 °C.⁹⁹ Confocal microscopy of live cells treated with a fluorescently labelled CPP often shows localisation of the peptide in cellular vesicles, suggesting an energy dependant route is taken.⁹⁹⁻¹⁰⁰

Additionally, internalisation of cationic peptides such as Tat and polyarginine appears to be dependent on interactions with anionic cell surface proteoglycans such as heparan sulfate proteoglycans (HSPG). The electrostatic interaction of arginine and lysine residues with HSPG draws the CPP into close proximity to the cell membrane.¹⁰¹ This interaction may then promote signalling cascades leading to activation of the protein Rac, which then promotes F-actin reorganisation, an essential step in lamellipodia formation and macropinocytosis.¹⁰²⁻¹⁰³

Endocytic uptake of CPPs is now generally accepted as the primary mechanism for CPP internalisation. However, the exact route is still unclear and it is likely that a variety of endocytic pathways are used by CPPs, for example, caveolae mediated clathrin mediated endocytosis, clathrin and caveolin independent endocytosis and macropinocytosis.¹⁰⁴⁻¹⁰⁶ Additionally, there are some examples of arginine rich peptides internalising *via* energy independent routes using live cells.¹⁰⁷ Overall, the exact mechanism of internalisation is likely to be dependent on cell type, CPP concentration, the CPP properties and the attached cargo.^{108,101}

In support of the endocytic uptake mechanism is the entrapment of CPPs and the attached cargo in cellular vesicles. Tünnemann *et al.* (2006) showed that the destination of Tat was dependant on the size of the attached cargo. Small cargo (<50 amino acids), were able to escape the endosomes and localise in the cytoplasm. However, with increasing size (>50 amino acids) the amount of cargo in the endosomes increased.⁷³

Importantly, many biologically active molecules require delivery to the cytosolic compartment for activity. Direct penetration of amphipathic peptides by disruption of the phospholipid membrane leads to the delivery of an attached cargo directly to the cytosol.⁸² However, endocytic uptake involves encapsulation of the CPP and attached cargo in cellular vesicles.⁹⁹ Initially after internalisation the CPP will be contained in the early endosomes.⁷⁴ Unless the endosome is disrupted, allowing for release of the contents into the cytoplasm, the CPP and cargo are destined for the late endosomes and eventually lysosomes where degradation will occur.⁷⁴

There have been a number of peptides and polymers that have been demonstrated to display endosomolytic properties. Table 1-3 shows a selection of molecules that display endosomolytic properties.

Table 1-3: A selection of endosomolytic agents

#	Endosomolytic agents	Reference
<u>Polymer based</u>		
15	poly(propylacrylic acid)	Cheung <i>et al.</i> (2001) ¹⁰⁹
16	poly(acrylic acid)	Philippova <i>et al.</i> (1997) ¹¹⁰
17	poly(ethyleneimine)	Alexis <i>et al.</i> (2006) ¹⁷
<u>Peptide based</u>		
18	HA2; GLFGAIAAGFIEGGWTGNIDGWYG	Wadia <i>et al.</i> (2004) ¹¹¹
19	H5WYG; GLFHAIHFIHGGWHGLIGGWGYG	Pichon <i>et al.</i> (2001) ¹¹²
20	10HIS; HHHHHHHHHH	Lo <i>et al.</i> (2008) ¹¹³
21	4 ₃ E; LAELLAELLAEL	Ohmori <i>et al.</i> (1997) ¹¹⁴

Many of the peptide based endosomolytic agents mimic the mechanisms used by viruses to escape the endosomes. Indeed, HA2 **18** and H5WYG **19** are derived from the influenza virus.¹¹¹⁻¹¹² These virus derived peptides change conformation in the low pH of the endosome to form a hydrophobic, amphipathic α -helix. The peptide then inserts into the membrane disrupting the endosome, ultimately leading to the release of the contents into the cytoplasm.¹¹⁵ Alternatively, the histidine rich peptides and endosomolytic polymers disrupt the endosome membrane by a ‘proton sponge’ effect.¹¹³ Once in the acidic environment of the endosome, the secondary and tertiary amines of the endosomolytic agent are protonated. This results in an influx of chloride ions, increasing the ionic concentration, and leading to osmotic swelling and rupturing of the endosomes.¹¹⁶

A number of the endosomolytic peptides have been used to increase the cytoplasmic delivery of HIV Tat-protein conjugates and DNA/Tat complexes. For example, Wadia *et al.* (2004) demonstrated that co-treatment of a fibroblast cell line with a Tat₄₉₋₅₇-HA2 fusion peptide and a Tat-Cre fusion protein significantly enhanced endosomal release of the Tat-Cre compared to when the Tat-Cre was used alone.¹¹¹ Similarly, Lo *et al.* (2008) demonstrated that a Tat₄₉₋₅₇-10His/DNA complex displayed approximately 7000 fold greater DNA transfection efficiency compared to a Tat₄₉₋₅₇/DNA complex, this is presumably a result of increased release of the DNA from cellular vesicles.¹¹³

The nature of the CPP-cargo linkage also appears to be influential on the intracellular delivery and cellular localisation of the cargo. Several studies have suggested that the biological effect of CPP-cargo conjugates is enhanced by the use of a reversible linkage. For example, Stein *et al.* (1999) showed that an anti-tetanus toxin F(ab')₂ conjugated to Tat₃₇₋₇₂ via a disulfide bond neutralised the toxin in chromaffin cells to a greater extent than the thioether linked F(ab')₂-Tat conjugate.⁷⁰ Similarly, Chen *et al.* (2001) demonstrated that the ϵ PKC inhibitor ψ ϵ RACK reversibly conjugated to R₇ via a disulfide linkage significantly reduced ischemia-induced cell damage, whereas the thioether linked ψ ϵ RACK-R₇ conjugate had no significant effect.¹¹⁷ These reports suggest that intracellular release of the CPP is important for the desired activity of the cargo, presumably to reduce interference of the CPP with the cargo or altering its co-localisation within the cell.¹¹⁸ However, there are also many examples of non-reversible CPP-protein conjugates being successful used to induce biological responses, thus the influence of the CPP-cargo linkage is possibly cargo and CPP dependent.

Understanding the processes of CPP internalisation is important for the effective application of CPPs for the intracellular delivery of macromolecules. The choice of CPP, application of endosomolytic peptides, and the nature of the CPP-cargo conjugation are all important factors that should be considered to ensure that a CPP-cargo conjugate induce the desired biological effect.

1.4.2 The application of CPPs *in vivo*

A number of *in vivo* pharmacological studies using diseased mouse models show promise for CPP mediated delivery of therapeutic cargo. However, there are few studies that address the pharmacokinetics (PK), ADME (absorption, distribution, metabolism and elimination) and the safety of CPPs, thus making it difficult to assess the therapeutic potential of protein-CPP conjugates.

The study by Lee *et al.* (2001) is one of a few that address the PK properties of a protein-CPP conjugate.¹¹⁹ In this study, a radiolabeled Tat₄₈₋₅₈-biotin/streptavidin (SA) complex was intravenously (*i.v.*) administered to rats. The percentage injected dose per gram of target tissue (% ID/g) calculated for the Tat₄₈₋₅₈-biotin/SA complex

suggested a modest increase in uptake of SA by the brain, liver, kidney, heart and lung relative to the native SA. Additionally, the authors reported that the Tat₄₈₋₅₈-biotin/SA complex possessed increased membrane permeability compared to the native SA. This resulted in rapid blood clearance, thus having a negative effect on %ID/g and suggesting uptake by peripheral tissues.¹¹⁹

A few studies have also addressed the tissue distribution of protein-CPP conjugates, giving further insight into the effect of CPP conjugation on the *in vivo* properties of an attached protein. One example by Schwarze *et al.* (1999) reported widespread tissue distribution in mice of a 116 kDa β -galactosidase-Tat₄₇₋₅₇ fusion protein.¹²⁰ Interestingly, enzyme activity was observed in brain tissue suggesting transport across the blood-brain barrier. However, a study by Kameyama *et al.* (2006) showed less widespread distribution of a ¹²⁵I labelled Fab fragment (polyclonal Fab mixture) conjugated with Tat₄₈₋₆₀, HIV-1 Rev₃₄₋₅₀ or Antp₄₃₋₅₈. This study showed that tissue distribution may also be dependent on the CPP used. For example, the highest levels of radioactivity for the ¹²⁵I labelled Fab-Tat₄₈₋₆₀ conjugate were observed in the liver and spleen, whereas for Fab-Antp₄₃₋₅₈ and Fab-HIV-1 Rev₃₄₋₅₀ conjugates this was in the liver, spleen and adrenal gland. For the unconjugated ¹²⁵I labelled Fab, radioactivity was seen in the thyroid gland, gastrointestinal contents, renal cortex and skin.⁶⁹

Niesner *et al.* (2002), using a mouse tumour model, observed lower tumour retention of an scFv specific for the ED-B domain of fibronectin conjugated to Tat₄₄₋₅₇, compared to the unconjugated scFv. However, increased retention in the liver, spleen and kidney was observed.⁶² Fibronectin is overexpressed and present in higher quantities in the extracellular matrix associated with tumour vasculature,¹²¹ therefore the decrease in tumour retention of the scFv upon Tat₄₄₋₅₇ conjugation is presumably a result of faster blood clearance and non-specific tissue uptake of the conjugate.

The findings of the aforementioned studies were recently supported by Sarko *et al.* (2010). In this study, the biodistribution in mice of 10 different ¹¹¹In or ⁶⁸Ga radiolabelled CPPs was determined. The authors reported rapid clearance from circulation (four hours after injection, <1% ID/g was in circulation) and non-specific uptake into almost all organs.¹²²

The non-specific tissue uptake of CPP conjugates may explain why relatively large doses (mg/kg) are required to obtain a biological response. These high doses may result in toxicity issues caused by the CPP.¹¹⁹ For example, the CPP octa-arginine has been shown to be a potent inhibitor of the proteasome and the enzyme Furin.¹²³⁻¹²⁴ A number of other CPPs, such as Antp and Tat have also shown cellular toxicity at high doses.¹²⁵⁻¹²⁷ Thus, a high dose coupled with the non-specific tissue uptake of a CPP could increase ‘off-target’ biological effects.

Local delivery may overcome some of the problems associated with CPPs *in vivo*. This was illustrated by Rothbard *et al.* (2000) reporting that topical administration of cyclosporine-polyarginine (R₇) significantly reduced skin inflammation in a mouse model of dermatitis.¹²⁸ Notably, Chen *et al.* (2001) developed an effective PKC δ inhibitor for the treatment of ischemia/reperfusion injury by conjugation of the cell impermeable PKC δ peptide inhibitor δ V1-1 to Tat₄₇₋₅₇ **22**.¹²⁹

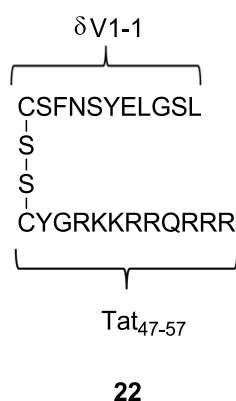


Figure 1-6: The cell permeable PKC δ peptide inhibitor δ V1-1-Tat₄₇₋₅₇ conjugate **22**.

Several studies have demonstrated that **22** reduces cardiac damage in a porcine model of acute myocardial infarction (AMI) after intracoronary injection.¹³⁰⁻¹³¹ Furthermore, **22** is currently in phase II clinical trials to assesses its safety and efficacy for the reduction of infarct size in AMI patients.¹³²⁻¹³³

Further *in vivo* tissue distribution, PK and toxicity studies will provide greater understanding of the PK and clearance mechanisms of protein-CPP conjugates. PK studies investigating the effect of CPP conjugation to antibody fragments will also provide insight into the therapeutic potential of transbodies and on how CPPs may be modified to optimise PK properties of an antibody-CPP conjugate.

1.4.3 Modulation of CPP *in vivo* properties

Recently, several approaches have been reported to reduce the non-specific uptake of CPPs by targeted delivery or targeted activation of CPP internalisation. A number of interesting examples are discussed in this section.

Tan *et al.* (2006) described the targeted delivery of Tat₄₇₋₅₈ to breast cancer cells overexpressing the receptor ErbB2. This was achieved by conjugation of an anti-ErbB2 peptide to the C-terminus of Tat₄₇₋₅₈ to afford the chimeric peptide **23**. This peptide showed greater uptake into cells overexpressing ErbB2 than cell expressing lower levels both *in vitro* and *in vivo*.¹³⁴ Myrberg *et al.* (2008) describe a similar approach using a tumour-homing peptide that was identified from a phage display library.¹³⁵ This ‘tumour-homing’ CPP **24** was composed of the CPP p-VEC, linked to a cyclic tumour specific peptide. This peptide showed *in vivo* tumour-homing properties and greater uptake into breast tumours than pVEC alone. This group later published another breast tumour-homing CPP **25**, which consists of a linear tumour targeting peptide conjugated to pVEC.¹³⁶

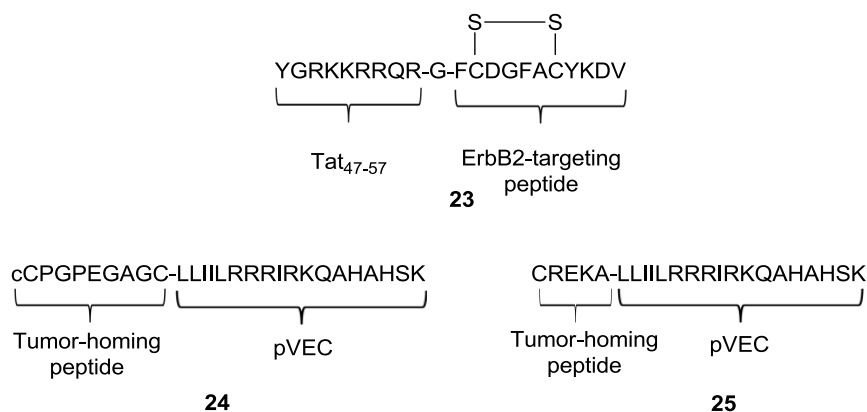


Figure 1-7: Examples of chimeric ‘tumour-homing’ cell penetrating peptides

The targeting of CPPs to specific tissues is a promising approach, however this may not significantly reduce non-specific tissue uptake due to the cationic charge of the CPP. In the context of the tissue targeting approach, an alternative is the targeted activation of a CPP.

Recently, Zhang *et al.* (2011) described the design and synthesis of an acid-activated CPP based on the CPP Transportan-10 **26**.¹³⁷ This was achieved by replacing the lysine residues contained in Transportan-10 with histidine residues to afford the peptide TH **27**. At pH 7.4, TH **27** is uncharged and unable to internalise into cells. However, in a slightly acidic environment (pH <6.5) the imidazole side chains of the histidine residues are protonated resulting in a net positive charge allowing for peptide internalisation. This acid-activated CPP may preferentially enter cancer cells in the acidic environment of a hypoxic tumour.

AGYLLGKINLKKLAKL(Aib)KKIL-[NH₂]

26

Aib = alpha-aminoisobutyric acid.

AGYLLGHINLHHLAHL(Aib)HHIL-[NH₂]

27

In 2003, the Tsein group described an elegant approach to targeting CPP activation with a modified CPP referred to as an ‘Activatable Cell Penetrating Peptide’ (ACPP) **28**.¹³⁸ This peptide consisted of a fluorescein labelled nona-arginine connected *via* a cleavable linker to nona-glutamate. This formed a peptide hairpin that was unable to internalise into cells, the nona-arginine was then released from the hairpin upon cleavage of the linker by a protease. After separation of the cleaved peptide, the nona-arginine was able to internalise into cells (Figure 1-8).

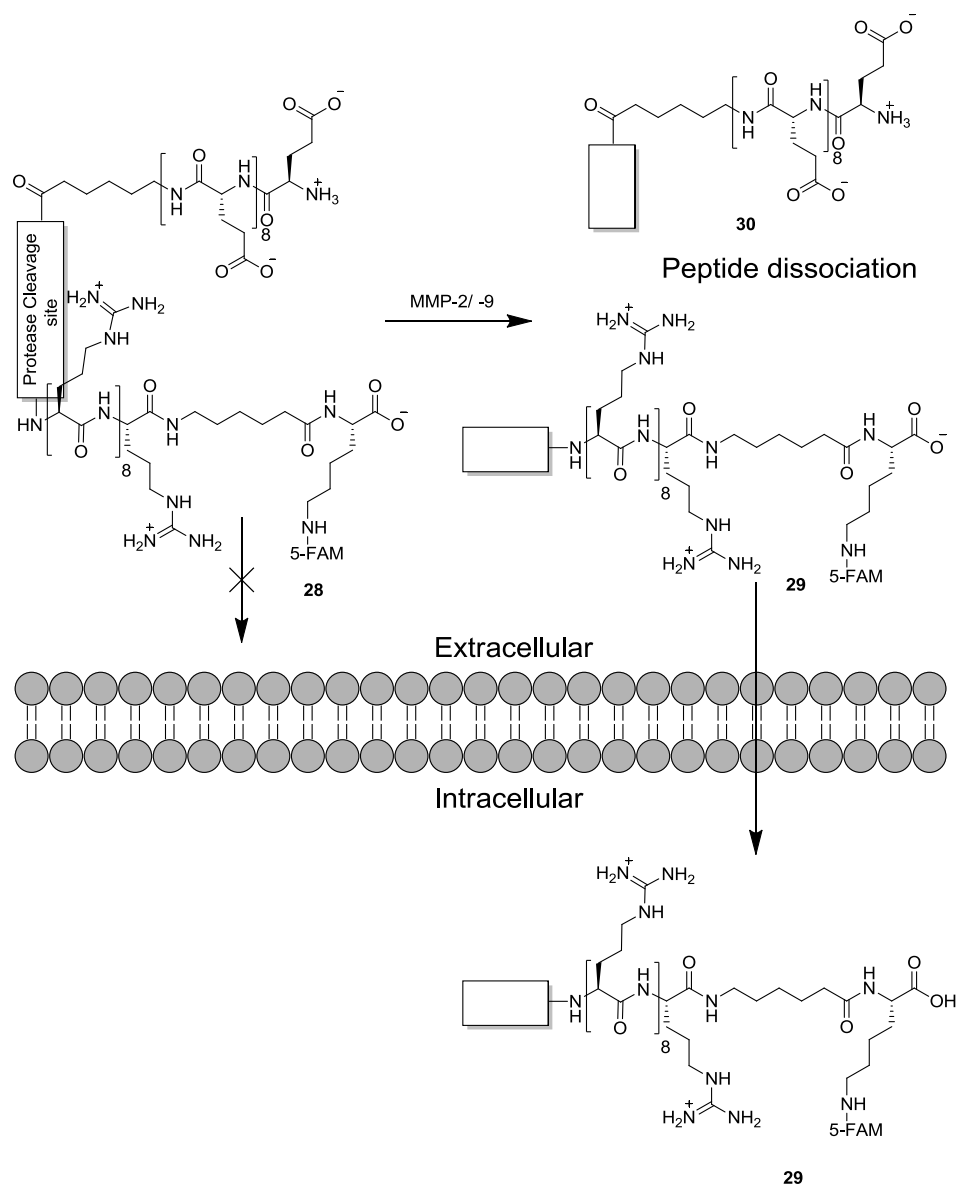


Figure 1-8: The activatable CPP (ACPP) **28** consists of nona-arginine linked to nona-glutamine via a proteolytic linker cleavable by the proteases MMP-2. In the uncleaved ACPP is unable to penetrate cells. The peptide is cleaved by matrix metalloproteinases-2 (MMP-2), which is over-expressed by several types of cancer cells. Cleavage results in the dissociation of the nona-glutamine peptide **30** from the nona-arginine **29**, thus allowing the nona-arginine **29** to internalise into the cancer cell.

The anionic and cationic peptides of ACPP **28** were linked together with the recognition sequence for matrix metalloproteinases-2 (MMP-2), an enzyme which is overexpressed by a variety of tumours and plays an important part in tumour invasion and metastasis.¹³⁹ Using a mouse xenograft model, the ACPP was shown to localise in a MMP-2 positive tumour to a greater extent than an ACPP containing a scrambled linker.¹³⁸ Additionally, Aguilera *et al.* (2009) demonstrated that *i.v.* injection of nona-

arginine in healthy mice resulted in localisation primarily around the injection site, which eventually re-distributed to the liver. In contrast, the ACPD was distributed uniformly in all tissues.¹⁴⁰ However, a recent study using a dual isotope labelled MMP-2 cleavable ACPD, allowing for discrimination between the uncleaved and cleaved peptide after *i.v.* administration in mice, demonstrated that activation of the ACPD was tumour-independent. The authors also suggested that tumour uptake of the ACPD is not a result of tumour specific activation but an effect of the increased permeability and tissue retention of the activated CPP and the 'leaky' vasculature of a tumour.¹⁴¹

Another interesting approach for the targeted activation of CPP intracellular delivery is based on tissue targeting using antibodies. In 2001, Liang *et al.* described a prodrug system for tissue specific delivery.¹⁴² This delivery system, called 'ATTEMPTS' (antibody targeted, [protamine] triggered, electrically modified pro-drug strategy) involves a tissue targeting component conjugated to heparin, for example a tissue specific antibody-heparin conjugate, and a drug component modified with a cationic peptide. The two components form an antibody-heparin/drug-peptide conjugate.¹⁴²⁻¹⁴³ This approach was successfully utilised for the site-specific delivery of plasminogen activators (tPA) by using an anti-fibrin IgG to target blood clots. Upon administration of protamine, an FDA approved antidote for heparin, the tPA was released from the complex by protamine displacing the cationic peptide to form a protamine/heparin complex. Interestingly, Kwon *et al.* (2008) applied the core principle of ATTEMPTS to Tat mediated intracellular delivery of macromolecules.¹⁴⁴ The authors demonstrated that Tat mediated internalisation of the enzyme Asparaginase (*E.C.* 3.5.1.1, ASNase) could be inhibited by forming an ASNase-Tat/heparin complex. The addition of protamine then released the ASNase-Tat allowing for intracellular delivery of the enzyme (Figure 1-9).¹⁴⁴⁻¹⁴⁵

1) Administration of
mAb-Heparin/CPP-Cargo complex

2) Administration of Protamine
and displacement of CPP

3) Internalisation of
CPP-cargo

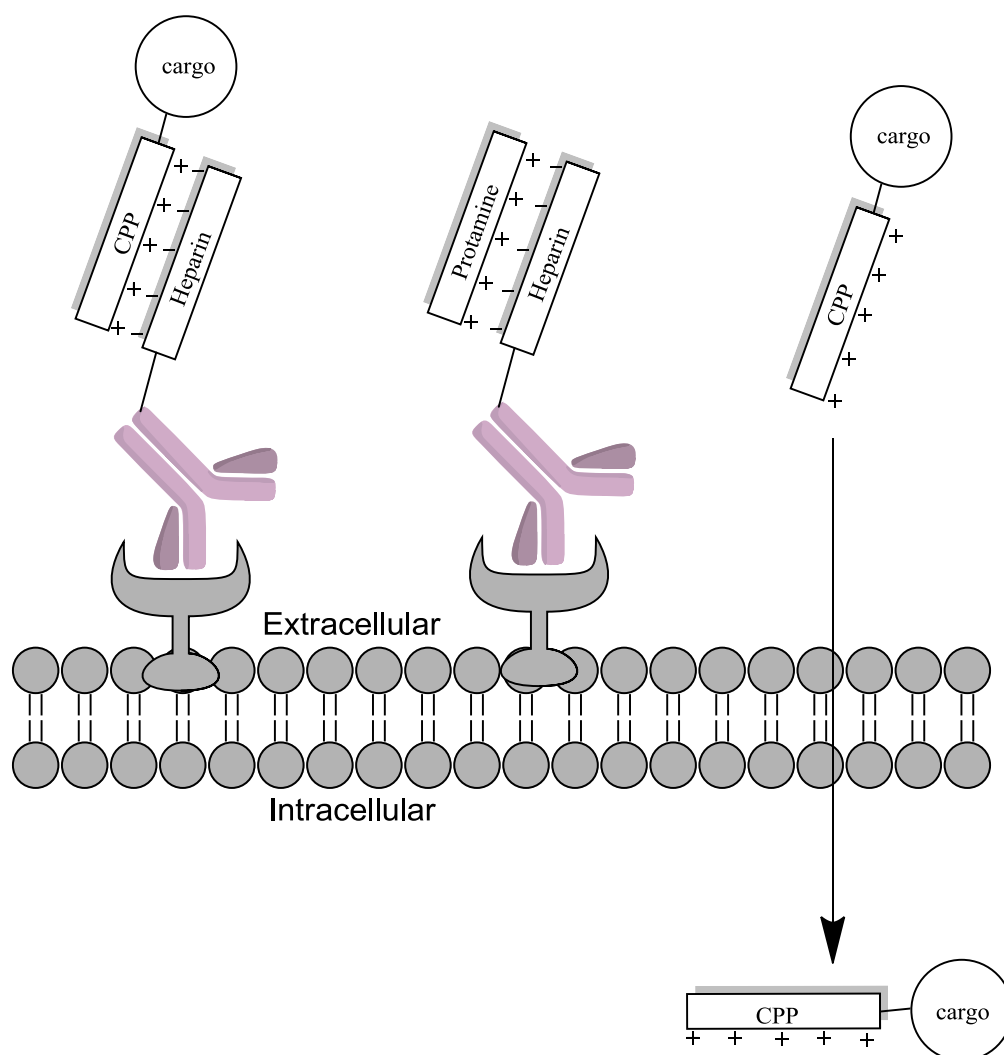


Figure 1-9: The principle of targeted CPP mediated delivery using the ATTEMPTS approach i) the targeting antibody-heparin conjugate is administered as a complex with the CPP-cargo conjugate ii) protamine is then administered and competes with the CPP-cargo for binding to heparin, resulting in the displacement of the CPP-cargo at the target site iii) the released CPP-cargo is then free to internalise into the cell.¹⁴⁴

This proof-of-principle study illustrates that the core concept of ATTEMPTS can be used to target the Tat-mediated intracellular delivery of macromolecules. This concept would allow for site-specific activation of TAT-cargo conjugate, reducing the non-specific interactions of CPPs seen *in vivo*. To date, the *in vivo* application of this system has not been reported, nevertheless, this novel approach to tissue targeting of a CPP-cargo conjugate looks promising.

A novel and simple alternative to the aforementioned approaches would be to individually mask the cationic side-chains of a CPP with hydrolytically or catalytically labile protecting groups. This could be achieved by using established prodrug moieties used for the masking of amines and guanidine functional groups.¹⁴⁶⁻¹⁴⁷ A generic approach to CPP activation based on peptide deprotection by hydrolysis or serum esterase activity could increase circulation time allowing for higher organ uptake and lower uptake by peripheral tissues. This concept will be explored in detail later in this thesis.

1.5 Making Transbodies

The approach taken for the preparation of an antibody-CPP is an important step for the successful use of the transbody. Any limitation in the ability to produce useful quantities of active transbodies could significantly hinder the optimisation stages. Furthermore, the many variables that can influence the cellular penetration of a CPP and attached cargo must also be taken into account.

The preparation of a transbody is generally achieved either by genetic fusion of a CPP to an antibody fragment to allow for expression of an antibody-CPP fusion protein, or by chemical conjugation of a CPP to give an antibody-CPP conjugate (see Table 1-1).

Synthetic IgGs and antibody fragments are generally produced by expression in a biological system. The expression system used is extremely important and often a limiting factor for the preparation of antibody reagents. The expression of IgGs is most suited to mammalian expression systems. The size, complexity and mammalian origin of IgGs make them difficult to express in bacterial systems. The expression of IgGs in Chinese Hamster Ovary cells (CHO) is now a well-established method.¹⁴⁸

In contrast, the relative simplicity of antibody fragments, e.g. scFv, makes bacterial systems most convenient for expression. *E. coli* is the most commonly used system because of its well characterised genetics and relatively low cost. There are many approaches for the expression of scFv in *E. coli*. The expression of an antibody fragment in the reducing environment of the *E. coli* cytoplasm often results in the formation of inclusion bodies. However, refolding of proteins from isolated inclusion

bodies is possible.¹⁴⁹ Alternatively, the use of engineered *E. coli* strains that possess an oxidising cytoplasmic environment and overexpressed molecular chaperones have been shown to increase the expression of antibody fragments.¹⁵⁰ Often the favoured approach is directing scFv to the oxidising periplasmic space by addition of a leader sequence such as, *PelB* to the *N*-terminus of the protein construct. Using this approach, yields in the range of 0.2-20 mg/L culture of active scFv can be achieved.¹⁵¹⁻¹⁵² However, expression yields have been shown to be related to primary sequence, thus meaning expression levels often vary between different scFvs.¹⁵³

The vast majority of CPP fusion proteins have been expressed in *E. coli* systems. Recently, the development of a mammalian system for the expression of CPP fusion proteins has also been described.¹⁵⁴⁻¹⁵⁵ However, Shaw *et al.* (2008) noted that with increasing cationic charge of the CPP the yield and secretion of the CPP fusion protein was greatly reduced.¹⁵⁵ Therefore, this approach may be less suitable for the highly cationic CPPs, such as poly-arginine and Tat.

Although there are many examples of CPP fusion proteins, this approach limits the range of CPP modifications that are possible. For example, regioselective labelling of a CPP with fluorescent probes or the incorporation of non-canonical amino acids would be difficult to achieve.

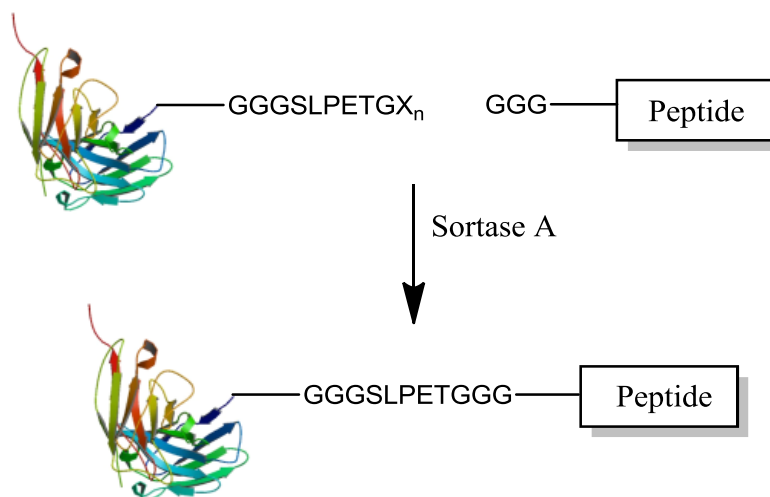
1.5.1 Chemical conjugation of CPPs to antibodies

Chemical conjugation offers an attractive alternative to fusion proteins. However, an inherent difficulty associated with chemical conjugation is the control of stoichiometry and site of conjugation. These are important variables that must be controlled to avoid any detrimental effects to protein activity. The ϵ -amine of lysine residues is frequently used for the conjugation of fluorescent probes.¹⁵⁶ However, the abundance of lysine residues in many proteins makes site-specific conjugation difficult.

An interesting approach to achieve site-specific modification of proteins was developed by Mao *et al.* (2004). The authors described the application of the transpeptidase Sortase A (SrtA) for the site-specific ligation of a selection of peptides

to Green Fluorescent Protein (GFP).¹⁵⁷ Scheme 1-1 illustrates the protein-peptide ligation catalysed by SrtA.

Scheme 1-1: Sortase A catalysed protein-peptide conjugation



SrtA catalysed ligation is achieved by introduction of the recognition sequence LPETGX_n to the protein and GGG to the peptide. SrtA can then catalyse the formation of an amide bond between these two substrates, and expelling GX_n.¹⁵⁷ Interestingly, SrtA was able to catalyse the ligation of (D)-peptides, synthetic branched peptides and small molecules possessing the SrtA recognition sequence to the C-terminus of a recombinant protein.¹⁵⁷

Alternatively, site-specific protein modifications can be achieved by introducing chemically modified amino acids as bioorthogonal handles to a protein. In principle, the two reactive components are required to be mutually reactive to each other but inert to the remaining functional groups present in the protein.¹⁵⁸ By using an *E. coli* methionine auxotroph, amino acids possessing bioorthogonal moieties, such as alkenes and azides, have been incorporated into proteins.¹⁵⁹ Functional groups can also be introduced by chemical or enzymatic methods.¹⁵⁸

One of the most promising functional groups for protein-peptide conjugation is the azide moiety. The reaction of an azide with an alkyne moiety in the presence of Cu^(I) by a Huisgen-[3+2]-cycloaddition results in the formation of a non-reversible 1,2,3-triazole linkage.¹⁵⁸ Recently, copper-free strain-promoted alkyne-azide cycloaddition

has also been described for the modification of proteins, thus avoiding the use of copper (Figure 1-10).¹⁶⁰

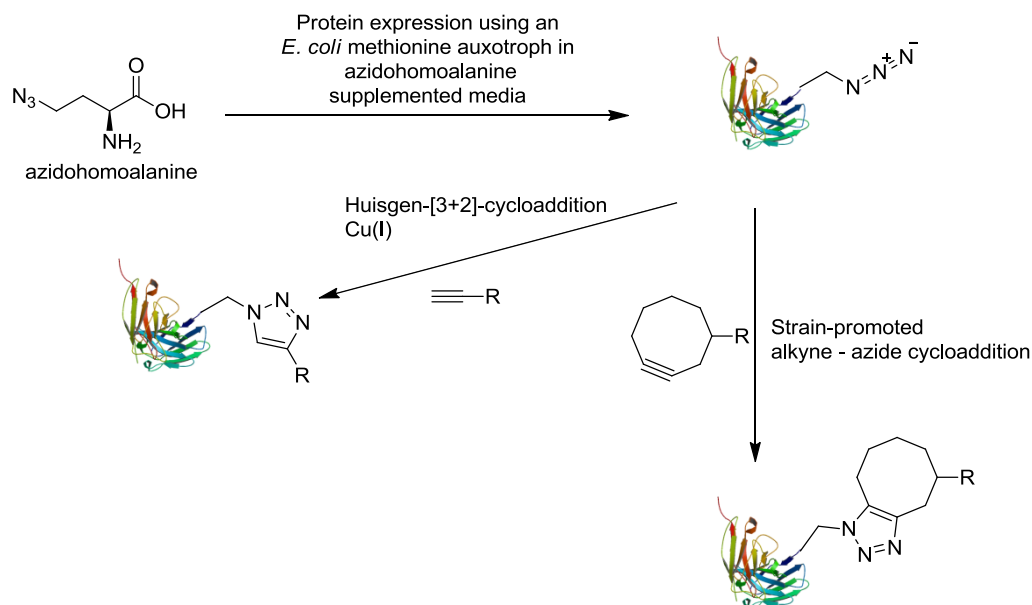


Figure 1-10: Protein-peptide conjugation by either Cu(I) catalysed Huisgen-[3+2]-cycloaddition or copper-free strain-promoted alkyne-azide cycloaddition.

An established approach for the site-specific modification of proteins is achieved by the introduction of an unpaired cysteine to the protein construct. The cysteine residue can then be modified using thiol reactive groups. Generally, native cysteine residues are involved in disulfide bonds and buried within the centre of the protein, thus making it possible to site-specifically label an unpaired cysteine residue. Commonly used thiol reactive groups for protein-peptide conjugation are illustrated in Figure 1-11.

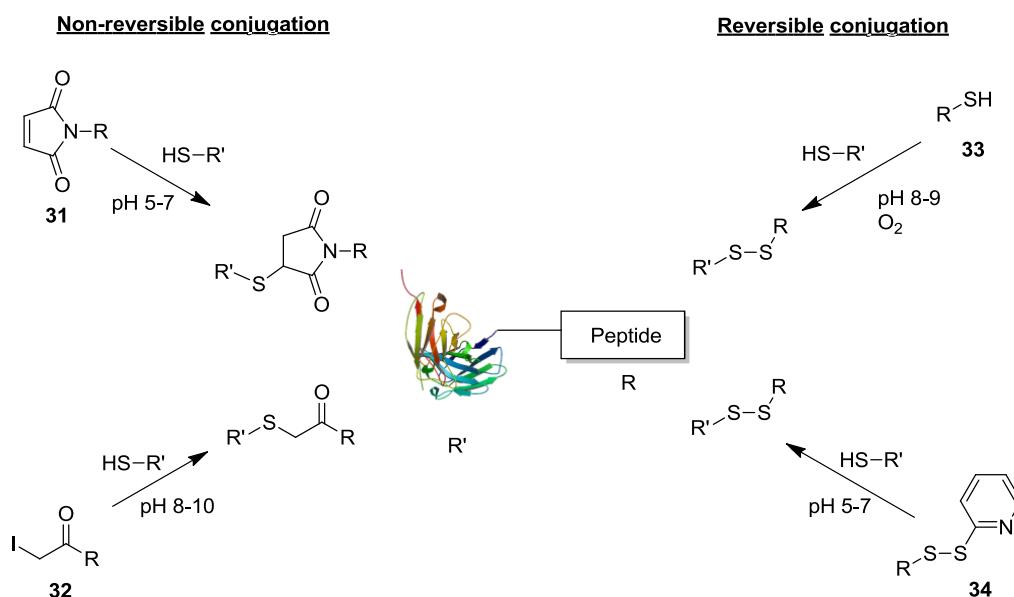
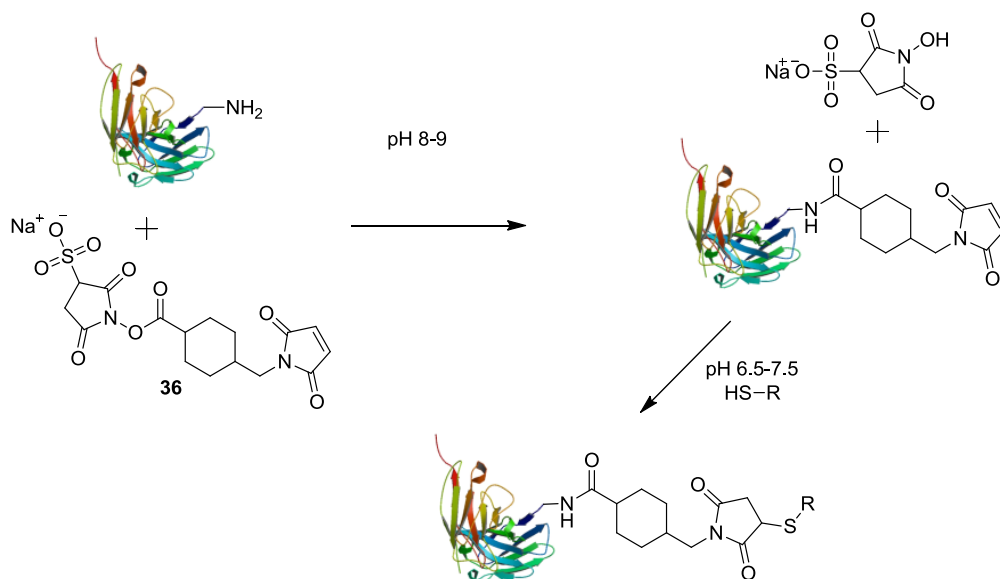


Figure 1-11: A selection of thiol reactive groups commonly used for protein-peptide conjugation. These include the maleimido **31**, iodoacetyl **32**, free thiol **33** pyridyl disulfide **34** moieties.

The thiol-reactive maleimido **31** and iodoacetyl **32** groups are commonly employed for thiol-specific peptide-protein conjugation.¹⁶¹ In slightly alkaline conditions (pH 7.5-9.0) a thiol reacts with the iodoacetyl moiety *via* a S_N2 reaction to form a thioether bond. At lower pH the iodoacetyl group are able to react with imidazolyl, methionine and primary amines.¹⁶¹ In contrast, the maleimido moiety reacts with a thiol in slightly acidic conditions (pH 5-7). The reaction of a thiol with the unsaturated imide of a maleimido moiety *via* a Michael addition forms a thioether bond. At more alkaline pH, reactivity towards primary amines increases.¹⁶¹

The maleimido group is a well-established thiol reactive group for protein-peptide and protein-protein conjugation. There are a number of heterobifunctional cross-linking reagents possessing maleimido moieties that are commercially available. Two established heterobifunctional reagents for protein conjugation are succinimidyl-4-*N*-(maleimidomethyl)cyclohexane-1-carboxylate (SMCC) **35** and the water soluble sulfo-SMCC derivative **36**.¹⁵⁶ These two reagents have found wide application for the preparation of protein-protein and protein-peptide conjugates. The NHS ester moiety can be used to react with primary amines of a protein, allowing for conjugation of a sulfhydryl to the maleimido moiety (Scheme 1-2).

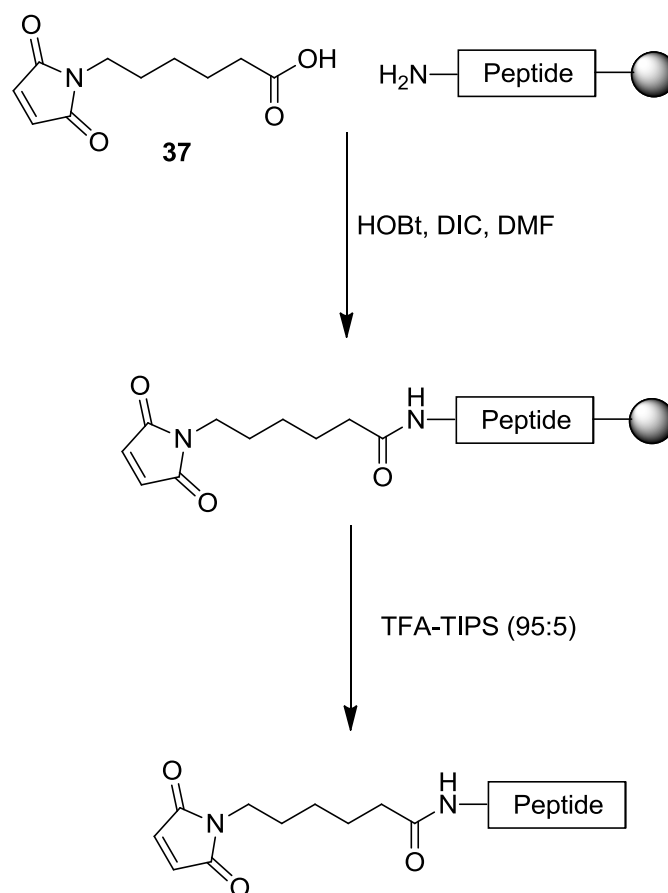
Scheme 1-2: Protein modification using succinimidyl-4-*N*-(maleimidomethyl)cyclohexane-1-carboxylate (SMCC) **36**.



Alternatively, a robust method for protein-peptide conjugation is the application of maleimido functional peptides. This approach allows for easy characterisation of the maleimido functional group introduced to the peptide and purification using HPLC. This can be difficult if the maleimido moiety is introduced to the protein.

There have been a number of approaches described for the synthesis of maleimido functional peptides.¹⁶²⁻¹⁶⁴ A simple and robust approach using Fmoc solid-phase peptide synthesis (Fmoc SPPS) is described by Hansen *et al.* (1998).¹⁶³ The authors described the introduction of 6-maleimidohexanoic acid **37** to the *N*-terminus of a peptide by carboxyl activation of acid with the coupling reagent HOBt and *N,N'*-diisopropylcarbodiimide (DIC).¹⁶³ Cleavage of the peptide from the resin is then achieved using TFA and the scavenger triisopropylsilane (TIPS) to afford the desired *N*-maleimido peptide in high purity (Scheme 1-3). This approach provides a maleimido functionalised peptide that can then be conjugated to a protein possessing an unpaired cysteine residue.

Scheme 1-3: Synthesis of maleimido functionalised peptides.¹⁶³



The maleimido moiety, although utilised extensively for site-specific protein-peptide conjugation, is limited by the irreversible nature of the conjugation. Furthermore, there are only two sites that can be functionalised, the nitrogen and the unsaturated imide, thus limiting the conjugation to only two components.

Recently, Tedaldi *et al.* (2009) and Smith *et al.* (2010) reported the development and application of mono-bromomaleimide **38** and di-bromomaleimide **39** as a reversible and selective reagent for the modification of sulfhydryls.¹⁶⁵⁻¹⁶⁶ These maleimide derivatives allow for both reversible and non-reversible protein-peptide conjugation and possess three points of functionalisation (Figure 1-12).

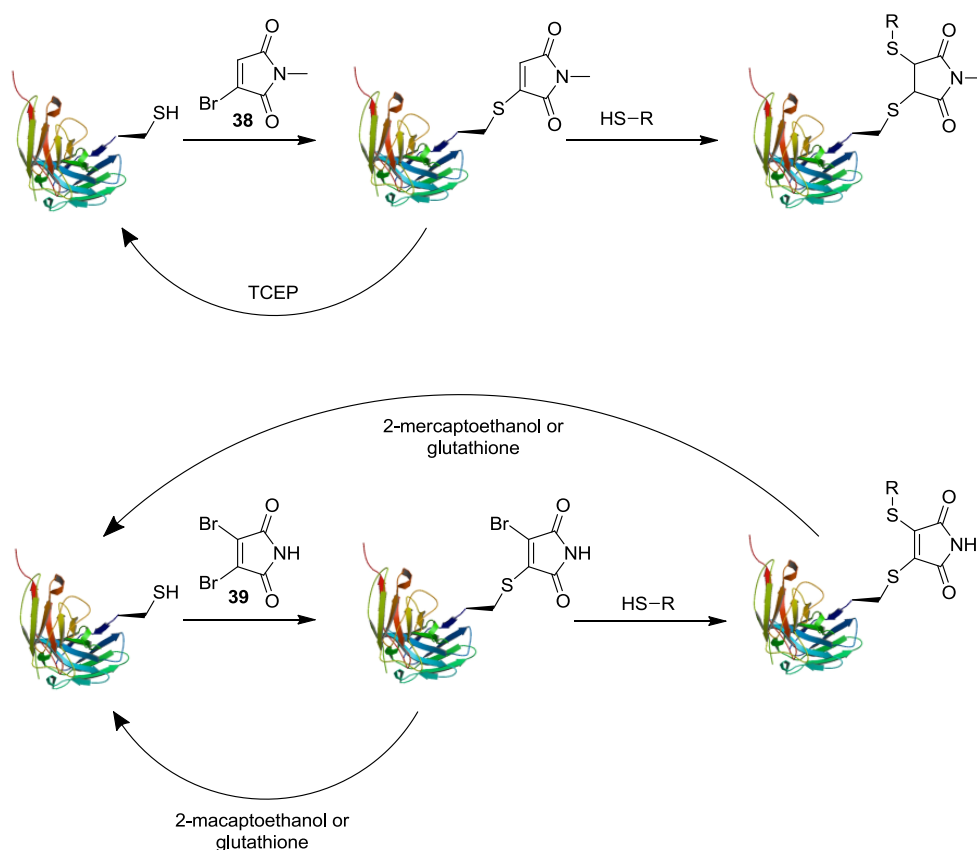


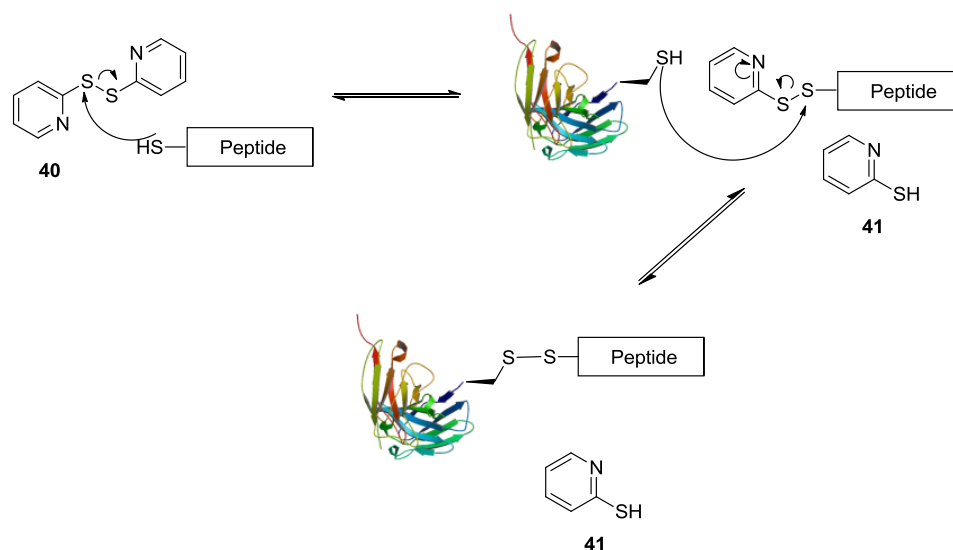
Figure 1-12: Modification of a protein using either mono-bromomaleimide **38** or di-bromomaleimide **39** allowing for conjugation of a second molecule that possesses a sulfhydryl moiety to the protein. The reaction can be reversed using the reducing agents TCEP, 2-mercaptoethanol or glutathione.

Both bromomaleimides **38** and **39** present a versatile alternative to the established maleimido moiety. The ability to reverse the conjugation using reducing agents allows for regeneration of the starting unconjugated protein. In a cellular context, this may also allow for dissociation of the conjugate in the reducing intracellular environment.¹⁶⁶

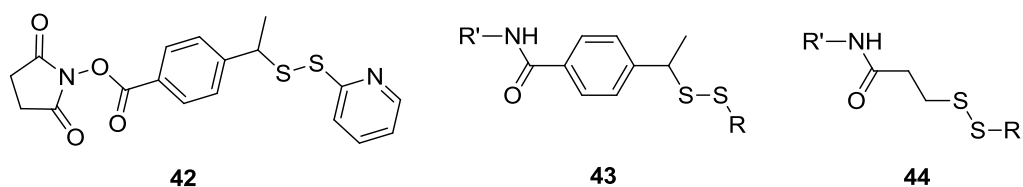
Alternatively, conjugation *via* a disulfide bond between an unpaired cysteine residue and a peptide possessing a sulfhydryl allows for reversible protein-peptide conjugation. Disulfide bonds can be formed by oxidation of two thiols without the use of any activating agents. The disadvantage of this approach is the generation of homodimers. To overcome this, disulfide exchange functional groups can be used such as, pyridyl disulfides.¹⁶¹⁻¹⁶⁷ An established method to achieve this is using 2-dithiodipyridine **40**. Initially, the free sulfhydryl of one of the components (i.e. the peptide) is activated with **40** in a disulfide exchange eliminating 2-mercaptopyridine **41** and forming the pyridyl disulfide intermediate. This mixed disulfide is then

susceptible to further disulfide exchange with another sulfhydryl-containing molecule. The addition of the second component (i.e. protein) possessing a sulfhydryl will then furnish the desired conjugate *via* a disulfide linkage (Scheme 1-4).

Scheme 1-4: Protein-peptide conjugation using 2-dithiodipyridine **40** *via* a mixed disulfide mechanism.



The stability of a disulfide linkage can also be increased by using hindered disulfide bonds, which can alter the rate of conjugate dissociation *in vivo*. Thorpe *et al.* (1987) demonstrated this by developing the heterobifunctional cross-linking reagent 4-succinimidylloxycarbonyl- α -methyl- α -(2-pyridyldithio)toluene (SMPT) **42** for the preparation of immunotoxin conjugates.¹⁶⁸ The immunoconjugate possessing the hindered disulfide linkage **43** possessed an *in vivo* half-life of 22 h, which was approximately twice as long as an unhindered disulfide **44**. The use of similarly hindered disulfide linkages may also be important for the *in vivo* application of antibody-CPP disulfide linked conjugates.



The chemical conjugation of a CPP offers greater flexibility for modification to the CPP and also the nature of the protein-CPP conjugation compared to CPP fusion proteins. Furthermore, it is important to consider the variables that are involved when

utilising CPPs for intracellular delivery of proteins. Thus, utilisation of the appropriate techniques to prepare antibody-CPP conjugates is paramount to the successful therapeutic application of transbodies.

1.6 Research aims and objectives

Transbodies hold the potential for the modulation of almost any intracellular target. This thesis aims to develop a systematic approach to modifying antibody reagents to enable the cell penetration and inhibition of an intracellular protein-protein interaction.

As discussed in this chapter there are a number of obstacles associated with using CPPs for the delivery of antibodies and antibody fragments into cells. There are three key requirements that need to be addressed for transbodies to be successfully used as therapeutic molecules:

- i) Efficient intracellular delivery of attached antibody fragment.
- ii) Delivery of the antibody fragment into the correct cellular compartment allowing for target inhibition.
- iii) An antibody-CPP conjugate possessing *in vivo* properties that allow for therapeutic quantities to reach target tissues.

The intracellular delivery of antibody fragments can be achieved using CPPs, however, endosomal entrapment is an inherent issue in this delivery approach. Additionally, the cationic charge of a CPP is required for activity but is also responsible for the non-specific, wide-spread tissue uptake seen *in vivo*, thus rendering CPP-mediated cargo delivery unsuitable for many therapeutic applications.

It is the major goal of this project to address some of these issues, to obtain insight into how antibody fragments can be modified with CPPs to possess cell penetrating capabilities, whilst possessing suitable *in vivo* properties. This thesis focuses on developing methodologies for systematic modification of antibody fragments.

The objectives of this thesis are;

1. Isolation of scFvs that inhibit a model intracellular protein-protein interaction.
 - ❖ It is proposed that by screening a naïve scFv library using antibody phage display it will be possible to identify scFvs that are specific and neutralising to the anti-apoptotic protein Bcl-2.
2. Investigate the use of CPPs to achieve intracellular delivery of neutralising anti-Bcl-2 scFvs into the cytoplasm to induce a biological response.
 - ❖ Develop a systematic approach for the comparison of different CPPs and for the optimisation of scFv internalisation.
 - ❖ Develop methodology to allow for the robust and reproducible production of a panel of scFv-CPP conjugates.
3. Investigate novel methods to modify the properties of cationic CPPs to improve *in vivo* properties.
 - ❖ Inhibit the internalisation of a CPP by protecting individual guanidinium moieties.
 - ❖ Develop a protection strategy for the guanidinium moieties of a CPP that can be catalytically/hydrolytically removed, allowing for controlled release of CPP activity.

The first stage of this study is the isolation of single chain variable fragments (scFv) that are specific and neutralising towards the anti-apoptotic protein Bcl-2, which is involved in the intrinsic apoptotic pathway. Overexpression of Bcl-2 is associated with a variety of cancers. Moreover, Bcl-2 is a well-characterised protein with a number of small molecule Bcl-2 inhibitors being reported. Bcl-2 inhibits the onset of apoptosis by forming heterodimers with pro-apoptotic members of the intrinsic apoptotic pathway. It is this clinically relevant, but well characterised protein-protein interaction that will be the model therapeutic target in this project.

Following the initial phase of this project, the main aim is to develop a systematic approach to modifying anti-Bcl-2 scFvs to possess cell penetrating capabilities using CPPs. Concurrent, development of a novel approach to modulate the *in vivo* properties and cellular internalisation of a CPP is also undertaken.

Thus, it is anticipated that this thesis will provide a general approach for the modification of a scFv to enable cellular penetration and inhibition of an intracellular PPI, whilst retaining therapeutically desirable *in vivo* properties.

Isolation of neutralising single chain antibodies specific to Bcl-2

The first stage of this study is the isolation of single chain variable fragments (scFvs) that are specific and neutralising towards a model intracellular protein-protein interaction. It was proposed that the anti-apoptotic protein Bcl-2 would be an ideal model target due its clinical relevance, extensive characterisation and the availability of small molecule Bcl-2 inhibitors, which will allow comparison of neutralising anti-Bcl-2 scFv with established data.

2.1 Bcl-2 - The model target

Apoptosis, or programmed cell death is vital for tissue homeostasis and protection from cytotoxic insults. Apoptosis is regulated by two main signalling cascades; the extrinsic and intrinsic apoptosis pathways. The extrinsic pathway is activated by ligand binding to cell surface receptors in the tumour necrosis factor (TNF) receptor family. This activates caspase-8, which then activates the downstream ‘effector caspases’, caspase-3, -6 and -7.¹⁶⁹ These caspases initiate cellular destruction, which eventually leads to apoptosis.¹⁶⁹ The intrinsic pathway is activated by developmental cues and cytotoxic insults, such as DNA damage and growth factor deprivation. This

pathway is regulated by members of the Bcl-2 protein family.¹⁶⁹⁻¹⁷⁰ The deregulation of the intrinsic apoptosis pathway is a critical step in tumour development.²

Bcl-2 is the founding member of the Bcl-2 family. All Bcl-2 family members have one of four regions of homology with Bcl-2, termed the Bcl-2 homology domains (BH1-4).¹⁶⁹ There are three subtypes of the Bcl-2 family, the pro-apoptotic, anti-apoptotic and the BH3-only proteins.¹⁶⁹⁻¹⁷⁰ The pro-apoptotic proteins BAX, BAK and BOK induce mitochondrial outer membrane permeabilisation resulting in the release of cytochrome c and subsequent activation of apoptosis. Figure 2-1 illustrates the extrinsic and intrinsic apoptosis pathways.

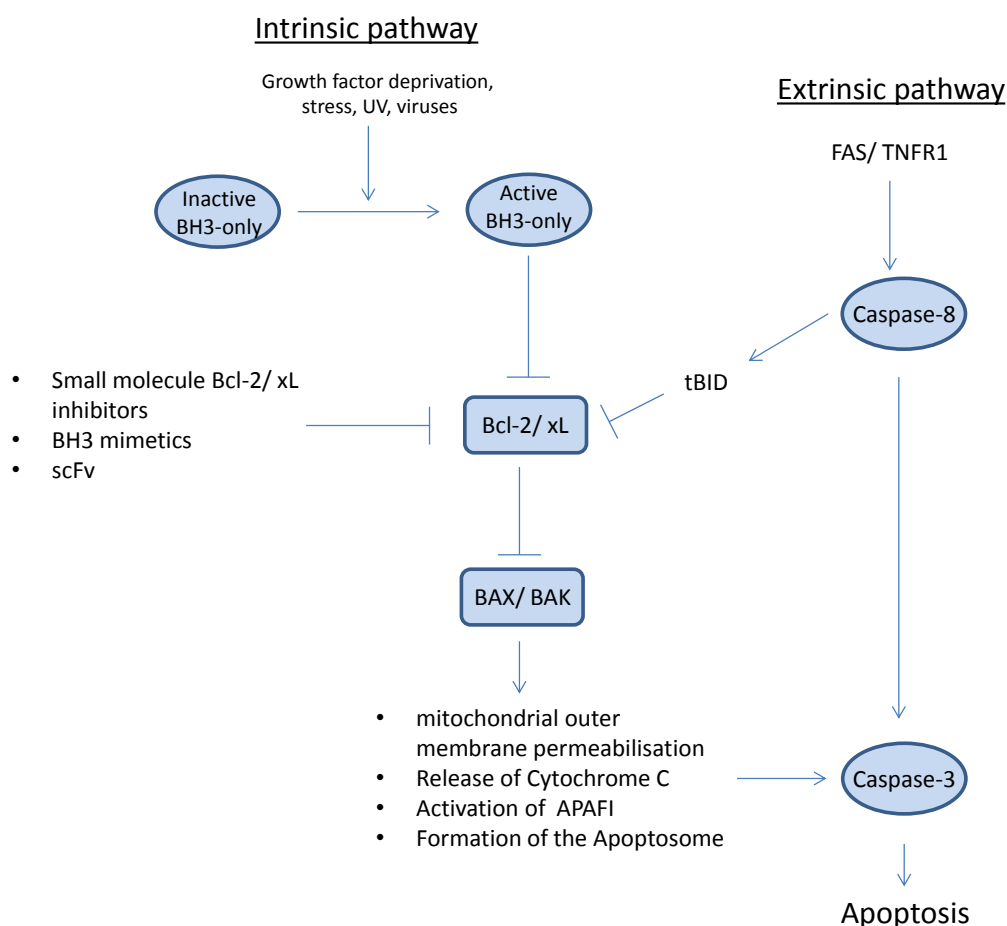


Figure 2-1: The intrinsic and extrinsic apoptosis pathways. In healthy cells Bcl-2/xL forms a heterodimer with BAX or BAK stopping the activation of apoptosis. Activation of the BH3-only proteins by cellular stress leads to displacement of Bcl-2/xL from the dimer allowing for BAX or BAK to initiate the onset of apoptosis. Overexpression of Bcl-2/xL deregulates this pathway. Bcl-2/xL inhibitors act by inhibiting Bcl-2/xL heterodimer formation with BAX and BAK. The figure is modified from Youle *et al.* (2008).¹⁷⁰

Heterodimerisation between the pro-apoptotic proteins and the anti-apoptotic proteins, such as Bcl-2, Bcl-xL, Bcl-w, Mcl-1, Bcl-B and A1, stops the pro-apoptotic proteins activating apoptosis.¹⁶⁹⁻¹⁷⁰ It is the balance between heterodimer and free pro-apoptotic protein that determines activation of apoptosis.¹⁶⁹⁻¹⁷⁰ A further level of control is provided by the BH3-only proteins, such as BAD, BIK, BID, HRK, BIM, BMF, NOXA and PUMA. Upon cytotoxic insult the expression and post-translational modification of the BH3-proteins is up-regulated, allowing binding to the anti-apoptotic proteins and competing with the pro-apoptotic proteins. This results in an increase in free pro-apoptotic proteins and subsequent activation of apoptosis.

The BH1, 2 and 3 domains of the anti-apoptotic proteins fold into a globular domain forming a hydrophobic groove displayed on the surface of the protein. The amphiphilic α -helical BH3 region of the pro-apoptotic and BH3-only proteins fit into this groove.¹⁷¹ Figure 2-2 shows the crystal structure of Bcl-xL in complex with the BH3 region of the pro-apoptotic protein BAK.

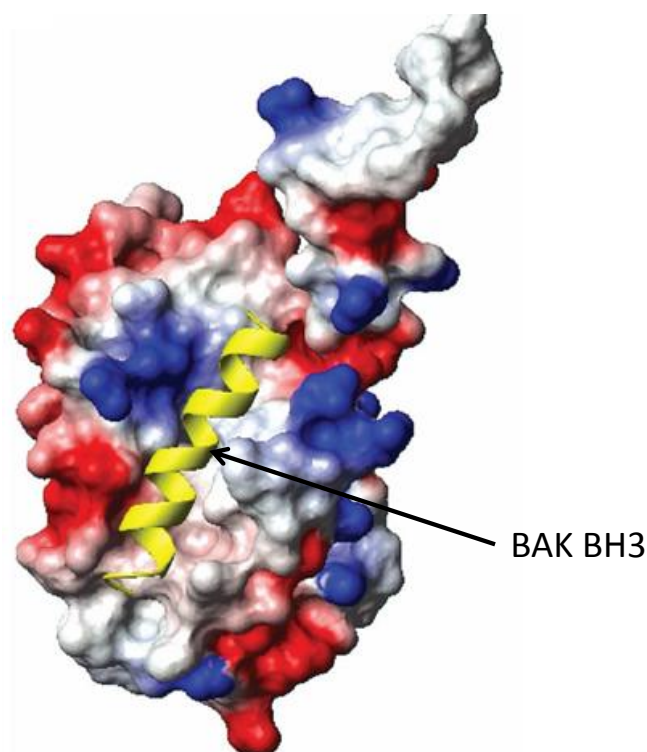
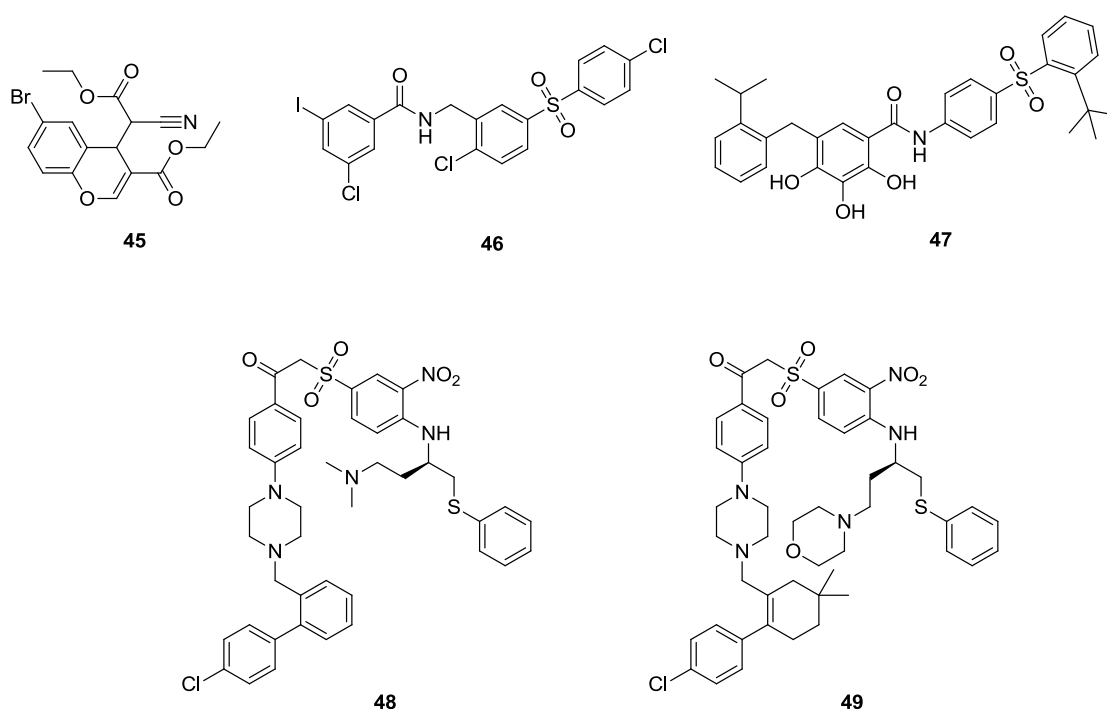


Figure 2-2: Surface representation of the BAK BH3/ Bcl-xL interaction, modified from Ji *et al.* (2006).¹⁷²

The overexpression of the anti-apoptotic proteins is a critical step in tumour development. Overexpression inhibits the onset of apoptosis allowing for the survival of cells possessing other oncogenic mutations.² Bcl-2 and Bcl-xL are overexpressed in a wide range of cancers, for example follicular lymphoma, leukaemia, lung and breast cancer.¹⁶⁹⁻¹⁷⁰

The importance of Bcl-2 and Bcl-xL in tumour development has led to extensive research into the design of Bcl-2 and Bcl-xL inhibitors that induce apoptosis in cancer cells relying on overexpression of Bcl-2/xL for survival. The hydrophobic groove of Bcl-2 and Bcl-xL is often the target for the rational design of small molecule inhibitors and BH3 peptide mimetics. A number of small molecule Bcl-2 inhibitors have been developed, for example HA14-1 **45**¹⁷³, BH3I-2s **46**¹⁷⁴, and TW-37 **47**.¹⁷⁵ One of the most promising Bcl-2 inhibitors is ABT-737 **48** and the next generation bioavailable derivative ABT-263 **49**, which is currently in phase I clinical trials.¹⁷⁶⁻¹⁷⁷



BH3 peptides have also been used to inhibit Bcl-2 and Bcl-xL. The application of BH3 peptides has mostly been limited to diagnostic purposes in studies investigating key members of the intrinsic apoptosis pathway. However, there are several examples of BH3 peptides being developed for therapeutic purposes. Notably, Walensky *et al.* (2004) reported a novel approach to using BH3 peptides for inhibition of Bcl-xL by

developing a ‘stapled’ BH3 helix that displayed improved stability and affinity to Bcl-xL.¹⁷⁸ The stapled BH3 helix also possessed cell penetrating capabilities.¹⁷⁸⁻¹⁷⁹ The use of CPPs to mediate the intracellular delivery of BH3 peptides has also been reported.¹⁸⁰⁻¹⁸¹

The role of Bcl-2 and Bcl-xL in deregulating the intrinsic apoptotic pathway is well characterised, and a number of small molecule Bcl-2/xL inhibitors have been reported. Thus, it is expected that scFv that bind to Bcl-2 and/or Bcl-xL and inhibit dimer formation with the pro-apoptotic proteins will induce apoptosis in the same manner as the small molecule Bcl-2/xL inhibitors.

2.2 Isolation of anti-Bcl-2 and Bcl-xL scFv using antibody phage display

It was predicted that by screening naïve scFv phage display libraries for scFv specific for Bcl-2 and Bcl-xL it would be possible to identify scFvs that inhibit Bcl-2 and Bcl-xL binding to the pro-apoptotic proteins.

Phage display has proven to be a powerful technique for the isolation of antibodies. The introduction of scFv-encoding DNA to the *N*-terminal region of a phage coat protein gene results in the expression of a scFv-coat protein fusion, resulting in presentation of the scFv on the surface of the phage particle.¹⁸² This effectively links the genotype with the phenotype of the antibody fragment. Using this approach, antibody libraries of naïve or immune origin (ideally containing 10^9 - 10^{11} clones) can be cloned into the phage genome to afford an antibody phage display library.¹⁸³

Commonly, M13 filamentous bacteriophage is used for antibody phage display.³⁰ This bacteriophage infects *E. coli* and replicates using the host DNA replication machinery. The phage genome is a single-stranded DNA molecule of approximately 6,400 nucleotides and consists of 11 genes, 5 of which are coat proteins.³⁰ Each phage particle comprises of approximately 2700 copies of the major coat protein pVIII, and 5 copies each of coat proteins pIII, pVI, pVII and pIX, which form the tips of the phage particle.³⁰ Insertion of scFv-encoding DNA to the *N*-terminal region of the *pIII* gene results in the scFv being expressed as a fusion with the coat protein (Figure 2-3).³⁰

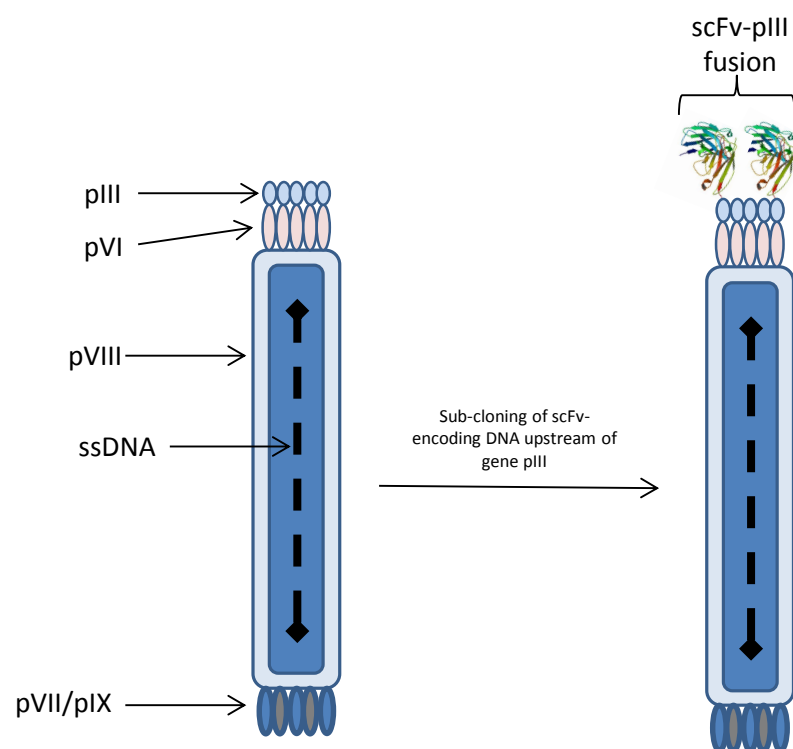


Figure 2-3: M13 phage structure; the phage particle consists of 5 coat proteins, pIII, pVI, pVII, pVIII and pIX. The sub-cloning of scFv-encoding DNA upstream of the *pIII* gene results in the presentation of the scFv on the surface of the phage particle upon assembly as a pIII-scFv fusion protein.

For the generation of a scFv phage library, the application of a phagemid is generally favoured. A phagemid is a plasmid that contains an *f1* origin of replication, phage coat protein gene and antibiotic resistance gene.³⁰ *E. coli* containing a phagemid requires infection with a helper phage to supply the phage genes required for phage assembly and packaging of the phagemid within the phage particle.³⁰ The application of phagemids for scFv phage display allows for a large scFv phage display library to be created.^{30,184}

Many techniques used for probing scFv libraries involve the immobilisation of the target antigen, thus allowing for isolation of the antigen/phage complexes from the non-specific scFv-phage contained in the library. An established selection technique is soluble selection using streptavidin coated magnetic beads and biotinylated antigen.³¹ Figure 2-4 outlines the principle of soluble selection of scFv from a phage display library.

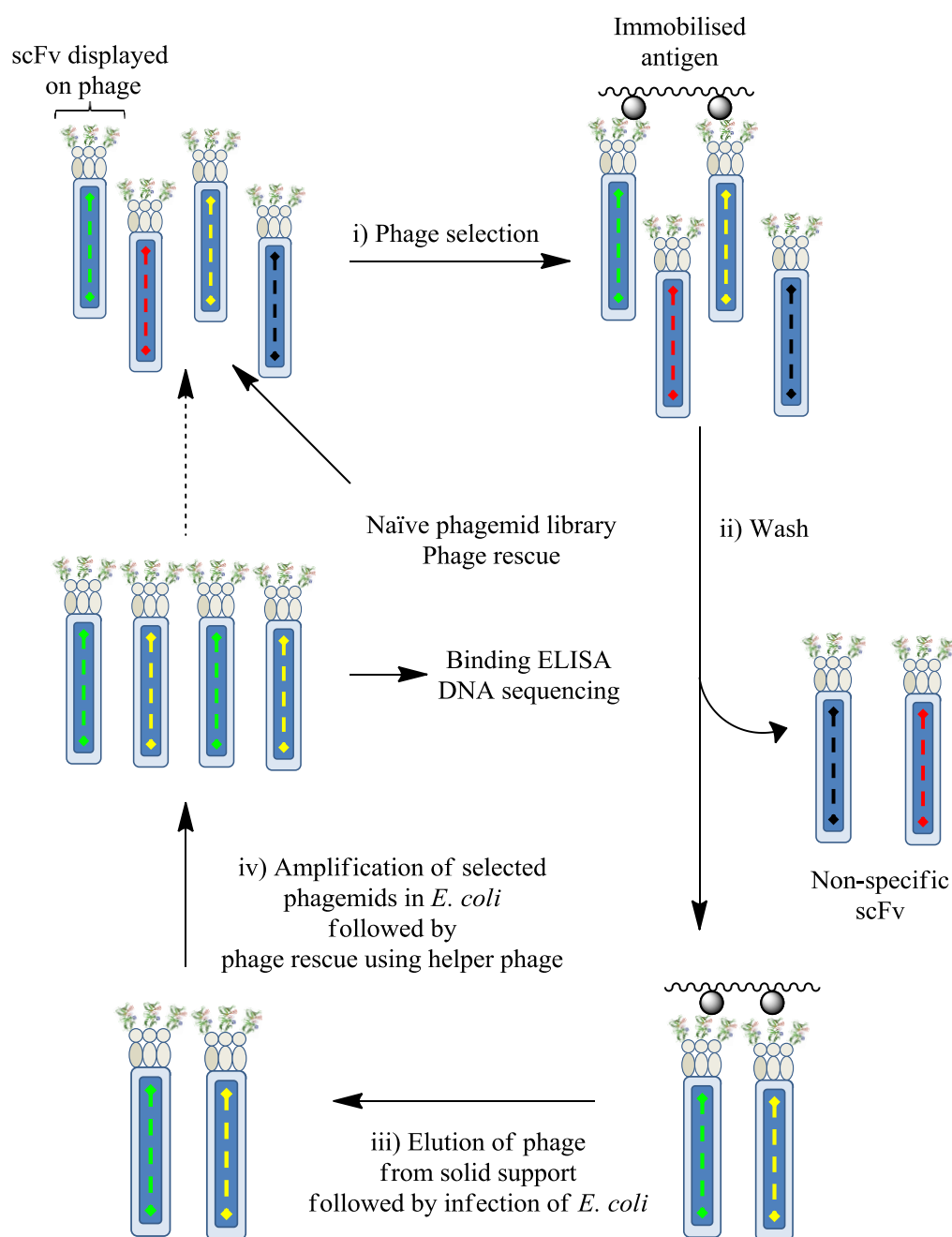


Figure 2-4: Process of soluble selection of scFv using a naïve phage display library

It was proposed that neutralising anti-Bcl-2 and anti-Bcl-xL scFv could be identified by soluble selection of anti-Bcl-2 and anti-Bcl-xL scFv from a naïve scFv phage display library, followed by screening of the enriched libraries using a competition assay for the Bcl-2/xL interaction with a BH3 peptide.

Additionally, the screening of naïve libraries for scFv that are cross-selective to both Bcl-2 and Bcl-xL was investigated. For a scFv to be cross-selective for Bcl-2 and Bcl-

xL an epitope common to both proteins is required. Table 2-1 shows the homology between the BH regions of Bcl-2 and Bcl-xL.

Table 2-1: The sequence line-up of human Bcl-2 and human Bcl-xL, BH1-4 domains. The homology for BH1, 2, 3 and 4 were calculated as 95, 81.8, 53.3 and 57.1 % respectively.

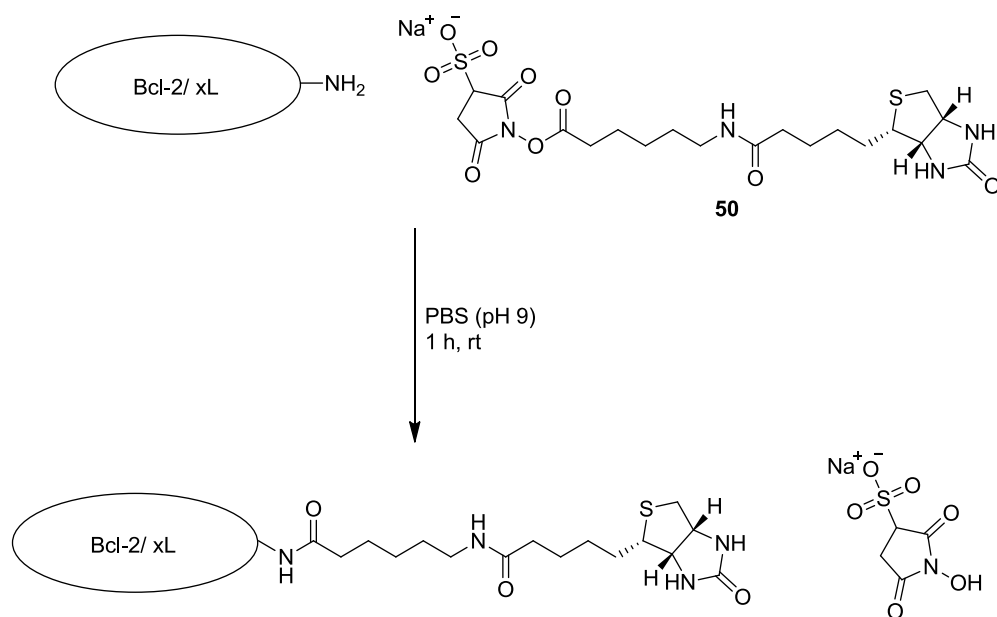
Bcl-2/xL conserved region	Amino acid sequence	% Homology
BH1	Bcl-2: ELFRDGVNWGRIVAFFSFGC Bcl-xL: ELFRDGVNWGRIVAFFEFGC	95%
BH2	Bcl-2: WIQDNGGWDAF Bcl-xL: WIQENGGWDTF	88%
BH3	Bcl-2: VHLTLRQAGDDFSRR Bcl-xL: VKQALREAGDEFELR	53%
BH4	Bcl-2: DNREIVMKYIHYKLSQRGYEW Bcl-xL: SNRELVDFLSYKLSQKGYSW	57%

The high degree of homology in the BH regions increases the possibility of isolating cross-selective anti-Bcl-2/xL scFv. Furthermore, as the BH regions are involved in heterodimer formation, it is possible that binding to these regions will inhibit Bcl-2 and Bcl-xL activity.

2.2.1 Selection of anti-Bcl-2 and anti-Bcl-xL scFvs

The first step in the soluble selection of anti-Bcl-2/xL scFvs was the biotinylation of Bcl-2 and Bcl-xL, thus allowing for immobilisation to streptavidin coated magnetic beads. The biotinylation of Bcl-2 and Bcl-xL is outlined in Scheme 2-1.

Scheme 2-1: Biotinylation of Bcl-2 and Bcl-xL using sulfosuccinimidyl-6-(biotinamido) hexanoate **50**.



A 4x molar excess of sulfosuccinimidyl-6-(biotinamido) hexanoate **50** was added to either Bcl-xL or Bcl-2 at rt. After 1 h the reaction was analysed using MALDI-TOF MS (Figure 2-5).

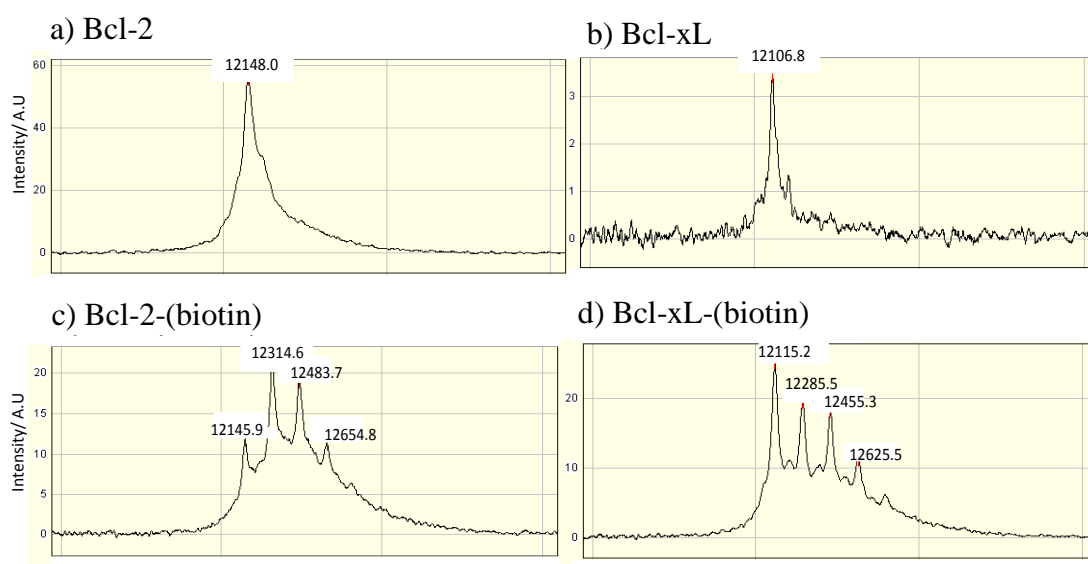


Figure 2-5: MALDI-TOF MS of the $[M+2H]^{2+}$ species of a) Bcl-2, b) Bcl-xL, c) Bcl-2-(biotin) and d) Bcl-xL-(biotin).

The successful biotinylation of Bcl-2 was confirmed by MALDI-TOF MS with four major peaks being detected at m/z 12145.9, 12315.6, 12483.7 and 12654.8 (Figure 2-5, c). These peaks correspond to the $[M+2H]^{2+}$ species for the Bcl-2, Bcl-2-(biotin), Bcl-

2-(2x biotin) and Bcl-2-(3x biotin) conjugates, respectively. Similarly, MALDI-TOF MS of the Bcl-xL biotinylation reaction mixture revealed four major peaks at m/z 12115.2, 12285.5, 12455.43 and 12625.5, assigned as the $[M+2H]^{2+}$ species for Bcl-xL, Bcl-xL-(biotin), Bcl-xL-(2x biotin) and Bcl-xL-(3x biotin) conjugates, respectively (Figure 2-5, d). The purification of Bcl-2 and Bcl-xL from the reaction mixture was achieved by size exclusion using Sephadex G-25 (PD-10, GE Healthcare).

To ensure that the Bcl-2 and Bcl-xL structure was unaffected by biotinylation, a binding enzyme-linked immunosorbent assay (ELISA) using three commercial anti-Bcl-2 and anti-Bcl-xL antibodies was performed. Additionally, the ability of biotinylated Bcl-2 and Bcl-xL to bind to the BH3 region of BID was determined using a phage binding ELISA with phage displaying BID BH3 (data shown in Appendix I). The biotinylated Bcl-2 and Bcl-xL successfully bound to BID BH3 and was also recognised by the commercial anti-Bcl-2 and anti-Bcl-xL antibodies, thus suggesting that the integrity of the proteins was retained.

The next step in isolating anti-Bcl-2/xL scFvs was the soluble selection of scFvs from three naïve scFv phagemid libraries (MedImmune, U.K) contained in the phagemid pCANTAB6.¹⁸⁵ This phagemid is approximately 4.5 kb and contains the phage coat protein *pIII* gene and an Ampicillin resistance gene. The scFv-encoding DNA is cloned at the *N*-terminal region of the *pIII* gene. The selection approach that was employed to enrich the naïve libraries with specific and cross-selective anti-Bcl-2 and anti-Bcl-xL scFv is outlined in Figure 2-6.

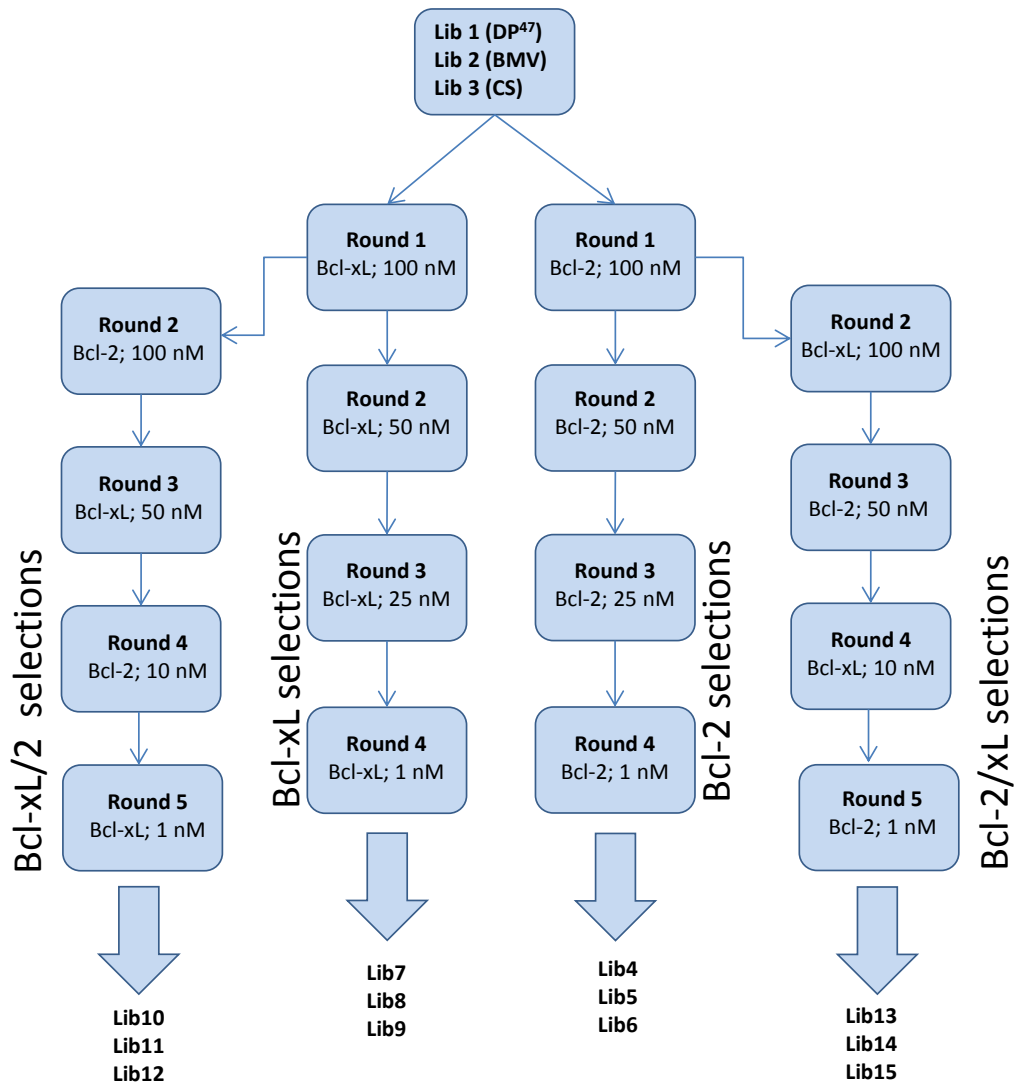


Figure 2-6: Selection pathways for soluble selection of anti-Bcl-2 and anti-Bcl-xL scFv from the naïve scFv phagemid libraries; DP⁴⁷ (Lib 1), BMV (Lib 2) and CS (Lib 3). The predicted outcome of the soluble selections is scFv specific for Bcl-xL and Bcl-2 and also scFv that are cross-selective for both antigens.

It was predicted that by alternating the selection antigen with each round it would be possible to select cross-selective anti-Bcl-2/xL scFvs. After each selection round, a representative population (~96 clones) of phage were screened for binding to Bcl-2 and Bcl-xL using a phage binding ELISA. Additionally, selected scFv were also screened against insulin and streptavidin to identify non-specific scFv. Figure 2-7 illustrates the increase in Bcl-2 and Bcl-xL specific scFv after four rounds of phage selection for the Bcl-2, Bcl-xL and the cross-selective Bcl-2/xL libraries.

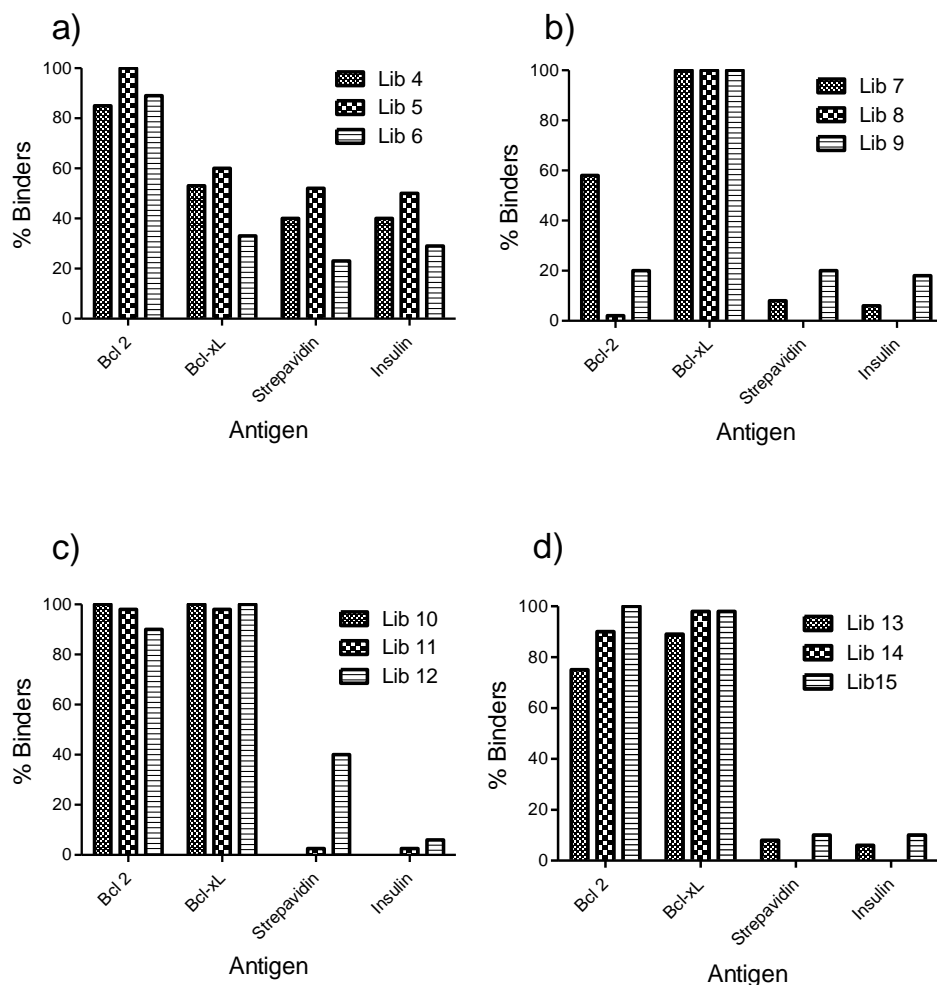


Figure 2-7: Phage binding ELISA of a representative population of phage isolated after four rounds of phage selection against either Bcl-2 or Bcl-xL. The binding of phage displaying scFv to Bcl-2, Bcl-xL and the negative controls; biotinylated insulin and streptavidin is shown. Phage libraries were selected against a) Bcl-2, b) Bcl-xL, and also selected against both c-d) Bcl-2 and Bcl-xL.


The percentage of scFvs specific for Bcl-2 and Bcl-xL present in the libraries increased throughout the selection rounds, ranging from 2-10% in round 1 to 85-100% in round 4 (Figure 2-7, a and b). However, the number of non-specific binders to insulin and streptavidin also increased throughout rounds, with the majority of libraries showing non-specific binders at the level of 15-25% in round 4. The cross-selective libraries contained approximately 70-100% cross-selective scFv after four rounds of selection (Figure 2-7, c and d).

DNA sequencing of the enriched libraries after each selection round allowed for determination of the scFv sequence diversity. Of the six CDRs the V_H CDR3 is often the most variable in a scFv population¹⁸⁶, thus only the V_H CDR3 amino acid

sequence was taken into account. It is desirable to obtain an enriched library that has a high V_H CDR3 diversity together with a high percentage of antigen specific scFvs, thus increasing the likelihood of isolating scFvs with the desired properties and antigen affinity. Table 2-2 shows the diversity of the V_H CDR3 amino acid sequences for each library selected against Bcl-2 and Bcl-xL as the selection rounds progressed.

Table 2-2: The percentage amino acid sequence diversity of the V_H CDR3 for a representative population (~96 clones) of scFv present in each library after four rounds of selection against either Bcl-2, Bcl-xL or both proteins

Library Number	% Sequence Diversity of V _H CDR3			
	R1	R2	R3	R4
1	83	n.d.	65	19
2	100	73	60	29
3	90	70	56	43
4	87	50	38	22
5	90	88	62	41
6	92	83	66	60
7	83	75	63	35
8	100	43	8	3
9	90	73	65	43
10	87	77	72	35
11	90	58	56	3
12	92	83	63	30
13	90	58	56	3
14	87	77	72	35
15	92	83	63	30


 Decrease in scFv V_H CDR3 amino acid sequence diversity

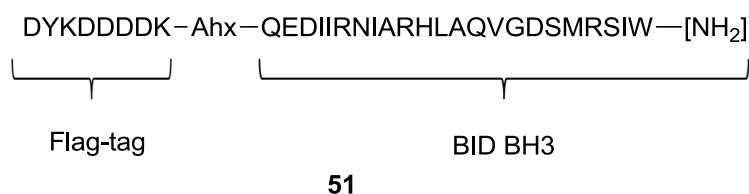
The selection of scFvs specific for Bcl-2, Bcl-xL or cross-selective to both proteins was successful with libraries containing anti-Bcl-2, anti-Bcl-xL and cross-selective scFv being obtained. Additionally, high sequence diversity was maintained throughout four rounds of selection, thus increasing the possibility of isolating scFv that have high affinity and are neutralising towards Bcl-2 and Bcl-xL.

2.3 Identification of scFv neutralising towards Bcl-2 and Bcl-xL

A representative population from each of the round 4 libraries were selected for screening in a functional assay to identify scFv that inhibit Bcl-2 and Bcl-xL binding to the BH3 region of BID.

The first step for the functional screening of the scFv libraries was the development of a high-throughput assay. An established technique for high-throughput screening of scFv phagemid libraries is the use of crude scFvs expressed in the periplasm of *E. coli*.^{187,31} However, as the scFvs are used without purification it is possible that potent scFv with low expression levels could be overlooked. Therefore, the functional assay is required to be highly sensitive to inhibitors.

It was proposed that an amplified luminescent proximity homogeneous assay (Alpha screen[®]) could be used to identify scFv that inhibit Bcl-2 and Bcl-xL activity. The principle of this assay is based on a donor bead containing the photosensitiser phthalocyanine and acceptor bead containing a thioxene derivative.¹⁸⁸ The donor bead converts ambient oxygen to ¹O₂ upon excitation at 680 nm, the ¹O₂ then transfers energy to the acceptor bead, which then emits light at 520-620 nm. This energy transfer only occurs when the two beads are in close proximity (< 200 nm).¹⁸⁸ The assay developed in this project utilises streptavidin coated donor beads, allowing for binding of biotinylated Bcl-2 or Bcl-xL and anti-flag antibody coated acceptor beads, allowing for binding of BID BH3-flag peptide **51**.



The interaction of **51** with the hydrophobic groove on the surface of Bcl-2 or Bcl-xL draws the two beads into close proximity allowing for energy transfer between the beads and subsequent detection of the protein interaction. A scFv that binds to Bcl-2/xL but does not inhibit this interaction will not be detected. Whereas a neutralising scFv will inhibit the formation of the BH3/Bcl-2 complex inhibiting the emission signal from the acceptor bead. Figure 2-8 illustrates the principle of the Bcl-2/xL Alpha screen assay.

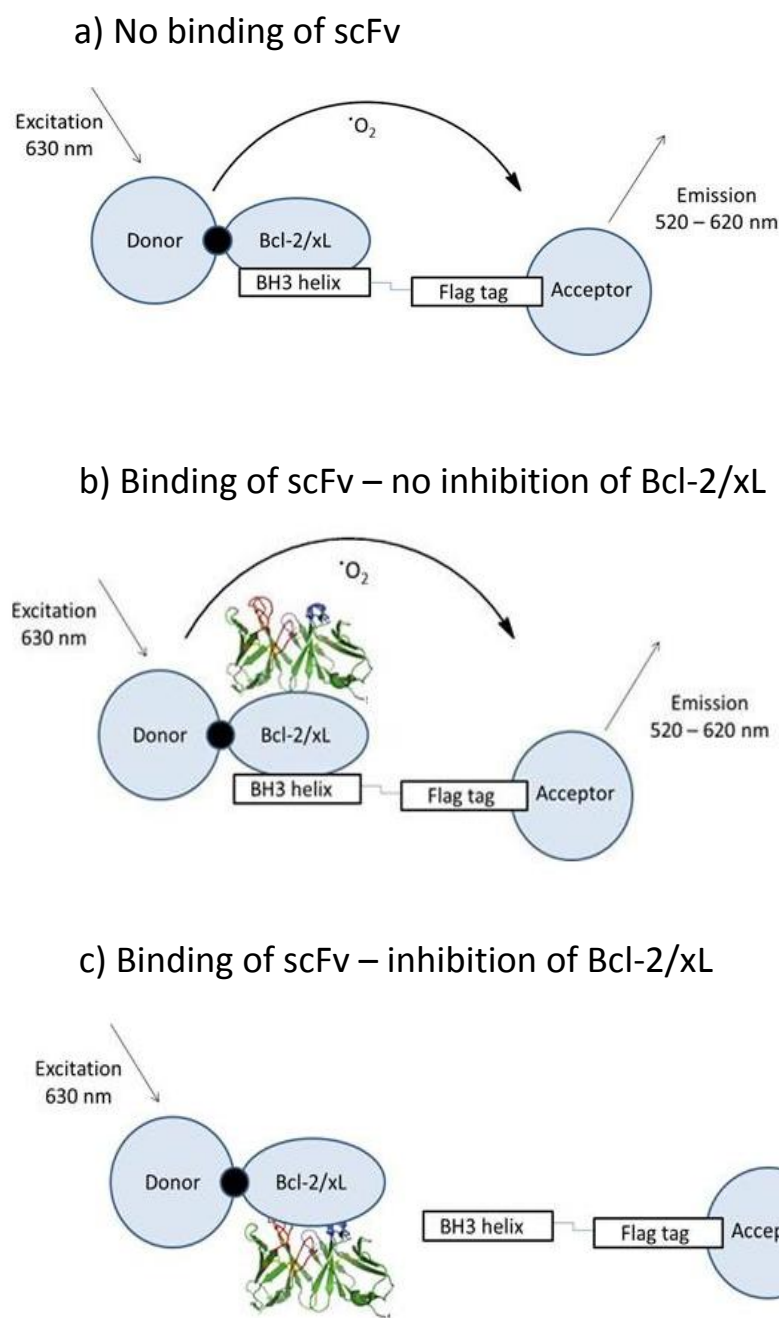


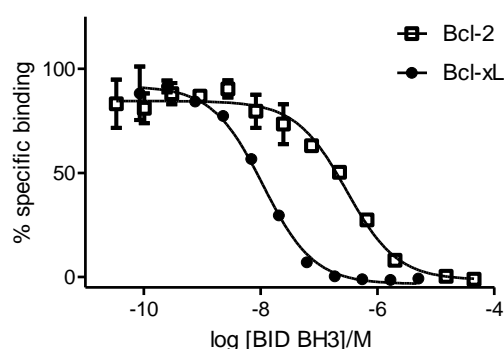
Figure 2-8: Bcl-2 and Bcl-xL Alpha screen assay set up, binding of Bcl-2 to BH3 results in a signal at 520-620 nm, addition of an anti Bcl-2 scFv to the assay may inhibit this interaction resulting in loss of signal.

Initial range finding studies were performed to determine the ideal concentration of Bcl-2/xL and BH3-flag required for a suitable signal to background ratio. The concentration of Bcl-2, Bcl-xL and BID BH3-flag **51** that were used in the assay are shown in Table 2-3.

Table 2-3: The assay concentrations of biotinylated Bcl-2, Bcl-xL and BH3-flag used in the Alpha screen competition assays.

	Biotinylated Bcl-2/xL, nM	BH3-flag, nM
Bcl-xL assay	1.95	0.49
Bcl-2 assay	7.8	7.8

Figure 2-9 shows a homologous competitive binding experiment for the competition of unlabelled BID BH3 (without flag-tag) for the Bcl-2 and Bcl-xL interaction with BH3-flag.



	BH3-flag, IC ₅₀ nM
Bcl-xL assay	10 ± 3
Bcl-2 assay	293 ± 5

Figure 2-9: Alpha screen sensitivity assay, the Bcl-2 and Bcl-xL interaction with BH3-flag was inhibited using unlabelled BH3 peptide (without flag-tag) to generate an inhibition curve, giving insight into the assay sensitivity. Each inhibition curve shows the range bars for the duplicate assay points. Each experiment was also performed at n=3, allowing for the determination of the IC₅₀ values.

The IC₅₀ value of the unlabelled BH3 is approximately 10 ± 3 nM in the Bcl-xL assay and 293 ± 5 nM in the Bcl-2 assay. Reported K_d values for Bcl-xL and Bcl-2 binding to BID BH3 are in the range of 2-12 nM and 200-270 nM, respectively.^{178, 189-190} The lower affinity of Bcl-2 for BID BH3 also explains the higher concentrations of Bcl-2 and BH3-flag that are required to obtain a suitable assay signal. However, the higher concentration of Bcl-2 used in the assay could lead to potent inhibitors that have low expression being overlooked in the high-throughput screen. For this reason a Dissociation-Enhanced Lanthanide Fluorescent Immunoassay (DELFI) assay adapted from the assay described by Rega *et al.* (2007) was investigated as an alternative format to screen anti-Bcl-2 scFv libraries.¹⁹¹ The heterogeneous nature of this assay allows for the addition of larger quantities of crude cell lysate without

affecting the final assay signal reading. Figure 2-10 illustrates the principle of the Bcl-2 DELFIA assay.

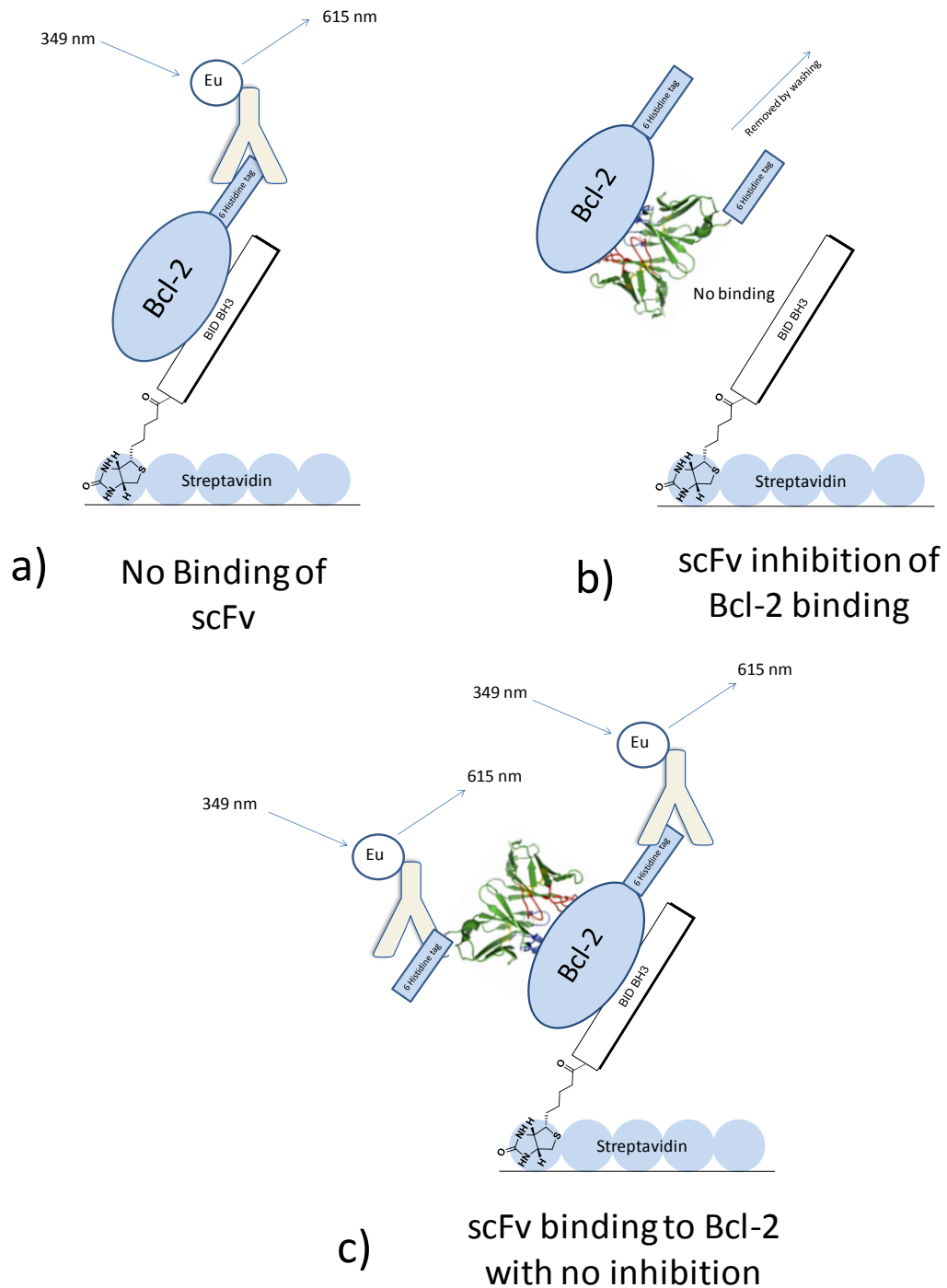


Figure 2-10: Bcl-2 DELFIA assay. Biotinylated BID BH3 was coated onto a streptavidin coated 96-well microtitre plates. Bcl-2 and the crude scFv are then added to each well. Finally, the addition of anti-histidine detection antibody labelled with Eu³⁺ allowed for detection of Bcl-2 binding to BH3 through emission at 615 nm. Washing was introduced between steps. ScFv that inhibit this interaction result in signal inhibition as a result of scFv/Bcl-2 complexes being removed from the well during the washing step. Figure modified from Rega *et al.* (2007).¹⁹¹

The scFvs were expressed from pCANTAB6 in *E. coli* and directed to the periplasm. The addition of a sucrose rich buffer was used to disrupt the bacteria membrane releasing the scFv into the supernatant. Supernatants were then used in each assay without purification. For both assays, total binding and non-specific binding control was used to calculate the total specific binding of Bcl-2 and BH3-flag of each well.

Using the Alpha screen assay, 384 individual colonies from the Bcl-xL (Lib 7-9), and cross selective (Lib 10-15) libraries were screened. Assay wells with a signal that corresponded to <30% of the total binding signal for the Bcl-xL/BH3-flag interaction were classified as positive hits. Using the DELFIA assay, 288 colonies from Bcl-2 libraries (Lib 4-6) were screened. Inhibitors of the BID BH3/Bcl-2 interaction were identified by a signal that was <5% of the total specific binding signal. Table 2-4 shows the number of positive hits for scFv neutralising to Bcl-2 or Bcl-xL binding to BH3. Additionally, DNA sequencing of each scFv clone screened in the functional assay allowed for identification of unique scFvs neutralising towards Bcl-2 and Bcl-xL.

Table 2-4: Positive hits identified from the high-throughput assays for the inhibition of Bcl-2 or Bcl-xL binding to BID BH3.

Selection Antigen	Library	Positive hits	Unique sequences
Bcl-xL	7-9	101	22
Bcl-xL/2	10-15	347	34
Bcl-2	4-6	92	44

The highest number of unique positive hits was seen from Bcl-2 selection libraries (Lib 4-6). The lowest number of positive hits was from the Bcl-xL selection libraries (Lib 7-9). The high-throughput screen successfully identified a number of scFvs that inhibit the binding of Bcl-2 and Bcl-xL to BID BH3.

2.3.1 Profiling of positive hits

A total of 40 unique scFvs identified as inhibitors of Bcl-2 or Bcl-xL in the high-throughput screens were expressed on a small-scale in *E. coli* TG1 and purified using His-tag affinity purification by the high-throughput expression team at MedImmune (U.K) using the method described by Vaughan *et al.* (1996).³¹ The purified scFvs

were then used in the Alpha screen assay to calculate the IC₅₀ values for inhibition of the Bcl-2 and Bcl-xL interaction with BID BH3-flag. In the first instance, scFvs were screened in either the Bcl-2 or Bcl-xL assay dependant on the antigen used to select the scFv (i.e. Bcl-xL, Bcl-2 or cross-selective libraries). The most potent scFvs were then also screened in both the Bcl-2 and Bcl-xL assays to confirm antigen specificity (Table 2-5).

Table 2-5: IC₅₀ values for anti-Bcl-2 and anti-Bcl-xL scFvs, identified using either an Alpha screen or DELFIA high-throughput assay. IC₅₀ values are calculated for the inhibition of either the Bcl-2 or Bcl-xL interaction with BID BH3. The full amino acid sequences of the scFvs are shown in Appendix III.

scFv #	IC ₅₀ , nM		V _H CDR3 amino acid sequence
	Bcl-xL	Bcl-2	
19	1191	nd	DGLQFDIDAFDM
20	1044	nd	ENSNYDAFDI
21	53	-	ENSKYDY
22	21	-	TGEYSGYDTSGVEL
23	1150	nd	VAGDTPIDY
24	2	-	DATTAPFYYYMDV
25	327	nd	ATGDPSGYNWFDP
26	157	nd	DCSSVGCYTSLDY
28	58	nd	DMIRLDWGDLSIDNWFDP
29	173	nd	DFGNWNYYYYYYYGMDV
30	73	nd	DSWGAGGVDAFDV
31	683	nd	QDRYGSCTSCYYEXYFDV
32	123	nd	DRLEWLGINYYYGMDV
68	94	nd	GVSGFTLPFDS
69	50	-	ASYQHFDWSPLGVDS
70	23	-	ETGYDAFDL
73	480	nd	ENSEYDSVDMDS
74	1787	nd	DLNYDFWWSGSGMDV
42	-	11	DPLSLYPYFDS
43	nd	220	WDYSSAFDI
44	-	2	DLWELLADAFDI
45	-	6	SKFLWFGGRNYFDP
46	nd	832	LGTSGWPFYYHYMDV
49	-	4	PSYDYWSAYPQRNYFYHGMDV
53	-	24	SRHMSDFWGSYLLPSGFFDV
54	-	23	IDCIGDFCDASGSSSFYD
55	-	5	EDCGTTCLGADS
56	-	50	ESQHIVGAAYLDP
57	-	47	DQWLAPFDYDS
59	-	72	HSGSGWYDHYFDH

60	-	16	GVSATYYEPYYFDF
61	2	18	ALSQTYWGFFPTYFDS
65	13	190	DSNTFWRGFWGYFNV
67	22	14	SGSSSWYRPDDAFDI
77	6	85	VSKWDRPGYLDY

nd; not determined, (-) no inhibition

A number of scFvs were isolated that showed potent inhibition of Bcl-2 and Bcl-xL. Additionally, four cross-selective scFvs were identified that inhibited both Bcl-2 and Bcl-xL (scFv53, 65, 67 and 77). Notably, a high number of scFvs with IC₅₀ values of <10 nM were identified from the Bcl-2 selection libraries with scFv44, 45, 49 and 55 showing the most potent inhibition of Bcl-2 binding to BID BH3.

Unfortunately, upon closer inspection of scFv67, the most potent cross-selective inhibitor of Bcl-2 and Bcl-xL, it became apparent that there was an amber stop codon present in the V_H domain. This was suppressed in the TG1 *E.coli*, however, expression of scFv67 in other *E. coli* strains or in mammalian cells will result in a truncated scFv. Thus, for scFv67 to be utilised in further studies this amber stop codon must be removed using site-directed mutagenesis.

The small molecule Bcl-2/xL inhibitor ABT-737 was also screened in both the Bcl-xL and Bcl-2 Alpha screen assays to determine the IC₅₀ values (Figure 2-11).

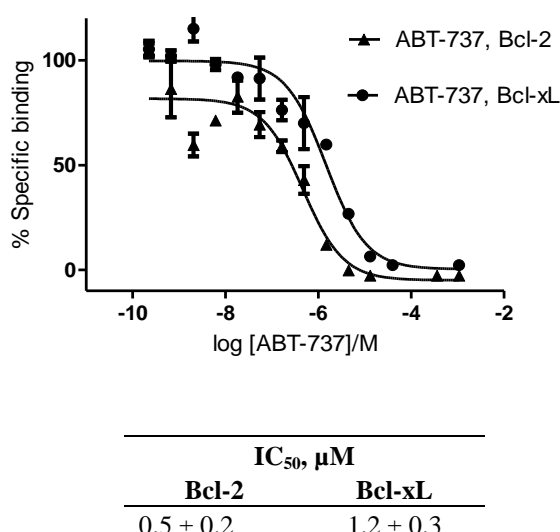


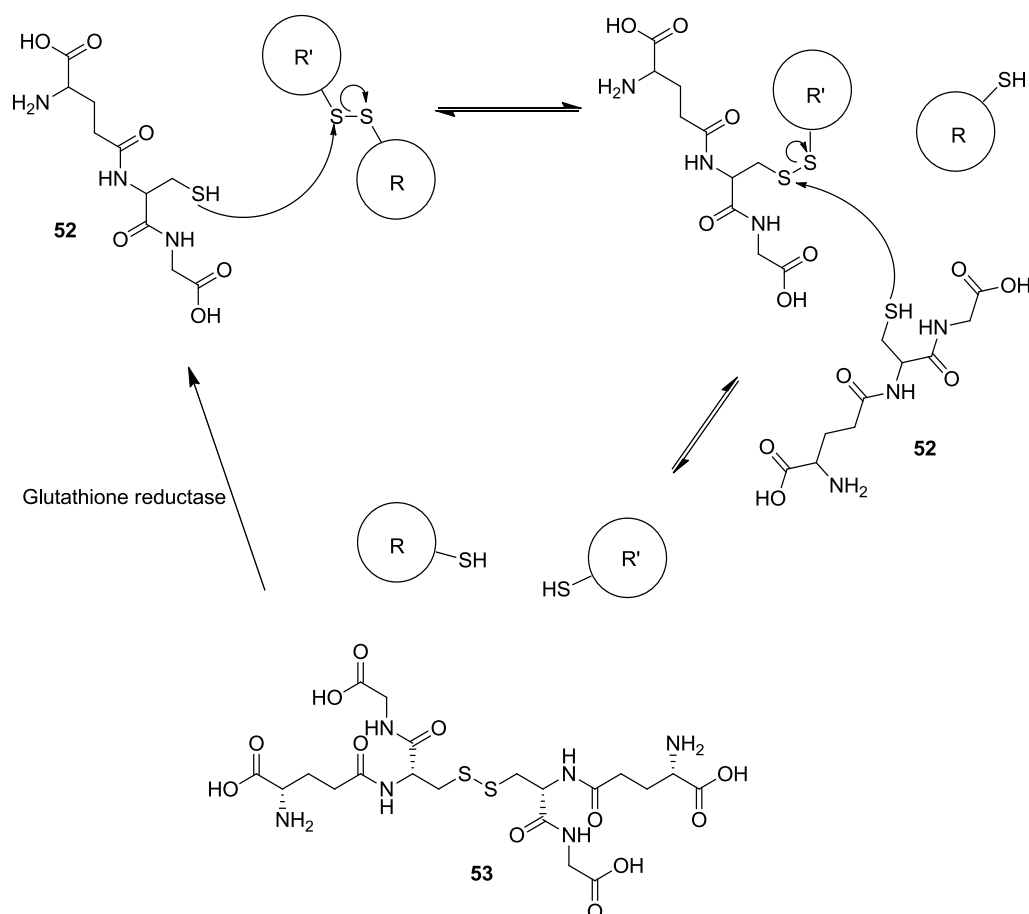
Figure 2-11: ABT-737 inhibition of the Bcl-2 and Bcl-xL interaction with BH3-flag, determined using an Alpha screen competition assay. Each inhibition curve shows the range bars for the duplicate assay points. Each experiment was also performed at n=3, allowing for the determination of the IC₅₀ values.

The IC₅₀ value for ABT-737 inhibition of Bcl-2 and Bcl-xL binding to BID BH3-flag was calculated as $0.5 \pm 0.2 \mu\text{M}$ and $1.2 \pm 0.3 \mu\text{M}$, respectively. Thus, a number of the isolated scFv are significantly more potent inhibitors of both Bcl-2 and Bcl-xL than this small molecule inhibitor.

2.3.2 Binding of scFv in reducing environment

An important requirement for isolated scFv is the ability to bind to Bcl-2 and Bcl-xL in the reducing intracellular environment of a cell. Intracellular reduced glutathione **52** is responsible for reducing non-native disulfide bonds and preventing the folding of proteins in the cytosol, thus deactivating proteins that should not be in that cellular compartment.¹⁹² The concentration of reduced glutathione in the cytosol can be as high as 10 mM.¹⁹² Reduced glutathione reduces a disulfide bond by a mixed disulfide mechanism shown in shown in Scheme 2-2.

Scheme 2-2: Mechanism of disulfide bond reduction by reduced glutathione **52**.¹⁶⁷



To assess the stability of the isolated scFvs in a reducing environment a model system was developed. This was based on a binding ELISA, involving a pre-incubation step of the scFv with reduced glutathione at 37 °C. After this incubation step, the ability of the scFvs to bind to Bcl-2 and Bcl-xL was determined. Figure 2-12 shows the results from this ELISA for the most potent scFvs isolated, scFv24, 44 and 77.

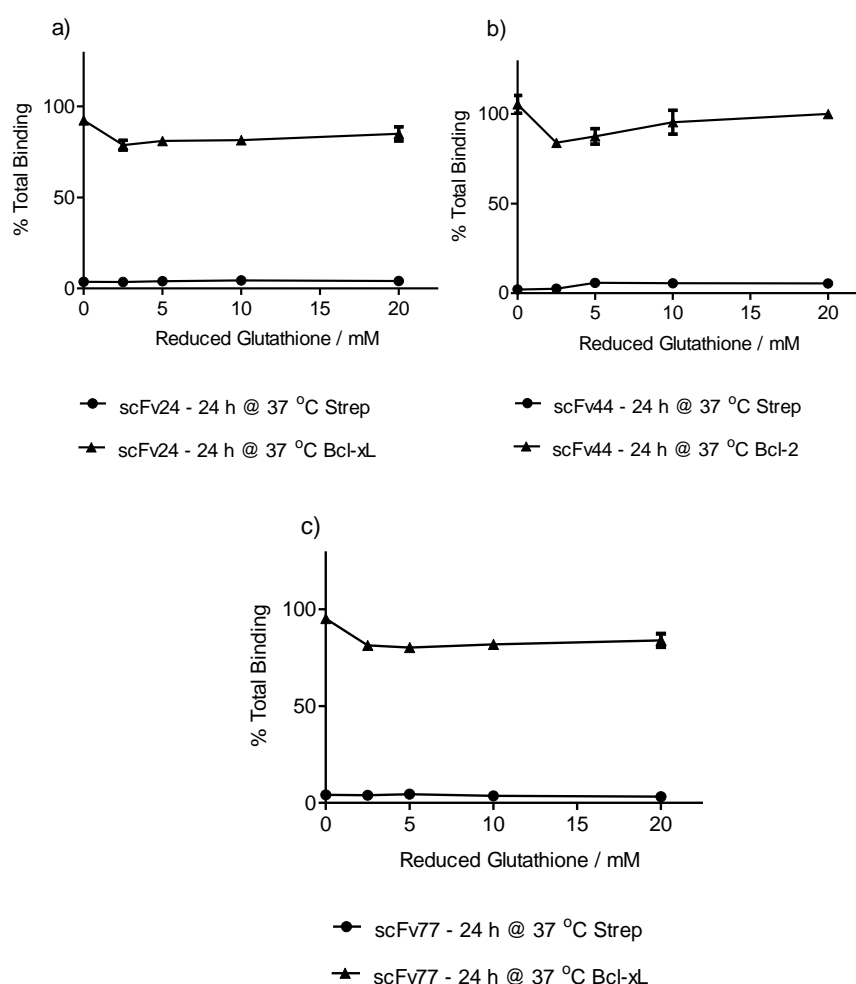


Figure 2-12: The percentage total binding of scFv24 and 77 to Bcl-xL, and scFv44 to Bcl-2 after incubation at 37 °C with increasing concentrations of reduced glutathione. The binding of scFv was also assessed using the non-specific antigen streptavidin to ensure that non-specific binding of the scFv did not increase. Total percentage binding is calculated relative to the total binding of a fresh sample of scFv.

Figure 2-13 shows the scFv binding to Bcl-2 and Bcl-xL as a percentage of the total binding of a fresh sample of scFv that had not been incubated at 37 °C or in the presence of glutathione. Incubation of scFv24, 44 and 77 at 37 °C for 24 h with reduced glutathione at concentrations of 0, 2.5, 5, 10 and 20 mM had minimal influence on the scFv binding to Bcl-2 and Bcl-xL. The scFv incubated at 37 °C for

24 h without glutathione showed approximately 95% total binding, thus the scFvs are stable at 37 °C. Incubation with increasing glutathione concentrations reduced the binding of the scFv to approximately 80-95% total binding. Therefore, the glutathione concentration appears to have a minimal effect on the stability of the scFv. This is not unexpected as the V_H and V_L intradomain disulfide bonds in an Fv fragment are buried, thus protecting them from reducing agents.^{193,58} This experiment demonstrates that scFv24, 44 and 77 are still able to bind to Bcl-2/xL after incubation at 24 h at 37 °C and at high concentrations of glutathione. Although this assay is a simplified model of the intracellular environment it is encouraging that the scFv tested retained antigen specificity. This also suggests that after intracellular delivery the anti-Bcl-2 and anti-Bcl-xL scFvs will be able to bind to cellular Bcl-2 and Bcl-xL.

2.4 Conclusions

Neutralising scFvs specific for Bcl-2 and Bcl-xL have been isolated from three naïve phagemid libraries (Lib1, Lib2 and Lib3) with several scFvs showing low IC₅₀ values in an Alpha screen competition assay for the inhibition of the Bcl-2 and Bcl-xL interaction with BID BH3. Table 2-6 shows the isolated scFvs showing the most potent inhibition of Bcl-2 and Bcl-xL.

Table 2-6: A selection of IC₅₀ values determined for the isolated anti-Bcl-2/xL scFv for the inhibition of the Bcl-2/xL interaction with BID BH3 in an Alpha screen assay.

scFv #	IC ₅₀ , nM		V _H CDR3 amino acid sequence
	Bcl-xL	Bcl-2	
44	-	2	DLWELL LADAFDI
45	-	6	SKFLWFGGRNYFDP
22	21	-	TGEYSGYDTSGVEL
24	2	-	DATTAPFY YMDV
61	2	18	ALSQTYWGFFPTYFDS
67[†]	22	14	SGSSSWYRPDDAFDI

[†]contains amber stop codon in V_H domain.

Neutralising scFvs that cross-selectively inhibit Bcl-2 and Bcl-xL were isolated together with scFvs that are specific and neutralising to either Bcl-2 or Bcl-xL only. Notably, the lead scFvs showed IC₅₀ values for the inhibition of the Bcl-2/xL interaction with BID BH3 lower than that calculated for the small molecule Bcl-2/xL inhibitor ABT-737.

Furthermore, several studies utilising the same libraries that were used in this chapter have reported the isolation scFvs with very high affinity to a target antigen.^{194,31} For example, Vaughan *et al.* (1996) reported the isolation of several scFvs possessing K_d values of <10 nM for a particular antigen.³¹ The fact that high affinity antibodies have previously been isolated from the libraries used in this project, and from similarly sized naïve scFv libraries, gives promise for the lead anti-Bcl-2 and anti-Bcl-xL scFv isolated in this project to also possess high affinities.

Additionally, the leads scFv24, 44 and 77 show good stability at 37 °C in the presence of reduced glutathione (2.5-20 mM). This suggests that the scFv will be stable in the reducing intracellular environment, which is an important requirement for intracellular antibodies.

Finally, in future studies it will be important to verify the specificity of the isolated scFv for Bcl-2 and Bcl-xL and also to other members of the Bcl-2 family such as, Mcl-1, A1 and Bcl-w. Nevertheless, a number of isolated antibodies show potent inhibition of Bcl-2 and Bcl-xL binding to BID BH3. Thus, these scFvs are expected to induce apoptosis in cells reliant on the overexpression of Bcl-2 and/or Bcl-xL for survival.

2.5 Materials and Methods

All agar plates and media were made with 2TY medium (16 g Tryptone, 10 g Yeast Extract, 5 g NaCl in 1 litre of H₂O), additional reagents and antibiotics added to 2TY media are as follows; Ampicillin and glucose (2TYAG, 100 µg/ml Ampicillin, 2% glucose), Kanamycin (2TYK, 50 µg/ml Kanamycin) and Ampicillin and Kanamycin (2TYAK, 100 µg/ml Ampicillin and 50 µg/ml Kanamycin). *E. coli* TG1 (Gibson, 1984) suppressor strain (K12, D (*lac-pro*), *supE*, *thi*, *hsdD5/F' traD36*, *proA⁺B⁺*, *lacI^q*, *lacZDM15*) was used for all phage production. The recombinant human Bcl-2 and Bcl-xL used for the phage selections was purchased from R&D systems. All His-tag purified scFv used for high-throughput screening was performed by the high-throughput expression team at MedImmune (Cambridge, U.K.). All phage display and ELISA protocols described are based on methods described by McCafferty *et al.* (1994)²⁹ and standard protocols established at MedImmune (Cambridge, U.K.). Finally, the human scFv naïve phagemid libraries DP^{47tp} (Lib1) BMV^{tp} (Lib2) and CS^{tp} (Lib3) used for all scFv selections are described by Tomlinson *et al.* (1992)²⁴⁵, McCafferty *et al.* (1994)²⁹, and Lloyd *et al.* (2004)¹⁹⁴, respectively. Each library was generated from non-immunised individuals from isolated spleen and bone marrow tissue and estimated to contain 10¹⁰ unique scFv sequences. In all libraries the V_L and V_H domains are linked together by a 15 amino acid (Gly₄Ser)₃ linker.

2.5.1 Biotinylation of Bcl-2 and Bcl-xL

EZ-Link Sulfo-NHS-LC-Biotin (sulfosuccinimidyl-6-(biotinamido) hexanoate **50** (Pierce, Thermo Scientific) was used to non-specifically label primary amines of human Bcl-2 (25.4 kDa), and human Bcl-xL (24.4 kDa) purchased from R&D systems. The proteins were supplied in 25 mM HEPES-KOH (pH 7.4), 0.1 M KCl, 10% Glycerol. To increase the biotinylation reaction, the buffer pH was increased by addition of saturated NaHCO₃ to give a final 10% solution.

A 1 mg/ml solution of sulfosuccinimidyl-6-(biotinamido) hexanoate **50** (1797 pmol/ml) was added at a 1:4 molar excess to either Bcl-2 or Bcl-xL. After a 1 h incubation at rt the reaction mixture was analysed using MALDI-TOF MS. If the

biotinylation was unsuccessful, further EZ-Link Sulfo-NHS-LC-Biotin was added (1:4 ratio) until the desired number of biotins (1-2 on average) was added to the protein.

The proteins were then purified by size exclusion using a PD-10 de-salting column (GE Healthcare, Sephadex G-25 Medium, 85-260 μ m, exclusion limit Mw 5000) pre-equilibrated with 30 ml 1x PBS. Fractions were collected at 0-2.75 ml (dead volume), 2.75-3.9 ml (protein) and 3.9-4.9 ml (salts and smaller particles). Fraction 2.75-3.9 ml was analysed by MALDI-TOF MS and the percentage of biotinylation was calculated from the MS peak intensities.

Protein concentration was determined using an Eppendorf BioPhotometer at 280 nm. The protein integrity and activity was determined using the direct binding ELISA protocol.

2.5.2 Direct binding ELISA

Biotinylated antigens were titrated (2x dilution) starting at 10 μ g/ml on a 96-well Greiner plate. 50 μ l of each dilution was transferred to the corresponding well of 96-well streptavidin-coated plate (Strepmax, costar 96-well plate, Thermo scientific) to give a range of antigen concentrations from 10.00-0.01 μ g/ml. Biotinylated insulin (1 μ g/ml coating concentration) and streptavidin coated wells were also used as negative controls to detect non-specific antibody binding.

Antigen was allowed to bind to the plate overnight at 4 °C or for 30 min at 37 °C. Following incubation the plates were washed 3x with PBS to remove unbound antigen. Plates were then blocked using 200 μ l/well of 3% (w/v) milk powder in 1x PBS (3% MPBS) and incubated for 1 h at rt. Plates were then washed 3x with PBS, followed by the addition of 50 μ l of detection antibody, diluted according to manufacturer's recommendation in 3% MPBS. Detection antibodies used included, mouse anti-Bcl-2 (Calbiochem, binding to amino acids 41-54 of rhBcl-2, Clone Ab-1) and mouse anti-Bcl-xL (Sigma-Aldrich, binding to amino acids 3-14 of rhBcl-xL, Clone 2H12). Plates were then washed 3x with PBS/0.1% Tween, followed by the addition of 50 μ l of goat anti-mouse horse radish peroxidase (HRP) antibody conjugate (R&D systems) to each well, which diluted according to manufacturer's recommendation in 3% MPBS.

Finally, plates were washed 3x with PBS/0.1% Tween, followed by addition of 50 μ l of peroxidase substrate 3,3',5,5'-Tetramethylbenzidine (TMB, Sigma-Aldrich) to each well. The plates were developed for 5-20 min at rt, followed by the addition of 50 μ l of 0.5 M H₂SO₄ to each well. Plates were read using an Envision plate reader (Perkin Elmer) at 450 nm.

2.5.3 Phage selection protocol

All naïve scFv libraries were contained in the pCANTAB6 phagemid (Figure 2-13).²⁹

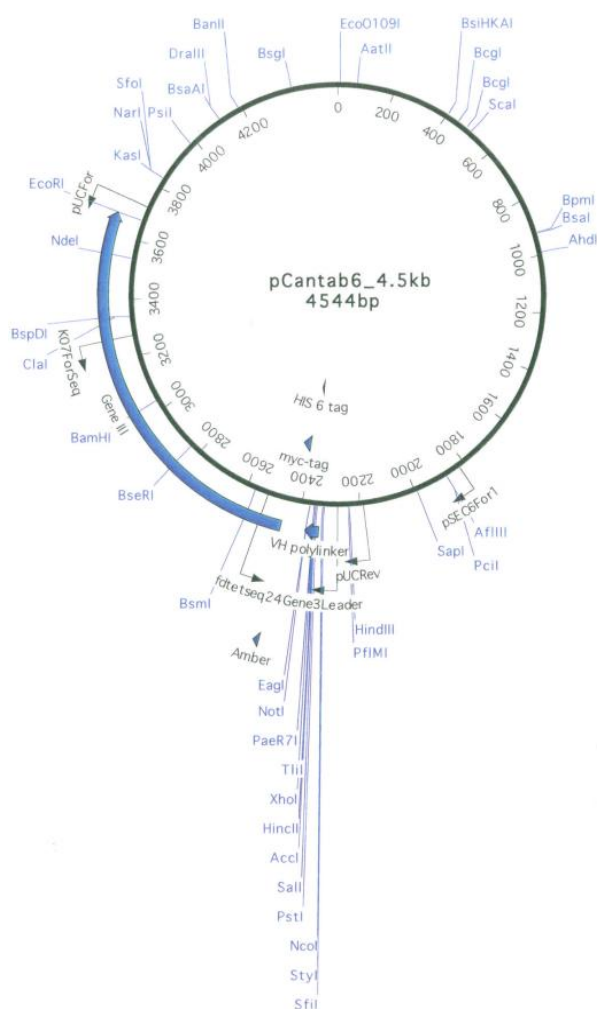


Figure 2-13: Vector map of pCANTAB6.

In the first step, 250 ml of 2TY media was inoculated with a single colony of TG1 *E. coli* cells. The culture was grown at 37 °C until mid-log phase was reached, corresponding to OD₆₀₀ 0.5-1.00.

For the first round of selections naïve antibody phage libraries DP^{47tp} (Lib1) BMV^{tp} (Lib2) and CS^{tp} (Lib3) were used (10¹⁰ cfu/ml). 50 µl of the rescued naïve phage library was blocked using 450 µl of 3% MPBS for 1 h at rt. 100 µl of streptavidin coated magnetic beads (Dynal-280, Invitrogen) were also blocked using 1 ml of 3% MPBS at rt for 1 h, beads were then removed using a magnetic block and resuspended in 100 µl of 3% MPBS. ScFv specific for streptavidin were removed from the phage libraries by addition of 50 µl blocked magnetic beads. Beads were then removed and discarded. Biotinylated Bcl-2 or Bcl-xL was then added to give a concentration of 100 nM for round 1 (antigen concentration was decreased with each round to increase selection stringency).

After 1 h incubation, 50 µl of beads were added and incubated for a further 5 min. Beads were then removed and washed 5 times in 1 ml PBS/0.1% Tween using a Kingfisher 96 magnetic particle processor (Thermo Scientific). Selected phage was eluted using 200 µl trypsin solution (10 µg/ml trypsin in 0.1 M sodium phosphate buffer, pH 7.4) at 37 °C on an orbital plate shaker at 600 rpm, thus cleaving the phage from scFv bound to biotinylated antigen/streptavidin complex.

Eluted phage was used to infect mid-log phase TG1 *E. coli* cells at 37 °C for 1 h. Phage output titres were calculated by serial dilution of infected TG1s. Diluted cells were plated onto 2TYAG plates at dilutions of 10⁻², 10⁻³, 10⁻⁴ and 10⁻⁵ and incubated overnight at 30 °C. Colonies were counted on each plate using an ACOLYTE colony counter. Phage output titres were expressed as the number of colony forming units (cfu/ml).

The infected *E. coli* was also plated on bioassay plates and grown at 30 °C overnight. The bacterial lawn was harvested with 10% glycerol 2TY media and either frozen or used directly for further phage rescue and selection rounds.

2.5.4 Phage rescue for subsequent selection rounds

In order to carry out subsequent phage display selection rounds, the bacteria collected and stored as a glycerol stock (output from previous round) were used to express phage particles. Phage libraries of selection outputs were prepared ready for immediate use as they are not suitable for storage.

25 ml of 2TYAG medium was inoculated with 0.25-0.5 ml of the glycerol stock, from the selections, to give a starting culture OD₆₀₀ of ~ 0.1. Cultures were grown at 37 °C to OD₆₀₀ = 0.5-1.0. Cells were then infected with 2.5 µl of M13K07 helper phage stock (3x10¹³ pfu/ml) and slowly shaken (150 rpm) at 37 °C for 1 h. Cells were then harvested at 2000 g for 10 min followed by resuspension in 0.5 ml 2TYAK medium, allowing for proliferation of cells containing phagemid (Ampicillin resistant) and helper phage (Kanamycin resistant). The resuspended cells were transferred into a clean 250 ml flask containing 25 ml 2TYAK media and grown overnight at 25 °C.

1 ml of overnight culture was centrifuged for 5 min and the supernatant, containing phage, removed and used in selections. Phage input titres were calculated to determine the amount of phage used for each selection round. This was achieved by adding 10 µl of the input phage stock to 990 µl of 2TY medium (10⁻² dilution). 10 µl of the diluted phage was then added to a second tube containing 990 µl 2TY medium (10⁻⁴ dilution), this was mixed thoroughly. 10 µl of this dilution was then added to a 96 deep-well plate containing 990 µl of mid-log phase TG1 *E. coli* (10⁻⁶ dilution). Infected cells were incubated for 1 h at 37 °C with shaking (150 rpm). Cells were further diluted to give samples of 10⁻⁸, 10⁻⁹, 10⁻¹⁰ and 10⁻¹¹ dilution. 100 µl of cells was spread onto 2TYAG petri dishes and grown overnight at 30 °C. Colonies were counted and phage titres calculated to determine phage input.

2.5.5 Analysis of selected phage

Single colonies from the phage output titre plates were picked into individual wells of a Costar 96-well plate containing 100 µl of 2TYAG and grown for 8 h at 37 °C. Glycerol was added to each well to give a final 20% glycerol solution to allow storage at -70 °C. Individual colonies (a representative population from each library,

approximately 96 colonies) were used for DNA sequencing using Sanger's method¹⁹⁵, by the DNA chemistry team at MedImmune (Cambridge, U.K.) using the primer MYC (Appendix II). ScFv sequences were analysed and annotated using Blaze2 software[®]. 96-well plate glycerol stocks were also used for phage ELISA to assess the number of antigen specific scFv collected from the selections.

2.5.6 Phage ELISA

96-well glycerol stocks from selections were used for inoculation of 96-well plates containing 900 µl of 2TYAG media, cultures were grown to an OD₆₀₀ of 0.5-1.0. Phage production was started by the infection with helper phage M13K07 (100 µl/well of 1.5×10^{10} pfu/ml solution) for 1 h at 37 °C. Cultures were then centrifuged at 2000 g for 10 min, the media was then changed to 500 µl of 2TYAK per well. Plates were then incubated overnight at 25 °C to allow for accumulation of progeny phage in the supernatant.

The following day, 500 µl of 6% MPBS was added to each well and incubated for 1 h at rt. Plates were then centrifuged at 2000 g for 5 min. Biotinylated Bcl-2, Bcl-xL or Insulin was coated onto 96-well streptavidin coated plate at a concentration of 1.25 µg/ml by addition of 50 µl of the protein sample to each well, followed by incubation of the plate at 37 °C for 0.5 h, and finally washing of the plate 3x with PBS. 50 µl of supernatant from the 96 deep-well plates containing phage was then added to corresponding wells on the Bcl-2, Bcl-xL, Insulin or streptavidin plates. Incubations and washes followed that described for Direct binding ELISA. Anti-M13 mAb HRP conjugate (R&D systems) was used as a secondary antibody and diluted by 1:5000 in 3% MPBS. 50 µl of the secondary antibody was then added to each well, followed by incubation for 1 h at rt and then washing of the wells 3x with PBS. Plates were developed and read as previously described in the direct binding ELISA protocol (Section 2.5.2). ScFv which bind specifically to the antigen of interest were defined by having at least >3 fold signal over that seen on an irrelevant antigen.

2.5.7 High-throughput screening

All materials were purchased from PerkinElmer and are as follows; OptiPlate-384 (Prod#6007299), AlphaScreen[®] FLAG[®] (M2) Detection Kit, 10000 assay points (Prod#6760613M, Donor Streptavidin beads and Acceptor anti-flag beads). Further materials used were; (Biotin)-Bcl-xL (366 µg/ml), BH3-flag (MedImmune, 24 µM stock solution, DYKDDDDK-linker-QEDIIRNIARHLAQVGDSMDRSIW), assay buffer (100 mM Tris (pH 8), 0.1% BSA, 0.01% Tween-20).

2.5.7.1 Expression of scFv in *E. coli* periplasm

96-well glycerol stocks from a selected library were replicated into a 96 deep-well plate containing 900 µl of 2TYAG media. Plates were incubated at 37 °C until cultures had an OD₆₀₀ of ~0.6. 100 µl of IPTG was added to each well at a concentration of 1 mM, giving a final well concentration of 0.1 mM. Plates were grown overnight at 30 °C to allow protein expression. The next day plates were centrifuged at 3000 g for 10 min, supernatant was removed and the cell pellets were resuspended in 400 µl of MES buffer (50 mM MOPS, 0.5 mM EDTA, 50 mM sucrose, pH 7.4), followed by incubation on ice for 30 min. Plates were again centrifuged at 3000 g for 10 min. The required volume of supernatant was then taken for use in high-throughput screening.

2.5.7.2 Alpha Screen Bcl-xL high-throughput screen

An Alpha screen competition assay was set up to identify scFv that inhibit the binding of Bcl-2/xL to BID BH3. Upon binding of Bcl-2/xL to BH3 a signal is emitted allowing for the interaction to be detected. Upon addition of an inhibiting scFv a loss in signal is observed.

For high-throughput screening, a final assay concentration of 1.95 nM of Bcl-xL and 0.49 nM of BH3-flag were used. ScFv library periplasm preparations in 96-well plates were transferred onto a 384 OptiPhase plates using a Mini track well dispenser, so that each well contained one scFv clone. All other reagent additions were performed using a Multidrop Combi dispenser (Thermo scientific).

Controls included non-specific binding (BH3-flag only, no scFv or Bcl-2/xL) and total binding (BH3-flag and Bcl-2/xL only, no scFv) wells. Controls were repeated 6 times for each experiment.

The detection mix was prepared in assay buffer to give a final assay concentration of 20 µg/ml of both donor and acceptor beads. The procedure was carried out in a dark room under green light.

Each well contained the reagents added in the following order: 7.5 µl periplasm preparations, followed by 7.5 µl of biotinylated Bcl-xL (from a 7.8 nM stock solution). The plates were then incubated for 30 min at rt. Following this step, 5 µl/well of BH3-flag (from a 2.94 nM stock solution) was added to the plate and incubated for 60 min at rt. Lastly 10 µl of beads (60 µg/ml stock to give a 20 µg/ml final assay concentration) were added to each well and incubated for 90 min at rt. Finally, plates were read on an EnVision plate reader (Alpha screen filters and protocols as recommended by manufacture's guidelines). Positive hits were defined as < 5% of binding compared to the total binding controls.

2.5.7.3 Bcl-2 DELFIA High-throughput screen

The low sensitivity of the alpha screen Bcl-2 format led to the development of a second assay to screen Bcl-2 scFv library outputs. This was based on a dissociation lanthanide fluorescent assay DELFIA assay described by Rega *et al.* (2007).¹⁹¹ Range determining experiments allowed suitable concentrations of reagent to be used. All assay buffers were purchased from Perkin Elmer. Initially, periplasm samples of scFv, selected using Bcl-2, were prepared as previously described (Section 2.5.7.1).

BID-BH3 biotin (biotin-QEDIIRNIARHLAQVGDSMDRSI, >95% purity, synthesised by Pepscan Ltd,) was coated onto 96-well streptavidin coated plates at 37 °C for 30 min at a concentration of 125 nM. Plates were then washed 3x with 1x PBS, followed by blocking using 3% MPBS for 1 h at rt. Plates were then washed 3x with 1x PBS, followed by addition of 25 µl of Bcl-2 (R&D systems, 0.73 mg/ml, 27 kDa) at a concentration of 12.5 nM in 6% MPBS. 25 µl/well of periplasm preparations were then added to give a single clone in each well. This gives a final assay Bcl-2 concentration of 6.25 nM. Plates were then incubated at rt for 1 h and washed 3x with

PBS/0.1% Tween. 50 µl of anti-His-tag antibody conjugated to Eu³⁺ (Invitrogen) at a concentration of 100 ng/ml in DELFIA buffer was added to each well and incubated for 1 h at rt. Plates were then washed 10x with DELFIA buffer followed by addition of 50 µl DELFIA enhancement solution. Plates were finally read on an Envision Plate reader at 615 nm. Positive hits were defined as < 5% of binding compared to the total binding controls.

2.5.8 Alpha Screen profiling of His-tag affinity purified scFv.

All final assay concentrations were the same as that used in the high-throughput screen (Section 2.5.7.2). Titration of His-tag purified scFv was carried out in Grainer 96-well plate. A 1/3 serial dilutions were prepared by the addition of 15 µl scFv (or its dilution) into 30 µl assay buffer consecutively on 96-well plate. Dilutions were carried out for each sample in duplicate, 10 µl of scFv dilution was then added to an assay well (OptiPlate-384). The reagents were added in the following order: 10 µl of scFv dilution followed by 5 µl of biotinylated Bcl-2 (46.8 nM stock) or Bcl-xL (11.7 nM stock) and incubated for 30 min at rt. Following this step, 5 µl/well of BH3-flag (Bcl-2 assay: 46.8 nM stock and for Bcl-xL assay: 2.94 nM stock) was added and incubated for 60 min at rt. Lastly, 10 µl of beads (60 µg/ml stock to give a 20 µg/ml final assay concentration) were added and incubated for 90 min at rt. Finally, plates were read on an EnVision plate reader (alpha screen filters and protocols as recommended by manufactures guidelines required).

2.5.9 scFv binding ELISA in the presence of reduced glutathione

Purified scFv24, 44 and 77 were diluted to 24 µg/ml into PBS (pH 7.4). 50 µl of the diluted scFv were transferred to the required number of wells on a 96-well plate. To these wells was added a 50 µl solution of reduced glutathione (Sigma-Aldrich) in PBS at varying concentrations (scFv concentration of 12 µg/ml and glutathione concentration of 0, 2.5, 5, 10 or 20 mM). These samples were then incubated for 24 h at 37 °C).

Biotinylated Bcl-2 or Bcl-xL (1.25 µg/ml) was coated onto 96-well streptavidin-coated plates (Strepmax, costar 96-well plate, Thermo scientific) as previously described (Section 2.5.2). A streptavidin coated plate, without added antigen, was used as negative control to detected non-specific scFv. The plates were then washed 3x with PBS to remove unbound antigen. Plates were then blocked with 3% MPBS and incubated for 1 h at rt.

50 µl/well of scFv that had been incubated at the 37 °C for 24 h at a concentration of 12 µg/ml and in the presence of reduced glutathione (0-20 mM). The scFv were incubated in each well for 1 h at rt. The plates were then washed 3x with PBS/0.1% Tween, followed by the addition of 50 µl/well of anti-myc mAb (9E3) (1 µg/ml) in 3% MPBS for 1 h at rt. Plates were again washed 3x with PBS/0.1% Tween, followed by the addition of 50 µl/well of goat anti-mouse mAb HRP conjugate, diluted according to manufacturer's recommendation in 3% MPBS. Finally, plates were washed 3x with PBS/0.1% Tween and developed and read as previously described (Section 2.5.2).

Preparation and characterisation of scFv-CPP conjugates

Many biologically active peptides and proteins are unable to internalise into a cell and so are ineffective as therapeutics. A class of peptides called Cell Penetrating Peptides (CPPs) have been demonstrated to facilitate the internalisation of macromolecules into cells overcoming the cell membrane barrier.¹⁹⁶⁻¹⁹⁷

The use of CPPs for intracellular delivery of proteins has been described extensively in the literature. Of the many CPPs known, the most commonly used are Penetratin (Antp)⁷⁹, HIV Tat⁹⁰ and octa-arginine (R₈).⁸⁹ In this chapter, site-specific labelling of anti-Bcl-2 and anti-Bcl-xL scFvs with CPPs is described. The wide number of variables that could affect the *in vivo* properties and efficacy of scFv-CPP conjugates such as, the nature of chemical conjugation⁷⁰ and influence of the cargo⁷³ were all considered when developing the CPP derivatives.

The major goals of this chapter are to induce apoptosis in cancer cells by inhibiting Bcl-2 and/or Bcl-xL using neutralising anti-Bcl-2 and anti-Bcl-xL scFv-CPP conjugates, and to develop methodology that allows for systematic optimisation of a scFv-CPP's cell penetrating capabilities.

3.1 Synthetic approaches for scFv-CPP conjugation

A common approach for the site-specific labelling of proteins is through incorporation of an unpaired cysteine residue in the protein construct, thus allowing chemoselective labelling using thiol reactive groups. It was proposed that CPP derivatives modified at the *N*-terminus with either an isobutyryl Cys or maleimido moiety could be conjugated to scFv possessing an unpaired cysteine residue (scFv-Cys), thus affording either a reversible or non-reversible scFv-CPP conjugate (Figure 3-1).

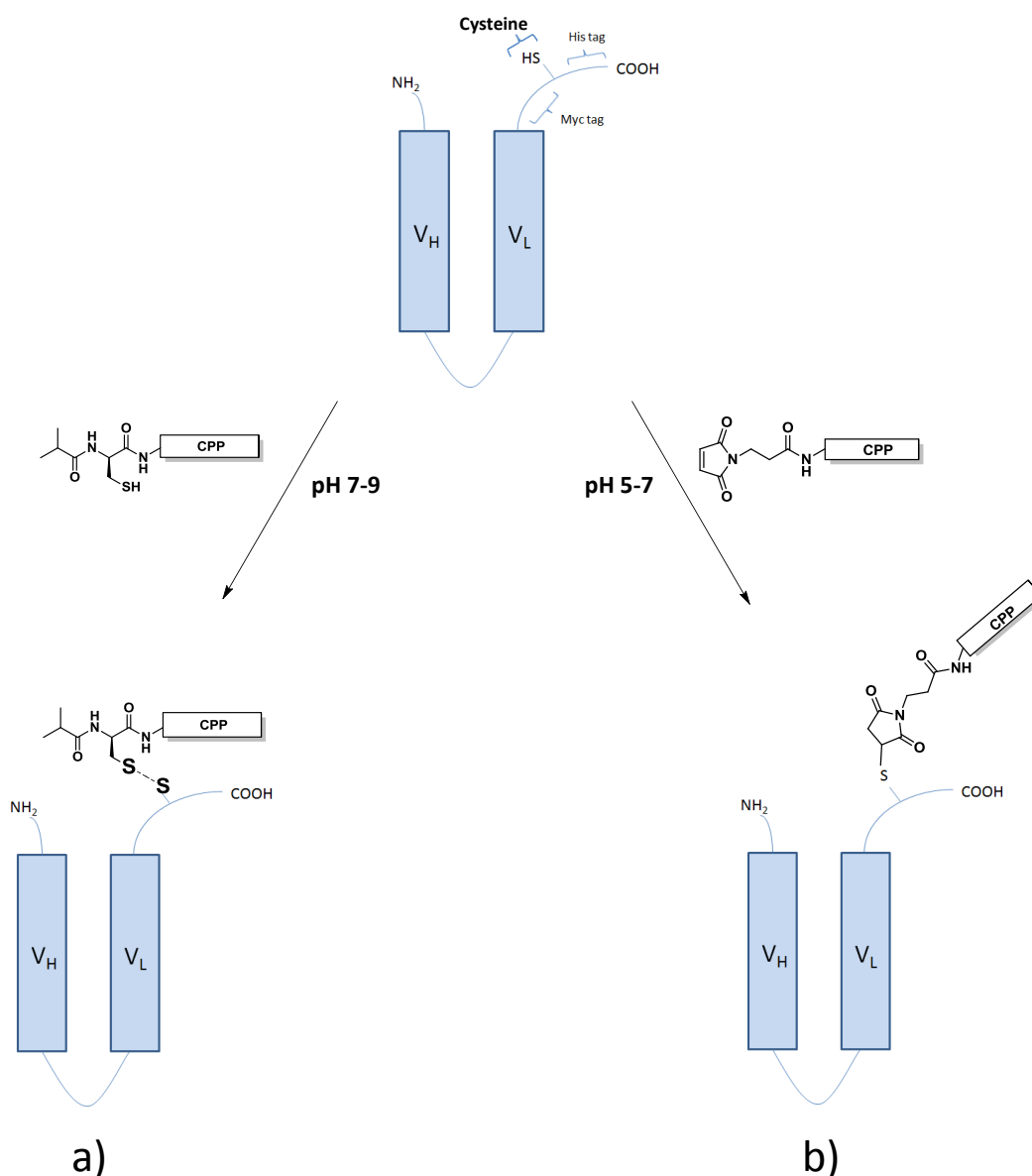


Figure 3-1: The introduction of a C-terminal cysteine to the scFv construct will allow for site-specific labelling through a) disulfide bond formation with the *N*-terminal cysteine residue of a CPP, or b) formation of a thioether bond with a *N*-maleimido CPP. A C-terminal His-tag will allow for purification of scFv by affinity chromatography and the myc tag (EQKLISEEDL) will allow for detection of scFv in ELISA and immunoblotting using anti-myc mAb (9E3).

The first step of the proposed synthesis of scFv-CPP conjugates was the preparation of scFv that possess a C-terminally located unpaired cysteine residue. Additionally, an important requirement is a robust method for the medium-scale production of a panel of scFv-Cys. *E. coli* is the most convenient method for the production of scFv due to *E. coli*'s well characterised genetics, ability to grow rapidly to high density, and is relatively inexpensive compared to alternative expression systems.¹⁹⁸⁻¹⁹⁹ However, expression of scFv in *E. coli* can give marked variations in yield, which is thought to be largely dependent on the scFv primary sequence.¹⁵³

3.2 Expression of scFv-Cys

The expression of scFv24, 44, 49, 61 and 77 in *E. coli* was investigated using the phagemid vector pUC119MCH (Medimmune, U.K). Additionally, expression of an anti-human carcinoembryonic antigen scFv (Cea6)³¹ was also investigated. It was predicted that the high specificity of this scFv for the extracellular carcinoembryonic antigen would make this molecule an ideal negative control for biological assays investigating the intracellular delivery of the anti-Bcl-2 and Bcl-xL scFvs. The production of scFv using this vector is driven by a *lac* promoter system. This vector also contains a *pelB* leader sequence to direct scFv to the oxidising *E. coli* periplasm, thus aiding scFv folding and formation of intradomain disulfide bonds. The expressed scFv construct is illustrated in Figure 3-2.



Figure 3-2: The expressed scFv construct from the pUC119MCH vector. A C-terminal His-tag is included for affinity purification, and myc tag for scFv immunodetection using an anti-myc mAb (9E3). An unpaired cysteine residue is located between the two C-terminal tags allowing for CPP conjugation.

The scFv-encoding DNA was sub-cloned into the pUC119MCH vector by excision of scFv DNA from the pCANTAB6 vector used previously for phage display. This was achieved using the restriction endonucleases NotI and SfiI. The ligation of scFv DNA into previously NotI/SfiI digested pUC119MCH vector was then achieved using T4 Ligase (*E.C. 6.5.1.1*). The ligated plasmids were then used to transform competent *E. coli*. Selection of *E. coli* colonies possessing the pUC119MCH vector was achieved

by Ampicillin selection. A representative population of colonies were cultured and used for DNA sequencing to confirm successful and in-frame sub-cloning of the scFv-encoding DNA into the plasmid.

In the first instance, the expression of scFv24 and 61 in *E. coli* was investigated using the BL21 *E. coli* strain on a 400 ml culture scale. The expression of scFv-Cys was induced using 1 mM IPTG when the *E. coli* culture had reached mid-log phase (OD₆₀₀ 0.5). The *E. coli* cultures were then incubated for 3 h at 37 °C, followed by harvesting and lysis of the bacteria using lysozyme and sonication. The expressed scFv-Cys possessing a His-tag were then isolated by affinity purification using a Ni²⁺ chelating column. The nickel bound scFv-Cys was eluted from the column by increasing the imidazole buffer concentration linearly from 40-400 mM. The eluted scFv-Cys was then pooled and analysed by SDS-PAGE. Unfortunately, the isolated scFv24 and 61 were of extremely low purity. Figure 3-3 shows the polyacrylamide gel for purified scFv24.

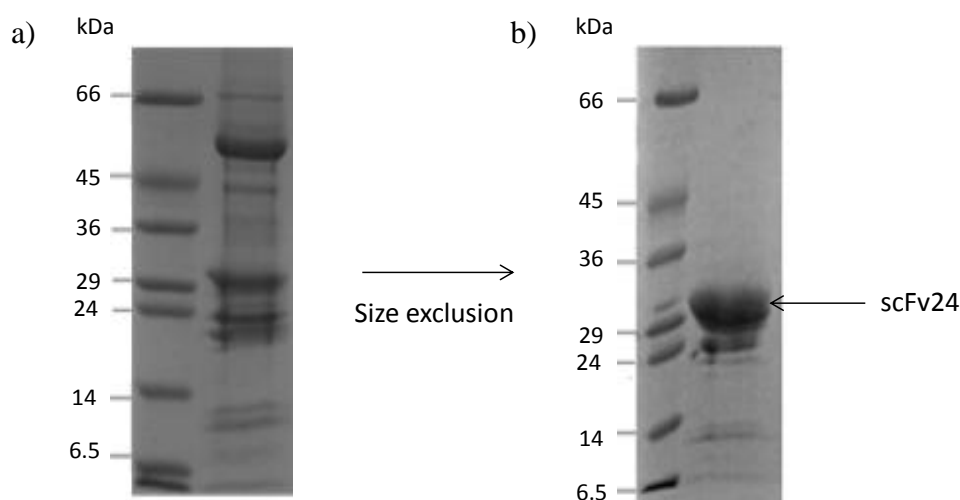


Figure 3-3: Reducing SDS-PAGE 15% acrylamide gel of scFv24 after affinity and size exclusion purification. The band corresponding to the scFv is approximately 30 kDa. a) His-tag affinity purified scFv24 b) scFv24 after size exclusion chromatography.

In repeated purifications, 20 mM imidazole and 10% glycerol was added to the *E. coli* lysate before loading onto the nickel column to reduce non-specific binding of bacterial proteins. Unfortunately, this had no significant impact on the scFv purity.

Thus, the partially purified scFv24 was subjected to size exclusion chromatography using a Superdex 75 (16/60) column (GE healthcare) to afford a pure sample in a yield

of 20% (Figure 3-3, b). The yields for scFv24 and 61 after the two purification steps were between 250-350 µg/L (Table 3-1).

Table 3-1: Isolation yields for scFv24 and 61 from *E. coli* expressed from the pUC119MCH vector.

scFv	Expression Yields, µg/L	Size exclusion yield
24	270	20%
61	340	32%

The expression yields for scFv24 and 61 obtained here are neither remarkably low, nor in the top bracket of the yields generally reported in the literature (0.1-20 mg/L).¹⁵¹⁻¹⁵² However, the low expression of scFv24 and 61 in *E. coli* using the pUC119MCH vector would require large culture volumes to gain useful quantities of scFv.

In an attempt to improve yields, the T7/*lac* promoter system was investigated for the *E. coli* expression of scFv-Cys. High yields of recombinant proteins can be obtained when using this promoter system in an *E. coli* strain possessing the T7 RNA polymerase gene (DE3λ lysogen).¹⁹⁹

The scFv24 encoding-DNA was sub-cloned into the expression vector p10HISCYS (MedImmune, U.K.) using the same method as described for the pUC119MCH vector. The p10HISCYS vector possesses a T7/*lac* promoter system and affords a protein construct with a C-terminally located His-tag and unpaired cysteine residue. Furthermore, this vector contains the *PelB* leader sequence to direct scFv to the periplasm. Interestingly, it has been reported that directing scFv to the periplasm together with high expression levels can result in leakage of the scFv into the culture media.¹⁹³ This can make purification significantly easier, allowing for efficient isolation of scFv in high yields. Thus, it was hypothesised that the T7/*lac* promoter system will dramatically increase expression levels, both allowing for increased isolation of soluble scFv from the periplasm and promote scFv leakage into the culture media. The scFv construct expressed from this vector is illustrated in Figure 3-4.

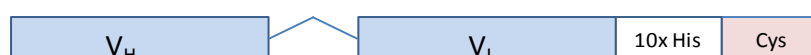


Figure 3-4: ScFv construct resulting from *E. coli* expression using the p10HISCYS vector; A C-terminal His-tag for affinity purification and C-terminal Cys is included for CPP conjugation.

Initially, the expression of scFv24 in *E. coli* was performed on a 10 ml scale using BL21 (DE3 λ) *E. coli*. Cultures were induced with 1 mM IPTG at mid-log phase followed by incubation for 16 h at 25 °C. The *E. coli* was harvested and lysed, followed by analysis of the bacterial fractions using SDS-PAGE and western blot (Figure 3-5).

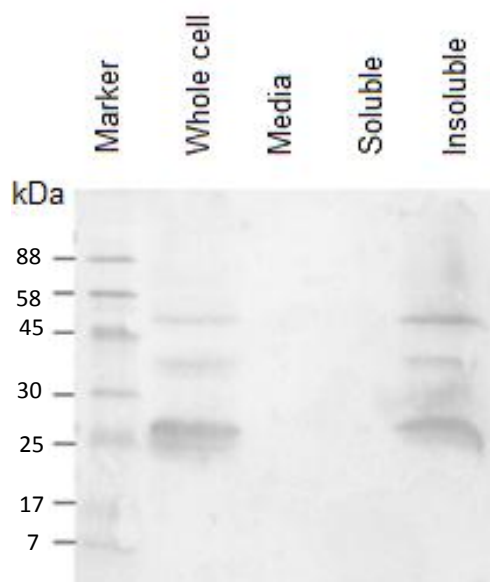


Figure 3-5: Western blot of scFv24 expressed in BL21 (λ DE3) from p10HISCYS. *E. coli* was induced at mid-log using 1 mM IPTG and incubated for 16 h at 25 °C. The bacteria were fractionated to give the whole cell, media, soluble and insoluble fractions. The nitrocellulose membrane was incubated with anti-polyhistidine mAb (R&D systems) followed by incubation with a goat-anti-mouse mAb (R&D systems) horseradish peroxidase conjugate and developed using 3,3',5,5'-Tetramethylbenzidine (TMB).

Unfortunately, no scFv24 was detected in any of the soluble fractions. However, scFv24 was detected in the insoluble fraction using an anti-polyhistidine mAb at approximately 28 kDa, as can be seen from the western blot in Figure 3-5.

The next step was to monitor the expression of scFv24 over 16 h at 16 °C to determine an optimum point to harvest *E. coli* and avoid the formation of inclusion bodies. After inducing the cultures with 1 mM IPTG, a 1 ml aliquot was removed at 1, 3, 6 and 16 h. The *E. coli* was harvested by centrifugation followed by lysis using lysozyme (1 mg/ml). The insoluble and soluble fractions were then analysed by reducing SDS-PAGE (Figure 3-6).

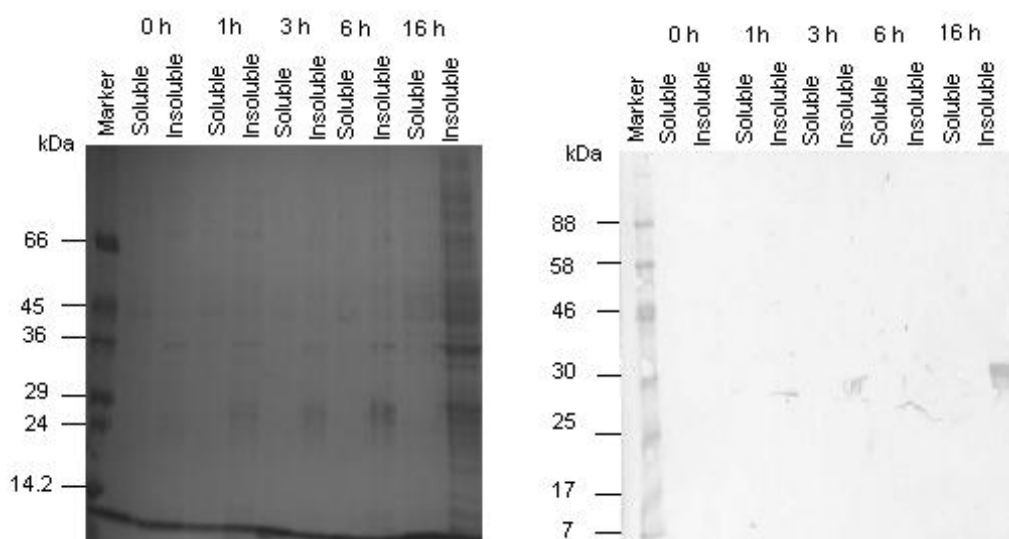


Figure 3-6: Time course of *E. coli* expression of scFv24 using the p10HISCYS vector in BL21 (λ DE3). *E. coli* was induced at mid-log with 1 mM IPTG and incubated for 16 h at 16 °C with samples being taken at specific time points. a) Bacterial fractions were analysed using a 15% SDS-PAGE gel and stained with Coomassie blue b) after the electoblot, the nitrocellulose membrane was incubated with anti-polyhistidine mAb followed by an goat anti-mouse mAb horseradish peroxidase conjugate and developed using 3,3',5,5'-Tetramethylbenzidine (TMB).

Unfortunately, the majority of scFv24 expressed from the pHIS10CYS vector appears in the insoluble bacterial fraction at 16 h post-induction (Figure 3-6). It was decided that the p10HISCYS vector was unsuitable for the expression of a panel of scFv in this study. Therefore, an alternative approach to obtain useful quantities of scFv was investigated.

3.2.1 Mammalian expression of scFv-Cys

The expression of lead scFv in a mammalian expression system established at MedImmune (Cambridge, U.K) was investigated. ScFv24, 77, 49 and the controls scFv84⁶³ and Cea6³¹ were sub-cloned into the mammalian expression vector pEOMCH. The scFv construct from the pEOMCH vector is identical to that produced by the pUC119MCH vector (see Figure 3-2).

A variant of Chinese Hamster Ovary cells (CHO), called CEP6 were used for the expression of scFv-Cys. Small-scale expression was carried out using a 10-20 ml suspension of CEP6 cells (5×10^5 cells/ml). The transient transfection of CEP6 cells with the pEOMCH vector was achieved using the transfection reagent

polyethylenimine (PEI). An aqueous solution of PEI (10 mg/ml) was added in equal volume to a solution of purified plasmid (0.25-0.5 mg/ml). This mixture was then transferred to the CEP6 cultures to give a final concentration of 1 µg DNA/ml of cells. The transfected cultures were incubated at for 10 days 37 °C with shaking, followed by cell harvesting and analysis of the culture media using a western blot to detect secreted scFv (Figure 3-7).

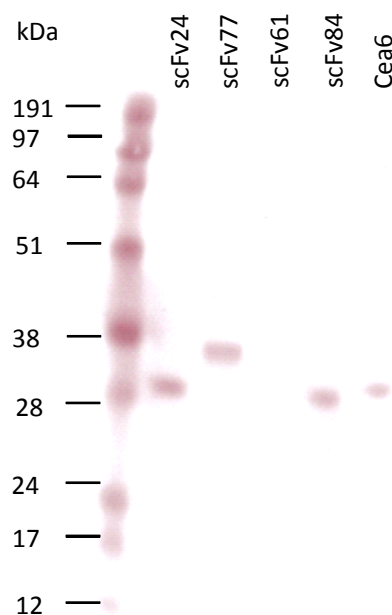


Figure 3-7: Western blot of CEP6 expression of scFv24, 77, 61, 84 and Cea6 using the pEOMCH vector. Cells were transiently transfected and incubated for 10 days at 37 °C. Culture media was analysed by western blot using a 4-12% polyacrylamide gel followed by transfer to nitrocellulose membrane. The membrane was incubated with anti-myc mAb (9E3) followed by goat anti-mouse mAb horseradish peroxidase conjugate and developed using an acridan-based substrate and read at 440 nm.

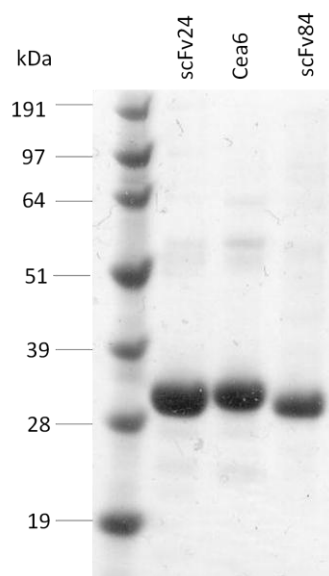
The small-scale expression of scFv24, 84 and Cea6 in CEP6 cells was successful. However, no detectable expression of scFv61 was observed (Figure 3-7). Although scFv77 was expressed in good levels the observed mass by western blot was ~35 kDa (Figure 3-7). The greater mass observed compared to that calculated for scFv77 (29 kDa) may be attributable to glycosylation at an *N*-glycosylation recognition sequon (Asn-Xaa-Thr) present in the *C*-terminus of the scFv (Figure 3-8).²⁰⁰⁻²⁰¹



Figure 3-8: SDS-PAGE analysis of scFv77 showing a band at ~35 kDa. scFv77 amino acid sequence shows the presence of an Asn-Xaa-Thr sequon. A 4-12% polyacrylamide gel was used and stained using Coomassie blue.

The good expression of scFv77 still makes this a suitable scFv for further investigation. If glycosylation has occurred, the close proximity of the glycosylation site to the C-terminal cysteine residue may have a negative effect on both CPP conjugation and subsequently cellular internalisation. Therefore, removal of the N-glycosylation site by replacing the asparagine with a glutamine residue using site-direct mutagenesis is required.

The expression of scFv24, 84 and Cea6 was scaled up to a 0.5 L culture volume. The CEP6 cells were transiently transfected as previously described followed by incubation of the culture for 10 days 37 °C. The cells were harvested and the expressed scFv possessing a His-tag were isolated from the culture media by affinity purification using a Ni²⁺ chelating column. The obtained expression yields and SDS-PAGE analysis of the purified scFv24, 84 and Cea6 are shown in Figure 3-9.

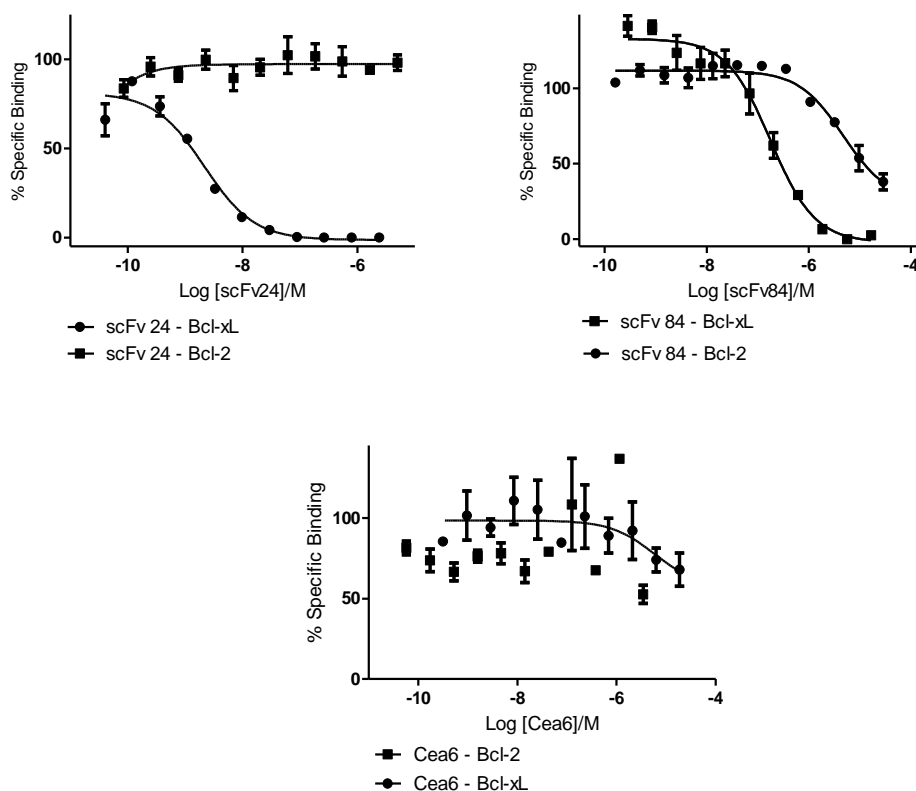


scFv	Yields, mg/L
scFv24	26.2
Cea6	59.2
scFv84	26.3

Figure 3-9: The expression yields from CEP6 cells for scFv24, Cea6 and scFv84 using the pEOMCH vectors. SDS-PAGE analysis shows pure protein with a single band at ~30 kDa. 4-12% polyacrylamide gel was used and stained using coomassie blue.

The medium-scale expression of scFv24, 84 and Cea6 in CEP6 cells was successful, allowing for isolation of scFv in good yields of 26.2, 59.2 and 26.3 mg/L, respectively. These yields are significantly higher than yields achieved in *E. coli*. Notably, minimal optimisation of the transfection and expression conditions were required to achieve high isolation yields for each scFv providing a universal expression system for the panel of lead anti-Bcl-2 and anti-Bcl-xL scFv.

An important requirement from the mammalian expression system is the production of active scFv-Cys. Hence, the ability of purified scFv to inhibit Bcl-2 and Bcl-xL binding to the BH3 region of BID was determined using an Alpha screen assay. The inhibition curves for scFv24, 84 and Cea6 are shown in Figure 3-10.



	IC ₅₀ , nM	
	Bcl-2	Bcl-xL
scFv24	-	6 ± 2
Cea6	-	-
scFv84	> 4000	153 ± 2

Figure 3-10: The inhibition curves for scFv24, scFv84 and Cea6 in an Alpha screen assay, curves show the inhibition of Bcl-2/xL binding to BID-BH3 by a) scFv24, b) scFv84 and c) Cea6.

The IC₅₀ values determined for the inhibition of the Bcl-2 and Bcl-xL interaction with BH3 for scFv24, 84 and Cea6 corresponded to IC₅₀ values determined for the scFvs expressed on a small-scale using the phagemid vector pCANTAB6 (Chapter 2). The purified scFv24 inhibited the binding of Bcl-xL to BH3 with an IC₅₀ value of 6 ± 2 nM. Surprisingly, the positive control scFv84 that was isolated from phage display libraries by Cohen-Saidon *et al.* (2003) and demonstrated to inhibit Bcl-2, showed only minimal inhibition of Bcl-2 binding to BH3 in the Alpha screen assay.⁶³ However, this scFv did inhibit Bcl-xL with an IC₅₀ value of 153 ± 2 nM. This result is in contrast to the reported properties of scFv84.⁶³ Finally, Cea6 showed no inhibition

of Bcl-2 or Bcl-xL confirming its suitability for use as a negative control in cell based assays.

Mammalian expression of lead scFvs proved successful, with high yields being obtained (26-60 mg/L) for scFv24, 84 and Cea6. The expression conditions required minimal optimisation between different scFv constructs, thus addressing the first aim of this study. Additionally, practical quantities of active scFv-Cys were obtained. This will allow for the investigation of CPP-mediated cellular delivery of the lead scFv and provide material for the envisaged whole cell and *in vitro* assays. The next phase of the project is described, focussing on the synthesis of CPP derivatives for site-specific conjugation to scFv-Cys.

3.3 Fmoc solid-phase peptide synthesis of CPPs

In the first instance, CPPs that are well established for the cellular delivery of proteins were investigated for cellular delivery of lead scFv. Table 3-2 shows the CPP sequences that were chosen to be synthesised and conjugated to scFv-Cys.

Table 3-2: Cell penetrating peptides chosen for conjugation to scFv-Cys.

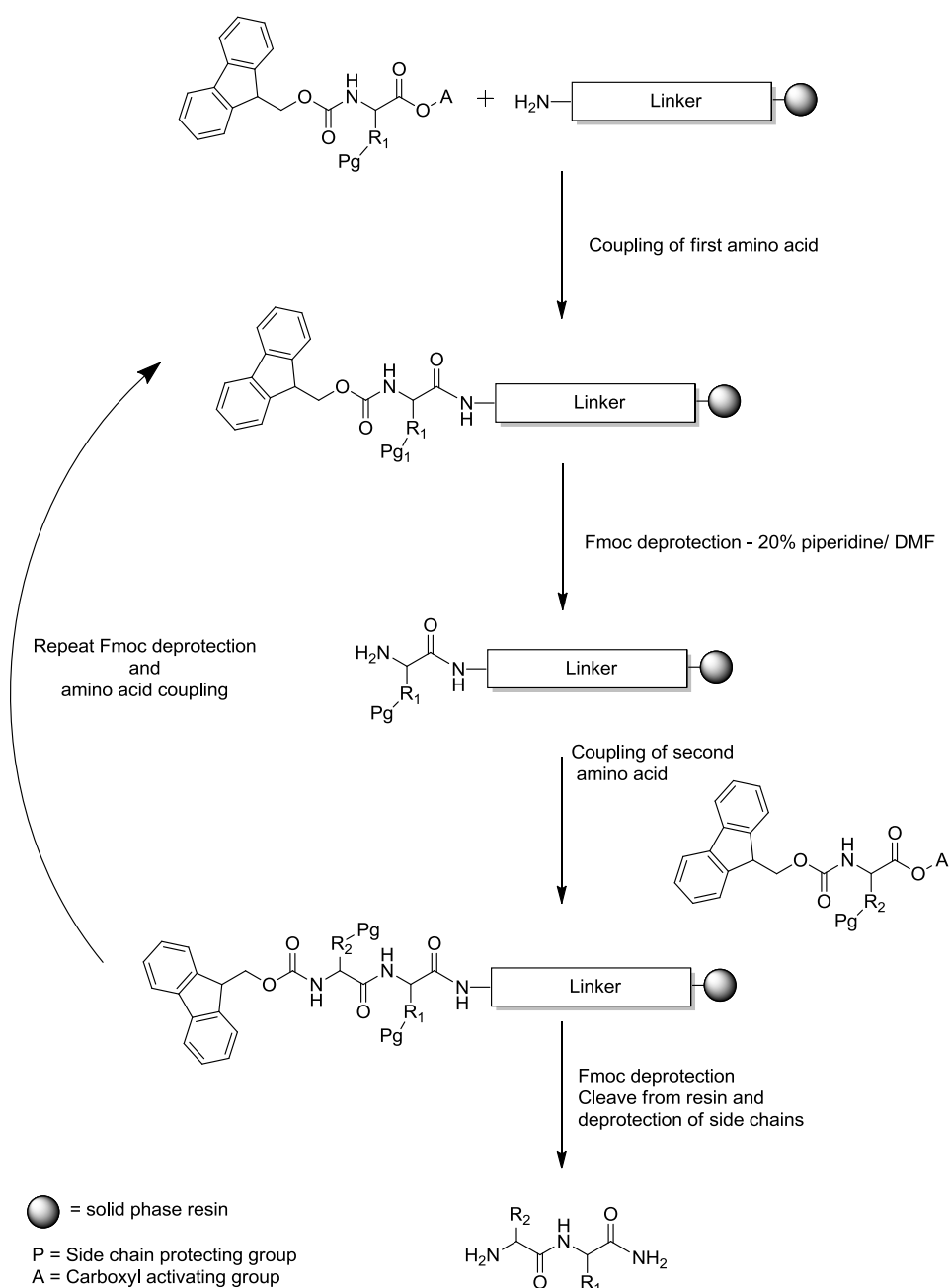
Derivatives	Sequence	Reference
<u>Penetratin derivatives</u>		
Antp ₅₂₋₅₈	RRMKWKK	Fischer <i>et al.</i> (2000) ²⁰²
Antp ₄₃₋₅₈	RQIKIWFQNRRMKKWKK	Derossi <i>et al.</i> (1996) ⁷⁹
<u>Polyarginine derivatives:</u>		
octa-arginine	RRRRRRRR	Wender <i>et al.</i> (2000) ⁸⁹
<u>HIV Tat derivatives</u>		
Tat ₄₉₋₅₇	RKKRRQRRR	Vives <i>et al.</i> (1997) ⁹⁰
<u>Polyproline derivatives</u>		
Pro ₁₄	PPPPPPPPPPPPPP	Crespo <i>et al.</i> (2002) ⁹⁵

Polyarginine, Penetratin and HIV Tat have been extensively used for the cellular delivery of proteins. Additionally, Crespo *et al.* (2002) describe the internalisation of FAM-(Pro)₁₄-OH **12** into NRK-49F cells.⁹⁵ Hence, it was proposed that conjugation

of (Pro)₁₄ to scFv could enable cell penetration. This peptide would be an interesting alternative to the polycationic CPPs as its non-cationic nature would be expected to result in significantly different *in vivo* properties compared to a cationic CPP.⁸¹

The synthesis of all CPP derivatives was achieved using Fmoc solid-phase peptide synthesis (SPPS). The Sheppard's Fmoc/*t*-Bu SPPS approach utilises the base labile 9-fluorenylmethyloxycarbonyl (Fmoc) group for α-amino protection in conjunction with acid-labile side-chain protection of amino acids.²⁰³ The general principles of Fmoc SPPS are outlined in Scheme 3-1.

Scheme 3-1: The general principles of Fmoc solid-phase peptide synthesis (SPPS).



The first step in Fmoc SPPS is the introduction of a N^α -Fmoc protected amino acid to a solid support *via* a linker. The Fmoc group is then removed using 20% piperidine/DMF prior to the addition of the second amino acid which is also in the N^α protected form. Amide bond formation is achieved by activation of the carboxyl group of the N^α -Fmoc protected amino acid promoting nucleophilic attack by the amino group of the peptidyl resin. The activation of a carboxylic acid can be achieved by substitution of the hydroxyl with an electron withdrawing group, thus increasing the electrophilicity of the carbonyl. A common method to activate a carboxyl group is by using aminium or phosphonium coupling reagents, such as HATU, HBTU, TBTU or PyBOP.²⁰⁴⁻²⁰⁵ An alternative method is through carbodiimide activation using N,N' -Diisopropylcarbodiimide (DIC) in the presence of an auxiliary nucleophile, for example 1-hydroxy-7-azabenzotriazole (HOAt)²⁰⁶ to form an activated ester. After introduction of the required amino acids to the peptidyl resin through repeated cycles of Fmoc deprotection, carboxyl activation and amide bond formation, the peptide can be cleaved and fully deprotected using 90% TFA to afford the desired peptide derivative.

3.3.1 Synthetic strategies for CPP derivatives

A standardised approach to the synthesis and design of CPP derivatives is important for the systematic optimisation of scFv-CPP conjugates. Therefore, a robust method for the introduction of thiol reactive groups to CPP derivatives was investigated. Another crucial component in this phase of the project is to provide a simple and robust method for the qualitative measurement of scFv-CPP cellular internalisation. This can be achieved through the addition of a fluorescent probe to the CPP construct. The general design of the CPP derivatives is shown Figure 3-11.

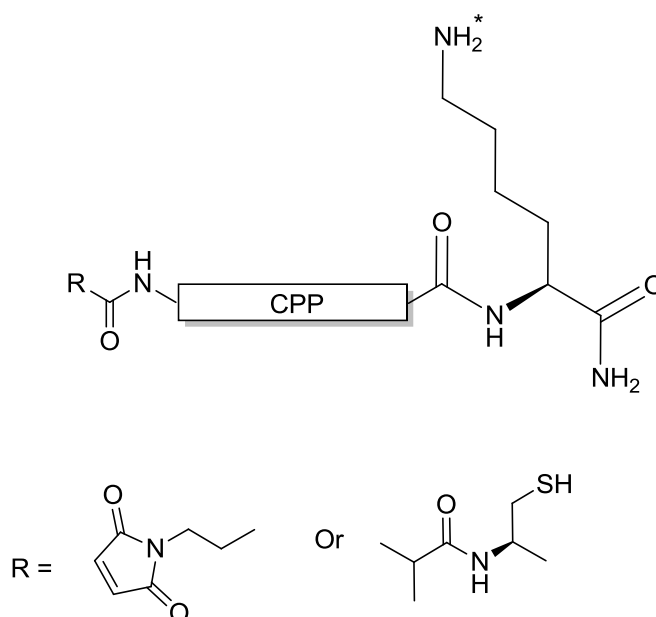


Figure 3-11: The general design of the CPP derivatives, a C-terminal lysine residue will allow for fluorescent labelling of the peptide. The N-terminus of the peptide will allow for coupling of either a maleimidopropionyl or isobutyryl cysteine moiety for site-specific conjugation to scFv-Cys

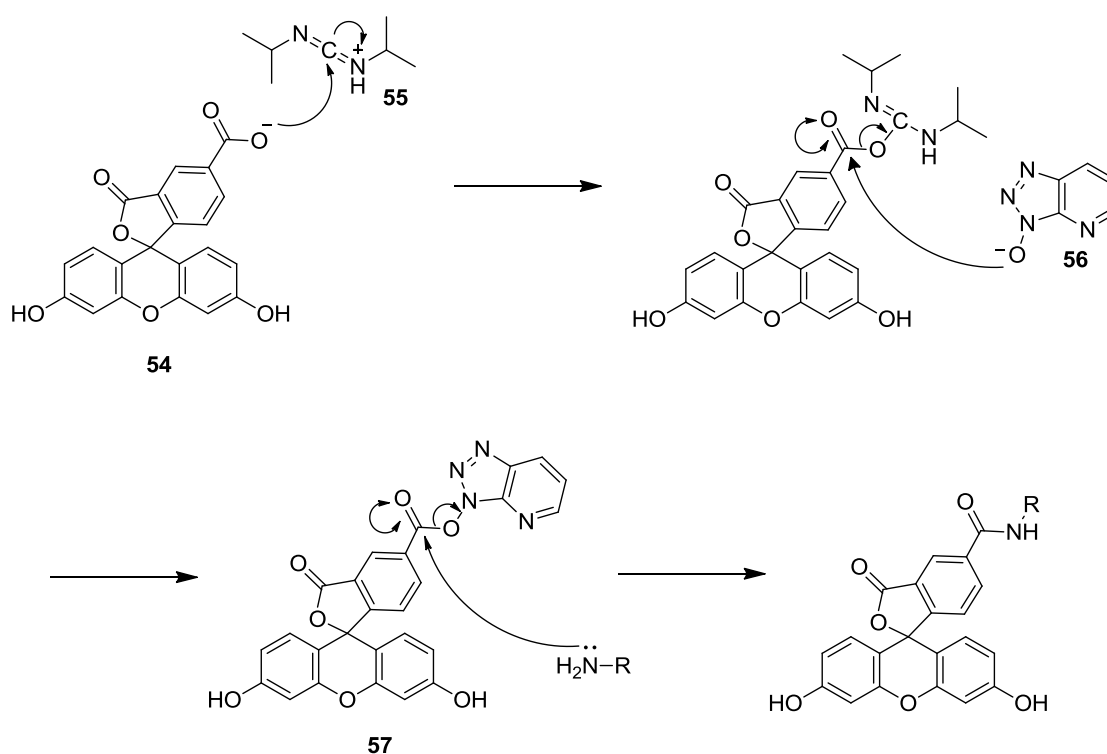
The CPP construct was designed for the introduction of both thiol reactive groups and fluorescent probes. The C-terminal lysine residue provides a reactive handle for modification with a fluorescent probe. An established method to achieve this is by introducing an orthogonally protected lysine residue to the peptidyl resin. This can then be deprotected for regiospecific introduction of a fluorescent probe followed by universal cleavage and deprotection to afford the labelled peptidic material.²⁰⁵

Two established orthogonal protecting groups for side-chain protection of a lysine residue are the hydrazine-labile ivDde^{204,207} and the acid sensitive methoxytrityl (Mmt) protecting groups.²⁰⁸ The ivDde protecting group is stable to 20% piperidine and >95% TFA, thus providing orthogonality with the Fmoc group and acid-labile protecting groups.²⁰⁷ The Mmt protecting group can be removed from the side-chain of Lys using 1% TFA in DCM allowing for deprotection in the presence of the Fmoc group and side-chain protecting groups that require >90% TFA for removal.²⁰⁸ Both protecting groups provide the orthogonality required for selective deprotection of a C-

terminal lysine residue, followed by the introduction of a fluorescent probe to the CPP derivatives.

5-Carboxyfluorescein **54** (5-FAM) is a versatile fluorescent probe and is commonly used to label peptides for imaging using confocal laser scanning microscopy (CLSM) and fluorescence microscopy. 5-FAM can be regioselectively introduced to a peptide during solid-phase synthesis. The coupling of 5-FAM **54** to an orthogonally deprotected lysine residue can be achieved using DIC **55** and HOAt **56** to activate the 5-carboxyl group. This affords the activated intermediate **57** allowing for the S_N2 substitution at the carbonyl of **57** by the ϵ -amine of Lys (Scheme 3-2).²⁰⁹

Scheme 3-2: Mechanism of 5-carboxyfluorescein **54** coupling to a primary amine using DIC **55** and HOAt **56**.



However, the 5-FAM phenolic groups can also attack the activated carboxyl group of 5-FAM to form polymeric phenyl esters. Base-catalysed aminolysis using 20% piperidine/DMF can be used to cleave ester bound 5-FAM.²¹⁰

The Rink Amide NovaGelTM resin was utilised for the synthesis of the CPP derivatives. Once the peptide has been assembled by step-wise introduction of N^α -protected amino acids to resin, the peptidic material is cleaved from the resin and

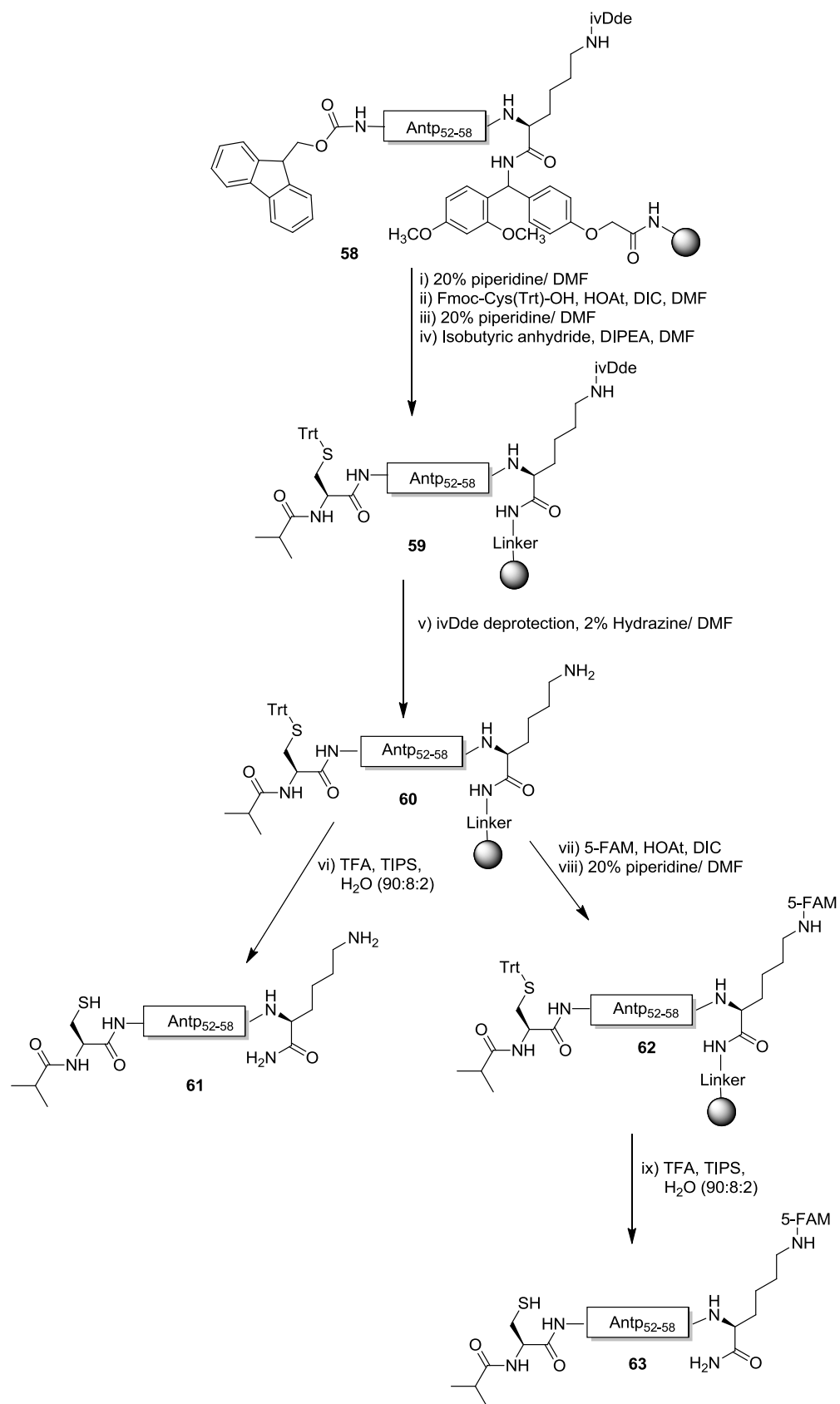
universally deprotected using a solution of TFA-TIPS-H₂O (90:2:8) to afford the peptide amide.²⁰⁵ The introduction of Fmoc-Lys(ivDde)-OH or Fmoc-Lys(Mmt)-OH to the rink amide linker allows for the orthogonal deprotection and regioselective modification of the lysine residue prior to the universal cleavage/deprotection step.

Furthermore, *N*-terminal functionalization of CPP derivatives with either a maleimido moiety or cysteine residue will allow for site-specific conjugation of the CPP to scFv-Cys. In the first instance, the synthesis of Antp₅₂₋₅₈ derivatives was investigated. The synthesised peptides were functionalised with either an *N*-terminal isobutyryl Cys or maleimido moiety, together with regiospecific labelling with 5-FAM.

3.3.2 Penetratin derivatives

Penetratin (Antp) is a well characterised CPP and has been demonstrated to deliver proteins into cells. Fischer *et al.* (2000)²⁰² showed that the eight amino acid truncated Penetratin derivative Antp₅₂₋₅₈ (⁵²RRMKWKK⁵⁸) efficiently penetrates cells and is the minimum sequence required for internalisation. This peptide was synthesised because of its simplicity and size, making it an attractive peptide for future studies in terms of scale-up synthesis. Additionally, the originally described full length Antp₄₃₋₅₈ (⁴³RQIKIWFQNRRMKWKK⁵⁸)⁷⁸ was also synthesised. The proposed synthesis of *N*-isobutyryl Cys Penetratin (Antp₅₂₋₅₈) derivatives is shown in Scheme 3-3.

Scheme 3-3: Synthesis of the *N*-isobutyryl Cys Antp₅₂₋₅₈ derivatives.



The first residue to be introduced to the resin linker was Fmoc-Lys(ivDde)-OH using HATU and DIPEA. All subsequent amino acids were then coupled to the peptidyl resin using HATU to afford intermediate **58**. The final Fmoc-Cys(Trt)-OH residue was coupled to the peptidyl resin using HOAt and DIC to reduce racemisation.²¹¹ This was followed by Fmoc deprotection and *N*-capping with an isobutyryl moiety using isobutyric anhydride to yield the peptidyl resin **59** (Scheme 3-3, steps i- iv).

The next step was the orthogonal deprotection of peptidyl resin **59** by removing the ivDde protecting group from the *C*-terminal lysine residue using 1% Hydrazine/DMF to afford intermediate **60** (Scheme 3-3, step v). The deprotection profile was monitored by detection of the chromophoric indazole reaction-product at 290 nm.²⁰⁷

Intermediate **60**, was universally deprotected and cleaved from the resin by acidolysis using 90% TFA to afford Antp₅₂₋₅₈ derivative **61** (Scheme 3-3, step vi). Alternatively, 5-FAM was coupled to **60** *via* the ϵ -amino group of the deprotected Lys using HOAt and DIC to afford intermediate **62** (Scheme 3-3, step vii-viii). Finally, the full deprotection of **62** and cleavage from the resin yielded the 5-FAM labelled Antp₅₂₋₅₈ derivative **63** (Scheme 3-3, step ix). The crude HPLC traces of the two *N*-isobutyryl cysteinyl Antp₅₂₋₅₈ derivatives **61** (t_R 3.12 min) and **63** (t_R 7.16 min) are shown in Figure 3-12 a) and b), respectively.

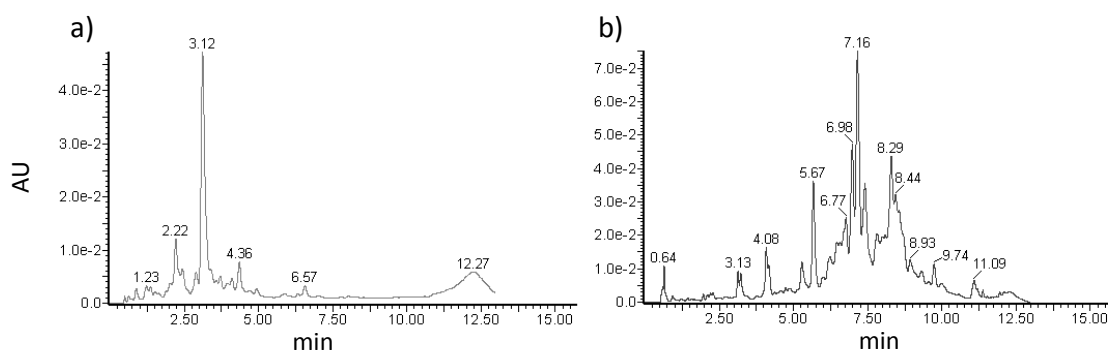


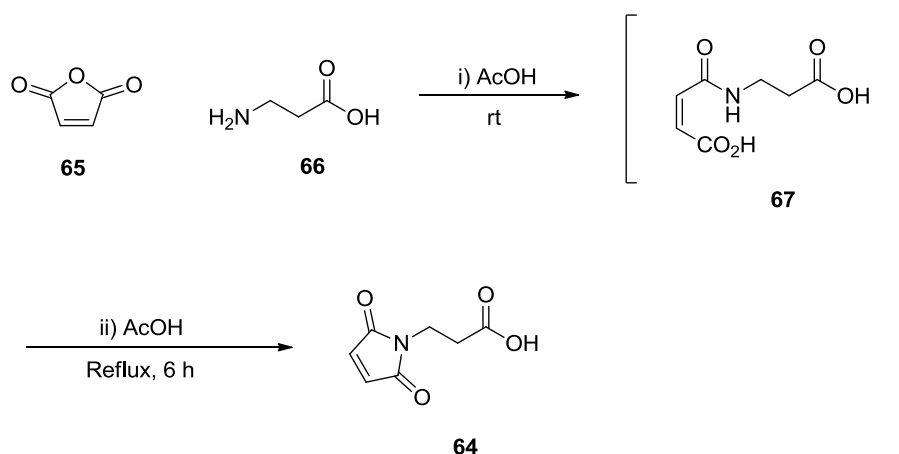
Figure 3-12: The crude HPLC trace of a) Antp₅₂₋₅₈ derivative **61** b) Antp₅₂₋₅₈ derivative **63**. Samples were run using the method; 10-40% B over 10 min, 3 ml/min. The column used was an Onyx Monolithic analytical C₁₈ column (100 x 4.6 mm).

The synthesis of both the Antp₅₂₋₅₈ derivatives **61** and **63** was successful, preparative HPLC was used to isolate the peptides in a purity of >85% and isolation yields of 51% and 46% for **61** and **63**, respectively. The general concepts outlined for the synthesis of

61 and **63** were applied to the synthesis of *N*-maleimido functional Antp₅₂₋₅₃ derivatives.

It was proposed that introduction of *N*-maleoyl- β -alanine **64** to the *N*-terminus of the Antp₅₂₋₅₈ peptidyl resin following the method described by Hansen *et al.* (1998) would afford the *N*-maleimidopropionyl Antp₅₂₋₅₈ derivative.¹⁶³ The first step taken was the synthesis of *N*-maleoyl- β -alanine **64** following the literature precedent (Scheme 3-4).²¹²

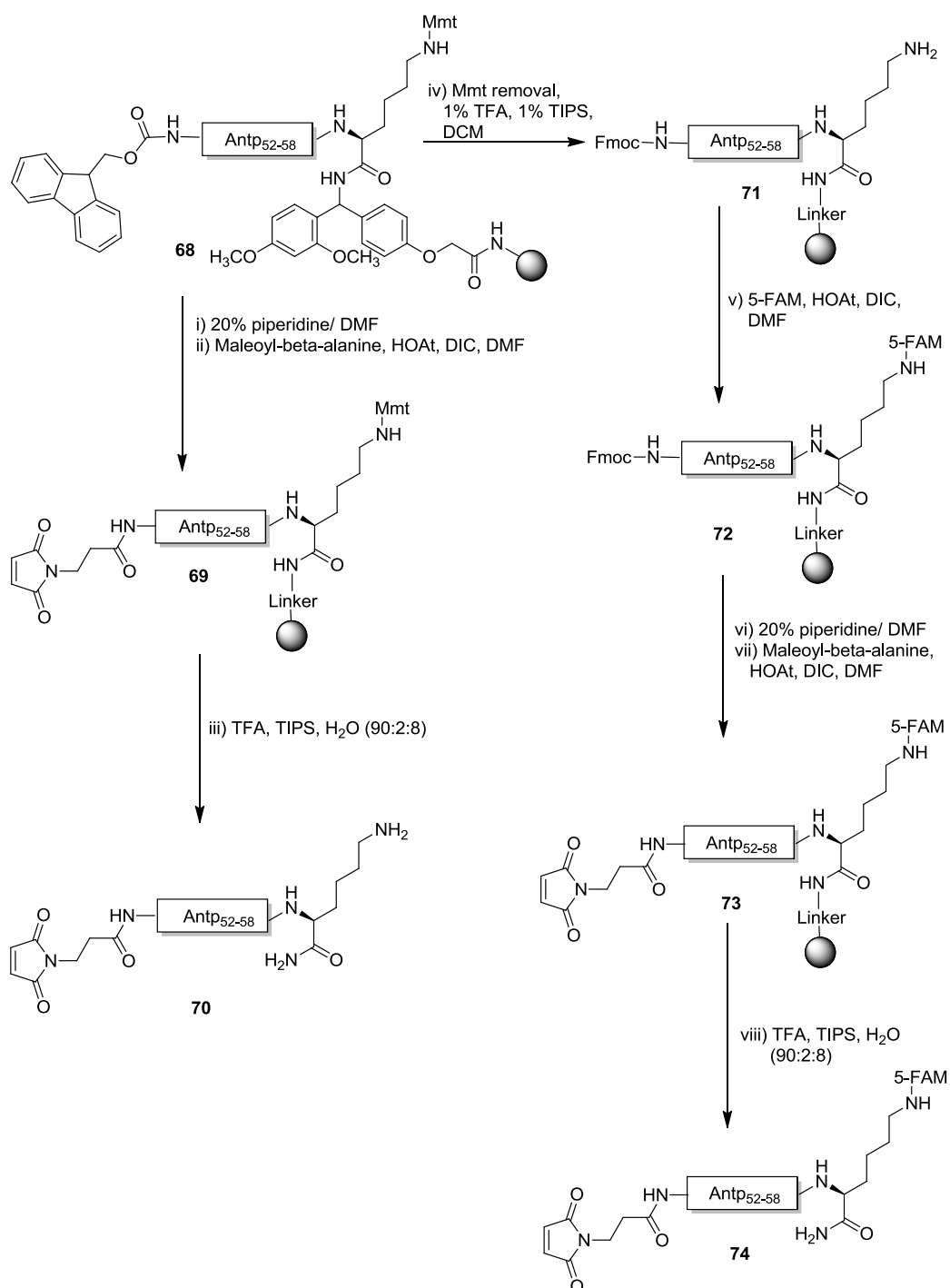
Scheme 3-4: Synthesis of *N*-maleoyl- β -alanine **64**.



The condensation of stoichiometric quantities of maleic anhydride **65** and β -alanine **66** in AcOH afforded the intermediate **67** at rt as a white precipitate (Scheme 3-4, i). The acid-catalysed intramolecular attack of the carbonyl group by the amide was then promoted by reflux of **67** in AcOH to afford the maleimide **64** after silica chromatography in a yield of 50% (Scheme 3-4, ii), which was spectroscopically identical to the literature.²¹² A scale-up of the reaction, to gram scale, resulted in no decrease in yield or purity.

The synthesis of *N*-maleimidopropionyl Antp₅₂₋₅₈ derivatives was achieved following Scheme 3-5. The first residue to be introduced to the rink amide resin was Fmoc-Lys(Mmt)-OH. The Mmt protecting group was used as an alternative to the hydrazine-labile ivDde protecting group. This was to avoid the potential Michael addition of hydrazine to the unsaturated imide of the maleimide moiety.

Scheme 3-5: Synthesis of *N*-maleimidopropionyl Antp₅₂₋₅₈ derivatives.



After the coupling of all the residues to the peptidyl resin, the *N*-terminal Fmoc group was deprotected, followed by introduction of *N*-maleimide-β-alanine **64** to peptidyl resin using HOAt and DIC to afford intermediate **69** (Scheme 3-5, steps i-ii). The full deprotection of **69** and cleavage from the resin using TFA-TIPS-H₂O (90:2:8) yielded the *N*-maleimidopropionyl Antp₅₂₋₅₈ derivative **70** as the major product (Scheme 3-5, step iii). Following this approach the longer Antp₄₃₋₅₈ derivative **75** was also

synthesised. Figure 3-13 shows the crude analytical HPLC of both *N*-maleimidopropionyl functional peptides **70** (t_R 3.02 min) and **75** (t_R 3.23 min).

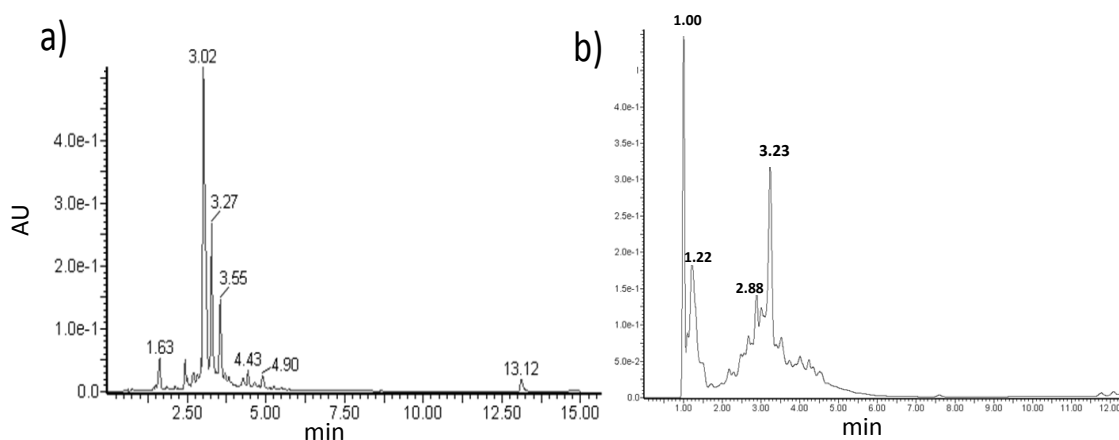


Figure 3-13: The crude HPLC trace of a) Antp₅₂₋₅₈ derivative **70** (t_R 3.02 min), b) Antp₄₃₋₅₈ derivative **75** (t_R 3.23 min). Peptide **70** was analysed using 20-30% B over 10 min and peptide **75** was analysed using 20-70% B over 10 min, 3 ml/min and an Onyx Monolithic analytical C₁₈ column (100 x 4.6 mm).

Following successful synthesis of peptides **70** and **75**, the introduction of 5-FAM to the maleimido functional Antp₅₂₋₅₈ derivative was investigated. In the first instance, the Mmt protecting group was removed from *N*-maleimidopropionyl functionalised intermediate **69** using 1% TFA, 1% TIPS in DCM. This was followed by the introduction of 5-FAM to the Lys side-chain using HOAt and DIC, as previously described. However, the final 20% piperidine/DMF step to removal 5-FAM polymeric phenolic esters proved problematic. It became evident that the order of *N*-maleoyl- β -alanine and 5-FAM coupling was extremely important. The final piperidine wash resulted in the addition of piperidine to the unsaturated imide of maleimide, thus deactivating the functional group. To overcome this, the Mmt deprotection was performed before the removal of the *N*-terminal Fmoc group, to afford intermediate **71** (Scheme 3-5, step iv). This allowed for the coupling of 5-FAM to the Lys side-chain (Scheme 3-5, step v) to yield **72**. Treatment of **72** with 20% piperidine/DMF removed the *N*-terminal Fmoc group allowing for the introduction of *N*-maleoyl- β -alanine using HOAt and DIC to give **73** (Scheme 3-5, steps vi-vii). Finally the full deprotection of **73** and cleavage from the resin by acidolysis yielded the 5-FAM labelled *N*-maleimidopropionyl Antp₅₂₋₅₈ derivative **74** as the major product (Scheme 3-5, step viii). The crude HPLC trace for 5-FAM labelled Antp₅₂₋₅₈ derivative **74** (t_R 4.34 min) is shown in Figure 3-14.

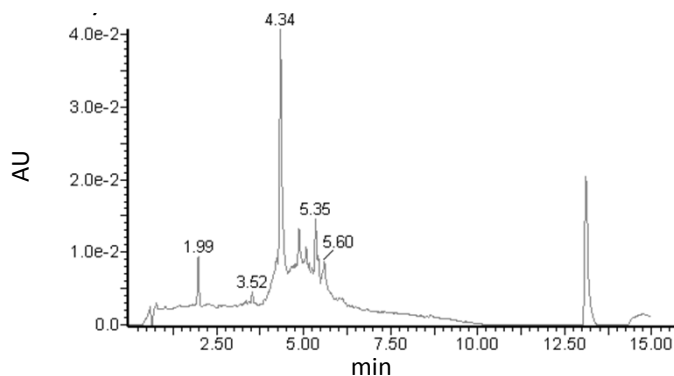
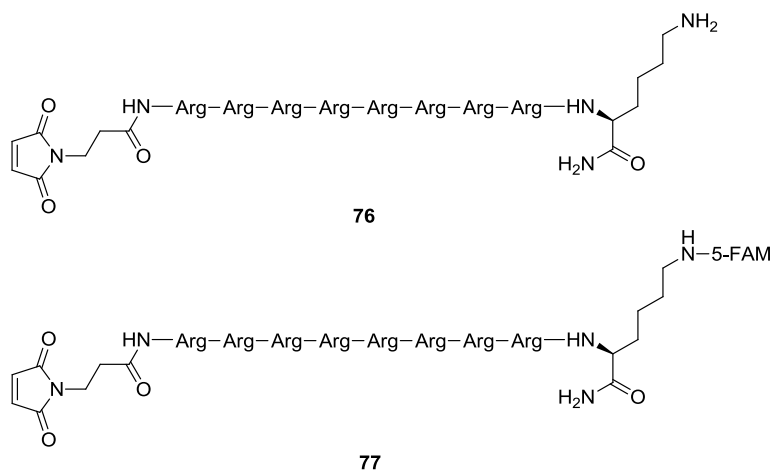


Figure 3-14: The analytical HPLC trace of crude peptide Antp₅₂₋₅₈ derivative **74** (t_R 4.34 min) analysed using 1-90% B over 10 min, 3 ml/min with an Onyx Monolithic analytical C₁₈ column (100 x 4.6 mm).

The synthetic strategies described in this section were applied to the synthesis of octa-arginine, HIV Tat and (Pro)₁₄ derivatives.

3.3.3 Octa-arginine derivatives

N-Maleimidopropionyl octa-arginine derivatives **76** and **77** were synthesised following the same method described for *N*-maleimidopropionyl Antp derivatives **70**, **74** and **75** (see Scheme 3-5).



The synthesis of the octa-arginine derivatives was achieved using the coupling reagent PyOxim[®].²¹³ The acylation reaction for each Fmoc-Arg(Pbf)-OH introduced to the peptidyl resin was repeated, before Fmoc deprotection, to insure complete coupling. The successful coupling of *N*-maleoyl- β -alanine followed by cleavage and deprotection afforded *N*-maleimidopropionyl octa-arginine **76** as the major product. Alternatively, 5-FAM was introduced to the peptidyl resin followed by cleavage and

deprotection of the peptide to afford the 5-FAM labelled octa-arginine **77** as the major product (Scheme 3-5, v-viii). Figure 3-15 shows the crude HPLC traces for **76** (t_R 3.00 min) and **77** (t_R 6.27 min).

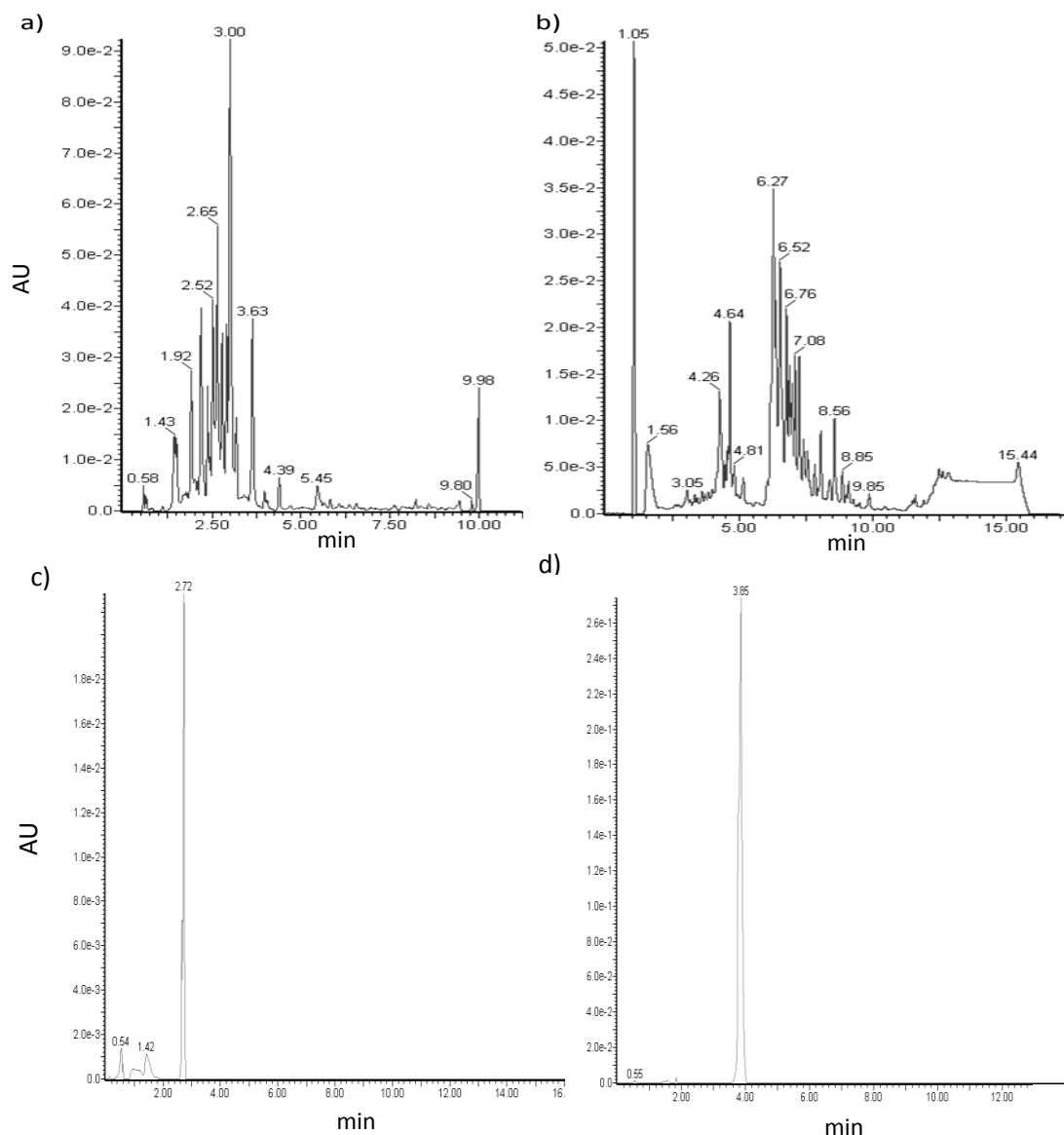


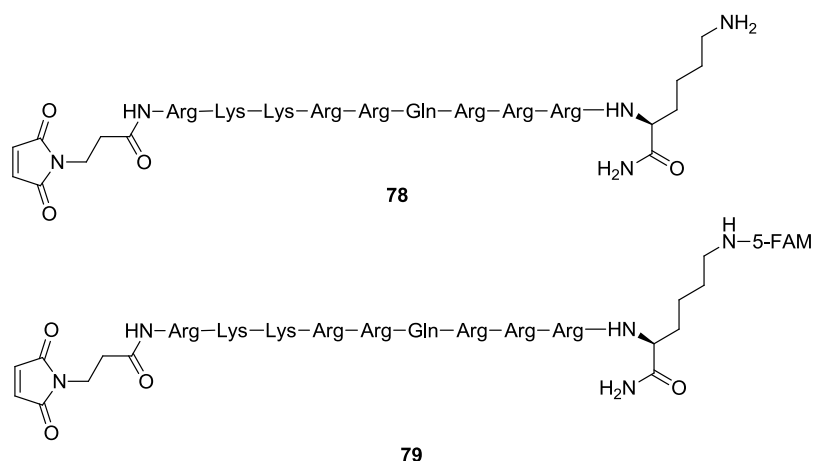
Figure 3-15: The analytical HPLC trace of crude peptide a) octa-arginine derivative **76** (t_R 3.00 min), 1-90% over 15 min, 3 ml/min b) octa-arginine derivative **77** (t_R 6.27 min), 1-50% B over 10 min, 3ml/min, c) purified **76** (t_R 2.72 min), 1-90% B over 10 min, d) purified **77** (t_R 3.85 min), 1-90% B over 10 min . Both crude and purified peptides were analysed using an Onyx Monolithic analytical C_{18} column (100 x 4.6 mm).

The relatively unclean synthesis of **76** and **77** is most likely attributable to incomplete coupling of Fmoc-Arg(Pbf)-OH. Nevertheless, the purity and yields achieved after

preparative HPLC were suitable for the current study, providing sufficient material for conjugation to scFv-Cys.

3.3.4 HIV Tat₄₉₋₅₇ derivatives

The synthesis of HIV Tat₄₉₋₅₇ derivative **78** and the 5-FAM labelled derivative **79** was achieved using the same method used for the Antp derivatives (see Scheme 3-5).



Initially, synthesis was performed using the coupling reagent HATU and DIPEA. However, no major product could be detected by analytic HPLC. Monitoring of the effluent from the Fmoc deprotections at 290 nm gave indication of difficult amino acid couplings. Difficult couplings were signified by a reduced Fmoc deprotection peak, notably the glutamine and following arginine residue showed significantly reduced Fmoc deprotection profiles. Based on these observations, the acylation reactions to introduce Fmoc-Gln(Trt)-OH and Fmoc-Arg(Pbf)-OH to the peptidyl resin were repeated before Fmoc deprotection. These alterations had little effect on the crude peptidic material obtained, with no major species being detected.

However, repetition of the synthesis using the coupling reagent PyOxim[®], together with repetition of the acylation reaction for each amino acid was successful affording the Tat₄₇₋₅₈ derivative **78** as the major product. Following Scheme 3-5, successful introduction of 5-FAM was also achieved to afford the 5-FAM labelled Tat₄₇₋₅₈ derivative **79**. The crude HPLC traces for the Tat₄₇₋₅₈ derivatives **78** and **79** are shown in Figure 3-16.

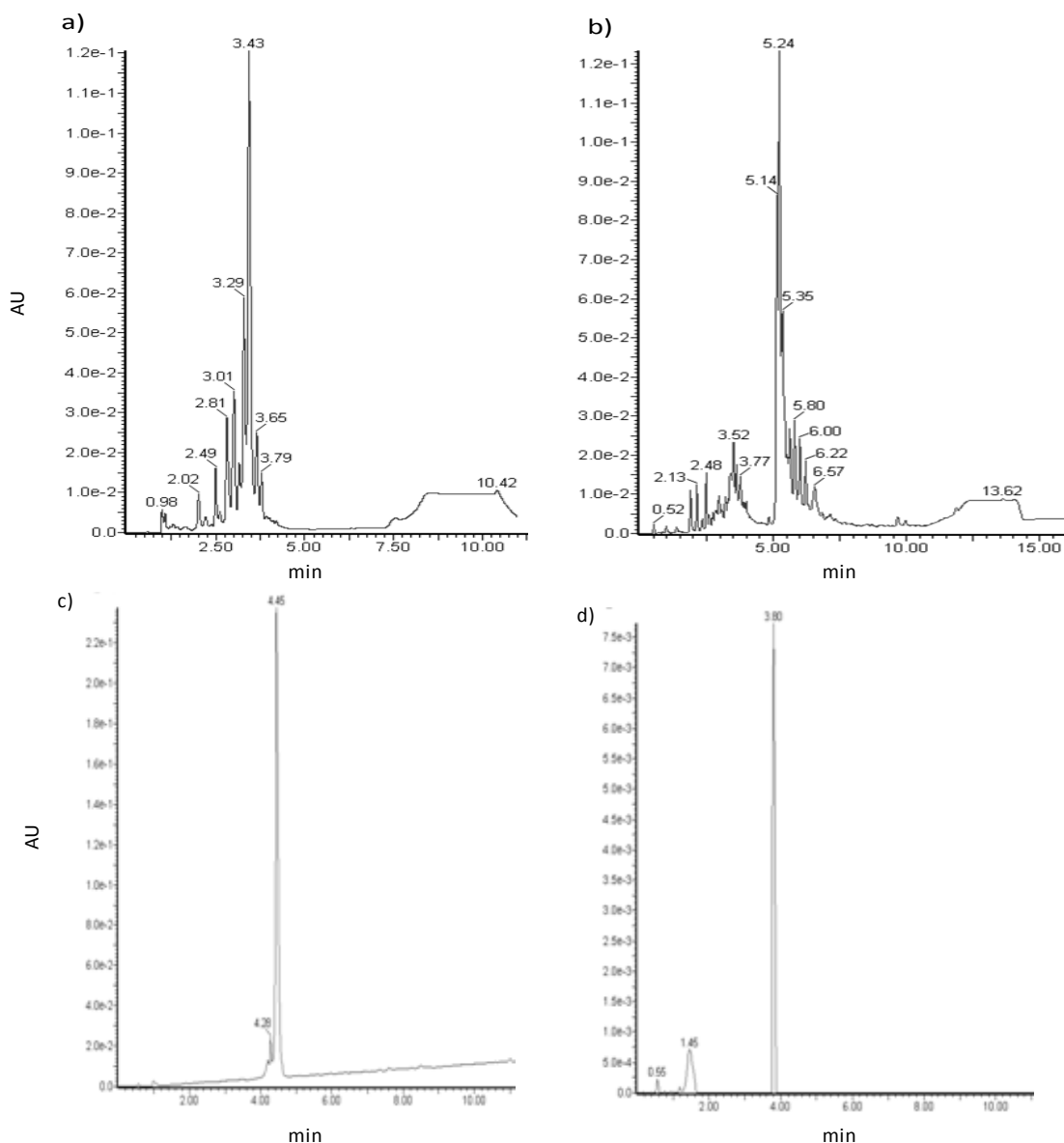
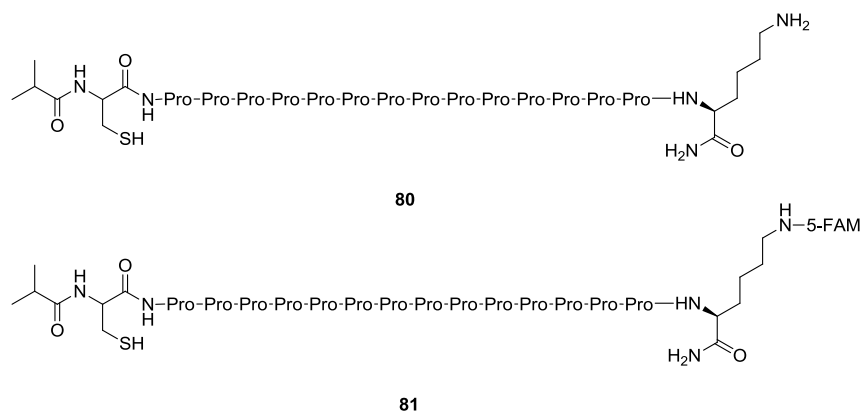


Figure 3-16: The crude HPLC trace of a) Tat₄₇₋₅₈ derivative **78** (t_R 3.43 min), 1-30% B over 6 min, 3 ml/min b) Tat₄₇₋₅₈ derivative **79** (t_R 5.24), 1-50% B over 10 min, 3 ml/min. c) purified **78** (t_R 4.45 min), 1-90% B over 15 min, d) purified **79** (t_R 3.80 min), 1-90% B over 10 min. Both crude and purified peptides were analysed using an Onyx Monolithic analytical C₁₈ column (100 x 4.6 mm).

The analytical HPLC traces of crude **78** and **79** show a major species at 3.43 and 5.24 min respectively, corresponding to the desired Tat₄₇₋₅₈ derivatives. The synthesis of **78** and **79** afforded material in yields and purity, after preparative HPLC, suitable for conjugation to scFv-Cys.

3.3.5 Pro₁₄ derivatives

The synthesis of *N*-isobutyryl Cys (Pro)₁₄-Lys amide **80** and *N*-isobutyryl Cys (Pro)₁₄-Lys(FAM) amide **81** was investigated to provide a (Pro)₁₄ derivative for conjugation to scFv. The cell penetrating capability of this scFv-(Pro)₁₄ conjugate can then be assessed using CLSM.⁹⁵ The synthesis of the Pro₁₄ derivatives was achieved following Scheme 3-3.



After assembly of the peptides and coupling of 5-FAM, the peptidyl resins were cleaved from the resin by acidolysis to afford the Pro₁₄ derivatives **80** and **81**. The crude HPLC traces for **80** (t_R 4.59 min) and **81** (t_R 7.33 min) are shown in Figure 3-17.

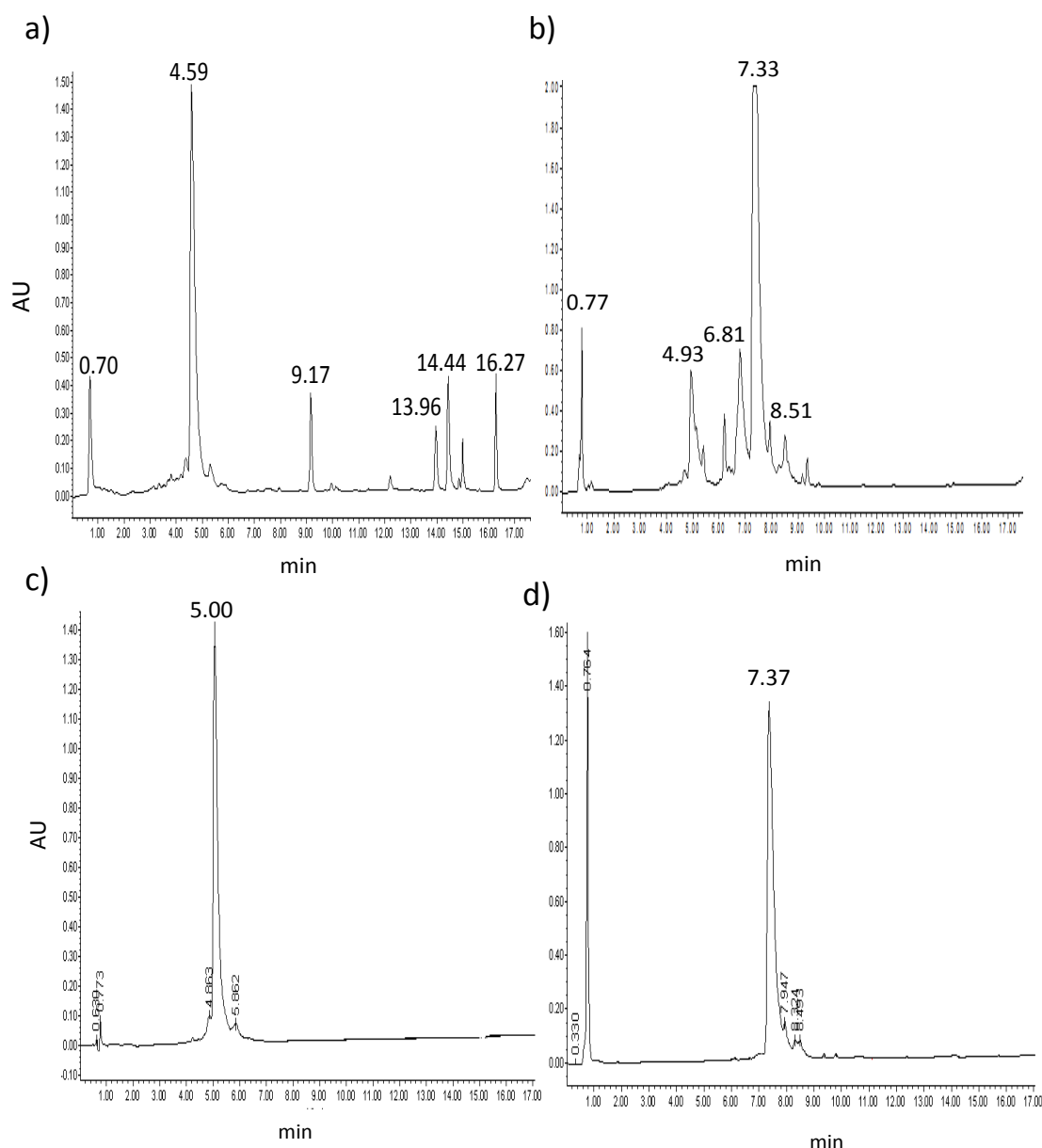


Figure 3-17: Crude HPLC trace of a) Pro₁₄ derivative **80** (t_R 4.59 min), b) Pro₁₄ derivative **81** (t_R 7.33 min), both peptides were analysed using 1-60% B over 12 min, 3 ml/min. c) purified **80** (t_R 5.00 min), 1-60% B over 12 min, d) purified **81** (t_R 7.37 min), 1-60% B over 12 min. Both crude and purified peptides were analysed using an Onyx Monolithic analytical C₁₈ column (100 x 4.6 mm).

The analytical HPLC of each peptide showed the presence of a major species. Further analysis of the major peak using TOF MS (ES⁺) showed the presence of a deletion sequence corresponding to (Pro)₁₄-Lys and (Pro)₁₄-Lys-(FAM) for **80** and **81**, respectively. The separation of these two species could not be achieved on a C₈ or C₁₈ column. As the deletion sequences will not interfere in the scFv conjugation both **80** and **81** were used as heterogeneous samples.

3.3.6 Summary of CPP derivative synthesis

A practical and robust synthetic approach for the synthesis of CPP derivatives has been developed. The described approaches allowed for labelling of peptides with 5-FAM and functionalisation of the *N*-terminus with either a maleimido or isobutyryl Cys moiety (Scheme 3-3 and Scheme 3-5).

Synthesis of *N*-maleimidopropionyl Antp derivatives **70**, **74** and **75** was high yielding with clean crude peptides being obtained. The synthesis of the arginine rich Tat₄₇₋₅₈ derivatives **78** and **79**, and octa-arginine derivatives **76** and **77** did not afford crude peptides of good purity. However, after purification, sufficient quantities of pure peptide were isolated for conjugation to scFv-Cys. The synthesised peptides were all purified by preparative RP-HPLC to afford peptides in good purity. The purity and HPLC isolation yields for each CPP derivative are shown in Table 3-3.

Table 3-3: CPP derivatives synthesised by Fmoc SPPS and purified by RP-HPLC with corresponding isolation yields and purity.

#	CPP	Sequence	Yield	Purity*	t _R / min [†]
61	Antp ₅₂₋₅₈	<i>i</i> But-C-RRMKWKK-K-[NH ₂]	51%	>85%	3.18
63	Antp ₅₂₋₅₈	<i>i</i> But-C-RRMKWKK-K(FAM)-[NH ₂]	46%	>90%	3.96
70	Antp ₅₂₋₅₈	Mal-RRMKWKK-K-[NH ₂]	69%	>90%	3.00
74	Antp ₅₂₋₅₈	Mal-RRMKWKK-K(FAM)-[NH ₂]	43%	>95%	4.30
75	Antp ₄₃₋₅₈	Mal-RQIKIWFQNRRMKWKK-K-[NH ₂]	20%	>90%	4.60
76	octa-arginine	Mal-(R) ₈ -K-[NH ₂]	15%	>90%	2.72
77	octa-arginine	Mal-(R) ₈ -K(FAM)-[NH ₂]	30%	>95%	3.85
78	Tat ₄₉₋₅₇	Mal-RKKRRQRRR-K-[NH ₂]	19%	>95%	2.55
79	Tat ₄₉₋₅₇	Mal-RKKRRQRRR-K(FAM)-[NH ₂]	36%	>95%	3.80
80	Pro ₁₄	<i>i</i> But-C-(P) ₁₄ -K-[NH ₂]	30%	>90%	4.72
81	Pro ₁₄	<i>i</i> But-C-(P) ₁₄ -K(FAM)-[NH ₂]	28%	>90%	5.00

* Peptide purity determined from intergration of HPLC peaks. † 1-90% B over 10 min, 3ml/min, Onyx monolithic C₁₈ (100 x 4.6 mm).

The synthesis of four different CPP derivatives possessing either an *N*-terminal maleimido or cysteine residue was successful, thus allowing for conjugation of the CPP derivatives to scFv-Cys. The successful introduction of 5-FAM to the CPP derivatives will allow for the investigation of scFv-CPP cell internalisation using CLSM or fluorescence microscopy.

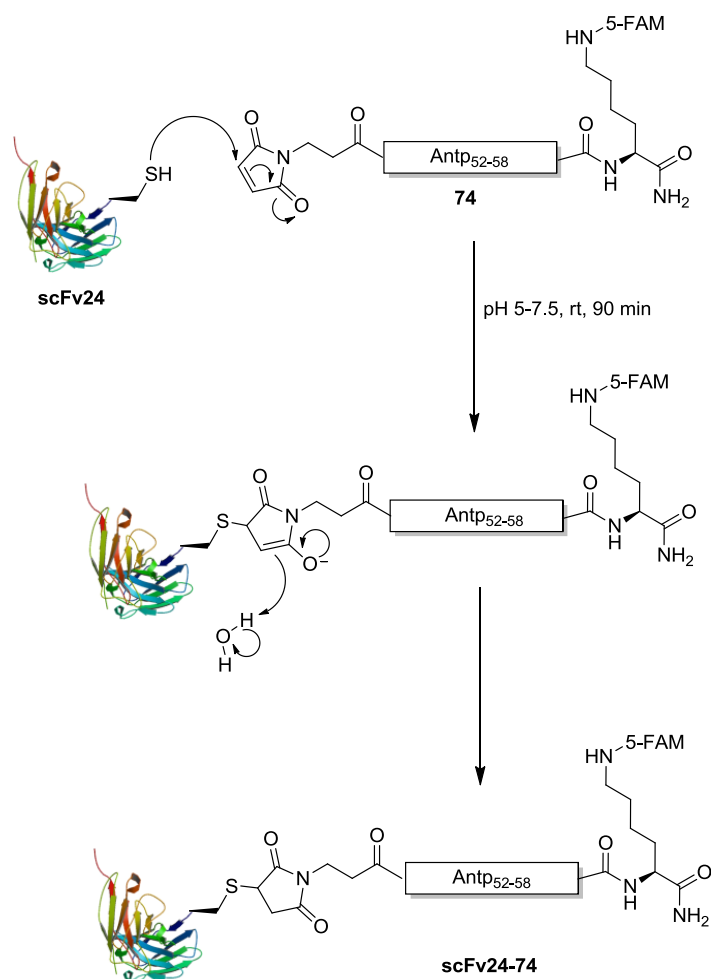
3.4 Preparation of scFv-CPP conjugates

It was previously proposed that an anti-Bcl-2/xL scFv-CPP conjugate will be able to internalise into cells, allowing for binding and inhibition of Bcl-2 or Bcl-xL. An important aspect of the scFv-CPP preparation is the development of efficient and simple methodology allowing for rapid screening of a panel of scFv-CPP conjugates in whole cell assays.

3.4.1 Thioether conjugation

Site-specific conjugation of *N*-maleimidopropionyl Antp₅₂₋₅₈-Lys(FAM) **74** to the previously expressed scFv-Cys (scFv24) was achieved following Scheme 3-6.

Scheme 3-6: Mechanism of *N*-maleimidopropionyl Antp₅₂₋₅₈ derivatives conjugation to scFv-Cys.



The conjugation of **74** to scFv24 was carried out in a sodium acetate buffer (pH 5.5) and in the presence of the reducing agent tris(2-carboxyethyl)phosphine (TCEP). This was to reduce any scFv-S-S-scFv dimers present, thus increasing the amount of scFv available for conjugation to **74**. A range of different TCEP concentrations were used to determine the optimum concentration for peptide conjugation. The scFv concentration was kept constant at 0.9 mg/ml in PBS (pH 7.4).

The first step was the addition of TCEP to scFv24 followed by incubation for 1 h at rt. The Antp₅₂₋₅₈ derivative **74** was then added at a 10x molar excess relative to the scFv. After 1 h, the conjugation of **74** was assessed using MALDI-TOF MS. Figure 3-18 shows the effect of the TCEP concentration on the percentage of **scFv24-74** formed in the conjugation reaction. The percentage of **scFv24-74** was determined from the MALDI-TOF MS peak intensities for the [M+H]⁺ species of scFv24 and **scFv24-74** observed at *m/z* 29000 and 30689, respectively.

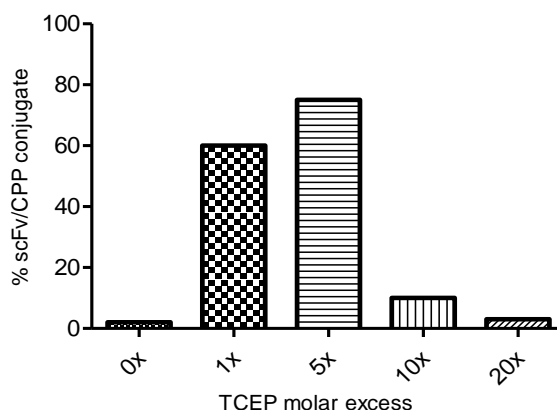


Figure 3-18: The effect of increasing TCEP concentration on maleimide conjugation to scFv-Cys. The percentage coupling was calculated from the peak intensity for the unlabelled and labelled scFv species using MALDI-TOF MS (sinapic acid matrix)

A 5x molar excess of TCEP allowed for 75% coupling of **74** to scFv24. However, an increase of TCEP to 10x and 20x molar excess resulted in a dramatic decrease in conjugation. Interestingly, the omission of TCEP resulted in no conjugation of **74** to scFv24, thus reduction of the scFv is an important step in this reaction. Although TCEP is advertised as being compatible with the maleimido moiety the findings here show that TCEP has a negative effect on the reactivity of the maleimido moiety, this is also supported by the similar findings of Getz *et al.* (1999) and Shafer *et al.* (2000).²¹⁴⁻²¹⁵

Moreover, the removal of TCEP by size exclusion, prior to the addition of peptide **74**, allowed for >95% conjugation of **74** to scFv24. This was confirmed by MALDI-TOF MS revealing a single peak at m/z 30689.0 assigned as $[M+H]^+$ for the **scFv24-74** conjugate. Figure 3-19 shows the MALDI-TOF MS spectra of the unlabelled scFv24 before treatment with TCEP, and the MS spectra of **scFv24-74**.

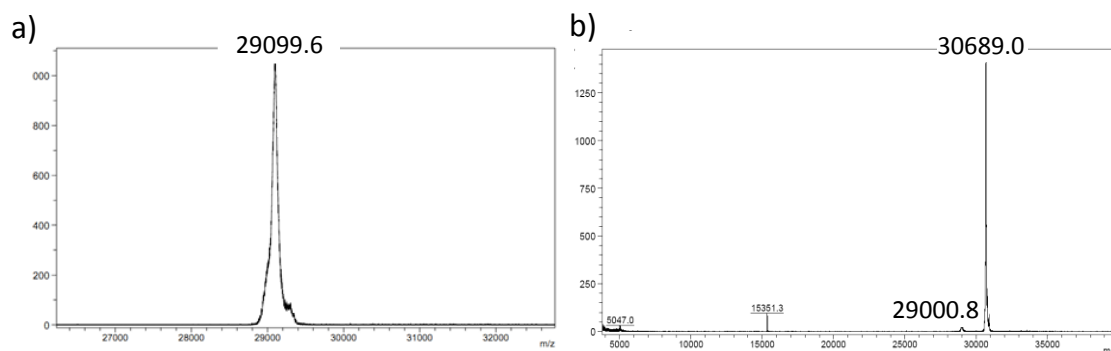


Figure 3-19: The MALDI-TOF MS traces for a) scFv24 and b) **scFv24-74** conjugate formed after treatment of scFv24 with TCEP followed by size exclusion and then addition of 10x molar excess of Antp₅₂₋₅₈-K(FAM) **74** and incubation for 1.5 h at rt.

In summary, >95% coupling of *N*-maleimidopropionyl Antp₅₂₋₅₈-Lys(FAM) **74** to scFv24 was achieved by initially treating the scFv with 5x molar excess of TCEP followed by removal, and then addition of a 10x molar excess of CPP. The method developed for conjugation of *N*-maleimidopropionyl CPPs to scFv24 was applied to the panel of synthesised CPP derivatives.

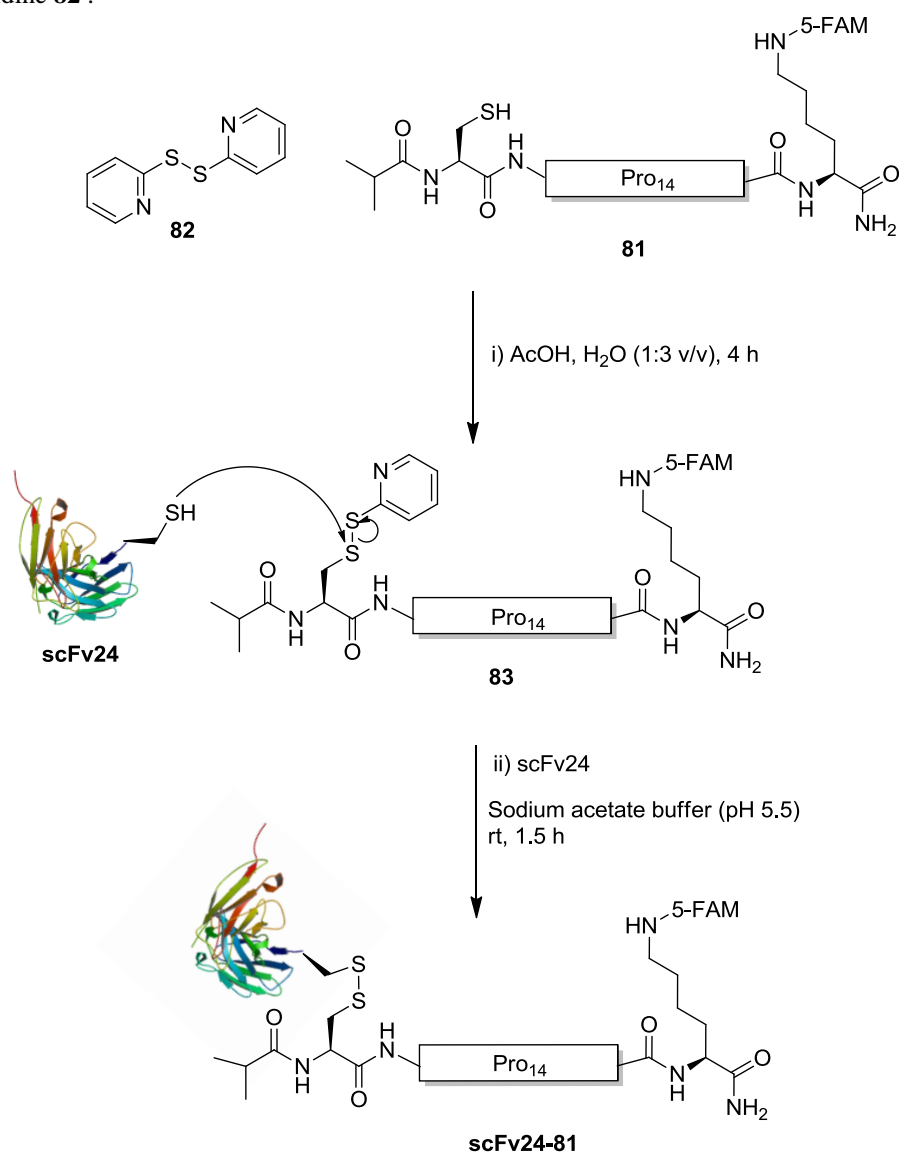
3.4.2 Disulfide conjugation

It was predicted that conjugation of a CPP derivative to scFv using a disulfide linkage would allow for cell internalisation and release of the scFv from the CPP in the reducing cellular environment.^{70,216} The formation of a disulfide bond between the C-terminally located cysteine residue of scFv24 and the *N*-terminal cysteine residue of *i*But-C-(P)₁₄-K(FAM)-[NH₂] **81** was investigated as a model reaction.

The first approach investigated for the conjugation of **81** to scFv24 *via* a disulfide bond was by air oxidation. In the first step, scFv24 was treated with 5x molar excess TCEP to reduce any scFv-S-S-scFv dimers. The reduced scFv solution was then buffer exchanged into deoxygenated PBS buffer (pH 8). This was followed by the addition of **81** at high dilution over 2 h with vigorous stirring until a 20x molar excess,

relative to scFv24 had been added. Unfortunately, this approach afforded only ~70% labelling of scFv24 with **77**. This was not improved with vigorous stirring and increased incubation time (24-48 h at rt). Using this approach, three possible species can be formed; CPP-S-S-CPP, CPP-S-S-scFv and scFv-S-S-scFv. Therefore, the formation of these dimers may have resulted in the low conjugation yields achieved. To encourage the formation of the scFv-S-S-CPP conjugate the cysteine residue of **81** was activated with 2,2-dithiodipyridine **82** using a method adapted from Rabanal *et al.* (1996)²¹⁷ (Scheme 3-7).

Scheme 3-7: Conjugation of *N*-maleimidopropionyl CPP derivatives to scFv-Cys using 2,2-dithiodipyridine **82**.



The activation of **81** was achieved using a 5x molar excess of 2,2-dithiodipyridine **82** in AcOH:H₂O (1:3). The reaction mixture was stirred for 4 h at rt, subsequent purification afforded the activated intermediate **83** in a yield of 65% (Scheme 3-7, i). The analytical HPLC of **83** showed the presence of one major species and synthesis of was confirmed by TOF MS (ES⁺) with a peak at m/z 1073.4878 being detected and assigned as the $[M+2H]^{2+}$ species.

ScFv24 was treated with a 10x molar excess of **83** in sodium acetate buffer (pH 5.5) for 1.5 h at rt, followed by analysis using MALDI-TOF MS (Figure 3-20).

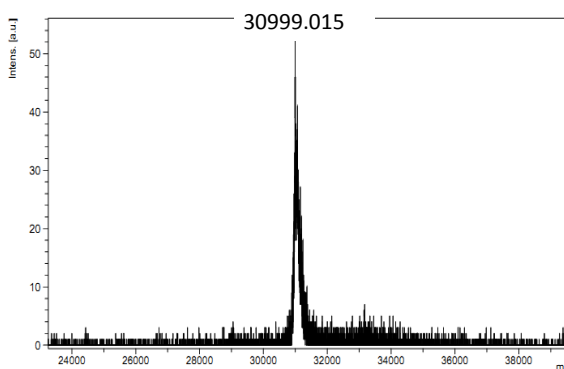


Figure 3-20: MALDI-TOF MS of **scFv24-81** after incubation with **136** for 1.5 h at rt.

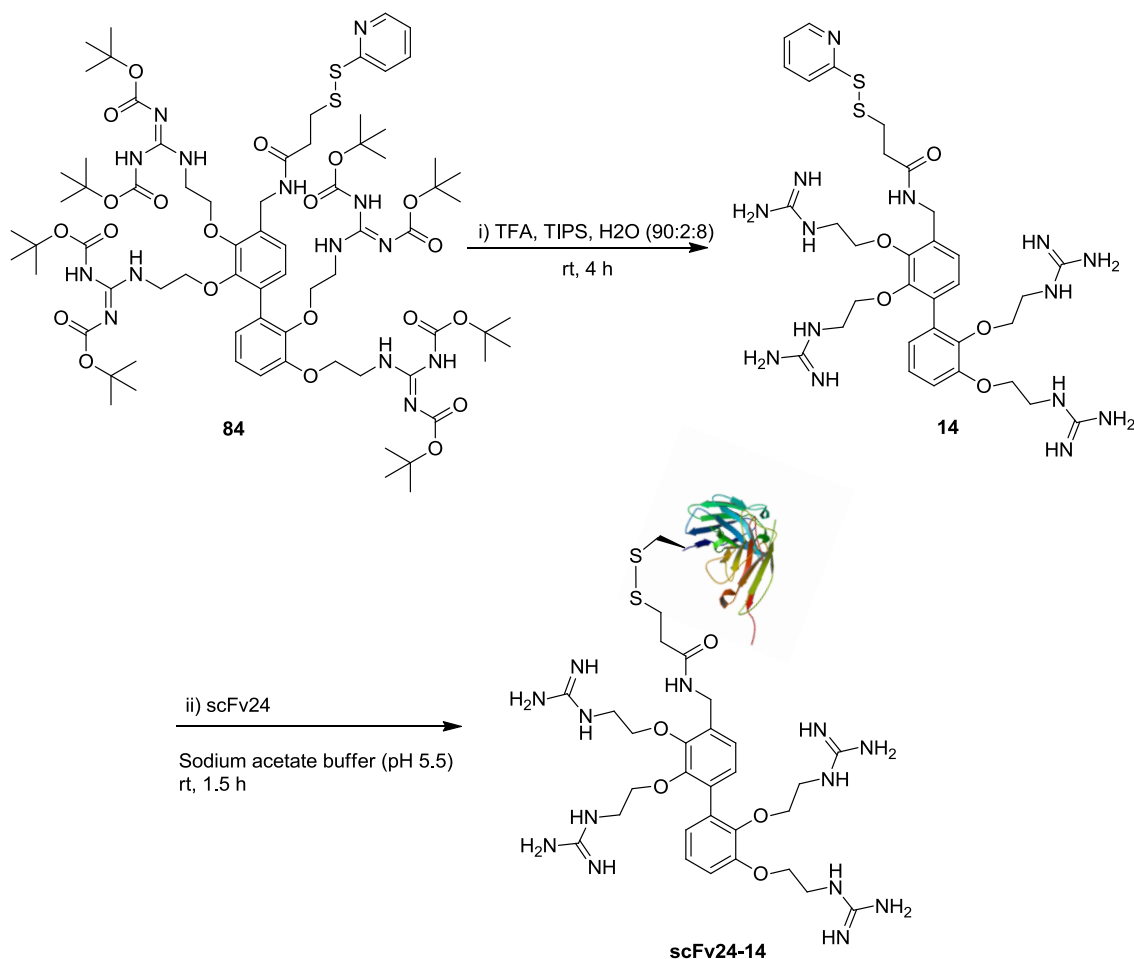
Figure 3-20 shows the complete conversion of scFv24 to form a single species at m/z 30999.0 assigned as the $[M+H]^+$ of **scFv24-81**. The activation of **81** with 2,2-dithiodipyridine **82** provides a simple and efficient method for coupling CPPs to scFv-Cys *via* a disulfide bond. This approach can be applied to the conjugation of other *N*-isobutryl Cys CPP derivatives.

3.4.2.1 ScFv conjugation to a small molecule carrier (SMoC)

To increase the possibility of achieving cellular internalisation of scFv24 and the induction of apoptosis, alternative delivery vectors were also investigated. Rebstock *et al.* (2008)⁹⁸ report the synthesis and application of a delivery vector based on a guanidine functionalised biphenyl scaffold. This small molecule carrier (SMoC) demonstrated efficient intracellular delivery of an attached biomolecule into a wide variety of cell types with good efficiency.⁹⁷ For this reason, the SMoC derivative **14** was conjugated to scFv24 and Cea6.

The Boc protected SMoC derivative **84** was synthesised by Charnwood Molecular Ltd. The Boc deprotection of **84** was achieved by acidolysis using 50% TFA in DCM to afford **14** in a quantitative yield (Scheme 3-8, i).⁹⁸

Scheme 3-8: Synthesis of scFv-SMoC conjugate **scFv24-14**.



The conjugation of **14** to scFv24 and Cea6 was achieved using the method described by Okuyama *et al.* (2007).⁹⁷ Briefly, a 10x molar excess of **14** was added to the scFv (3 mg/ml) in sodium acetate buffer (pH 5.5) (Scheme 3-8, ii). After 1.5 h at rt the reaction was analysed by MALDI-TOF MS (Figure 3-21).

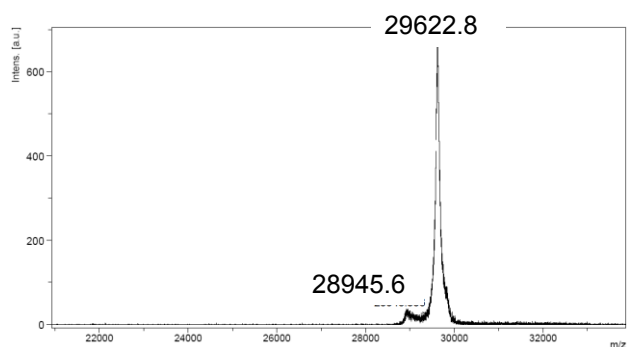


Figure 3-21: The MALDI-TOF MS trace for **scFv24-14** after incubation with SMOc **14** for 1.5 h at rt.

The successful conjugation of **14** to scFv24 and Cea6 was achieved with >95% conversion of the scFv to the **scFv24-14** and **Cea6-14** conjugate. **ScFv24-14** and **Cea6-14** were purified by size exclusion to afford the pure scFv conjugate in yields of 54% and 37%, respectively.

3.4.3 Summary of scFv-CPP conjugate preparation

The optimised conjugation methods allow for >90% conjugation of CPP derivatives to scFv. After the formation of scFv-CPP conjugates, unreacted CPP was removed by size exclusion using a HiPrep™ 26/10 desalting column (GE healthcare).

Table 3-4 shows the percentage conjugation of CPP derivatives to scFv24 and Cea6 together with the yields achieved after the conjugation and purification steps. The 5-FAM labelled CPP derivatives were also conjugated to scFv24 for determination of scFv24-CPP internalisation using fluorescence microscopy and CLSM.

Table 3-4: Summary of scFv-CPP conjugates purified by size exclusion.

scFv conjugate	Peptide	Yield	% of scFv labelled with peptide	MALDI-TOF MS, m/z [M+H] ⁺	
				Calc.	Obs. [†]
scFv24-74	Mal-RRMKKWKK-K(FAM)-[NH ₂]	31%	>95%	30696	30689
scFv24-76	Mal-(R) ₈ -K-[NH ₂]	78%	>95%	30573	30578
Cea6-76	Mal-(R) ₈ -K-[NH ₂]	33%	>95%	30423	30454
scFv24-77	Mal-(R) ₈ -K(FAM)-[NH ₂]	32%	>95%	30931	30928
scFv24-79	Mal-RKKRRQRRR-K(FAM)-[NH ₂]	34%	>95%	31004	31007
scFv84-79	Mal-RKKRRQRRR-K(FAM)-[NH ₂]	37%	~20%*	30142	n.d
Cea6-79	Mal-RKKRRQRRR-K(FAM)-[NH ₂]	32%	~35%*	30855	n.d
scFv24-81	iBut-C-(P) ₁₄ -K(FAM)-[NH ₂]	34%	>95%	31064	30999
scFv24-14	SMoC	54%	>95%	29621	29623
Cea6-14	SMoC	37%	>95%	29554	29553

*determined only from absorbance of 5-FAM using eq. 3. † The observed m/z for all scFv-CPP conjugates is within <0.2% error of the calculated m/z .

The successful conjugation of the CPP derivatives to scFv24 was confirmed by MALDI-TOF MS revealing [M+H]⁺ peaks for all of the scFv24-CPP conjugates (Table 3-4). A slightly lower yield for the scFv-CPP(FAM) conjugates was achieved compared to the scFv-CPP conjugates. This is attributable to greater precipitation of the scFv during the conjugation reactions when using the FAM labelled peptides. It is possible that the 5-FAM destabilised the protein upon conjugation, resulting in greater protein precipitation. The conjugation of 5-FAM labelled Tat₄₇₋₅₈ derivative **79** to scFv84 and Cea6 was also successful, however, MALDI-TOF MS did not detect the **scFv84-79** and **Cea6-79** conjugates. Thus, the successful conjugation of **79** to the scFv was confirmed from the absorbance ratio of the scFv and 5-FAM using eq. 3. The percentage conjugation was significantly lower than that achieved for the conjugation of **79** to scFv24. This may be attributable to the observed instability of these scFv compared to scFv24, resulting in greater protein precipitation during the conjugation reaction. Further investigation into the CPP conjugation conditions for scFv84 and Cea6 are required to increase yields and the percentage of CPP conjugation.

$$\text{Fluorophore/protein ratio} = \frac{A_{\text{max of labelled protein}}}{\epsilon * \text{protein concentration (M)}} * \text{dilution factor} \quad (\text{eq. 3})$$

A_{max} = Absorbance of sample measured at the wavelength maximum (λ_{max}) for the dye molecule
 ϵ = Molar extinction coefficient of 5-FAM ($M^{-1} \text{ cm}^{-1}$)

The activity of scFv-CPP conjugates was confirmed by ELISA. The retention of the scFv specificity for Bcl-2 and Bcl-xL is essential for the envisaged studies using these scFv-CPP conjugates. Figure 3-22 shows the positive binding of the scFv24-CPP conjugates to Bcl-xL, and **scFv84-79** binding to Bcl-2, determined using a direct binding ELISA.

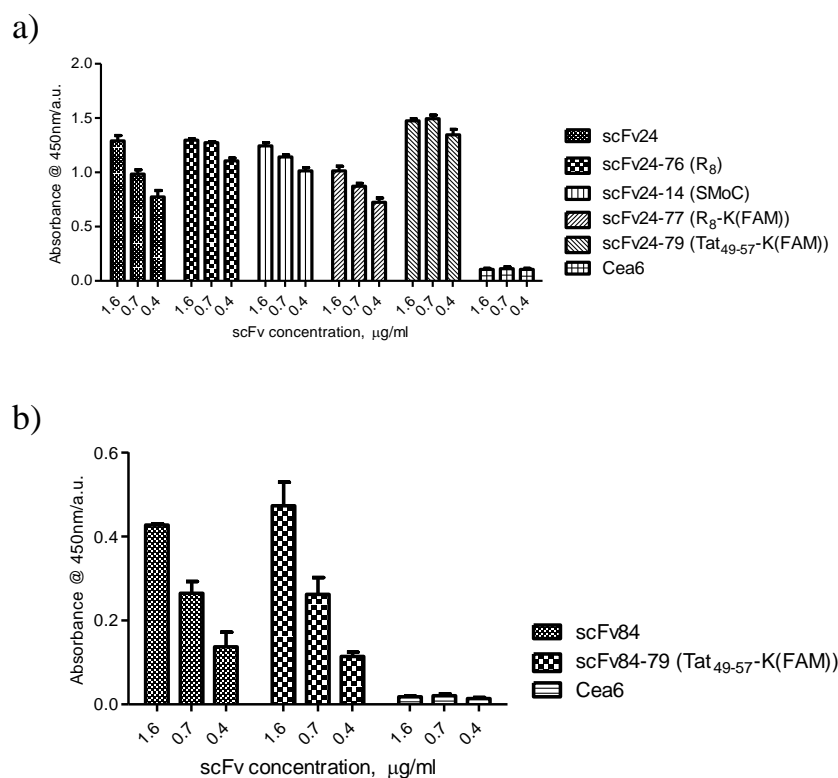


Figure 3-22: Analysis of scFv-CPP binding to Bcl-xL and Bcl-2 using a binding ELISA. Biotinylated Bcl-xL or Bcl-2 was coated onto streptavidin 96-well plates, followed by incubation with the corresponding scFv-CPP. After washing, bound scFv was detected using anti-myc mAb (9E3) and goat anti-mouse HRP conjugate, and finally developed with TMB. The plate was then read on an Envision plate reader at 450 nm. a) scFv24, scFv24-CPP and Cea6 binding to Bcl-xL. b) scFv84, **scFv84-79** and Cea6 binding to Bcl-2.

The antigen specificity of all of the scFv-CPP conjugates was retained, with similar binding to Bcl-2 and Bcl-xL being observed as the unconjugated scFv. Overall, the optimised methods for the preparation of scFv-CPP conjugates has allowed for >90% conjugation of the CPP derivatives to the purified scFv-Cys. Importantly, the antigen-binding of the scFv was retained after CPP conjugation, allowing for investigation into the cell internalisation and the biological effects of the scFv-CPP conjugates.

3.5 Cellular delivery of scFv-CPP(FAM) conjugates

The CPP mediated delivery of proteins can be determined using a variety of methods, for example flow cytometry²¹⁸, immunoprecipitation⁶³ and radiolabelling.⁶⁹ The most common approach is through attachment of a fluorophore to the CPP allowing for detection of cell internalised CPP using fluorescence microscopy or confocal laser scanning microscopy (CLSM).^{63, 65}

When investigating the internalisation of CPP conjugates using fluorescent probes it is important to ensure that false positives are not obtained and that the limitations of the technique used are taken into account. Cationic CPPs will adhere to the negatively charged cell membrane, which can lead to the overestimation of CPP internalisation.⁹⁹ The possibility of artefacts is also increased when using fixed cells, as this can permeabilise the cell membrane resulting in increased CPP uptake, leading to overestimation of CPP internalisation.⁹⁹ Thus, in this study only live cells were used to minimise the potential for artefacts.

3.5.1 Fluorescence microscopy

Fluorescence microscopy was used to assess the internalisation of scFv-CPP conjugates and to compare the effectiveness of each CPP derivative. Using fluorescence microscopy it is not possible to discriminate between membrane associated and intracellular fluorescence. However, removing membrane adsorbed peptides before fluorescence microscopy can avoid artefacts. A simple method to remove membrane bound CPPs described by Kameyama *et al.* (2007) is to wash cells treated with CPPs with an acidic buffer (3 M glycine, pH 3) before imaging.²¹⁹

The internalisation of the scFv-CPP(FAM) conjugates into HeLa cells was investigated by incubation of the cells with a 10 µM solution of scFv-CPP(FAM) for 30 min at 37 °C. Following incubation, the medium was removed and the cells were washed twice with an acid wash buffer (3 M Glycine, pH 3), twice with PBS (pH 7.4) and finally left in Hanks balanced salt solution (HBSS buffer) containing the membrane permeable nuclear stain Hoechst 33342. The fluorescence microscopy images for HeLa cells treated with 10 µM of scFv24 labelled with Antp₅₂₋₅₈ (**scFv24-**

74), octa-arginine (**scFv24-77**) and Tat₄₉₋₅₇ (**scFv24-79**) are shown in Figure 3-23. The nuclei are shown in blue and the scFv24-CPP conjugates are shown in green.

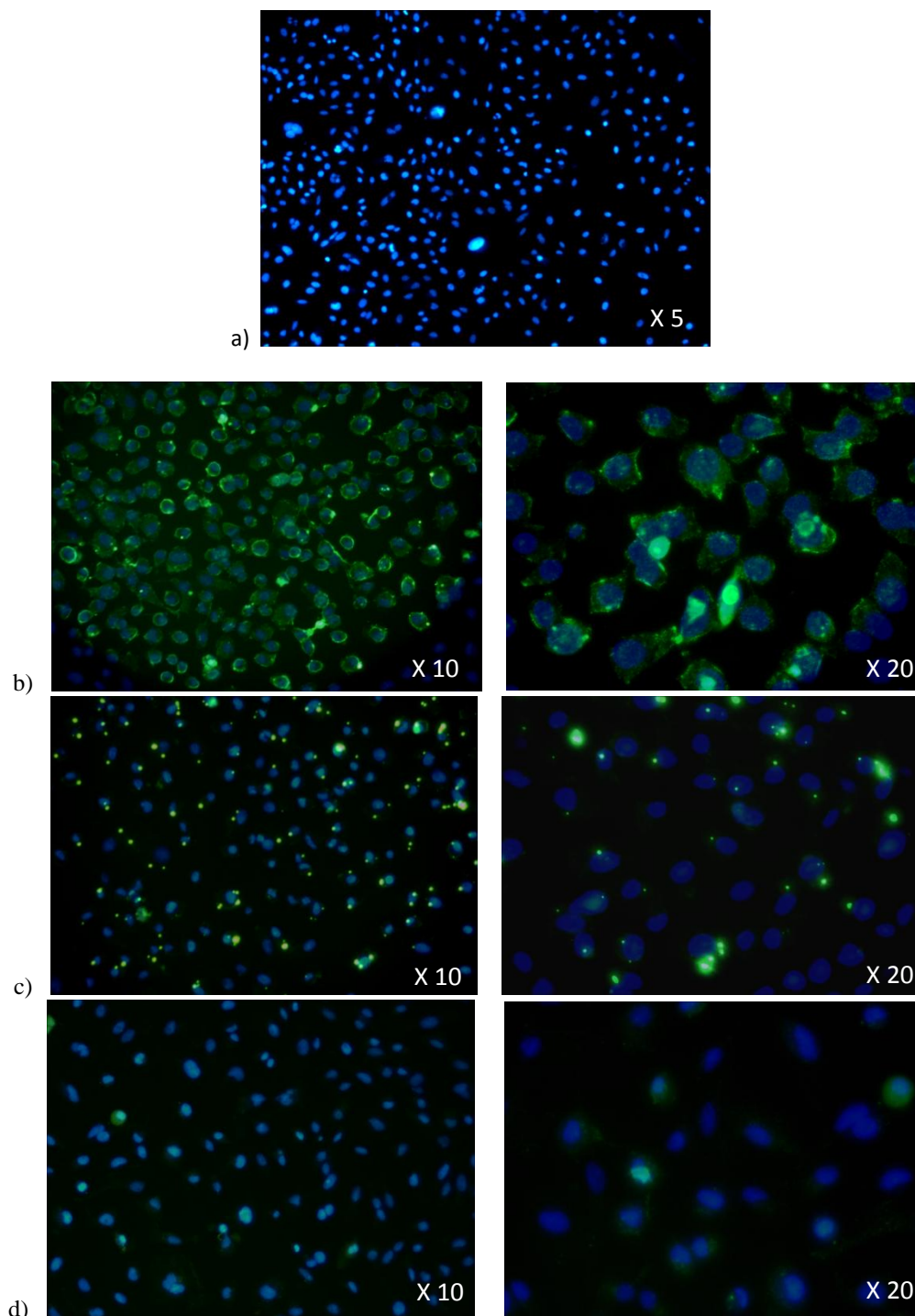


Figure 3-23: Fluorescence microscopy of HeLa cells treated with scFv-CPP(FAM) (Green) for 30 min at 37°C a) vehicle only control b) **scFv24-77**, 10 μ M c) **scFv24-79**, 10 μ M d) **scFv24-74**, 10 μ M. The cells were also incubated with the nuclear stain Hoechst 33342 (blue). The magnifications shown for each image are the objective magnification used.

The image of untreated HeLa cells (Figure 3-23, a) shows no auto-fluorescence, thus acting as a control for comparison to cells treated with scFv-CPP(FAM) conjugates. Figure 3-23 b) shows cells treated with the scFv-octa-arginine conjugate **scFv24-77**, the cell associated fluorescence of **scFv24-77** is of greater intensity than the other scFv-CPP conjugates and appears to be uniformly distributed throughout the cells.

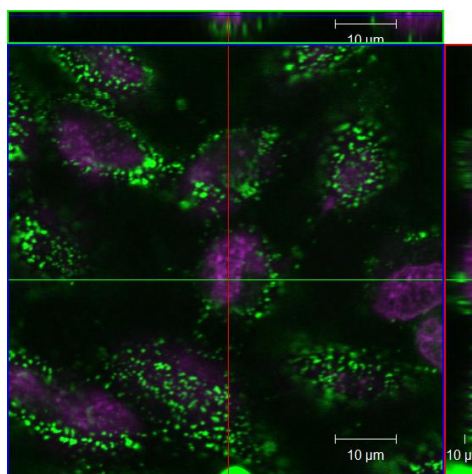
ScFv24 labelled with Tat₄₉₋₅₇ (**scFv24-79**) and Antp₅₂₋₅₈ (**scFv24-74**) (Figure 3-23, c and d) shows very different fluorescent localisation compared to **scFv24-77**. The punctate fluorescence of the HeLa cells treated with **scFv24-79** appears to be cell associated, suggesting localisation of the scFv in cellular vesicles. However, it is not possible using fluorescence microscopy to firmly determine if this fluorescence is membrane bound or intracellular. Notably, there is little cell associated fluorescence seen for the scFv-Antp₅₂₋₅₈ conjugate **scFv24-74**. Thus, it was concluded that Antp₅₂₋₅₈ was not a suitable for the intracellular delivery of scFv into HeLa cells.

3.5.2 Confocal Laser Scanning Microscopy (CLSM)

CLSM was used to confirm that the scFv-octa-arginine conjugate **scFv24-77** and the scFv-Tat₄₉₋₅₇ conjugate **scFv24-79** are internalised into cells. CLSM allows for in-focus imaging at selected depths of a sample by using a point source of light and pinhole to reject light that is not incident from the focal plane.²²⁰ In the context of this study this allows for focussing within the cell, distinguishing between membrane bound and cell internalised scFv-CPP conjugates, avoiding the possibility of artefacts associated with membrane adsorbed CPPs.

HeLa or Rat Basophilic Leukaemia (RBL-2H3) cells were incubated for 30-90 min at 37 °C with 10 µM of either **scFv24-77** or **scFv24-79**. After incubation, the cells were washed with PBS and incubated with 5 µM of the nuclear stain Draq5 (Ex 646 nm/Em 681 nm). The unfixed live cells were then imaged using an inverted x63 oil immersion lens. Figure 3-24 shows the confocal images taken at selected depths within the cell (z-sectioning) after HeLa cells were incubated with a 10 µM solution of **scFv24-77** for either 30 or 90 min at 37 °C.

a) 30 min



b) 90 min

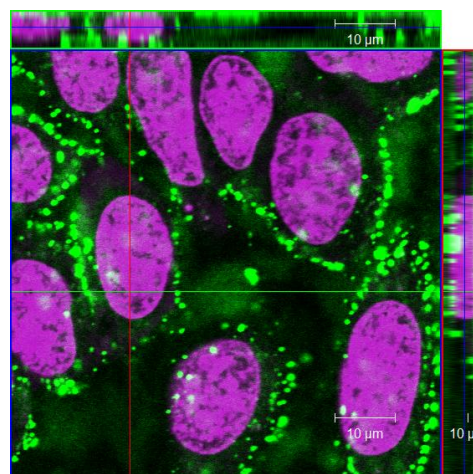


Figure 3-24: Z-sectioning using confocal microscopy of HeLa cells treated with 10 μ M of **scFv24-77** (Green) for a) 30 min at 37 °C and b) 90 min at 37 °C. Draq5 was used as a nuclear stain (Purple).

The punctate co-localisation of **scfv24-77** in the HeLa cells after 30 and 90 min incubate (Figure 3-24 a and b) is indicative of endosomal entrapment of a CPP⁹⁹, z-sectioning of the cells also confirmed that the fluorescence observed is intracellular, suggesting that **scFv24-77** is internalised into HeLa cells by an endocytic route. The z-sectioning of RBL-2H3 cells incubated with **scFv24-77** for 30 min is shown in Figure 3-25.

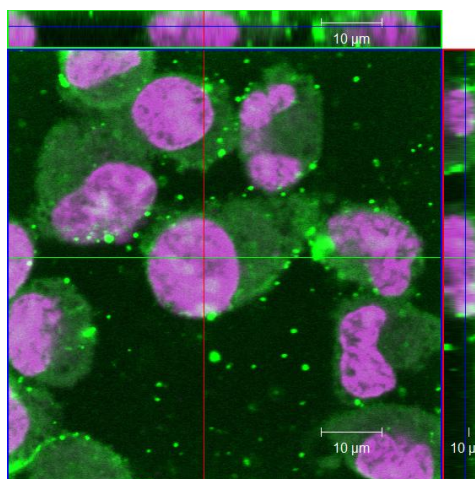


Figure 3-25: Z-sectioning using confocal microscopy of RBL-2H3 cells treated with 10 μ M of **scFv24-77** (Green) for 30 min at 37 °C. Draq5 was used as a nuclear stain (Purple).

Interestingly, RBL-2H3 cells incubated with **scFv24-77** show very different localisation compared to the HeLa cells. The uniform fluorescence of the whole cell suggests cytoplasmic localisation of **scFv24-77**. This encouraging data suggests that the **scFv24-77** conjugate will be able bind to Bcl-2 and Bcl-xL in RBL-2H3 cells. Figure 3-26 a) shows the z-sectioning of HeLa and RBL-2H3 cells incubated for 30 and 90 min with a 10 μ M solution of the Tat₄₉₋₅₇ conjugate **scFv24-79** at 37 °C.

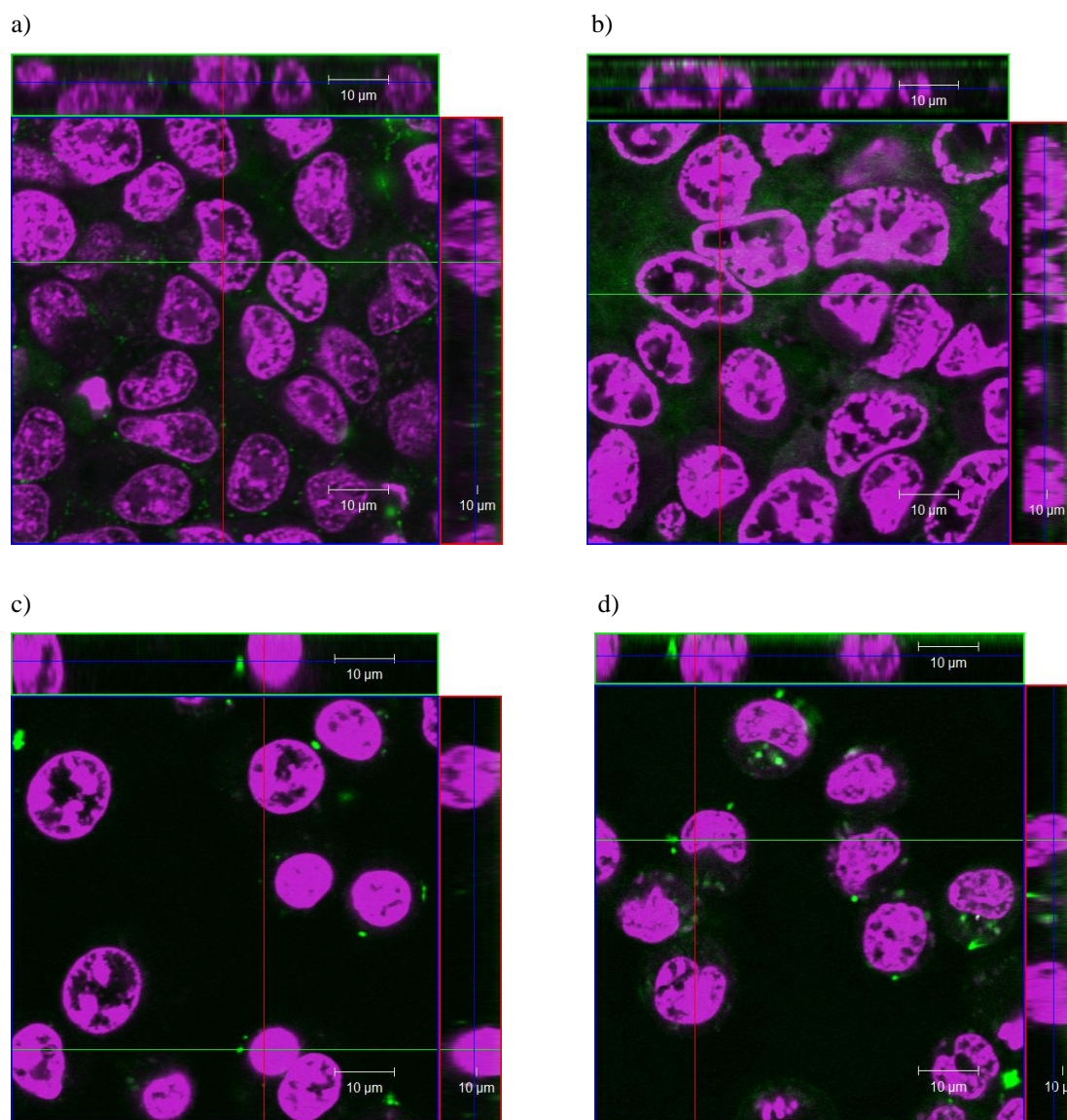


Figure 3-26: CLSM z-sectioning of HeLa and RBL-2H3 cells treated with 10 μ M of the scFv-Tat₄₉₋₅₇ conjugate **scFv24-79** (Green) a) HeLa cells, 10 μ M **scFv24-79**, 30 min at 37 °C b) HeLa cells, 10 μ M **scFv24-79**, 90 min at 37 °C, c) RBL-2H3 cells, 10 μ M **scFv24-79**, 30 min at 37 °C, d) RBL-2H3 cells, 10 μ M **scFv24-79**, 90 min at 37 °C. After incubation with **scFv24-79** the cells were incubated with 5 μ M Draq5 to stain the cell nuclei (Purple).

After incubation of **scFv24-79** with HeLa and RBL-2H3 cells for 30 min there was no significant cell associated fluorescence observed (Figure 3-26, a and c). After incubation of **scFv24-79** for 90 min with HeLa cells, single points of intense fluorescence are seen (Figure 3-26, b and d). This fluorescence appears to be intracellular and possibly a result of scFv localising in cellular vesicles. The incubation of RBL-2H3 cells with **scFv24-79** for 30 min gave similar results to that observed with HeLa cells. However, after 90 min the fluorescence intensity was significantly greater (Figure 3-26, d). The punctate fluorescence seen after incubation of **scFv24-79** with RBL-2H3 cells again suggests co-localisation of the scFv-CPP in cellular vesicles.

The distinctly different localisations seen for **scFv24-74** and **scFv24-79** after incubation with HeLa and RBL-2H3 cells suggests that the scFv-CPP conjugates are internalised by different mechanisms. A number of studies have reported that CPP internalisation varies dependant on the CPP, cell type, exposure time, temperature, peptide concentration and treatment of cells (un-fixed and fixed).^{99,82,221} Therefore, the differences in cellular localisation observed for **scFv24-74** and **scFv24-79** is possibly a result of both the cell line and the CPP used (i.e. octa-arginine and Tat₄₇₋₅₉). Further investigation of **scFv24-77** cellular internalisation using a wider panel of cell lines would provide insight into the general cellular localisation of **scFv24-77**. Nonetheless, the octa-arginine derivative **77** proved to be the most promising CPP investigated here for the intracellular delivery of scFv.

3.5.2.1 Cellular internalisation of **scFv24-Pro₁₄** conjugate

It was proposed that conjugation of Pro₁₄ derivative *i*But-C-(P)₁₄-K(FAM)-[NH₂] **81** to scFv24 would enable cellular internalisation of the scFv. Thus, HeLa cells were incubated with **scFv24-81** at a concentration of 10 µM for 90 min at 37 °C, followed by imaging using CLSM (Figure 3-27, a).

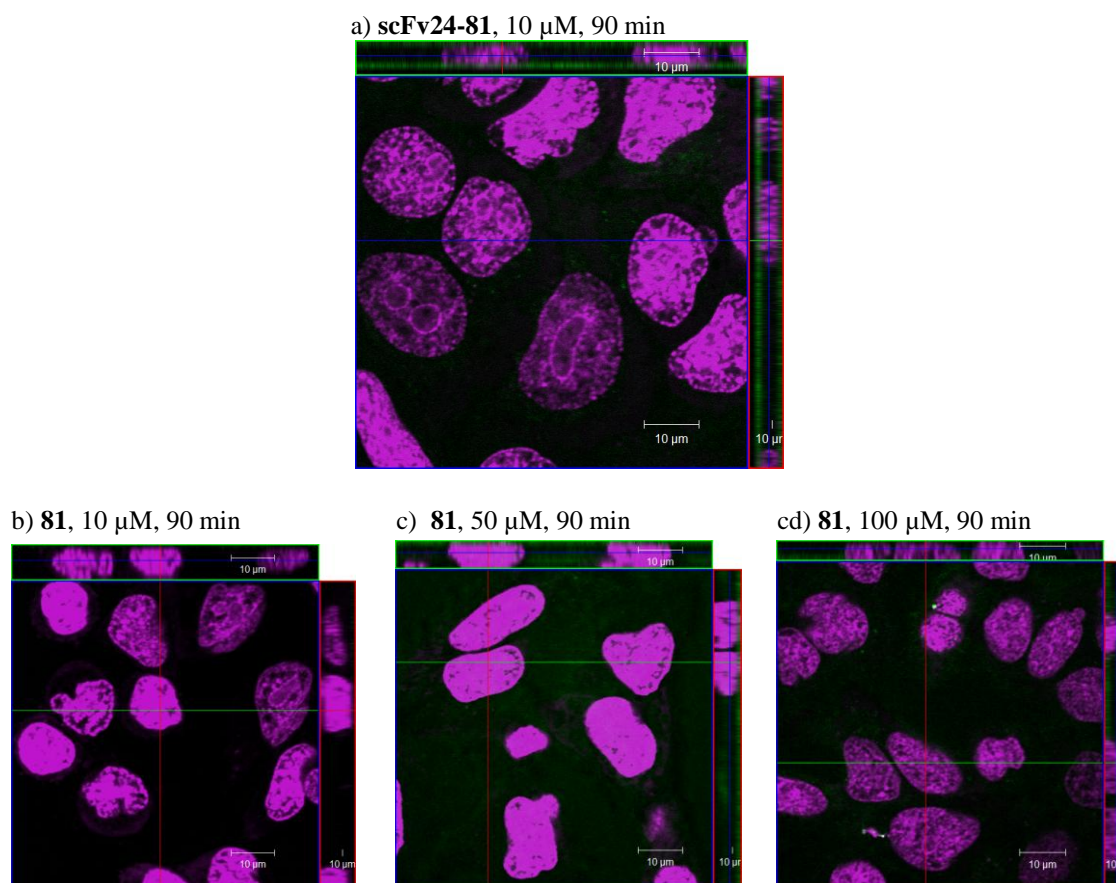


Figure 3-27: Z-sectioning using confocal microscopy of HeLa cells treated with a) **scFv24-81** (Green) for 90 min at 37 °C, 10 μ M b) treated with *i*But-C-(P)₁₄-K(FAM)-[NH₂] **81** at 10 μ M, c) 50 μ M and d) 100 μ M for 90 min at 37 °C. Draq5 was used as a nuclear stain (Purple).

It is clear that no cell associated fluorescence **scFv24-81** is observed after incubation for 90 min with HeLa cells (Figure 3-27, a). In a further experiment, cells were also incubated with *i*But-C-(P)₁₄-K(FAM)-[NH₂] **81** at 10, 50 and 100 μ M for 90 min at 37 °C, followed by CLSM (Figure 3-27, b, c and d). At 10 and 50 μ M no cell associated fluorescence for **81** was observed, minimal cell associated fluorescence was seen at 100 μ M suggesting internalisation of **81** at very high concentrations. The contrast between the results for **81** seen here compared to those seen by Crespo *et al.* (2002) are most likely attributable to the techniques employed.⁹⁵ CLSM of live cells avoids artefacts associated with membrane adhered peptide and permeabilisation of the cell membrane through cell fixing. However, Crespo *et al.* (2002), utilised fluorescence microscopy with paraformaldehyde fixed cells increasing the likelihood of overestimating cellular internalisation of the peptide.⁹⁹ Therefore, it was concluded that *i*But-C-(P)₁₄-K(FAM)-[NH₂] **81** was not a suitable delivery vector for scFv.

3.5.3 Summary of scFv-CPP cell internalisation

The cellular internalisation of scFv24 was successful. The octa-arginine derivative **77** proved the most efficient CPP to enable intracellular delivery of scFv, with apparent cytoplasmic delivery being achieved in RBL-2H3 cells. A summary of the cell internalisation of the scFv-CPP conjugates is shown in Table 3-5.

Table 3-5: scFv-CPP(FAM) internalisation and localisation; summary of CLSM and Fluorescence microscopy

scFv-CPP	CPP	Sequence	Localisation of scFv-CPP conjugate	
			HeLa	RBL-2H3
scFv24-77	octa-arginine	Mal-(R) ₈ -K(FAM)-[NH ₂]	cellular vesicles	cytoplasm
scFv24-79	Tat ₄₉₋₅₇	Mal-RKKRRQRRR-K(FAM)-[NH ₂]	Minimal internalisation, cellular vesicles	
scFv24-74	Antp ₅₂₋₅₈	Mal-RRMKKWKK-K(FAM)-[NH ₂]	Minimal cell internalisation	n.d
scFv24-81	Pro ₁₄	<i>i</i> Butyl-C-(P) ₁₄ -K(FAM)-[NH ₂]	extracellular	n.d

The comparison of the CPPs ability to deliver proteins into HeLa cells has been reported previously. Moosmeier *et al.* (2010) conclude that the order of efficiency for the internalisation of streptavidin by the CPPs used here is Antp₅₂₋₅₈ < Tat₄₉₋₅₇ < octa-arginine.²²² Although this is in agreement with the findings here, there are significant differences between the co-localisation of HIV Tat₄₉₋₅₇ (**scFv24-79**) and octa-arginine (**scFv24-77**) scFv conjugates that should be taken into account and could be influential on the biological effect of internalised scFv.

In conclusion, octa-arginine appears to be the most suitable CPP for delivering scFv24 into cells, thus it will be used to investigate the ability of scFv24 to induce apoptosis by inhibition of Bcl-xL.

3.6 Biological activity of scFv-CPP conjugates

Previously in Chapter 2, anti-Bcl-2 and Bcl-xL scFv were demonstrated to inhibit Bcl-2 and Bcl-xL binding to the BH3 region of BID in an *in vitro* Alpha screen competition assay. In a cellular context, cancer cells relying on the overexpression of Bcl-2 family members for cell survival will undergo apoptosis by inhibition of Bcl-2/xL. The pro-apoptotic proteins (BAK and BAX) are then able to induce downstream effector proteins, leading to the onset of apoptosis.¹⁶⁹

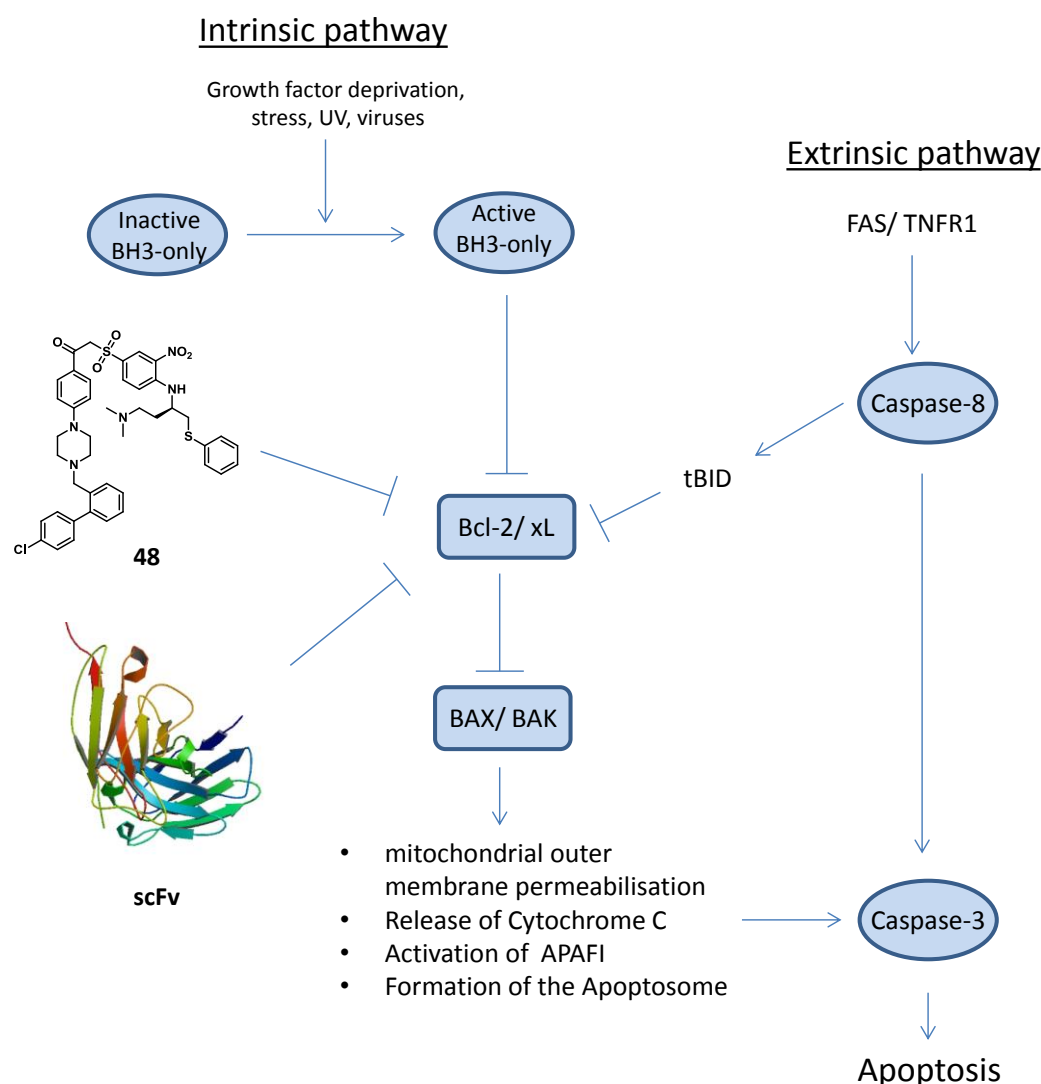
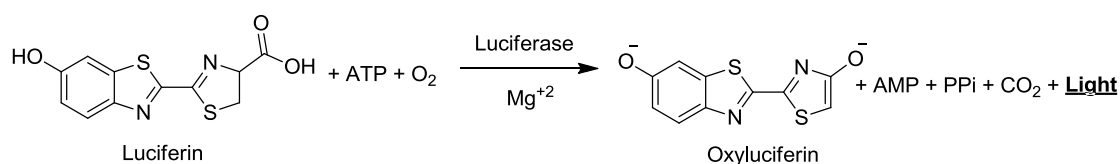


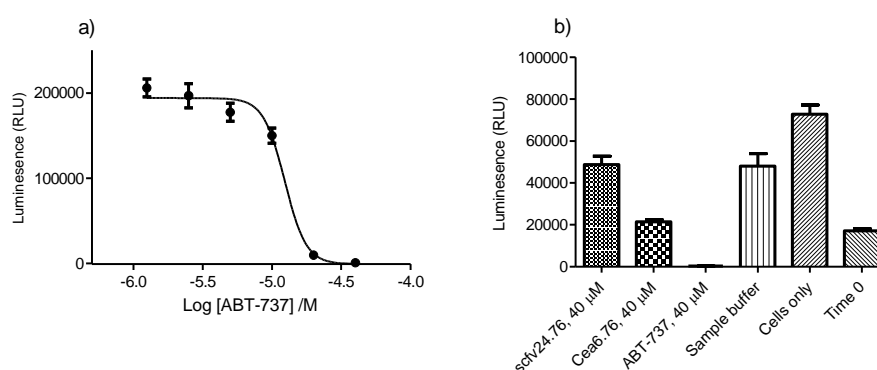
Figure 3-28: The intrinsic and extrinsic apoptosis pathways. In healthy cells, Bcl-2/xL forms a heterodimer with BAX/BAK stopping the activation of apoptosis. Activation of the BH3-only proteins by cellular stress leads to displacement of Bcl-2/xL from the dimer allowing for BAX/BAK to initiate the onset of apoptosis. Overexpression of Bcl-2/xL deregulates this pathway. Bcl-2/xL inhibitors act by inhibiting Bcl-2/xL heterodimer formation with BAX and BAK.

The comparison of the biological effect of anti-Bcl-2/xL scFv-CPP conjugates to the small molecule Bcl-2/xL inhibitor ABT-737 will provide insight into the effectiveness of the scFv-CPP conjugates to be internalised into a cell and inhibit Bcl-2/xL. The viability of cells after treatment with either ABT-737 or scFv-CPP conjugates was assessed using a luciferase-based ATP assay (Cell Titre Glo[®], Promega). The concentration of ATP has a direct relationship to the number of viable cells and a linear relationship with increasing cell numbers, thus making it a suitable marker to assess the effect of the scFv-CPP conjugates on cell viability. The principle of this assay is shown in Scheme 3-9.²²³

Scheme 3-9: The principle of the luciferase-based ATP cell viability assay, the reaction of luciferin with ATP is catalysed by luciferase in the presence of Mg²⁺.



Jurkat cells have previously been reported to be sensitive to Bcl-2/xL inhibition by ABT-737²²⁴⁻²²⁵ and also cell penetrable BH3 peptides.¹⁷⁸ Therefore, Jurkat cells were seeded at 3 x 10³ cells/well in 96-wells plates and treated for 48 h at 37 °C with either ABT-737 (Figure 3-29, a) or the Bcl-xL neutralising scFv24-octa-arginine conjugate **scFv24-76** (Figure 3-29, b).



	EC ₅₀ , µM
Jurkat	14.0 ± 0.6

Figure 3-29: a) ABT-737 and b) **scFv24-76** effect on Jurkat cell viability. Negative controls included **Cea6-76**, vehicle control, time 0 and cells only control.

The EC₅₀ calculated for ABT-737 with Jurkat cells was $14.0 \pm 0.6 \mu\text{M}$, this is slightly higher than the literature EC₅₀ value of $5 \mu\text{M}$.²²⁵ However, this difference could be related to cell line variability and experimental error. Unfortunately, the viability of the Jurkat cells was unaffected after incubation with $40 \mu\text{M}$ of **scFv24-76**. Unexpectedly, the non-specific scFv-octa-arginine conjugate **Cea6-76** did reduce the number of viable Jurkat cells, with a similar luminescence signal to time 0 wells being observed, thus suggesting that **Cea6-76** has a cytostatic effect on Jurkat cells. This is most likely a result of a non-specific interaction by Cea6 as this scFv is not specific for an intracellular target.³¹ Further investigations using **Cea6-76** are required to confirm the mechanisms involved in this apparent cytostatic effect.

3.6.1 The effect of scFv-CPP constructs on Rat basophilic leukaemia cell (RBL-2H3) viability

Cohen-Saidon *et al.* (2003) reported the isolation of an anti-Bcl-2 scFv and demonstrated that the scFv-Tat fusion protein was able to internalise in a rat basophilic leukaemia cell line (RBL-2H3) and induce apoptosis.⁶³ Using a trypan blue dye exclusion assay the authors observe a 50% decrease in cell viability after incubation with anti-Bcl-2 scFv ($15 \mu\text{g/ml}$, $0.5 \mu\text{M}$) compared to untreated cells and cells treated with a non-specific scFv.⁶³ This experiment was repeated using the same anti-Bcl-2 scFv (scFv84). In this study, however, scFv84 was conjugated to the 5-FAM labelled Tat₄₉₋₅₇ derivative **79** by a thioether bond to afford **scFv84-79**. RBL-2H3 cells were incubated with **scFv84-79** ($25 \mu\text{g/ml}$, $0.83 \mu\text{M}$) for 48 h followed by determination of cell viability using the Cell Titre Glo[®] assay (Figure 3-30).

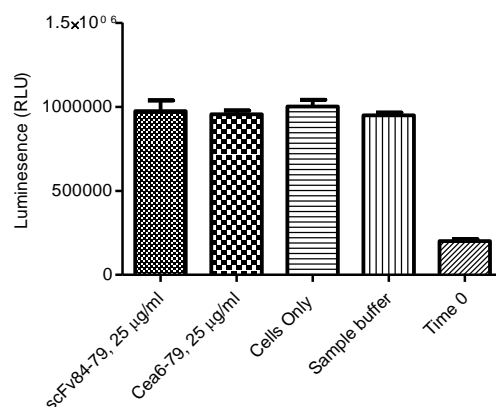


Figure 3-30: The effect on RBL-2H3 cell viability after incubation with **scFv84-79** for 48 h. Negative controls included **Cea6-79**, sample buffer and cells only control.

The viability of the RBL-2H3 cells was unaffected by treatment with **scFv84-79** over 48 h. This is contradictory to the findings reported by Cohen-Saidon *et al.* (2003)⁶³ using a scFv-Tat₄₇₋₅₇ (⁴⁷YGRKKRRQRRR⁵⁷) fusion protein, however, the 5-FAM labelled Tat₄₉₋₅₇ derivative **79** was conjugated to scFv84 by a thioether bond in this study. It is possible the results seen with **scFv84-79** could be related to the position and nature of the peptide conjugation and the presence of 5-FAM.

The treatment of RBL-2H3 cells with ABT-737 (Figure 3-31, a) and the octa-arginine conjugates **scFv24-76** and **Cea6-76** (Figure 3-31, b) at 40 µM had no effect on cell viability.

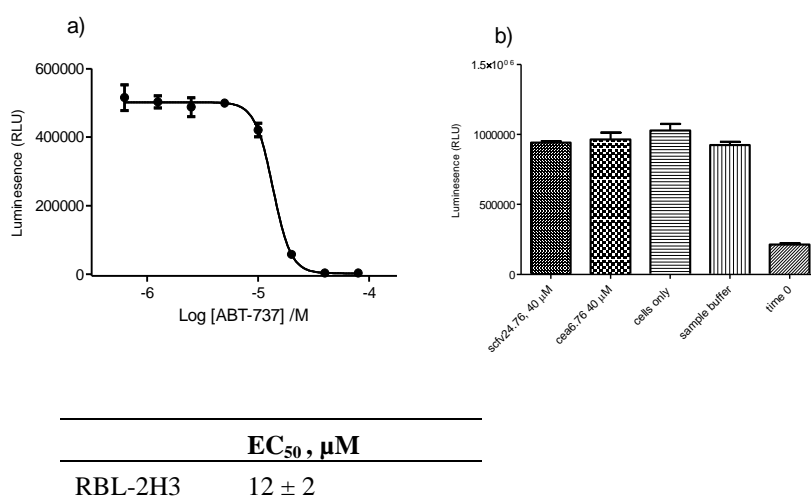


Figure 3-31: a) ABT-737 and b) **scFv24-76** effect on RBL-2H3 cell viability. Negative controls included **Cea6-76**, vehicle and cells only control.

The EC₅₀ value calculated for ABT-737 using RBL-2H3 cells was 12 ± 2 μ M, thus having similar sensitivity to ABT-737 as Jurkat cells. This suggests that cells may not be sensitive enough to Bcl-2/xL knockout for a 40 μ M solution of **scFv24-76** to induce apoptosis.

3.7 Conclusions

In the first phase of this study a mammalian expression system was used to produce usable quantities of scFv-Cys. This allowed for site-specific conjugation of a range of CPP derivatives to the C-terminally located cysteine residue of the scFv. The optimised conjugation conditions and high levels of scFv obtained from the mammalian expression system will allow for rapid screening of a panel of scFv-CPP conjugates without time consuming sample preparation in future studies.

Furthermore, it was demonstrated that conjugation of the octa-arginine derivative **77** to scFv24, affording the **scFv24-77** conjugate, enabled internalisation into HeLa and RBL-2H3 cells. Although the conjugate clearly localises in cellular vesicles of HeLa cells, in RBL-2H3 cells the conjugate appears to be localised in the cytoplasm, however this could also be an artefact of membrane bound scFv conjugate. In contrast, the Tat₄₉₋₅₇ conjugate **scFv24-79** showed minimal internalisation into HeLa and RBL-2H3 cells, furthermore, the internalised protein appeared to localise in cellular vesicles in both cell lines. Intracellular delivery of a protein using CPPs has been previously reported to result in endosome entrapment.⁹⁹ Additionally, Tünnemann *et al.* (2006) demonstrated that TAT fusion proteins (>50 amino acids) were taken up largely into cytoplasmic vesicles.⁷³ Cytoplasmic delivery of the scFv-CPP conjugates is necessary for scFv binding and inhibition of the targets Bcl-2 and Bcl-xL. Therefore, based on the CLSM imaging, it was concluded that scFv conjugated to the octa-arginine derivative **76** or the 5-FAM labelled **77** were the most suitable constructs for the cell viability assay.

Unfortunately, preliminary cell viability studies did not suggest induction of apoptosis by **scFv24-76**. In this assay the small molecule Bcl-2/xL inhibitor ABT-737 was used as a positive control with EC₅₀ values of 12 ± 2 μ M and 14.0 ± 0.6 μ M being calculated for Jurkat and RBL-2H3 cells, respectively. The low sensitivity of the two

cells lines to ABT-737 prompted the use of high concentration of **scFv24-76** to be used (40 μ M). Incubation of **scFv24-76** for 48 h with both RBL-2H3 and Jurkat cells showed no effect on cell viability. It is possible that the absence of a biological response is due to the low sensitivity of these cell lines to Bcl-2/xL inhibition. In order to induce cell apoptosis, significant amounts of scFv would be required to be internalised into the cells. Thus, it is possible that internalisation efficiency and endosomal entrapment of the scFv-CPP may be a limiting factor. This is also supported by the *in vitro* data that shows scFv24 to be a more potent inhibitor of Bcl-xL than ABT-737. Of equal importance, is that scFv24 is specific to Bcl-xL only, thus the sensitivity of the RBL-2H3 and Jurkat cells to Bcl-xL inhibition has to be considered.

A number of reports have investigated the sensitivity of different cell lines to ABT-737, thus using a cell line that displays high sensitivity to ABT-737 will increase the possibility of observing a biological effect for the **scFv24-76** conjugate (Table 3-6).

Table 3-6: EC₅₀ values for ABT-737 with a selection of cell lines.

Cell Line	EC ₅₀ , μM		Reference
	Culture conditions		
	10% FBS	Reduced FBS (%)	
HL-60	>10	-	High <i>et al.</i> (2010) ²²⁵
K562	>10	-	
Nalm6	>10	-	
Jurkat	5.00	-	
Molt4	0.92	-	
REH	0.68	-	
CEM	0.30	-	
Hal-01	0.19	-	
DoHH2	0.13	0.001 (3%)	Bruncko <i>et al.</i> (2007) ²²⁶
RS11380	0.15	0.014 (3%)	
SUDHL-4	0.85	0.220 (3%)	
NCI-H146	0.09	0.015 (0%)	Shoemaker <i>et al.</i> (2006) ²²⁷
A549	22.3	5.2 (0%)	

The design of the CPP derivatives will allow for further optimisation of scFv delivery. The C-terminal lysine residue could be used to incorporate endosomolytic peptides, a selection of peptides demonstrated to possess endosomolytic properties are shown in Table 3-7.

Table 3-7: A selection of endosomolytic peptides.

	Endosomolytic peptide	Reference
18	HA2; GLFGAIAGFIEGGWTGNIDGWYG	Wadia <i>et al.</i> (2004) ¹¹¹
19	H5WYG; GLFHAIHFIHGGWHGLIGGWGYG	Pichon <i>et al.</i> (2001) ¹¹²
20	10HIS; HHHHHHHHHH	Lo <i>et al.</i> (2008) ¹¹³
21	4 ₃ E; LAELLAELLAEL	Ohmori <i>et al.</i> (1997) ¹¹⁴

These endosomolytic peptides have been demonstrated to increase endosome escape of cargo internalised through CPP mediated delivery. Introducing one of these peptides to a scFv-CPP conjugate could increase the quantity of scFv being delivered into the cytoplasm, resulting in a larger quantity of scFv being able to inhibit Bcl-2/xL and induce apoptosis.

In summary, investigation into obtaining a sufficiently sensitive cell line to Bcl-2/xL knockout is required to increase the possibility of observing a biological response induced by scFv24-CPP conjugates. Future directions after this first objective should then be both focussed on optimising the cellular delivery and biological effect of the lead anti-Bcl-2 or Bcl-xL scFv-CPP conjugates.

3.8 Materials and Methods

All agar plates, culture media and buffers used are described in Chapter 2, unless otherwise stated. All vectors were kindly supplied by MedImmune, Cambridge. All DNA manipulations were performed using plasmid purified using a QIAGEN plasmid purification kit (QIAGEN) according to the manufacture's guidelines and using either TG1 (K12, D (*lac-pro*), *supE*, *thi*, *hsdD5/F' traD36*, *proA⁺B⁺*, *lacI^q*, *lacZDM15*) or Novablue (*endA1 hsdR17 (r_{K12-} m_{K12+}) supE44 thi-1 recA1 gyrA96 relA1 lac F'[proA⁺B⁺ lacI^qZAM15::Tn10] (Tet^R)*) *E. coli* strains. All protein concentrations were determined from the sample absorbance at A₂₈₀ using a NanoDrop spectrophotometer (Thermo Scientific).

3.8.1 SDS-PAGE and western blot analysis

SDS-PAGE was utilised to assess the purity of protein samples. 5 µl of NuPAGE[®] LDS Sample Buffer (Invitrogen) and 1 µl of 1 M TCEP were added to 10 µl of protein sample. The samples were heated for 2 min at 95 °C and then loaded onto either a 15% SDS polyacrylamide gel or a 2-12% NuPAGE[®] Bis-Tris gel (Invitrogen), submersed in running buffer (0.1% SDS, 25 mM Tris, 192 mM glycine). The samples were then separated using 180 V until the loading buffer reached the bottom of the gel. The gel was then washed with 20 ml of H₂O, followed by staining with Coomassie blue stain (1% Coomassie brilliant blue R-250, 10% AcOH, 40% isopropanol, 50% H₂O) for 1 h at rt. The gel was then destained using destain solution (20% isopropanol, 10% AcOH and 70% H₂O) until the protein bands were visible.

For western blot analysis gels were used before fixing and staining. Protein bands were electroblotted to a nitrocellulose membrane (Hybond C, 0.45µm, GE Healthcare) using transfer buffer (20% MeOH, 25 mM Tris, 192 mM glycine) as the transfer medium at 100 V for 2 h. The membranes were washed using 20 ml of 1x PBS and then blocked with 3% MPBS for 2 h at rt. All primary and secondary antibodies used are shown in Table 3-8 with corresponding concentrations used for the western blot.

Table 3-8: Primary and secondary antibodies used for western blotting

Antibody	Concⁿ	Supplier
<u>Primary</u>		
Anti-Myc mAb (9E3)	1 µg/ml	AbD Serotec
Anti-polyhistidine mAb (AD.1.1.10)	1 µg/ml	R&D systems
<u>Secondary</u>		
Goat Anti-Mouse IgG HRP conjugate	Used as a 1:1000 dilution	R&D systems

The primary and secondary antibodies were diluted into 3% MPBS. Membranes were incubated with a primary antibody for 1 h at rt (10 ml of antibody dilution), followed by washing of the membrane with 20 ml of wash buffer (1xPBS/0.1% Tween v/v). This wash step was repeated 3x before the addition of a secondary antibody (10 ml of antibody dilution). After incubation, the membranes were washed as before and then developed using 1.5 ml of the peroxidase substrate 3,3',5,5'-tetramethylbenzidine liquid substrate system for membranes (TMB, Sigma-Aldrich). The reaction was stopped by washing the membrane with PBS.

3.8.2 General sub-cloning procedure

All enzymes and buffers were purchased from New England Biolabs. All pCANTAB6 and pUC119MCH plasmid were purified using QIAgen midi plasmid purification kit, following manufacture's guidelines.

3.8.2.1 Digestion of scFv DNA and vector

The design of phagemid pCANTAB6 allows for the isolation of the scFv-encoding DNA from the vector using restriction enzymes NotI and NcoI or alternatively NotI and SfiI. For the vector pUC119MCH and pEOMCH, restriction enzymes SfiI and NotI were used to clone scFv DNA and for pHIS10CYS enzymes NotI and NcoI were used.

ScFv DNA and plasmid concentrations were determined using an Eppendorf BioPhotometer and agarose gel electrophoresis (1.5% agarose gel at 120 V). The following components were combined and performed in duplicate.

For the digestion of vector DNA and isolation of scFv DNA with the restriction enzymes NotI and NcoI each sample contained, ~2 µg of DNA, 1 µl of both NotI (10 U/ µl) and NcoI (10 U/µl), 5 µl of 10x restriction buffer 3, 0.5 µl of 10 mg/ml bovine serum albumin (BSA) and nuclease-free water to make the final reaction volume up to 50 µl. Samples were then incubated for 2-4 h at 37 °C.

Alternatively, for the digestion of DNA with the restriction enzymes SfiI and NotI, each sample contained ~5 µg of DNA, 1 µl of SfiI (10 U/µl), 5 µl of 10x restriction buffer 2, 0.5 µl BSA (10 mg/ml) and nuclease-free water to make the final reaction volume up to 50 µl. Samples were then incubated for 1.5 h at 50 °C. After incubation, 5 µl of 10x restriction buffer 2, 0.5 µl BSA (10 mg/ml), 2 µl of NotI (10 U/µl) and nuclease-free water to make the final reaction volume up to 100 µl was added, followed by incubation for 1.5 h at 37 °C.

Following all incubation steps, the digested DNA was analysed using gel electrophoresis on a 1.5% agarose gel at 120 V. The scFv inserts were identified at approximately 850 bp through comparison to a 1 kb marker. The DNA was purified from the agarose gel using a QIAgen gel purification kit following manufactures guidelines.

3.8.2.2 Ligation of inserts and vectors

For a typical ligation ~100 ng vector and ~100 ng of insert (approx. 5:1 molar ratio of insert ends: vector ends) is required. To each ligation reaction, 2 µl of cut vector (at 50 ng/µl, i.e. ~100 ng or $\sim 3 \times 10^{10}$ molecules) and 5 µl cut insert (at 20 ng/µl, i.e. ~100 ng or $\sim 10^{11}$ molecules) was added to 3 µl 10x T4 ligation buffer, 1 µl T4 DNA ligase and 19 µl nuclease-free water. Samples were then incubated overnight at 16 °C.

3.8.2.3 Transformation of ligated DNA into *E. coli*

Initially, chemically competent *E. coli* was thawed on ice. 10 µl of each ligation reaction was added into 100 µl competent cells and incubated for 30 min on ice. A positive and a negative transformation control were included by mixing 100 µl of *E. coli* with 10 ng undigested vector or no DNA. This was followed by heat shock of the

cells for 45 sec at 42 °C using a preheated thermal cycler. After heat shock, cells were incubated on ice for 2 min followed by addition of 900 µl 2TYG media. The *E. coli* was then incubated for 1 h at 37 °C with shaking at 120 rpm.

Cells were centrifuged at 2000 g for 10 min and resuspended in 200 µl of 2TY media. Cells suspension was then spread onto pre-dried 2TYAG bioassay plates for pCANTAB6 or 2TYK bioassay plates for pUC119MCH.

3.8.3 Expression of scFv-Cys in *E. coli* with pUC119MCH vector

ScFv-encoding DNA was excised from purified pCANTAB6 vector containing the desired scFv DNA sequence using the restriction enzymes NotI and SfiI as previously described (Section 3.8.2.1). Purified scFv-encoding DNA was then ligated into SfiI/NotI digested pUC119MCH vector (Figure 3-32). Successful sub-cloning was confirmed by DNA sequencing of the pUC119MCH vector using the PUC_R primer (Appendix II). Purified pUC119MCH containing scFv24-encoding DNA was used to transform competent *E. coli* BL21 (*fhuA2 [lon] ompT gal [dcm] ΔhsdS*).

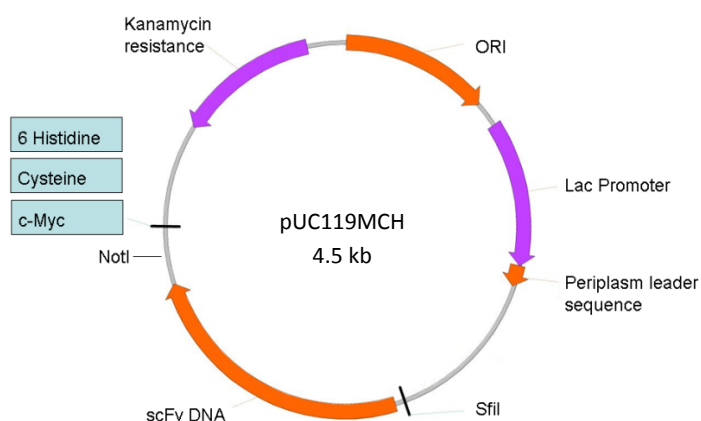


Figure 3-32: Vector map of pUC119MCH vector, the scFv constructs are sub-cloned into the vector using NotI and SfiI restriction sites.

A single colony of *E. coli* containing the pUC119MCH vector was used to inoculate 400 ml of TYK media. Cultures were incubated at 37 °C with shaking at 380 rpm. At an OD₆₀₀ between 0.5-1 cultures were induced using 1 mM IPTG followed by incubation of the culture at 37 °C with shaking at 380 rpm for 16 h. Bacteria were

harvested by centrifugation at 4 °C, 3000 g for 15 min. Pellets were snap frozen and stored at -80 °C until further use.

Approximately 3 g of *E. coli* pellet was suspended into 20 ml of lysis buffer (2xPBS, Roche protease Inhibitor cocktail (EDTA free), 1 mg/ml lysozyme (Sigma-Aldrich), pH 7.4) and incubated for 5 min at rt. The bacterial suspension was then sonicated at 75 W intermittently for 10 seconds, with 30 second intervals on ice. The lysate was centrifuged at 10000 g for 10 min at 4 °C, the supernatant was then removed and filtered through a 0.45 µm filter.

Affinity purification was carried out using a 5 ml HitrapTM FF crude nickel chelate column (GE Healthcare). The bacteria lysates were loaded onto the column using a peristaltic pump (0.5-1.0 ml/min) at 4 °C. All following wash steps were then performed on an ÄKTA primeTM purification system with a flow rate of 2 ml/min and a pressure limit of 0.3 MPa. Columns were washed with 10 column volumes (CV) of 2 x PBS, 10 CV of 40 mM imidazole (2x PBS) and eluted using a linear gradient 10 CV from 40 to 400 mM imidazole over 10 CV with the collection of 5 ml fractions. All fractions were analysed using SDS-PAGE and western blot. Fractions containing scFv were pooled and concentrated using a VivaspınTM centrifugal concentrator (5000 Mw cut off). Protein concentrations were determined from absorbance at A₂₈₀ using a NanoDrop spectrophotometer (Thermo Scientific).

Protein samples were purified by size exclusion using a 16/60 Superdex 75 column (GE Healthcare) pre-equilibrated using 2x PBS (pH 7.4) on an ÄKTA purifier at a flow rate of 0.3 ml/min with 0.5 ml fraction collection. Fractions were analysed by SDS-PAGE, the fractions corresponding to the scFv were pooled and concentration using a VivaspınTM centrifugal concentrator (Mw cut off <5000). Samples were snap frozen and stored at -20 °C.

3.8.4 Expression of scFv-Cys in *E. coli* with p10HISCYS vector

ScFv24-encoding DNA was sub-cloned into p10HISCYS vector (Figure 3-33) using the restriction enzymes NotI and NcoI as previously described. Successful sub-cloning was confirmed by DNA sequencing of the p10HISCYS vector using the T7 forward primer (Appendix II). Purified p10HISCYS containing scfv24-encoding DNA

was used to transform competent *E. coli* BL21 (*fhuA2 [lon] ompT gal (λ DE3) [dcm] ΔhsdS*).

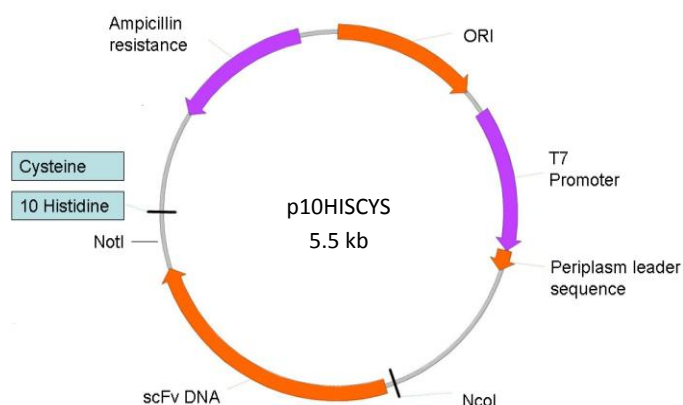


Figure 3-33: Vector map of p10HISCYS vector. ScFv constructs are sub-cloned into the vector using NotI and SfiI restriction sites

A single transformed *E. coli* colony possessing the p10HISCYS vector containing the scfv24-encoding DNA was cultured in 10 ml of 2TYAG media at 37 °C. This was then transferred to 16 °C when the culture reached OD₆₀₀ 0.4. At OD₆₀₀ 0.5-0.6 the culture was induced with 1 mM IPTG. At 1, 2, 4, 6 and 16 h a 1 ml sample was removed from the culture. The bacteria were harvested by centrifugation at 3000 g and 4 °C. Supernatant was used making the media fraction. The *E. coli* fractions were analysed using a modified method described in the Invitrogen QIAexpressionist™.²²⁸ Briefly, the pellet was suspended into 100 µl of lysis buffer (2x PBS, Roche protease Inhibitor cocktail (EDTA free), 1 mg/ml lysozyme (Sigma-Aldrich), pH 7.4) and incubated on ice for 30 min. The bacterial lysate was then centrifuged at 13,000 g at 4 °C. The supernatant (i.e. soluble fraction) was transferred to a fresh sample tube. The bacterial pellet was resuspended into 100 µl of 1x PBS to form the insoluble fraction. A 20 µl aliquot from each sample was added to 5 µl of NuPAGE® LDS Sample Buffer (Invitrogen) and 1 µl of 1 M TCEP and heated for 15 min at 95 °C. These samples were analysed by SDS-PAGE and western blotting as previously described.

3.8.5 Transient expression of scFv-Cys in Cep6 cells with pEOMCH vector

ScFv constructs were sub-cloned into pEOMCH vector (Figure 3-34) using the restriction enzymes NotI and SfiI as previously described. Successful sub-cloning was confirmed by DNA sequencing of the pEOMCH vector using the two primers AR138 and AR142 (Appendix II). The pEOMCH vector containing the desired scFv construct were purified using a QIAGEN plasmid Giga prep kit according to the manufacturer's protocol.

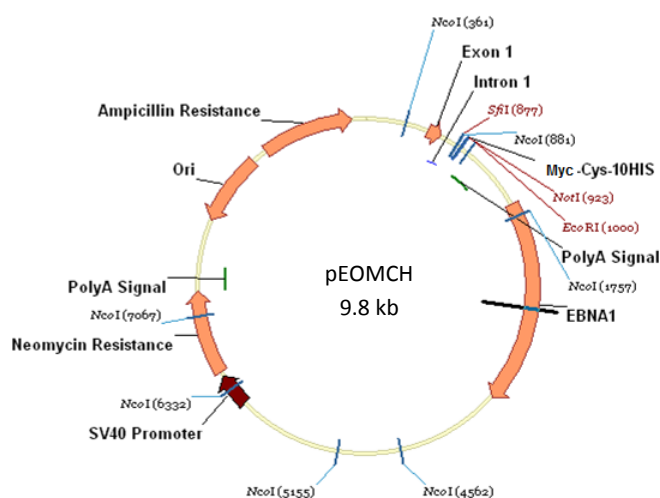


Figure 3-34: Vector map of pEOMCH vector. ScFv constructs are sub-cloned into the vector using NotI and SfiI restriction sites.

The CEP6 cells were sub-cultured by the tissue culture team at MedImmune (Cambridge, U.K.), 24 h before transfection the Cep6 cells were seeded at 5×10^5 viable cells/ml in 500 ml in CD-CHO medium, thus on the day of transfection it was assumed that the cell number would be approximately $1 \pm 0.5 \times 10^6$ viable cells/ml. Before transfection, the cultures were inoculated with penicillin (100 μ g/ml) and streptomycin (100 μ g/ml).

The purified pEOMCH-scFv plasmid was added to polyethylenimine (PEI, 10 mg/ml) at a 1:1 (v/v) ratio. The quantity of plasmid used was calculated so that it would give a final culture concentration of 1 μ g DNA/ml of cells at $1.0 \pm 0.5 \times 10^6$ cells/ml. For example, using a 500 ml culture; 10 ml of purified plasmid at 0.5 mg/ml was added to

10 ml of PEI (10 mg/ml), the 20 ml solution would then be added to the culture, thus resulting in approximately 1 µg DNA/ml of cells.

Before addition of the PEI/DNA mixture to the cultures the solution was vortexed for 10 seconds followed by incubation for 1 min at rt, this solution was then added to the cell culture. The cultures were supplemented with 50 ml of M20A feed (MedImmune, U.K. containing amino acids, vitamins, recombinant human insulin and plant hydrolysates) and 10% glucose. The cultures were incubated for approximately 10 days and supplemented every 2-3 days with 50 ml M20A feed and 10% glucose. After 10 days the cells were harvested by centrifugation at 3000 g for 30 min at 4 °C. Supernatants were then filtered through a 0.22 µm filter (Millipore, Stericup® Filter Units). The culture supernatants containing the secreted scFv were stored at 4 °C overnight before affinity purification.

Histidine purification was carried out using a 5 ml Hitrap FF crude column (GE Healthcare). The filtered media was loaded onto a column using a peristaltic pump at 1 ml/min. The loaded column was then washed with 5 CV of 2x PBS, 5 CV of 40 mM imidazole in 2x PBS and scFv eluted using 400 mM imidazole in 2x PBS with 2 ml fraction being collected. Figure 3-35 shows the SDS-PAGE analysis of a typical purification for scFv24, 84 and Cea6.

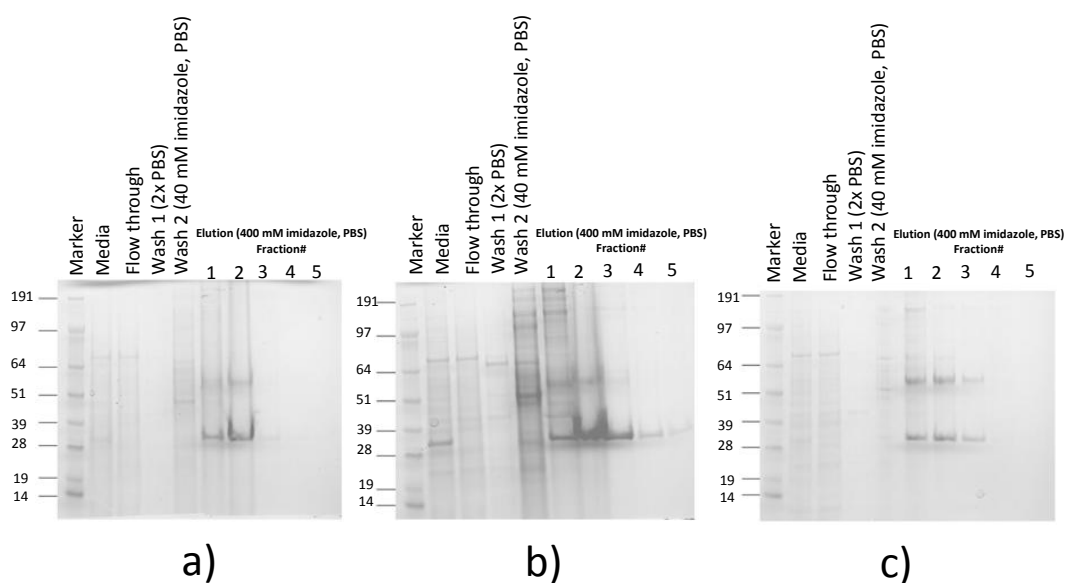


Figure 3-35: Reducing 2-12% SDS polyacrylamide gel of samples from affinity purification of a) scFv24 b) Cea6 and c) scFv84 from pEOMCH. Fractions shown include cell culture media before purification, flow through of media after loading onto 5 ml Hitrap™ FF crude nickel column, column washes followed by elution of scFv using 400 mM imidazole in 2x PBS. The gel was stained with coomassie blue.

The fraction were then analysed using SDS-Page. Fractions containing protein were pooled and buffer exchanged using a PD-10 column (GE Healthcare) into sodium acetate buffer (pH 5.5). The eluent was then concentrated to ~2 mg/ml using a Vivaspin™ centrifugal concentrator (5000 Mw cut off) and stored at -80 °C.

3.8.6 Preparation of scFv-CPP conjugates

Unless stated, all buffers were filtered through a 0.22 µm filter and degassed. Standard buffers used are as previously described. All scFv-Cys used were purified from Cep6 cells using the pEOMCH vector.

All reagent used for CPP conjugations were purchased from Sigma-Aldrich unless stated. Both *N*-maleimidopropionyl and *N*-isobutyryl cysteinyl CPPs were synthesised as described in Chapter 6 and used as 10 mg/ml solutions in deionised water. All scFv-Cys (1-4 mg/ml) used for conjugations were treated with 10x molar excess of TCEP for 1 h at rt. For example, to 15 ml of scFv24 (1.47 mg/ml, 0.74 µmol) was added TCEP (2.1 mg, 7.34 µmol) followed by incubation for 1 h at rt. The sample was then desalted into a deoxygenated sodium acetate buffer (pH 5.5) using a HiPrep™ 26/10 Desalting Column (8-10 ml/min, GE Healthcare) on an ÄKTA purifier at a flow rate of 8-10 ml/min with 2 ml fraction collection. Fractions corresponding to the scFv were pooled and concentrated to 2 mg/ml using a Vivaspin centrifugal concentrator (Mw cut off < 5,000).

3.8.6.1 Conjugation of *N*-maleimidopropionyl CPPs to scFv-Cys

The synthesised *N*-maleimidopropionyl CPPs were reconstituted into deionised water to a final concentration of 10 mg/ml. To a solution of 1 ml of scFv-Cys (2 mg/ml, 2 mg, 67 nmol) was added 10x molar excess of *N*-maleimidopropionyl CPP (670 nmol). The reaction was incubated for 1.5 h at rt or overnight at 4 °C. Samples were analysed for successful conjugation using MALDI-TOF MS using a Bruker Daltonics Ultraflex instrument and sinapic acid (50% MeCN/ H₂O) matrix. The data were processed using Bruker Daltonics Flexanalysis™ software. If the coupling was incomplete a further 10x excess of peptide was added to the reaction and incubated for a further 1.5

h at rt followed by analysis. Samples were purified using a HiPrep™ 26/10 Desalting Columns (8-10 ml/min, GE Healthcare) on an ÄKTA purifier using sodium acetate buffer (pH 5.5) at flow rate of 8-10 ml/min with 2 ml fraction collection. A typical purification trace is shown in Figure 3-36, the major peak at 13.09 min corresponds to the scFv-CPP conjugate and the minor peaks are the elution of excess unreacted peptide.

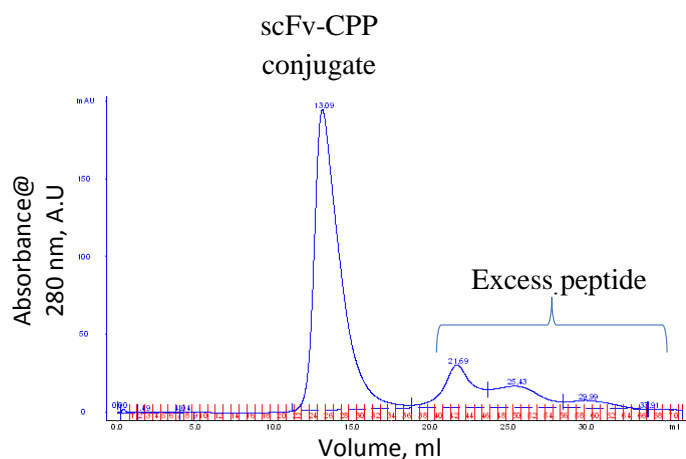


Figure 3-36: A typical elution trace obtained for the purification of scFv-CPP conjugates using a HiPrep™ 26/10 Desalting Columns (8-10 ml/min, GE Healthcare) on an ÄKTA purifier.

Fractions corresponding to the scFv-CPP conjugate were pooled and concentrated using a Vivaspın™ centrifugal concentrator (Mw cut off < 5000) to approximately 12 mg/ml. All scFv samples were then stored at -20 °C until further use.

3.8.6.2 Conjugation of peptide 136 and SMOc 14 to scFv-Cys.

The pyridyl disulfide activated *N*-isobutyryl cysteinyl peptide **136** or the small molecule carrier (SMoC) **14** was conjugated to scFv-Cys using the same protocol used for *N*-maleimidopropionyl CPPs (Section 3.8.6.1). Samples were again purified by size exclusion using a HiPrep™ 26/10 Desalting Columns and concentrated using a Vivaspın™ centrifugal concentrator (Mw cut off < 5000) to approximately 12 mg/ml. Each sample was then analysed using MALDI-TOF MS as previously described.

3.8.6.3 Direct binding ELISA – scFv-CPP antigen specificity

The specificity of the scFv-CPP conjugates for Bcl-2 or Bcl-xL was determined using the direct binding ELISA protocol (Section 2.5.2). Biotinylated Bcl-2 or Bcl-xL (1.25 µg/ml) was coated onto 96-well streptavidin-coated plates (Strepmax, costar 96-well plate, Thermo scientific) as previously described (Section 2.5.2). A streptavidin coated plate, without added antigen, was used as negative control to detect non-specific scFv. After coating, the plates were washed 3x with PBS to remove unbound antigen. Plates were then blocked using 200 µl/well of 3% MPBS and incubated for 1 h at rt.

Plates were then washed 3x with PBS, followed by the addition of 50 µl/well of scFv-CPP (1.6, 0.7 or 0.4 µg/ml) in 3% MPBS to the Bcl-xL, Bcl-2 and streptavidin only coated plates. The scFv-CPP was then incubated for 1 h at rt. The plates were then washed 3x with PBS/0.1% Tween, followed by the addition of 50 µl/well of mouse anti-Myc mAb (9E3) (1 µg/ml) in 3% MPBS followed by incubation at rt for 1 h. The plates were then washed 3x with PBS/0.1% Tween. 50 µl/well of mouse anti-mouse horse radish peroxidase (HRP) antibody conjugate (R&D systems), diluted according to manufacturer's recommendation in 3% MPBS was then added and incubated at rt for 1 h. Finally, plates were washed 3x with PBS/0.1% Tween and developed and the absorbance at 450 nm read as previously described (Section 2.5.2).

3.8.7 General cell culture protocol

All buffers used were either filtered through 0.2 µm filters or autoclaved. Standard buffers used are as follows; HBSS buffer (0.55 M Glucose, 0.137 M NaCl, 5.4 mM KCl, 0.25 mM Na₂HPO₄, 0.44 mM KH₂PO₄, 1.3 mM CaCl₂, 1.0 mM MgSO₄, 4.2 mM NaHCO₃, pH 7), Acid wash buffer (0.3 M Glycine, 150 mM NaCl, pH 3), Phosphate buffered saline (PBS; 2.67 mM potassium chloride, 1.47 mM potassium phosphate monobasic, 137.93 mM sodium chloride, 8.1 mM sodium chloride, pH 7.4).

Jurkat and RBL-2H3 cells were maintained by static culture in RPMI-1640 (Sigma-Aldrich) medium supplemented with 10% fetal bovine serum (FBS). HeLa cells were maintained in Eagle's Minimum Essential Medium (Sigma-Aldrich) supplemented with 10% FBS. All cell culture manipulations were performed in a Class II microbiological safety cabinet that was cleaned with 70% IMS prior to use. All FBS

used was heat inactivated (55-59 °C) for 30 min to denature complement proteins prior to use. The cells were cultured in a humidified incubator containing 5% CO₂ at 37 °C. The cell lines were sub-cultured into 75 ml Costar tissue culture flasks until confluence reached approximately 80%.

Sub-culturing of suspension cells was achieved by a 1/6 dilution of confluent cells into fresh culture media. For adherent cells, the media was aspirated and the cells were washed with 2 ml of sterile PBS. The cells were then treated with ~0.5 ml of 0.25% (w/v) trypsin 0.53 mM EDTA solution at 37 °C for 5 min or until all cells were visibly detached from the flask. To the suspended cells ~5 ml of culture media was added. The cells were then diluted into fresh culture media once more at approximately 1/6 dilution. Each cell line was sub-culture no more than 30 times before disposal.

3.8.8 Fluorescence microscopy

All fluorescence microscopy was carried out using a Nikon Eclipse 90i Fluorescent Microscope. HeLa cells were seeded at 1×10^5 cells/well in a 12-well cell culture plate (Nunc) and allowed to adhere at for 16 h at 37 °C. 500 µl of scFv-CPP(FAM) conjugates at 10 µM in RPMI-1640 media were then added to cells, and incubated for 30 min at 37 °C followed by aspiration of the media. Cells were then washed 3x with 1 ml of acid wash buffer (3 M glycine, pH 3) to remove membrane adsorbed scFv-CPP conjugates, followed by washing 3x with 1 ml PBS. The cells were then left in 2 ml of HBSS buffer containing Hoechst 33342 (0.5 µg/ml, Sigma-Aldrich, Prod# B2261) to stain cell nuclei. Cells were then imaged either at x5, x10 or x20 magnification. The Hoechst 33342 stain was imaged by UV absorbance using a mercury lamp.

3.8.9 Confocal scanning laser microscopy

All CSLM was carried out using a Zeiss LSM510 META Confocal Imaging System and Zeiss LSM510 operating software. Cells were imaged using an inverted 63x oil objective and Argon (458, 477, 488, 504 nm) and He-Ne 633 nm lasers, Z-sectioning was performed using the Zeiss LSM510 operating software.

Live-cell imaging was performed using a method adapted from that described by Chazotte *et al.* (2011).²²⁹ HeLa or RBL-2H3 cells were seeded at 1×10^5 cells/well using a 6-well cell culture plate (Nunc) containing glass coverslips. The cells were allowed to adhere at for 14 h at 37 °C. The scFv-CPP(FAM) conjugates were diluted into RPMI-1640 media to give a concentration of 10 μ M. The media in each well was removed followed by addition of 1 ml/well of the diluted scFv-CPP(FAM) samples. The cells were then incubated for 30 or 90 min at 37 °C. After incubation, the media was removed and the cells were washed 3x with 2 ml of PBS. The cells were then incubated with the nuclear stain Draq5[®] (5 μ M, 500 μ l, New England Biolabs) for 5 min at rt. Cells were again washed 2x with 2ml of PBS before the coverslips removed and placed onto cover slides with the cells facing down. To prevent the cells from drying out, 50 μ l of HBSS buffer was applied onto glass slides prior to placing the coverslip cells down, the coverslip was then held in place by application of nail varnish around the edges. The cells were then imaged and z-sections were taken using the Zeiss LSM510 operating software.

3.8.10 Biological activity of scFv-CPP conjugates - Cell Titre Glo assay[®]

The biological activities of the scFv-CPP conjugates and ABT-737 were assessed using an ATP/Luciferase based assay (Cell Titre Glo assay[®], Promega). Jurkat cells were seeded on the day of dosing in 96-well cell culture plates (Costar) at 3×10^3 cells/well in 20 μ l of fresh media. Alternatively, RBL-2H3 cells were seeded at 3×10^3 cells/well in 100 μ l of fresh media and given 16 h to adhere at 37 °C. After the cells were attached, 80 μ l of media was removed from each well to leave the cells in 20 μ l of media/well.

ScFv-CPP constructs (12-15 mg/ml, 0.4-0.5 mM stock solution) in sodium acetate buffer (pH 5.5) were diluted into RPMI-1640 media to give a working concentration of 50 μ M. The diluted sample was then filtered through a sterile 0.22 μ m syringe filter (PVDF, Millipore). 80 μ l of the filtered sample was then added to each well to give a final assay concentration of 40 μ M and well volume of 100 μ l.

Alternatively, ABT-737 (1.63 mg/ml, 2 mM stock in DMSO) was diluted into RPMI-1640 media to give a stock solution of 25 μ M, which was then further diluted to give

the serial dilutions; 12.50, 6.25, 3.13, 1.56 and 0.78 μM in RPMI-1640 media. 80 μl of each dilution was added to each well to give final ABT-737 concentrations of 0.63-20 μM in a well volume of 100 μl .

Each sample dilution was tested in triplicate. Negative controls included wells containing only 100 μl of RPMI-1640 media and wells containing RPMI-1640 media and sample vehicle. Additionally, a time 0 control plate containing 3×10^3 cells/well in 100 μl RPMI-1640 media was analysed, using the Promega Cell Titre Glo[®] protocol described below, at the time of dosing the cells.

Cells were incubated with the samples for 48 h at 37 °C. The cell viability of each well was then determined using the Promega Cell Titre Glo[®] protocol. The first step was the addition of 100 μl of luciferase/ATP assay solution to each well followed by agitation of the plate using an orbital plate shaker at 600 rpm for 2 min. Cells were then transferred to a white walled 96-well plate and incubated for a further 6 min at rt. Plates were read on a PerkinElmer Envision plate reader measuring the relative luminescence units (RLU).

Controlled unmasking of a cationic cell penetrating peptide for intracellular delivery

The highly basic nature of the arginine side-chain plays a major role in the cell penetrating capability of arginine rich CPPs.⁸⁹ Although CPPs have shown promise for the intracellular delivery of macromolecules they have had limited *in vivo* success. The conjugation of a cationic CPP to a protein results in non-specific uptake into almost all tissues together with rapid blood clearance.¹¹⁹ This wide-spread tissue uptake often means that relatively high doses (mg/kg) of CPP conjugates are required to induce a biological effect. As previously mentioned there have been a number of reported approaches that aim to reduce the non-specific uptake of CPPs using targeted delivery or targeted activation of CPP internalisation. A novel alternative to these methods is investigated in this chapter.

The aim of the research presented in this chapter is to control the cellular internalisation of a CPP by masking the cationic arginine residues with hydrolytically and/or enzymatically labile protecting groups. It is predicted that after *i.v.* administration of the CPP, the cationic charge will then be gradually unmasked by breakdown of the protecting groups by hydrolysis or deprotection by serum esterases. This slow unmasking will then allow for the CPP to interact with cell membranes

leading to internalisation. Figure 4-1 illustrates the principle of the approach investigated in this chapter.

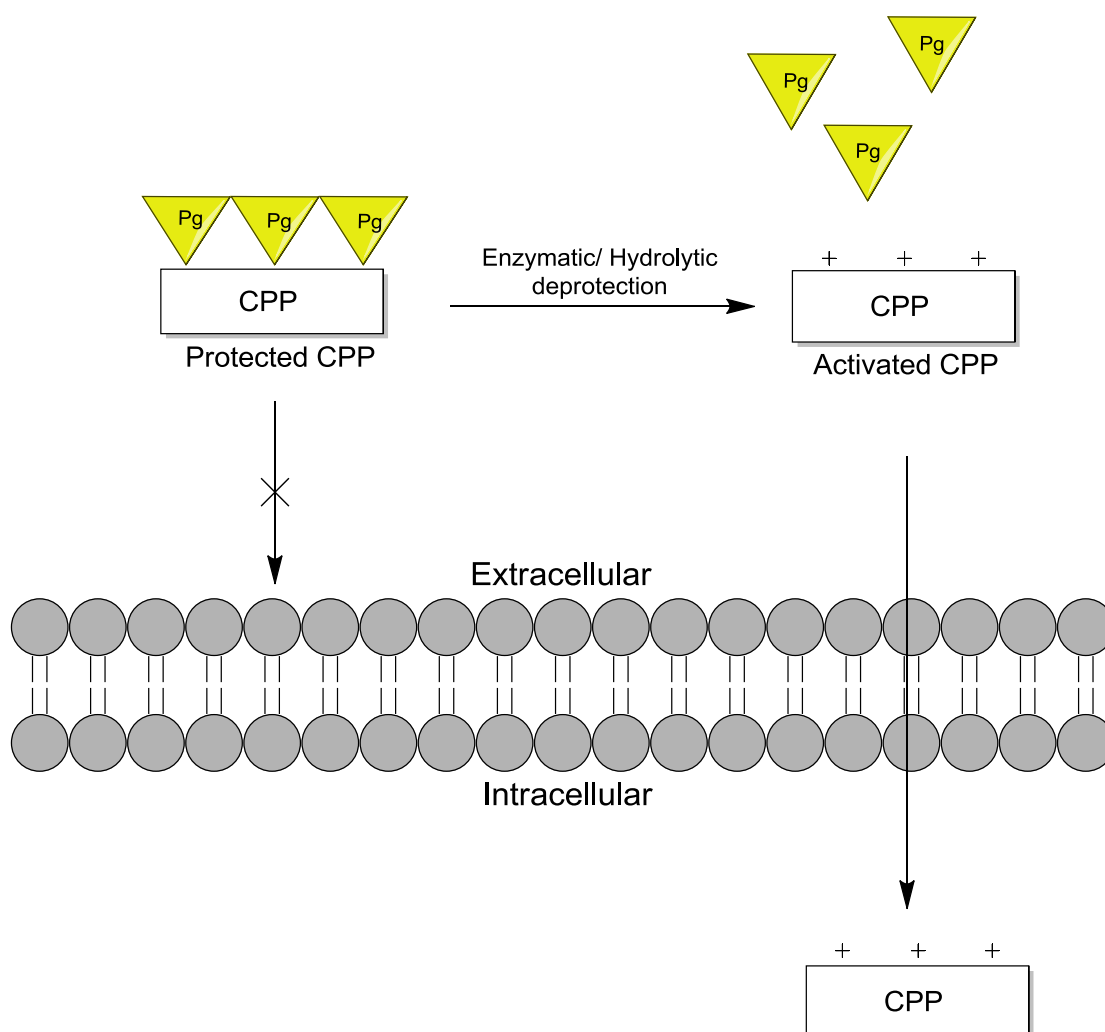


Figure 4-1: The protected guanidine functionalities of the CPP result in inhibition of cell internalisation. Slow hydrolysis of the protecting groups or deprotection by the activity of serum esterases then exposes the guanidine moieties allowing for internalisation of the peptide.

This approach could prolong the circulation time of a protein-CPP conjugate, allowing for organ uptake and reducing peripheral tissue uptake. The advantage of this method is that the activation step is separate from the targeting mechanism. Therefore, this approach could be used in conjunction with a range of cargo and tissue targeting molecules.

The research aims of this chapter are:

1. Proof-of-concept: does carbamate protection of the guanidine functionality of octa-arginine inhibit cell penetration?
 - ❖ Synthesis of 5-FAM labelled octa-ornithine derivatives.
 - ❖ In-solution guanidinylation of octa-ornithine derivatives to afford carbamate protected octa-arginine derivatives.
 - ❖ Cell internalisation studies comparing the protected and unprotected octa-arginine derivatives using confocal laser scanning microscopy (CLSM).
2. The application of esterase and hydrolytically sensitive carbamate protecting groups for the protection of octa-arginine.
 - ❖ Investigate the application of acyloxymethyl (AM) and acyloxy (AO) carbonyl groups for the side-chain protection of arginine.
 - ❖ Evaluate the esterase-sensitivity and hydrolytic stability of the AM and AO groups at the monomer level using a HPLC based assay.
 - ❖ Investigate the application of esterase-sensitive AM/AO groups for the protection of the guanidine functionality of octa-arginine.

The overall goal of this chapter is to establish if guanidine protection with labile protecting groups is a feasible and effective approach to modulating cell internalisation of the CPP octa-arginine.

4.1 Proof-of-concept: Inhibition of CPP cell internalisation by carbamate protection of the guanidine moieties

Carbamate protection of the guanidine functionality of octa-arginine was investigated as a method to inhibit its cell penetration. It was proposed that protected octa-arginine could be accessed by the in-solution guanidinylation of an octa-ornithine derivative using carbamate protected guanidinylation agents. Therefore, the initial step was the synthesis of 5-FAM labelled octa-ornithine derivatives to provide material for use in the rest of this study. Importantly, the regioselective labelling of the peptides with 5-FAM would provide a robust method to assess the cellular uptake of the octa-arginine derivatives using CLSM. Table 4-1 shows the peptides that will be used in this chapter.

Table 4-1: Octa-ornithine derivatives to be synthesised

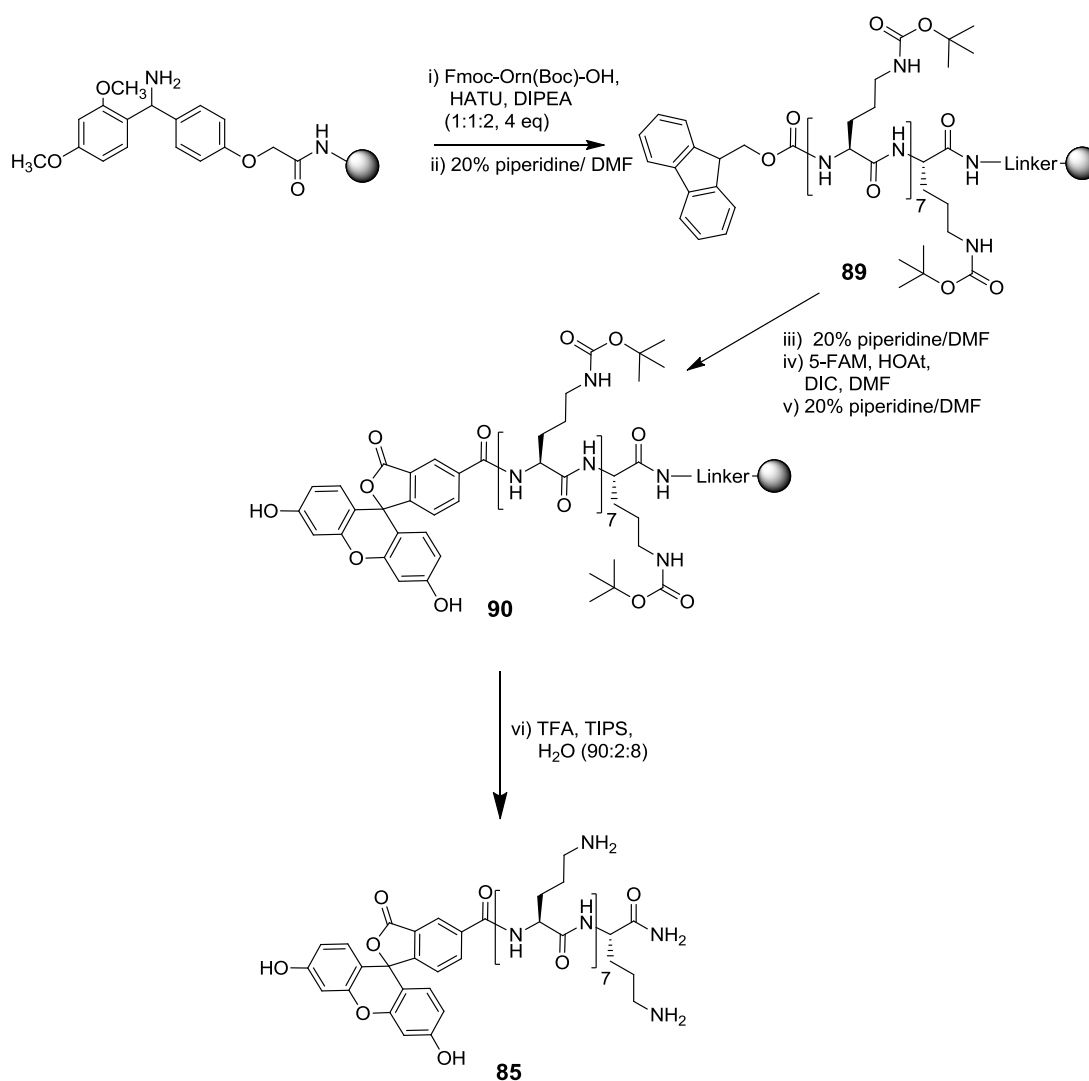
#	Peptide	Reference
<u>octa-ornithine derivatives</u>		
85	FAM-(Orn) ₈ -[NH ₂]	
86	FAM-(Orn-Ahx) ₈ -[NH ₂]	
<u>octa-arginine derivatives</u>		
87	FAM-(Arg) ₈ -[NH ₂]	Wender <i>et al.</i> (2000) ⁸⁹
88	FAM-(Arg-Ahx) ₈ -[NH ₂]	Rothbard <i>et al.</i> (2002) ²¹⁸

The 5-FAM labelled octa-ornithine derivative **85** was chosen based on the CPP octa-arginine **87**. This CPP is widely used for the intracellular delivery of a wide range of cargo.⁸⁹ Additionally, the 6-aminohexanoic acid (Ahx) spaced octa-ornithine derivative **86** was chosen. The corresponding spaced octa-arginine derivative **88** was reported by Rothbard *et al.* (2002) to possess superior cell penetrating ability compared to octa-arginine.²¹⁸ Moreover, octa-ornithine derivative **86** may be more suitable for the introduction of multiple protected guanidine moieties due to the spacing between the amino acid residues and flexibility of the peptide backbone relative to **85**.

The synthesis of octa-ornithine **85** was achieved using standard Fmoc solid-phase peptide synthesis (Fmoc SPPS) on a Rink amide NovaGel[®] resin. The first residue to be introduced to the resin was Fmoc-Orn(Boc)-OH using four equivalents of amino

acid and the carboxyl-activation mixture HATU and DIPEA, relative the resin loading (0.1 mmol). All subsequent amino acid residues were introduced to the peptidyl resin after repeated steps of Fmoc deprotection using 20% piperidine in DMF followed by coupling of Fmoc-Orn(Boc)-OH. This was repeated until a total of eight ornithine residues were introduced to the peptidyl resin to afford intermediate **89** (Scheme 4-1, i-ii).

Scheme 4-1: Synthesis of the 5-FAM labelled octa-ornithine derivative **85**.



In the next step of the synthesis, **89** was Fmoc deprotected using 20% piperidine in DMF. 5-FAM was then introduced to the peptidyl resin using the coupling reagents HOAt and DIC (Scheme 4-1, iii-iv). The reaction mixture was stirred intermittently for 16 h at rt. The resin was then washed with DMF to remove excess reagents.

Subsequent washing of the resin with 20% piperidine/ DMF removed any 5-FAM polymeric phenyl esters by base-catalysed aminolysis to afford peptidyl resin **90** (Scheme 4-1, v).²¹⁰ The final step of the synthesis involved treatment of **90** with TFA-TIPS-H₂O (90:2:8) to furnish the FAM labelled octa-ornithine derivative **90** in good yield and purity (>80%). Figure 4-2 shows the crude analytical trace of **85** (t_R 3.12 min).

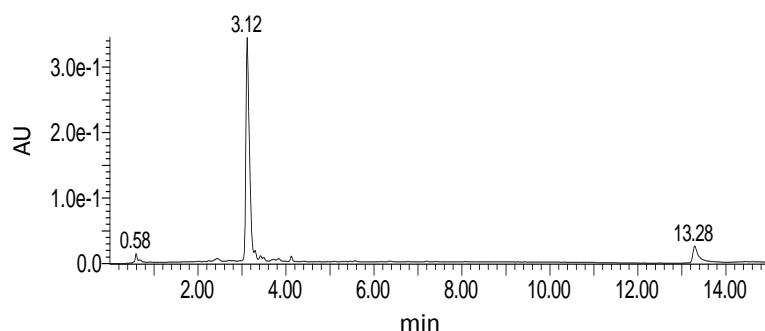
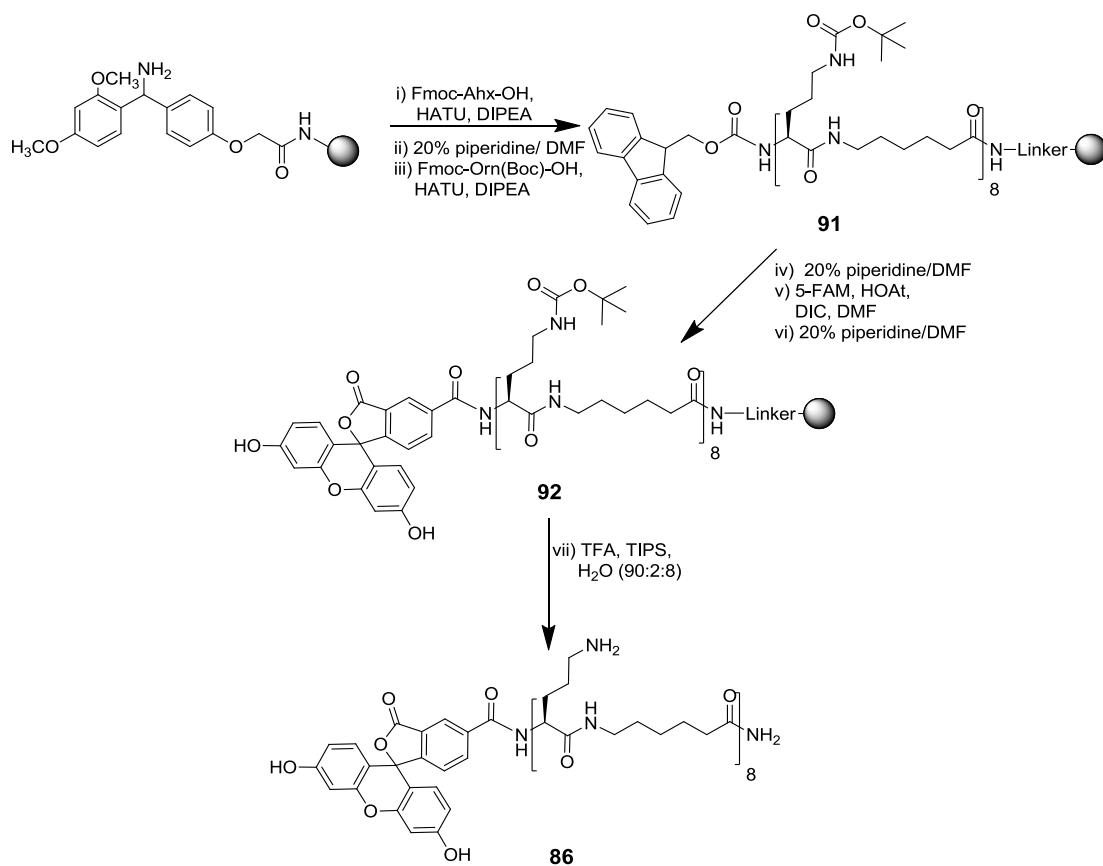


Figure 4-2: Analytical HPLC of crude FAM-(Orn)₈-[NH₂] **85** (t_R 3.12 min) analysed using a 1-90% B over 10 min, 3ml/min method on an Onyx Monolithic C₁₈ column (100 x4.6 mm).

The successful synthesis of **85** was confirmed by TOF MS (ES⁺) with a peak at m/z 644.8573 being detected and assigned as the $[M+2H]^{2+}$ species together with a single major product being observed by analytical HPLC (see Figure 4-2). The aforementioned synthetic approach was applied to the synthesis of the Ahx spaced octa-ornithine derivative **86**.

Scheme 4-2: Synthesis of the Ahx spaced 5-FAM labelled octa-ornithine derivative **86**.



Preparative HPLC of crude peptide **86** gave a peptide of good purity (>95%) and in an isolation yield of 46%. Figure 4-3 shows the analytical HPLC trace for the crude peptide **86** (t_R 2.77 min).

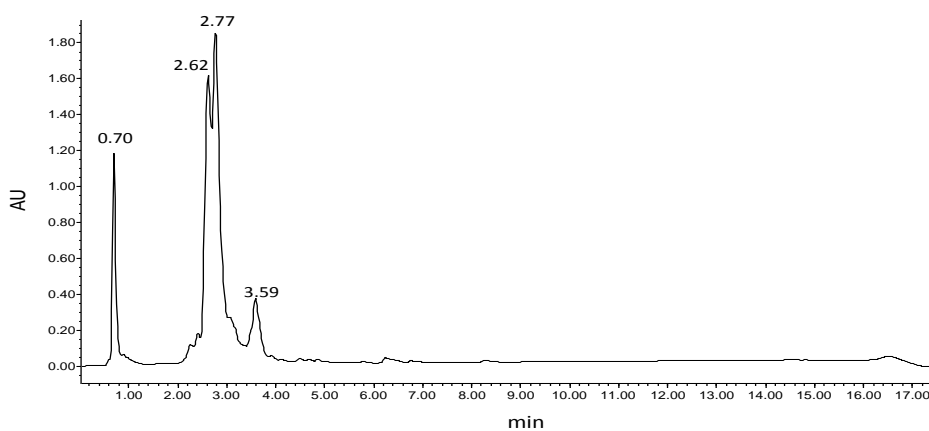


Figure 4-3: Analytical HPLC of crude FAM-(Orn-Ahx)₈-[NH₂] **86** (t_R 2.77 min) analysed using 1-100% B over 10 min, 3ml/min method on an Onyx Monolithic C₁₈ column (100 x 4.6 mm).

The successful synthesis of **86** was confirmed by TOF MS (ES^+) with peaks at m/z 1097.6907 and 732.1321 being observed and assigned as $[\text{M}+2\text{H}]^{2+}$ and $[\text{M}+3\text{H}]^{3+}$, respectively. The reduced yield of **86** was the result of incomplete coupling of the final ornithine residue, possibly due to aggregation of the peptide hindering access to the α -amine, thus reducing the efficiency of the residue coupling. Table 4-2 shows the synthesised octa-ornithine derivative and the corresponding yields.

Table 4-2: Isolation yields and purity of FAM-(Orn)₈-[NH₂] **85** and FAM-(Orn-Ahx)₈-[NH₂] **86**.

	Sequence	Yield	Purity*	t_R/min^\dagger
85	FAM-(Orn) ₈ -[NH ₂]	71%	>80%	3.12
86	FAM-(Orn-Ahx) ₈ -[NH ₂]	46%	>95%	3.45

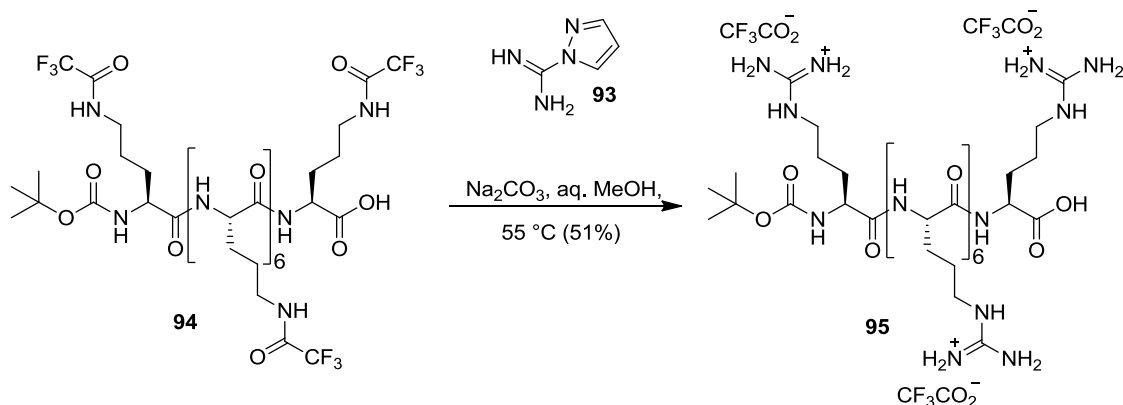
*Peptide purity determined from integration of HPLC peak.

† 1-90% B over 10 min, 3ml/min, Onyx monolithic C₁₈ (100 x 4.6 mm).

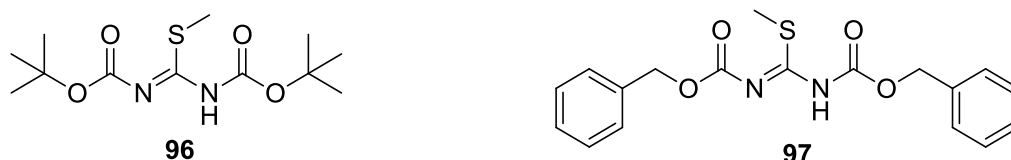
The two octa-ornithine derivatives **85** and **86** were used for subsequent reactions investigating the in-solution guanidinylation of the ornithine side-chain to afford protected octa-arginine derivatives.

In this context, the reported procedure by Wender *et al.* (2001) utilises pyrazole-1-carboxamide **93** to guanidylate a trifluoroacetamide protected octa-ornithine derivative **94** affording the octa-arginine derivative **95** in a yield of 50% (Scheme 4-3).²³⁰

Scheme 4-3: Synthesis of octa-arginine **95** by guanidinylation of trifluoroacetamide protected octa-ornithine derivative **94**.

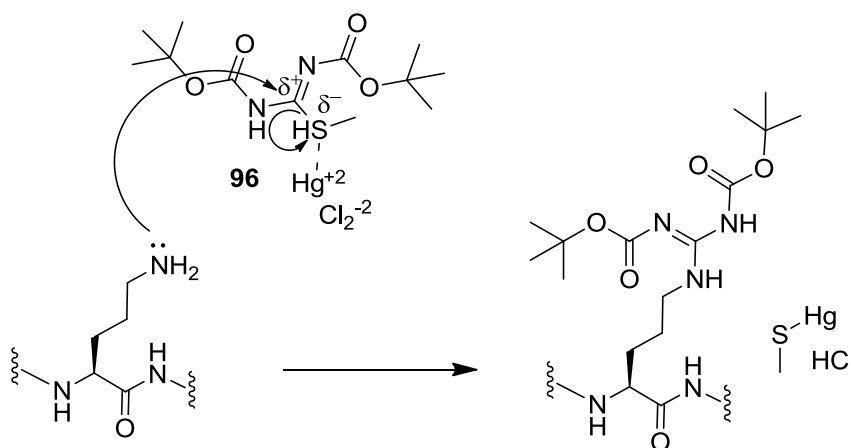


Overall, the octa-arginine was synthesised in 10 steps starting from the trifluoroacetamide protected ornithine monomer in an overall yield of 29%. Alternatively, a milder approach for introducing guanidine moieties to a molecule is the application of protected isothioureas such as, *N,N'*-bis(*tert*-butoxycarbonyl)-*S*-methylthiourea **96** and *N,N'*-bis(benzyloxycarbonyl)-*S*-methylthiourea **97**.²³¹



Usually, the conversion of an isothiourea to a guanidine requires an activation step. This can be achieved under mild conditions using the Lewis acid mercuric chloride.^{232,233} The guanidinylation reaction proceeds by $\text{Hg}^{\text{(II)}}$ bonding with the thioether of **96**, resulting in polarisation of the carbon-sulfur bond, which promotes the $\text{S}_{\text{N}}2$ substitution of the methyl thioether by an amine. The proposed mechanism for this reaction is illustrated in Scheme 4-4.

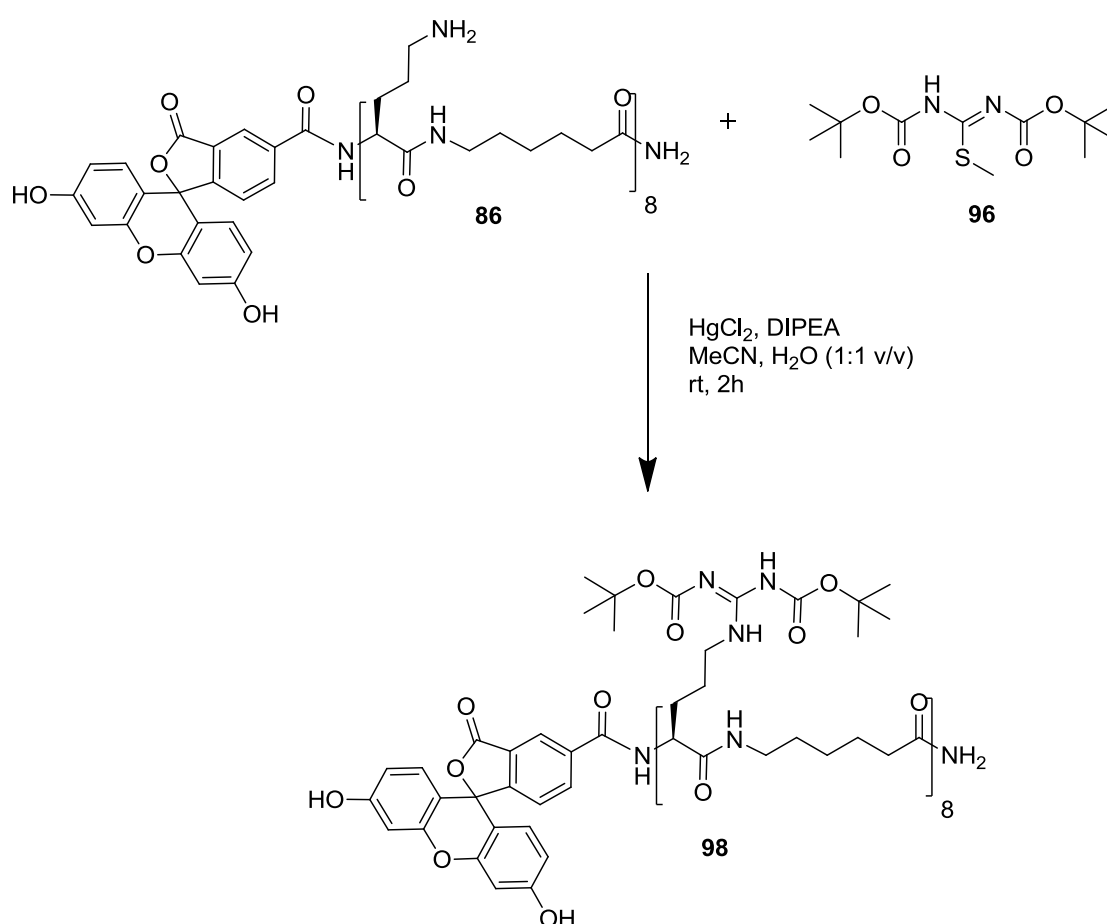
Scheme 4-4: The proposed mechanism for the guanidinylation of an amine with *N,N'*-bis(*tert*-butoxycarbonyl)-*S*-methylthiourea **96** in the presence of HgCl_2 .



This strategy was employed to introduce di-Boc protected guanidine moieties to an octa-ornithine derivative to afford the corresponding protected octa-arginine. The protected peptide will then be used to determine if cell internalisation is inhibited by protecting the guanidine moieties of arginine.

The guanidinylation of the octa-ornithine derivatives **85** and **86** using *N,N'*-bis(*tert*-butoxycarbonyl)-*S*-methylthiourea **96** and mercuric chloride was investigated. The Ahx spaced octa-ornithine derivative **86** was used to determine optimum reaction conditions. Peptide **86** was dissolved in water and treated with 10 eq. of DIPEA to scavenge TFA salts. Separately, **96** was dissolved into MeCN and pre-activated using a stoichiometric amount of mercuric chloride. Peptide **86** was then added dropwise to the activated guanidinating agent (Scheme 4-5).

Scheme 4-5: Synthesis of FAM-(R(di-Boc)-Ahx)₈-[NH₂] **98**.



The reaction was stirred for a further 2 h, followed by removal of the solvent *in vacuo*. The orange residue was suspended in MeCN and centrifuged at 13000 g for 20 min. This resulted in a white pellet and clear orange supernatant. The supernatant was then analysed by HPLC. The synthesis of FAM-(R(di-Boc)-Ahx)₈-[NH₂] **98** was successful. Analysis by TOF MS (ES^+) revealed peaks at m/z 1378.1024, 1033.8420 and 827.2668 that were assigned as the multiple ions $[\text{M}+3\text{H}]^{3+}$, $[\text{M}+4\text{H}]^{4+}$ and

$[M+5H]^{5+}$, respectively. Additional peaks corresponding to sequential loss of Boc groups were also detected, suggesting fragmentation of the peptide in the MS.

Preparative HPLC was used to isolate **98** in a yield of 57%. Surprisingly, subsequent analysis of the purified peptide by analytical HPLC indicated that the N^G -Boc protected peptide was unstable in aqueous conditions, indicated by the presence of four major peaks in the HPLC chromatogram (Figure 4-4).

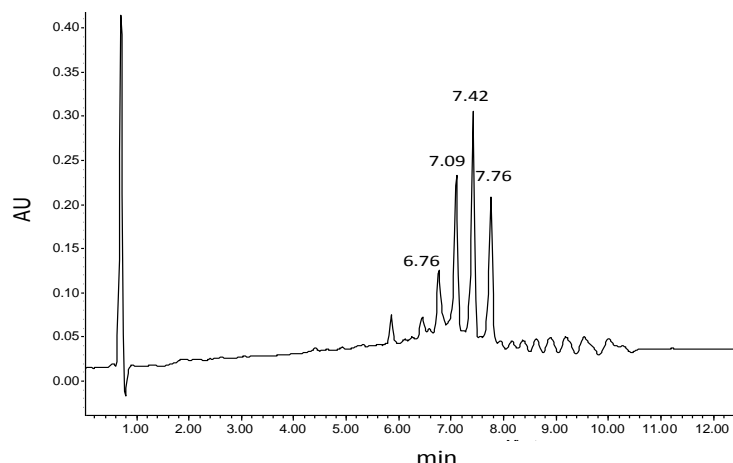
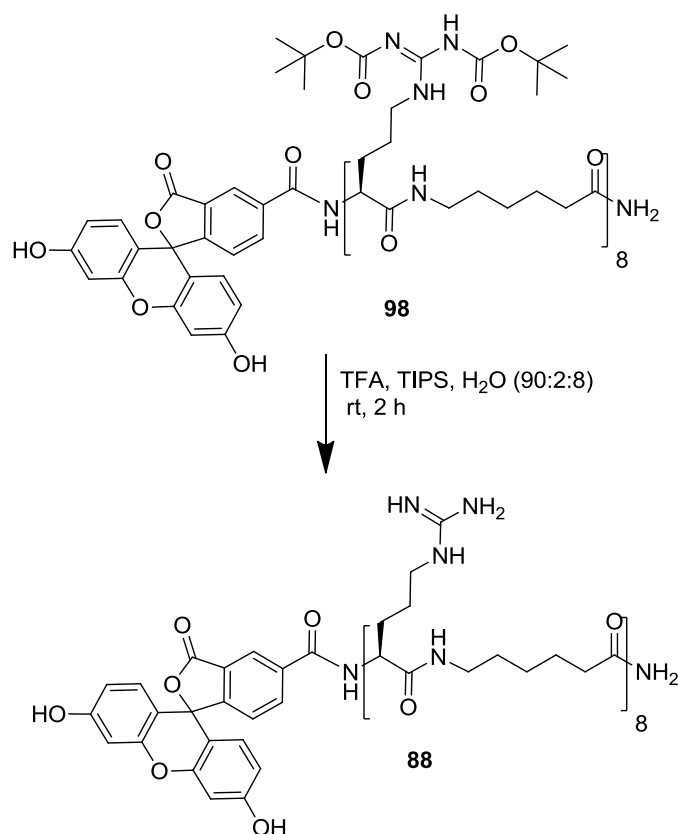


Figure 4-4: Analytical HPLC of purified FAM-(R(di-Boc)-Ahx)₈-[NH₂] **98** analysed using 1-100% B over 10 min, 3ml/ min method on an Onyx Monolithic C₁₈ column (100 x4.6 mm).

To confirm that the observed species seen in the HPLC were due to the loss of Boc groups peptide **98** was N^G -Boc deprotected by acidolysis (Scheme 4-6). Additionally, this would provide the unprotected octa-arginine derivative to be used as a positive control in the cell internalisation studies.

Scheme 4-6: Synthesis of FAM-(R-Ahx)₈-[NH₂] **88**.



FAM-(R(di-Boc)-Ahx)₈-[NH₂] **98** was *N*^G-Boc deprotected in a solution of TFA-TIPS-H₂O (90:2:8) with stirring for 2 h at rt. The TFA was then removed *in vacuo* to afford an orange residue. This residue was triturated with diethyl ether followed by lyophilisation. The resulting orange solid was analysed using analytical HPLC (Figure 4-5).

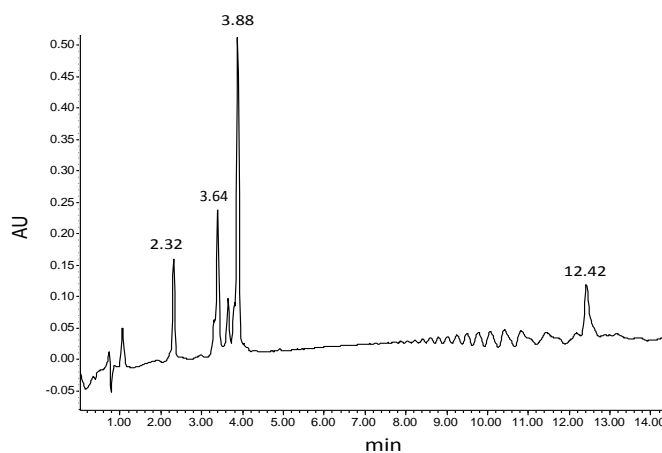


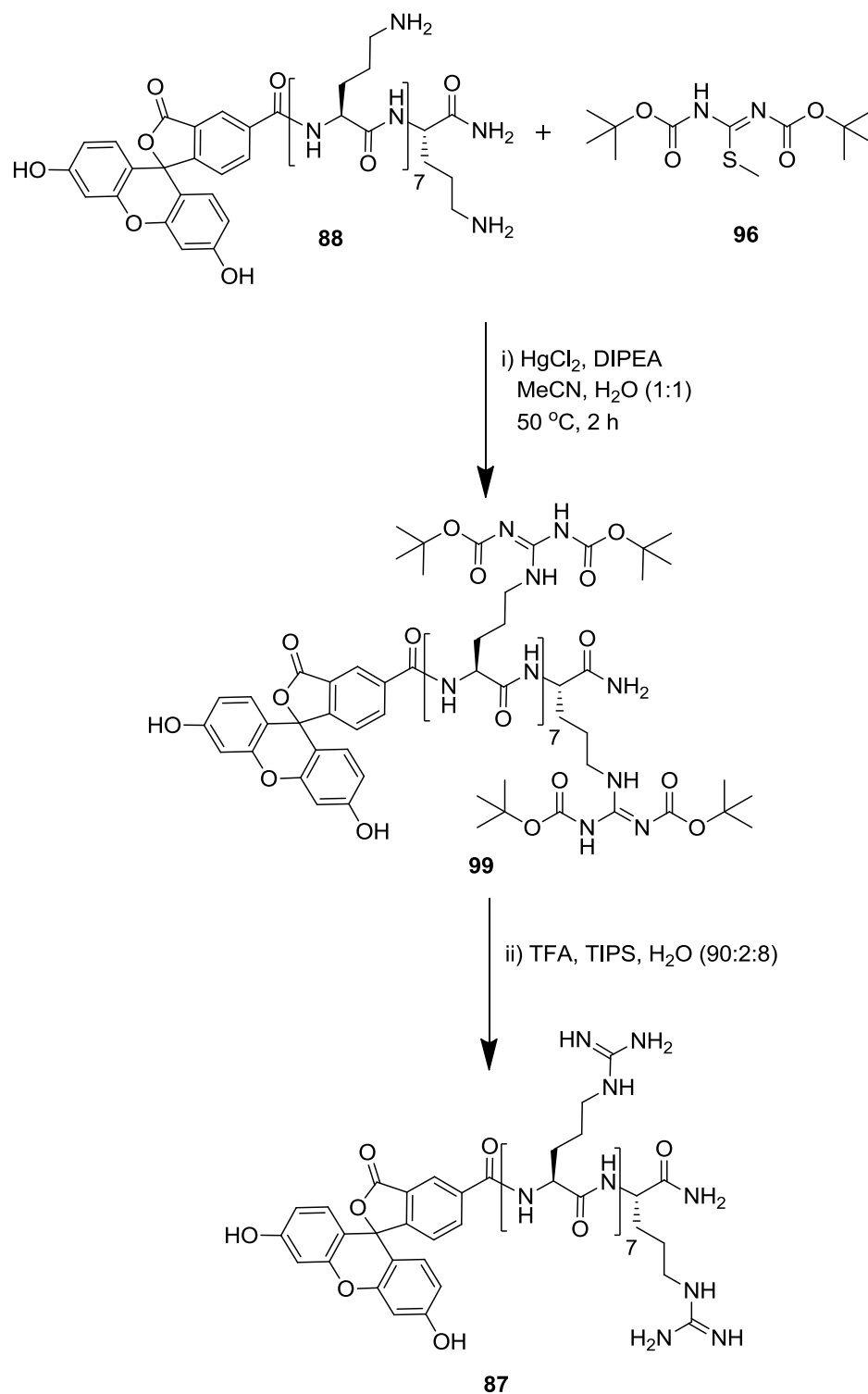
Figure 4-5: Analytical HPLC of crude FAM-(R-Ahx)₈-[NH₂] **88** (*t*_R 3.88 min) analysed using 1-90% B over 10 min, 3ml/ min method on an Onyx Monolithic C₁₈ column (100 x 4.6 mm).

The major peak at 3.88 min (Figure 4-5) was isolated by preparative HPLC to afford **88**. Notably, purified **88** was stable unlike the Boc protected peptide **98**. The successful isolation of **88** was confirmed by MALDI-TOF MS. A major species at m/z 2531.397 was observed, which is in agreement with the calculated value for the $[M+H]^+$ species of the fully deprotected octa-arginine derivative **88**.

Interestingly, the Boc deprotection of **98** resulted in one major species. This suggests that the multiple species seen in the analytical HPLC of **98** are due to hydrolysis of the Boc groups. TOF MS (ES^+) analysis of peptide **98** showed the presence of a number of species with different numbers of Boc groups, however it must be noted that this fragmentation may also occur due to ES ionisation. Nevertheless, comparison of the internalisation capabilities of the partially protected FAM-(R(di-Boc)-Ahx)₈-[NH₂] **98** and the unprotected FAM-(R-Ahx)₈-[NH₂] **88** should still be insightful.

The guanidinylation of octa-ornithine derivative **85** was achieved using the same method used for the synthesis of **98** (Scheme 4-5), however, at rt no reaction occurred. Alternatively, heating of the reaction to 50 °C with stirring for 2 h resulted in complete guanidinylation of peptide **85** to give the N^G -Boc protected octa-arginine **99** (Scheme 4-7).

Scheme 4-7: Synthesis of FAM-(R(di-Boc))₈-[NH₂] **99** and FAM-(R)₈-[NH₂] **87**.



The successful synthesis of **99** was confirmed by TOF MS (ES⁺) revealing a peak at m/z 807.4263 that was assigned at the [M+4H]⁴⁺ species. Preparative HPLC of the crude peptide afforded **99** in good purity and a yield of 23%. Interestingly, peptide **99** displayed greater stability under aqueous conditions compared to FAM-(R(di-Boc))-

Ahx)₈-[NH₂] **98**. This difference could be a result of **98** adopting a more compact conformation in solution compared to the Ahx spaced peptide **98**, thus protecting the Boc groups from hydrolysis.

The *N*^G-Boc deprotection of **98** was achieved using TFA-TIPS-H₂O (90:2:8) (Scheme 4-7, ii). The TFA was then removed *in vacuo* after 4 h and the resulting orange residue was triturated with diethyl ether. FAM-(R)₈-[NH₂] **87** was then isolated by preparative HPLC in good purity and an isolation yield of 40%. The successful synthesis of **87** was confirmed by MALDI-TOF MS with a peak at *m/z* 1625.86 being detected and assigned as the [M+H]⁺ species. Table 4-3 shows the yields and purity of both the synthesised *N*^G-protected and unprotected octa-arginine derivatives.

Table 4-3: Synthesised *N*^G-Boc protected and unprotected octa-arginine derivatives.

#	Sequence	Yield	Purity*	<i>t</i> _R / min [†]
98	FAM-(R(di-Boc)-Ahx) ₈ -[NH ₂]	57%	n.d	6.76, 7.09, 7.42, 7.76
88	FAM-(R-Ahx) ₈ -[NH ₂]	56%	>95%	3.88
99	FAM-(R(di-Boc)) ₈ -[NH ₂]	23%	>80%	8.95
87	FAM-(R) ₈ -[NH ₂]	40%	>95%	3.47

*Peptide purity determined from integration of HPLC peak. †1-90% B over 10 min, 3ml/min, Onyx monolithic C₁₈ (100 x 4.6 mm). Multiple peaks for **98** due to sequential *N*^G-Boc deprotection.

In summary, the in-solution guanidinylation of the octa-ornithine derivatives **85** and **86** was successful. Guanidinylation using the Boc protected isothiourea **96** afforded the *N*^G-Boc protected octa-arginine derivatives **95** and **99**. Notably, peptide **99** displays greater stability under aqueous conditions compared to the protected Ahx spaced octa-arginine **98**. Thus, peptide **99** is perhaps a more suitable peptide for CLSM studies comparing the cell internalisation of the protected and unprotected octa-arginine derivatives.

4.1.1 Cell internalisation of protected octa-arginine derivatives

The cell internalisation of the prepared peptides was assessed using CLSM. By comparing the cellular internalisation of the protected and unprotected octa-arginine derivatives the effect of protecting the guanidine functionality of an octa-arginine can be assessed. The unprotected octa-arginine derivatives FAM-(R)₈-[NH₂] **87** and

FAM-(R-Ahx)₈-[NH₂] **88** were used as positive controls. These peptides were compared to the protected peptide FAM-(R(di-Boc)₈-[NH₂] **99** and the partially protected FAM-(R(di-Boc)-Ahx)₈-[NH₂] **98** (Figure 4-6).

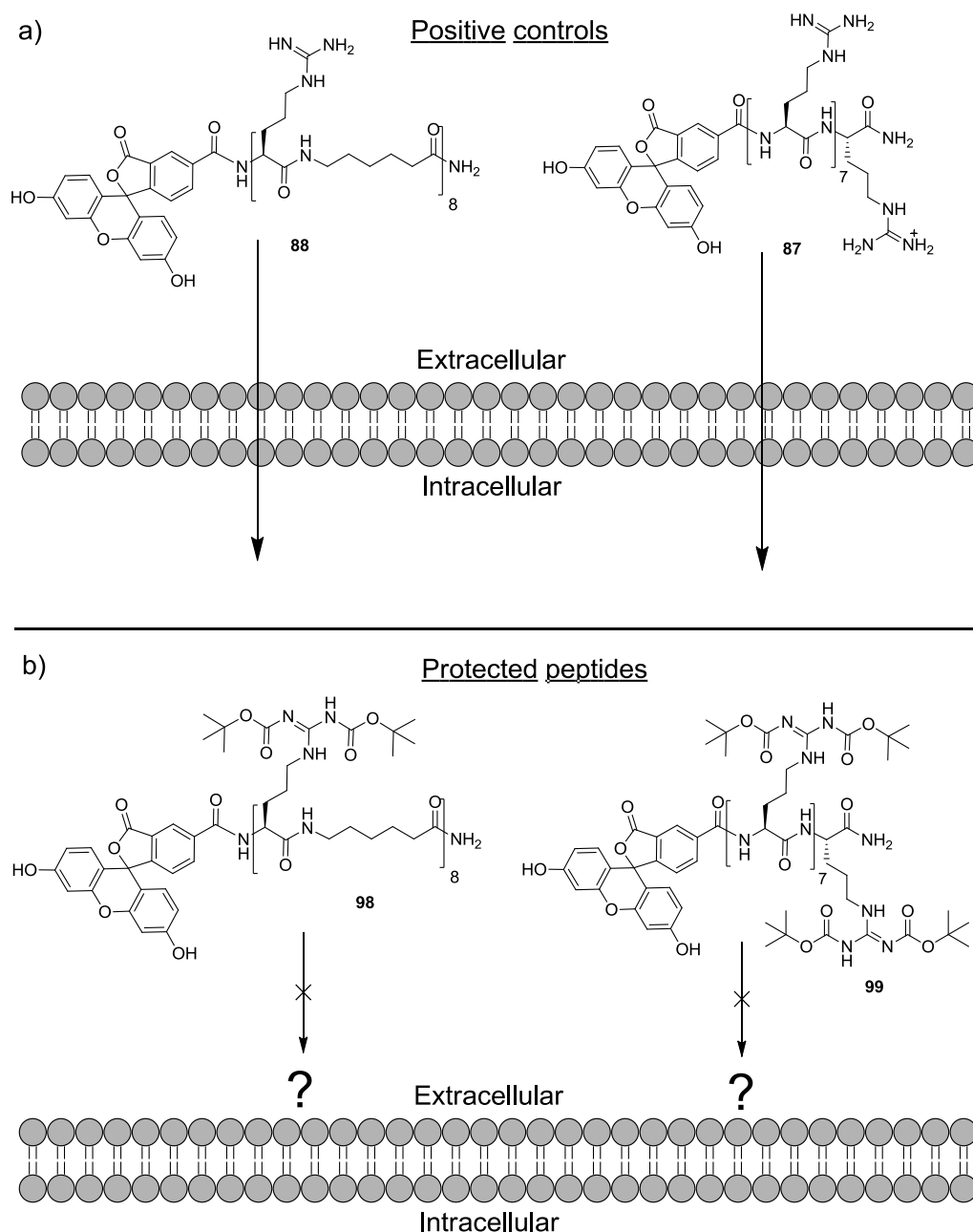


Figure 4-6: The cell internalisation of the a) unprotected and b) carbamate protected octa-arginine derivatives will be compared to determine if protection of the arginine side-chains inhibits internalisation. The peptides are labelled with 5-FAM allowing for internalised peptide to be imaged using CLSM.

HeLa cells were treated with either the N^G -Boc protected or the unprotected octa-arginine derivative at 10 μ M for 30 min at 37 $^{\circ}$ C. After incubation, cells were washed with PBS and incubated with 5 μ M of the nuclear stain Draq5 (Ex 646 nm/Em 697 nm). Finally, the live cells were imaged using an inverted x63 oil immersion lens. Z-sectioning using CLSM allowed for focusing within the cell, distinguishing between membrane and intracellular associated fluorescence. The prepared peptides all possess an *N*-terminal fluorescein (Ex 494 nm/Em 518 nm) allowing for detection of the peptide. Figure 4-7 shows HeLa cells treated with FAM-(R-Ahx)₈-[NH₂] **88** (Figure 4-7, b) and FAM-(R(di-Boc)-Ahx)₈-[NH₂] **98** (Figure 4-7, c).

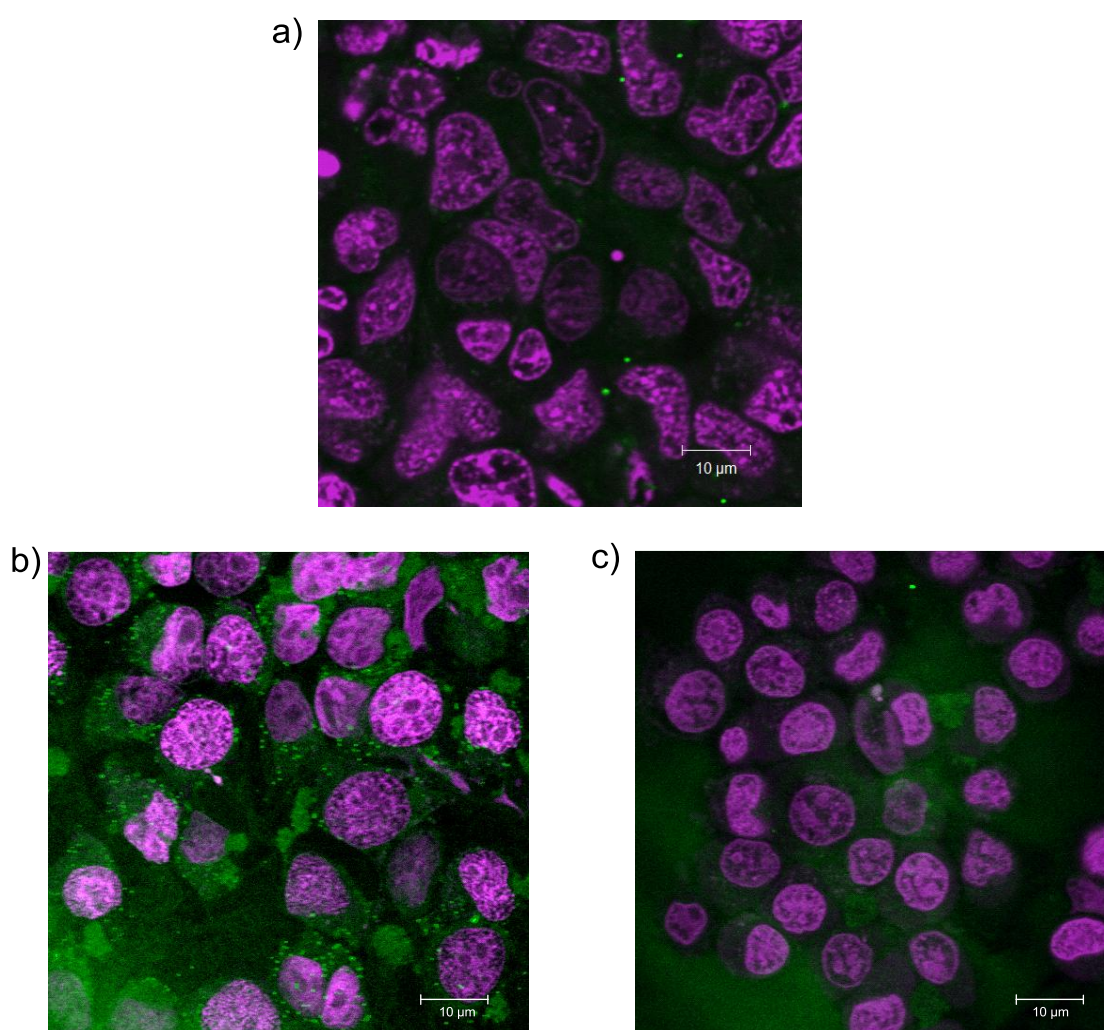


Figure 4-7: Cell internalisation of octa-arginine derivatives. HeLa cells treated with 10 μ M of 5-FAM labelled peptide (green), for 30 min at 37 $^{\circ}$ C. Cells were then washed and incubated with the nuclear stain Draq5 (purple) and imaged using CLSM with an inverted x63 oil immersion lens a) untreated cells, b) FAM-(R-Ahx)₈-[NH₂] **88** and c) FAM-(R(di-Boc)-Ahx)₈-[NH₂] **98**.

The partial protection of the arginine side-chains appears to inhibit cell internalisation of the Ahx spaced octa-arginine **98** (Scheme 4-7, c). However, the FAM-(R-Ahx)₈-[NH₂] **88** does not show intense cell associated fluorescence, suggesting that this peptide is not efficiently internalised into HeLa cells (Scheme 4-7, b). Despite this, there is still a difference between the cell internalisation of the partially protected **98** and unprotected peptide **88**.

The cell internalisation of the FAM-(R)₈-[NH₂] **87** and FAM-(R(di-Boc))₈-[NH₂] **99** was investigated using the same method as previously described. Figure 4-8 shows the CLSM images of HeLa cells treated with 10 µM of peptide (green) for 30 min, again the cell nucleus was stained with Draq5 (purple).

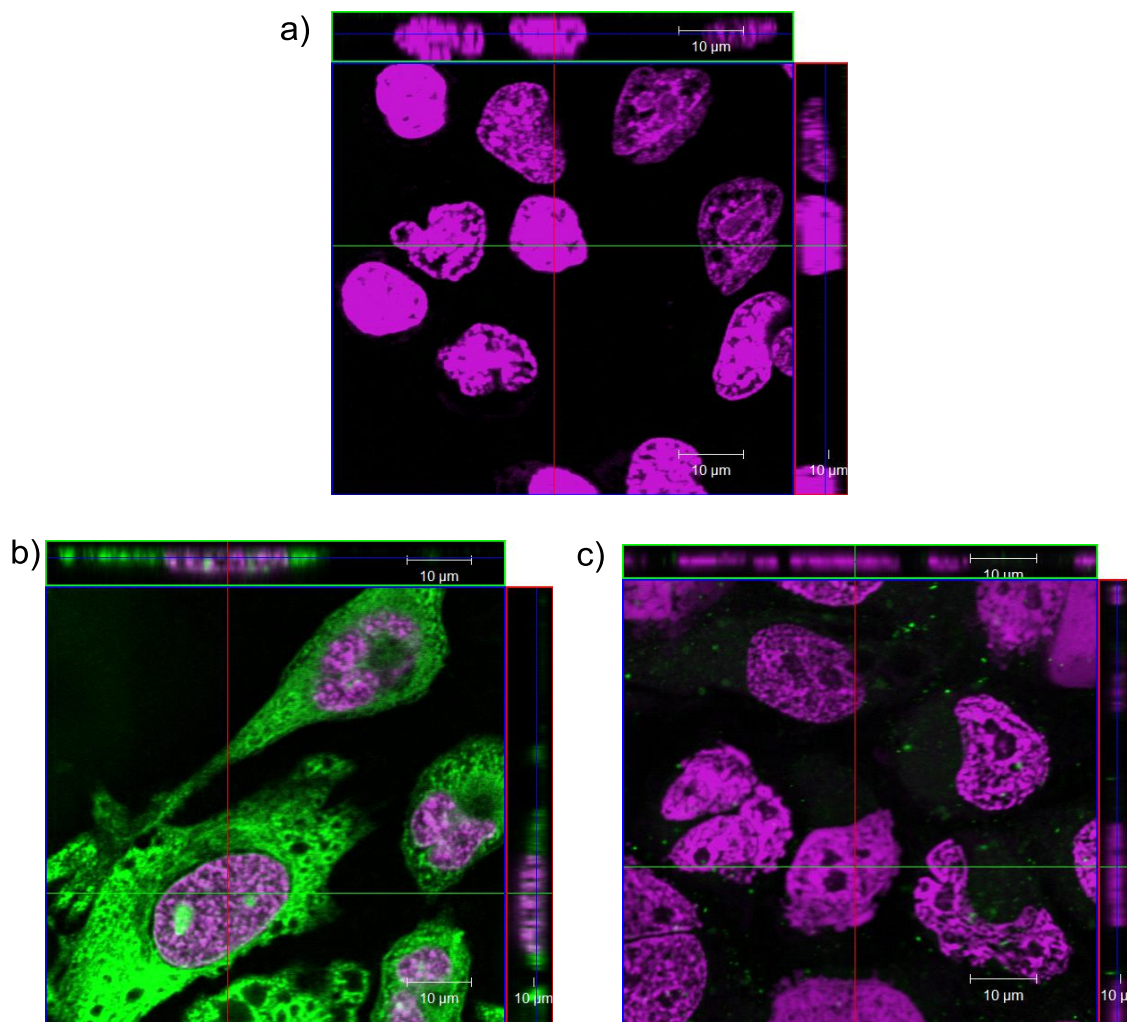


Figure 4-8: Cell internalisation of octa-arginine derivatives. HeLa cells treated with 10 µM of 5-FAM labelled peptide (green), for 30 min at 37 °C. Cells were then washed and incubated with the nuclear stain Draq5 (purple) and Z-sections of the cells were taken using CLSM with an inverted x63 oil immersion lens **a)** untreated cells, **b)** FAM-(R)₈-[NH₂] **87** and **c)** FAM-(R(di-Boc))₈-[NH₂] **99**.

FAM-(R)₈-[NH₂] **87** is clearly internalised, with uniform cellular fluorescence being observed (Figure 4-8, b). In contrast, minimal fluorescence is seen for the *N*^G-Boc protected peptide FAM-(R(di-Boc))₈-[NH₂] **99** (Figure 4-8, b).

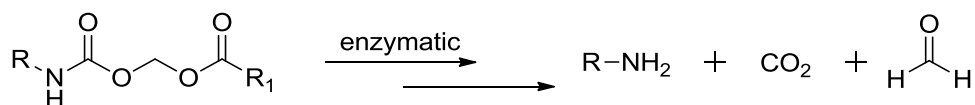
In summary, the inhibition of the cellular internalisation of octa-arginine was successfully achieved by protection of the guanidine moieties of the arginine side-chains using the Boc protecting group. The difference observed in the CLSM images is very significant. FAM-(R)₈-[NH₂] **87** shows the most efficient cellular uptake with intense cell associated fluorescence being observed. This cellular uptake was almost completely inhibited through *N*^G-Boc protection, demonstrated by treatment of cells with FAM-(R(di-Boc))₈-[NH₂] **99**. CLSM of cells treated with **99** showed no cell associated fluorescence, thus suggesting no cellular uptake of the peptide.

4.2 Protection of arginine side-chain with hydrolytic and esterase-labile protecting groups

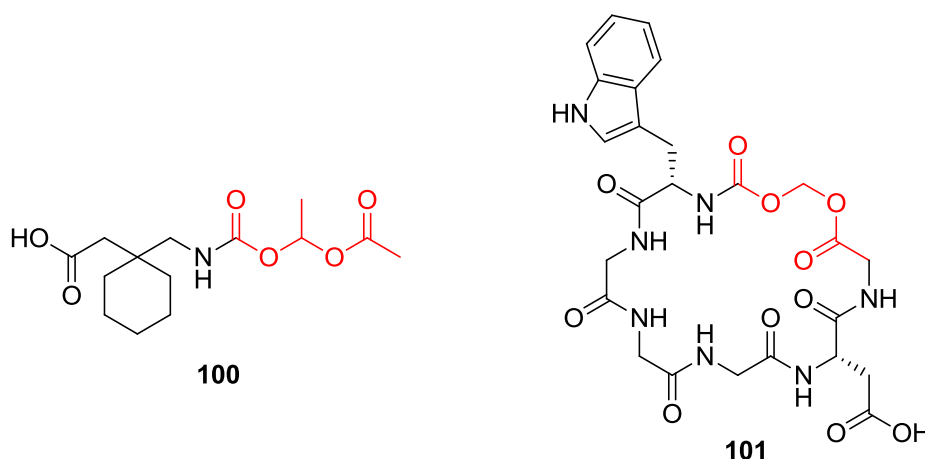
The aforementioned findings clearly demonstrated that CPP side-chain protection decreases cellular uptake. Thus, the use of hydrolytically or catalytically labile protecting groups was investigated. The protection of an octa-arginine derivative with labile protecting groups is predicted to result in unmasking of the cell penetrating properties of the peptide *in vivo*.

An established method for the protection of amine and guanidine moieties in drug molecules is the application of the esterase-sensitive acyloxymethyl carbonyl (AM) protecting group.¹⁴⁶ Therefore, this class of protecting group may be suitable for the protection of an octa-arginine derivative. Upon enzymatic cleavage of the ester moiety by serum esterases, the protecting group is removed to leave the unprotected amine (Scheme 4-8).^{146, 234-235}

Scheme 4-8: Enzymatic cleavage of an acyloxymethyl carbonyl (AM) protected amine by an esterase to afford the unprotected amine.¹⁴⁶

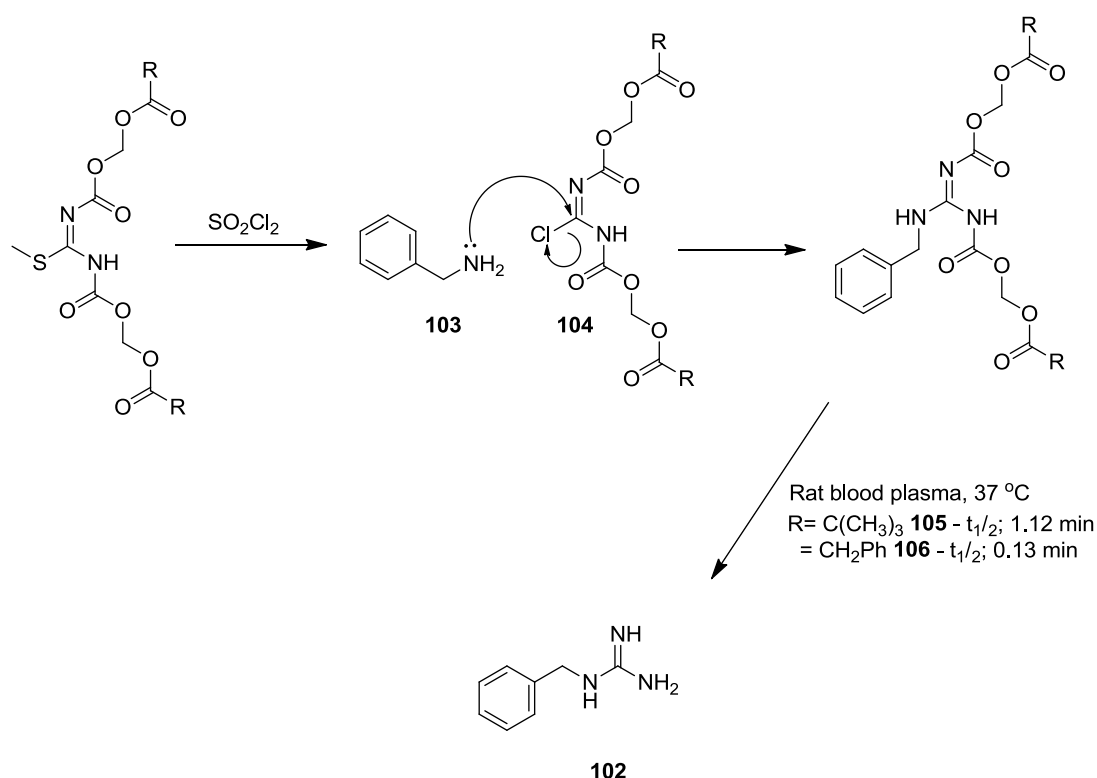


There are several examples of AM moieties being used in prodrugs. For example, Cundy *et al.* (2004) reported the synthesis of XP13512 **100**, a prodrug of Gabapentin, which is used for the treatment of neuropathic pain. This prodrug showed better bioavailability than the parent drug and was rapidly converted after absorption.²³⁶ Additionally, Gangwar *et al.* (1997) report the application of an AM group for the synthesis of the peptide prodrug **101**. Upon enzymatic cleavage of the ester, the linear peptide is produced.²³⁷ The half-life of the cyclic peptide in human blood plasma was 132 ± 4 min.



Of relevance to the aims of this chapter, Saulnier *et al.* (1994) demonstrated the application of AM groups for the protection of guanidine moieties. The authors utilised several AM groups to protect the guanidine moiety of the model compound *N*-benzylguanidine **102**. This was achieved by guanidinylation of benzyl amine **103** using an *N,N'*-bis(acyloxymethoxycarbonyl)-*S*-methylisothiourea that was pre-activated with sulfuryl chloride (Scheme 4-9).

Scheme 4-9: Guanidinylation of benzyl amine **103** with a thiourea using sulfuryl chloride.

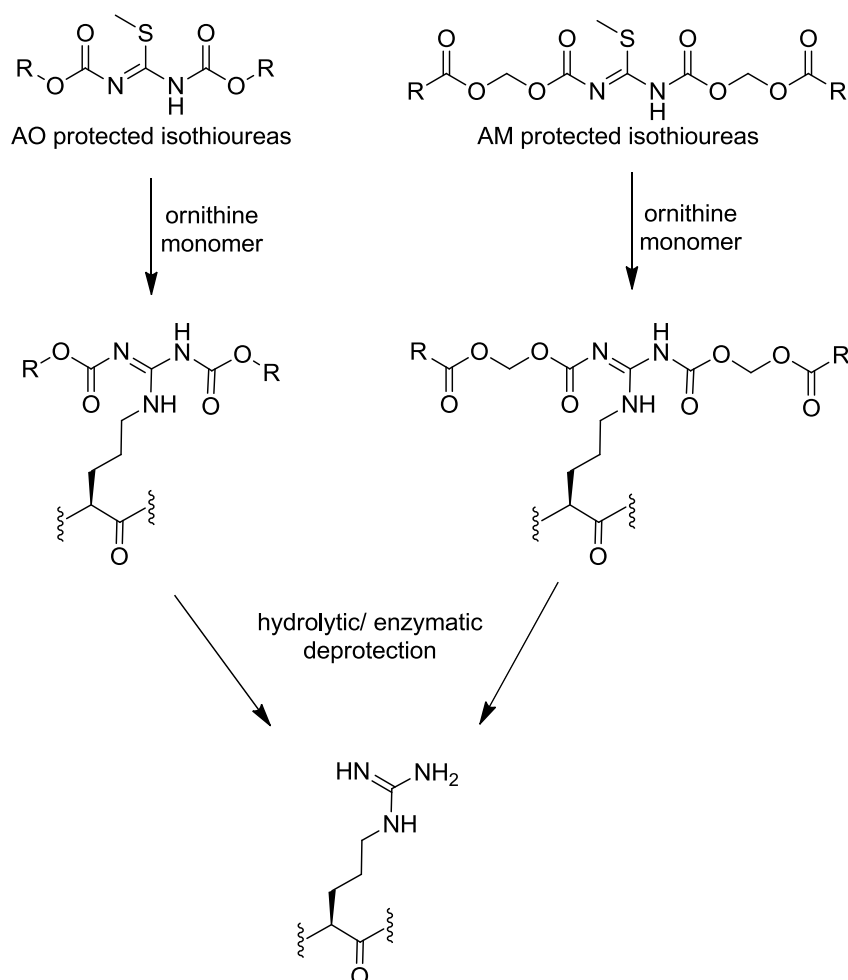


Initially, the isothiurea was pre-activated with sulfuryl chloride to afford the reactive intermediate **104**. This pre-activation step improved the chemoselectivity of the reaction by reducing the nucleophilic attack at the ester carbonyl of the isothiurea. The reported half-lives ($t_{1/2}$) of the protected guanidine moieties in rat blood plasma were 1.12 min and 0.13 min for the **105** and **106** respectively. Experiments using pig liver esterase (PLE) also confirmed that the deprotection of these groups was mediated by esterases.¹⁴⁷

Alternatively, acyloxycarbonyl (AO) protecting groups can also be used to mask amine and guanidine moieties. These simple carbamates have shown less promise for the protection of amines in drug molecules because of the relative chemical and enzymatic stability compared to AM group.¹⁴⁶ However, the application of AO protecting groups will be investigated in this chapter for the protection of an octa-arginine, primarily as a more stable alternative to the AM groups.

It was proposed that assessment of the hydrolytic and esterase-sensitivity of AM and AO protecting groups at the monomer level will give insight into their suitability for the protection of an octa-arginine derivative (Scheme 4-10).

Scheme 4-10: The proposed synthesis of AO and AM protected ornithine residue and either hydrolytic or enzymatic deprotection to give the unprotected arginine residue.

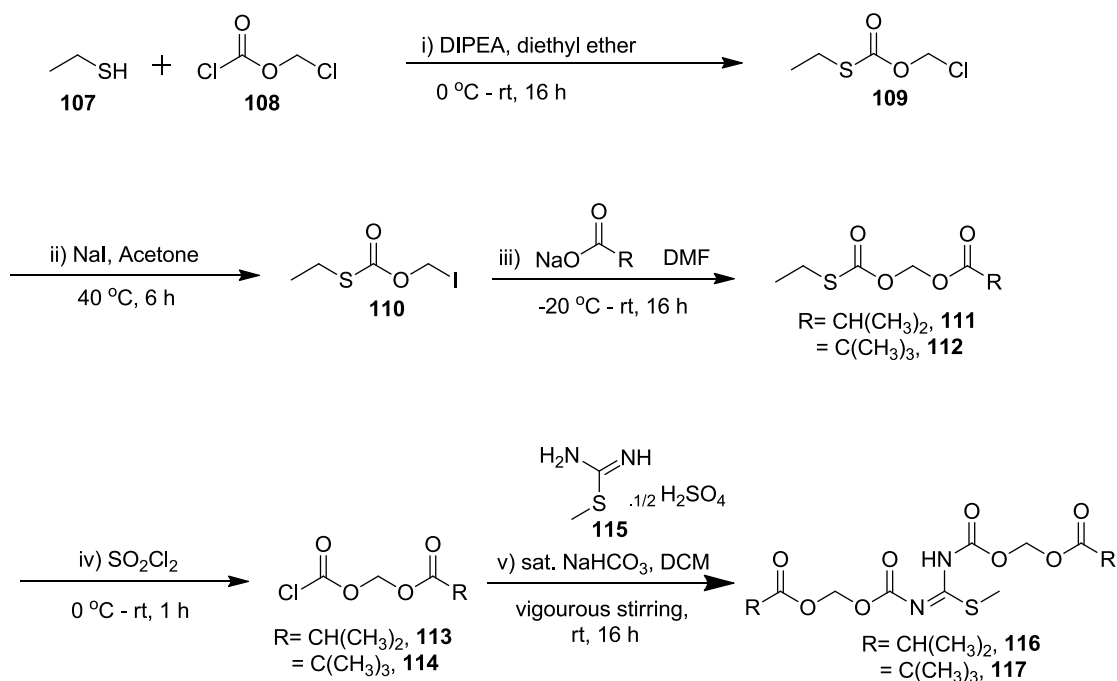


It is envisaged that the protected arginine monomers will provide material for stability assays to investigate the breakdown of the protecting groups in different aqueous conditions and in the presence of esterases using a HPLC based assay.

4.2.1 Synthesis of protected isothioureas

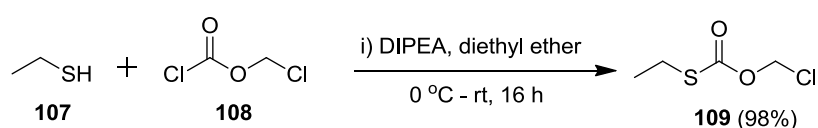
Initially a number of isothiourea starting materials needed to be synthesised. It was proposed that these intermediates could be accessed by a previously reported 5-step synthesis.^{147,238} For example, the synthesis of isobutanoyloxymethyl and pivaloyloxymethyl protected isothioureas is outlined in Scheme 4-11.

Scheme 4-11: Synthesis outline for *N,N'*-bis(acyloxymethoxycarbonyl)-*S*-methylothiourea.



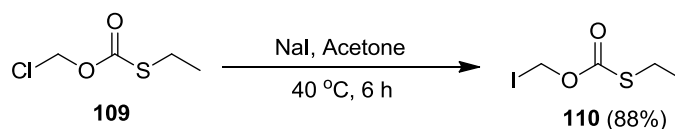
In the first step of the proposed synthesis²³⁷, an ethereal solution of ethanethiol **107** and chloromethyl chloroformate **108** was stirred for 16 h at rt. Subsequent purification of the crude reaction mixture afforded *O*-chloromethyl-*S*-ethyl carbonothioate **109** in a 98% yield (Scheme 4-11).

Scheme 4-12: Synthesis of *O*-(chloromethyl)-*S*-ethyl ester **109**.



The spectroscopic data for **109** was identical to that reported in the literature.²³⁸ To avoid nucleophilic attack at the carbonyl of **109**, the alkyl chloride was converted to an alkyl iodide by a Finkelstein reaction (Scheme 4-13).

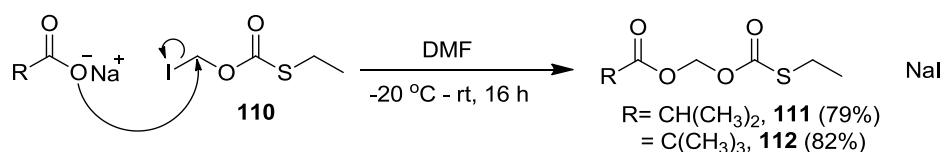
Scheme 4-13: Synthesis of *O*-(iodomethyl)-*S*-ethyl carbonothioate **110**.



Compound **109** was added to a solution of sodium iodide in acetone with stirring for 4 h at 40 °C. Subsequent work-up of the crude reaction mixture afforded the reactive intermediate *O*-(iodomethyl)-*S*-ethyl carbonothioate **110** in a yield of 88%. Exchange of the chloride for an alkyl iodide was confirmed by ¹H NMR with a slight downfield shift of the adjacent methylene protons from δ 5.77 to 5.98 ppm being observed, which was also in agreement with the literature.²³⁸

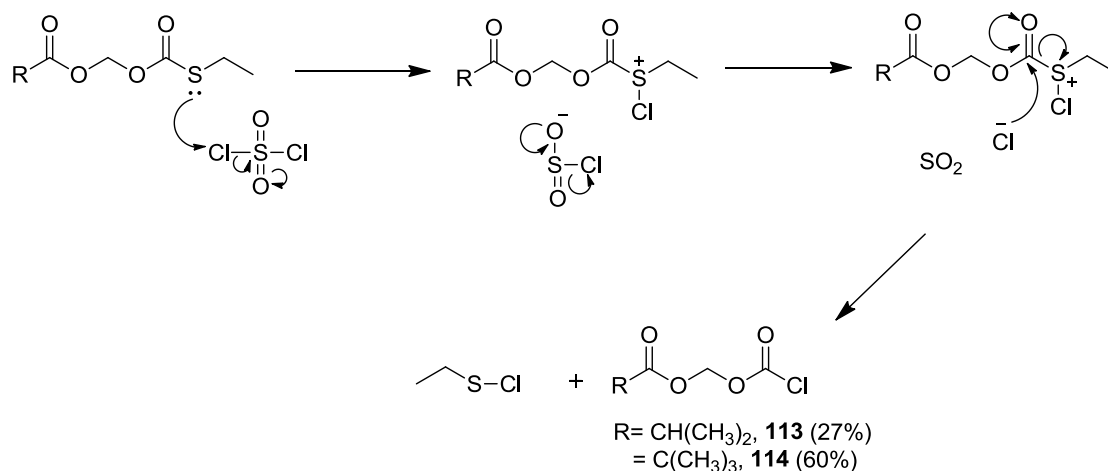
The next step of the synthesis involved the addition of **110** to a solution of either sodium isobutyrate or sodium pivalate in dry DMF at -20 °C. The solution was then warmed to rt and stirred for 16 h. The reaction proceeded by a S_N2 substitution of the alkyl iodide by the carboxylate anion to furnish the esters **111** and **112** in yields of 79% and 82%, respectively (Scheme 4-14).

Scheme 4-14: Synthesis of acyloxymethyl-*S*-ethyl carbonothioate **111** and **112**.



Successful synthesis of the **111** and **112** was confirmed using ¹H NMR with a slight upfield shift of the methylene protons from δ 5.98 ppm for **110** to 5.80 ppm for both **111** and **112** being observed. Additionally, FTIR showed the presence of two carbonyl peaks between 1720 and 1760 cm⁻¹ that are in agreement with the literature.²³⁸ The penultimate step of the synthesis involved the chlorination of **111** and **112** using sulfonyl chloride (Scheme 4-15).

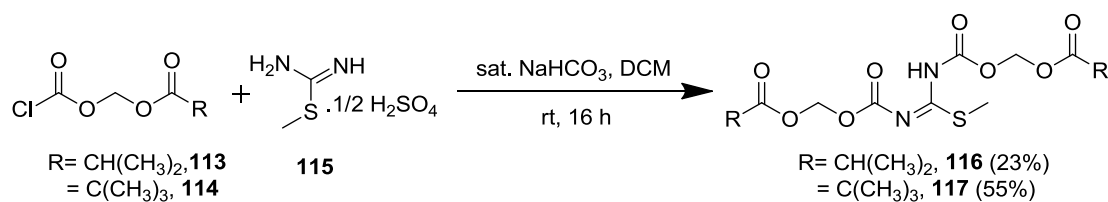
Scheme 4-15: Synthesis of acyloxymethyl carbonochloridate **113** and **114**.



Sulfuryl chloride (1.3 eq.) was added to **111** or **112** at 4 °C with stirring. The reaction mixture was allowed to warm to rt and stirred for 1 h. The by-product of the reaction, ethylsulfenyl chloride, was largely removed *in vacuo*. However, further purification was required by Kugelrohr distillation to afford the pure acyloxymethyl carbonochloridate **113** and **114** in yields of 27% and 60%, respectively. Successful chlorination of the esters was confirmed using FTIR with a change in the absorption of the carbonyl at 1720 cm⁻¹ for **111** and **112** to approximately 1790 cm⁻¹ for **113** and **114** being observed. Additionally, ¹H NMR showed the loss of a triplet at δ 1.32 ppm and quartet at δ 2.89 ppm, confirming substitution of the ethanthio moiety.

The successful synthesis of the acyloxymethyl carbonochloridate intermediates allowed for the synthesis of the *N,N'*-bis(acyloxymethoxycarbonyl)-*S*-methylisothioureas following the procedure described by Saulnier *et al.* (1994) (Scheme 4-16).¹⁴⁷

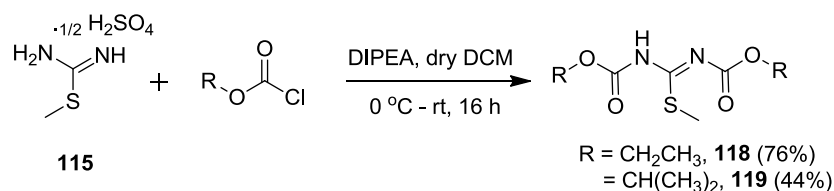
Scheme 4-16: Synthesis of *N,N'*-bis(acyloxymethoxycarbonyl)-*S*-methylisothioureas **116** and **117**.



In this final step, 2-methyl-2-thiopseudourea hemisulfate **115** was reacted with either acyloxymethyl carbonochloridate **113** or **114** using Schotten-Baumann conditions. **115** was dissolved in saturated NaHCO₃ followed by dropwise addition of 2.5 equivalents of the carbonochloridate in DCM followed by rigorous stirring for 24 h. Formation of the mono-protected 2-methyl-2-thiopseudourea was seen as a minor product. Silica chromatography allowed for isolation of the di-protected 2-methyl-2-thiopseudourea **116** and **117** in reasonable yields. Successful synthesis was confirmed by TOF MS (ES⁺) with molecular ion peaks detected at *m/z* 379.1197 and 407.1324 assigned as [M+H]⁺ for **116** and **117**, respectively.

It was proposed that the AO protected isothiureas could be accessed following a previously reported one-step synthesis.²³⁹ The intermediates *N,N'*-bis-(ethyloxycarbonyl)-*S*-methylthiourea **118** and *N,N'*-bis-(isopropylloxycarbonyl)-*S*-methylthiourea **119** isothiurea were synthesised following the proposed synthetic route shown in Scheme 4-17.

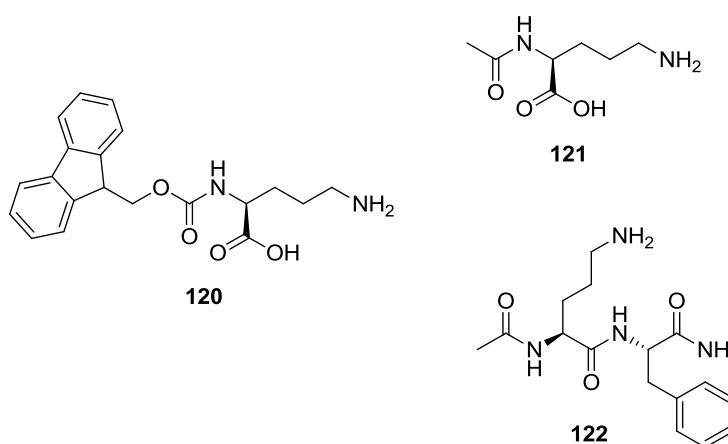
Scheme 4-17: Synthesis of *N,N'*-bis-(acyloxycarbonyl)-*S*-methylthioureas **118** and **119**.



Thus, 2-methyl-2-thiopseudourea **115** was dissolved in DCM followed by the addition of 3 equivalents of either ethyl chloroformate or isopropyl chloroformate. Subsequent work-up and purification afforded **118** and **119** in yields of 76% and 44%, respectively. The successful synthesis of **118** and **119** was confirmed by TOF MS (ES⁺) with molecular ions at *m/z* 235.0838 and 263.1097 being detected and assigned as the [M+H]⁺ species, respectively.

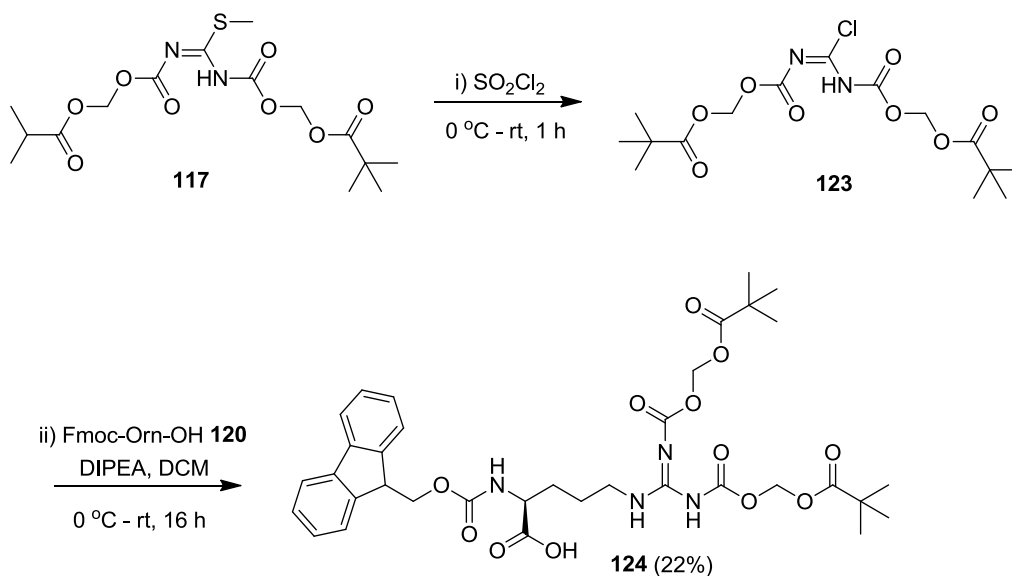
4.2.2 The stability of acyloxycarbonyl and acyloxmethoxy carbonyl protected arginine

To investigate the stability of the AM and AO protecting groups, a simple model system that utilised an ornithine monomer was developed. The first step in setting up the model system was the synthesis of AM and AO protected arginine derivatives. The guanidinylation of two different ornithine monomers, Fmoc-Orn-OH **120**, *N*-acetyl ornithine **121** and the dipeptide *N*-acetyl ornithyl phenylalanine amide **122** using the prepared protected isothioureas was investigated.



Initially, the guanidinylation of Fmoc-Orn-OH **120** was investigated, as the absorbance of the Fmoc group would allow for detection of small quantities of the compound and deprotected species in a HPLC assay. The guanidinylation of **120** using *N,N'*-bis-((pivaloyloxy)methyloxycarbonyl)-*S*-methylthiourea **117** was achieved following the procedure described by Saulnier *et al.* (1994) (Scheme 4-18).¹⁴⁷

Scheme 4-18: Synthesis of AM protected Fmoc-Arg-OH **124**.

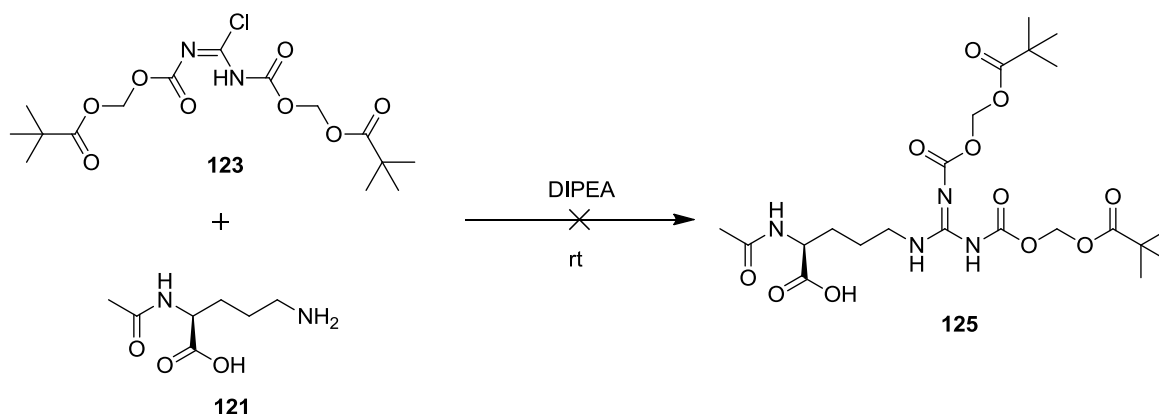


The first step involved the pre-activation **117** using sulfuryl chloride to afford the reactive intermediate **123**. The excess sulfuryl chloride and the sulfenyl chloride were then removed *in vacuo* (Scheme 4-18, i). Without purification, 2 equivalents of **123** were added to a solution of Fmoc-Orn-OH **120** in DCM and 4 equivalents of DIPEA (Scheme 4-18, ii). The reaction was stirred for 1 h at rt followed by purification by silica chromatography to afford **124** in a yield of 22%. The successful guanidinylation of **124** was confirmed by TOF MS (ES^+) with a base peak at m/z 713.2806 being detected, which was assigned as $[\text{M}+\text{H}]^+$.

Unfortunately, **124** was only sparingly soluble in aqueous solvents, thus could not be used to assess the hydrolytic or esterase stability of the AM protecting groups in aqueous buffers. This insolubility is possibly a result of the organic nature of the Fmoc group.

Alternatively, guanidinylation of *N*-acetyl ornithine was investigated. It was predicted this would yield an ornithine derivative with improved water solubility. The conditions used for the synthesis of **125** were applied to the guanidinylation of *N*-acetyl ornithine **121** (Scheme 4-19).

Scheme 4-19: Attempted synthesis of AM protected Fmoc-Arg-OH **125**.



N-acetyl ornithine was insoluble in DCM, thus alternative solvents and reaction conditions were investigated for the synthesis of **125**. The conditions that were investigated for this reaction are outlined in Table 4-4.

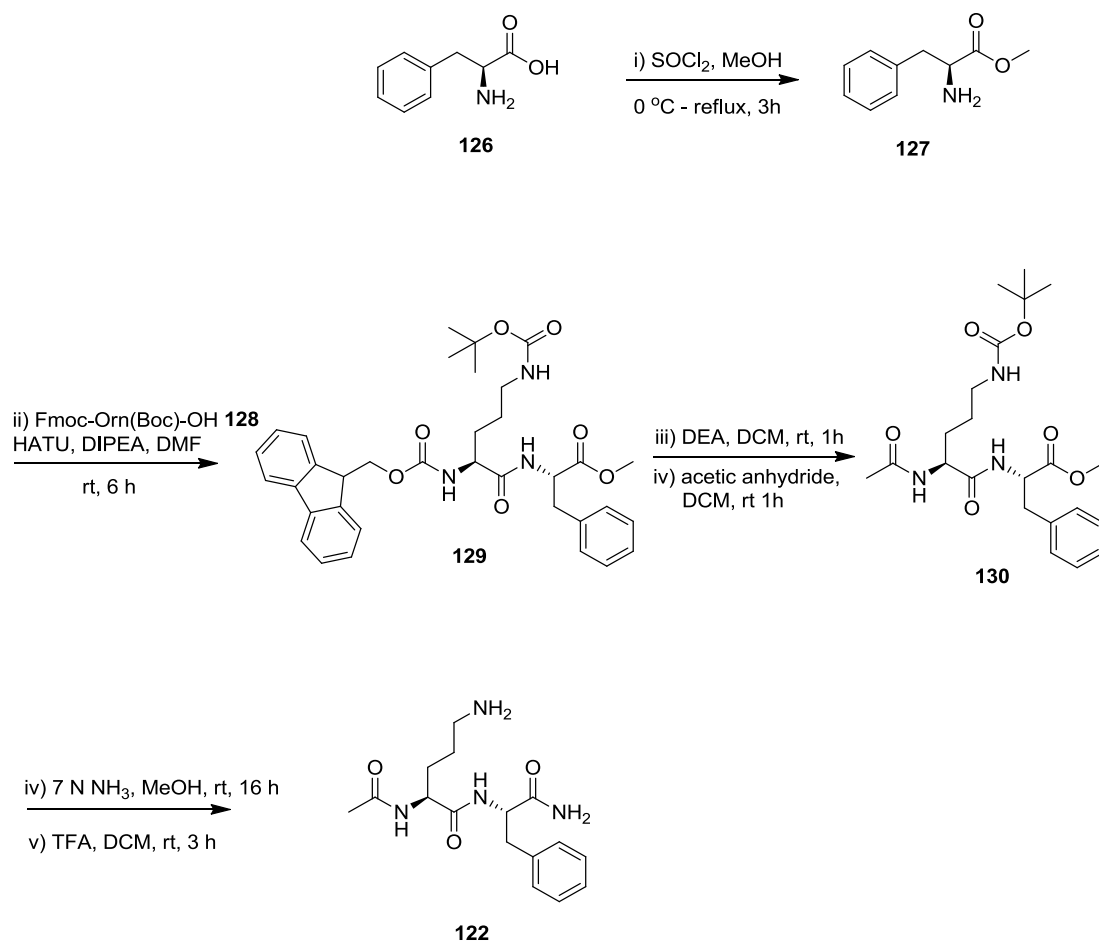
Table 4-4: Unsuccessful attempts to synthesise **125**.

Solvent	Base	Temperature	Result
DMF	DIPEA	rt	No reaction
DMF	DIPEA	50 °C	No reaction
DMF	DIPEA	80 °C, 1 h	Inseparable mixture
THF	DIPEA	rt, 16 h	No reaction, partial solubility of <i>N</i> -acetyl ornithine,
THF/ H ₂ O	DIPEA	rt, 16 h	No reaction

By heating the reaction at 80 °C in DMF it is possible that the rate of the desired reaction was increased. However, the rate of nucleophilic substitution at the ester carbonyl of **123** would have also increased leading to product decomposition, explaining the inseparable mixture obtained using these conditions.

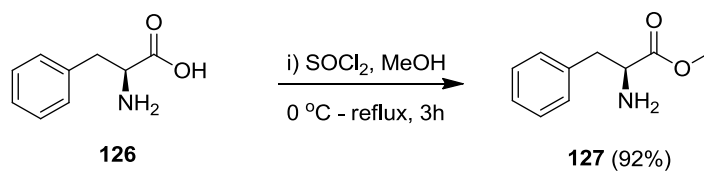
Thus, an alternative scaffold was investigated, in an attempt to obtain an arginine derivative of suitable solubility for both the guanidinylation reaction and application in an enzyme based assay using aqueous buffers. The dipeptide *N*-acetyl ornithyl phenylalanine amide **122** was investigated for this application. Additionally, this dipeptide was synthesised with the rationale that the phenylalanine side-chain would increase the UV absorbance of the dipeptide, thus enabling detection of small quantities of the compound in a HPLC based assay. The synthesis of **122** is outlined in Scheme 4-20.

Scheme 4-20: Proposed synthesis of *N*-acetyl ornithyl phenylalanine amide **122**.



In the first step of the proposed synthesis, thionyl chloride was added dropwise to a methanolic solution of phenylalanine **126** at 0 °C.²⁴⁰ The reaction mixture was warmed to rt followed by refluxing for 3 h (Scheme 4-21).

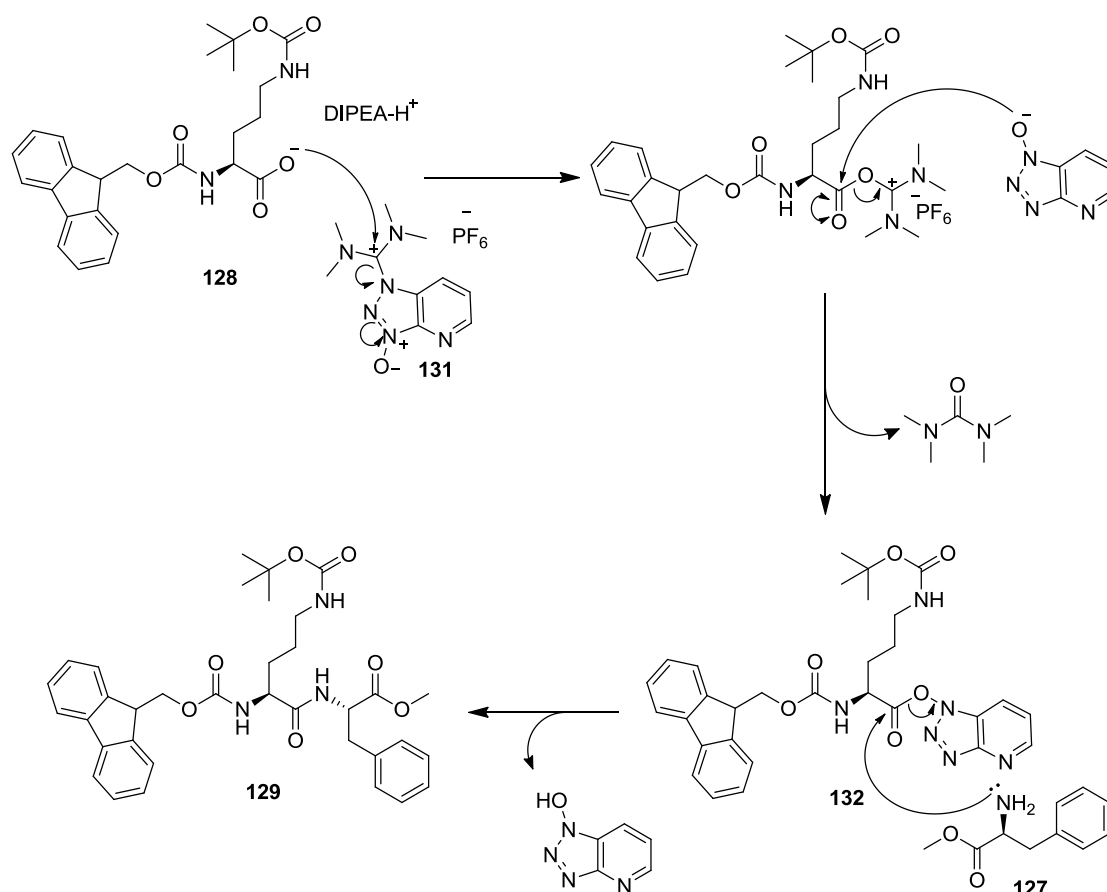
Scheme 4-21: Synthesis of phenylalanine methyl ester **127**.



Re-crystallisation of phenylalanine methyl ester **127** from the crude reaction mixture using methanol and diethyl ether was achieved in a yield of 92% which was spectroscopically identical to the literature.²⁴⁰

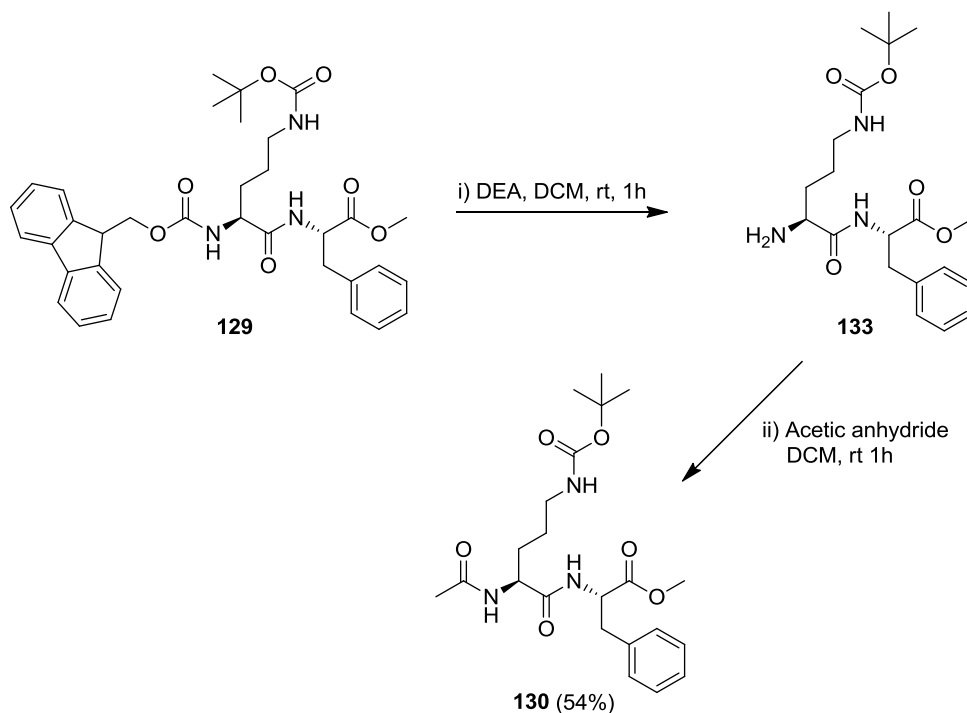
In the next step, compound **127** was coupled to Fmoc-Orn(Boc)-OH **128** by amide bond formation. A stoichiometric amount of **128** was added to the coupling reagent HATU **131** and DIPEA in DMF with stirring, to form the activated ester intermediate **132**. 0.5 equivalents of **127** was then added to this solution followed by stirring at rt for 3 h. The reaction proceeded by the mechanism shown in Scheme 4-22.²⁰⁵

Scheme 4-22: Mechanism of amide bond formation using the coupling reagent HATU **131**.



Subsequent purification of the crude reaction mixture afforded **129** in a yield of 78%. In the next step, the Fmoc group of **129** was removed using diethylamine (DEA) in DCM (Scheme 4-23, i).

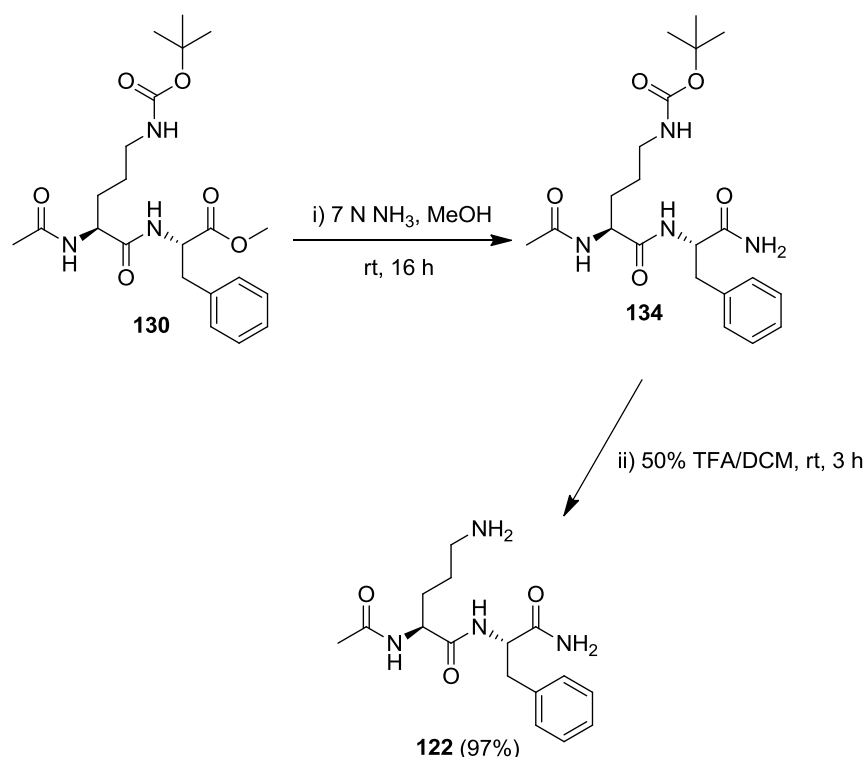
Scheme 4-23: Synthesis of *N*-acetyl(*N'*-(*tert*-butoxycarbonyl)ornithyl)phenylalanine methyl ester **130**.



The intermediate **133** was isolated by removal of the reaction solvent and DEA *in vacuo*. A solution of **133**, DIPEA and acetic anhydride in DCM was stirred for 16 h at rt (Scheme 4-23, ii). Subsequent work-up and purification of the reaction mixture furnished **130** in a yield of 54%.

In the penultimate step, the methyl ester of **130** was modified by aminolysis. This was achieved by dissolving **130** in a methanolic solution of 7 N ammonia and stirring of the reaction mixture for 16 h at rt followed by removal of the reaction solvent *in vacuo* (Scheme 4-24, i).

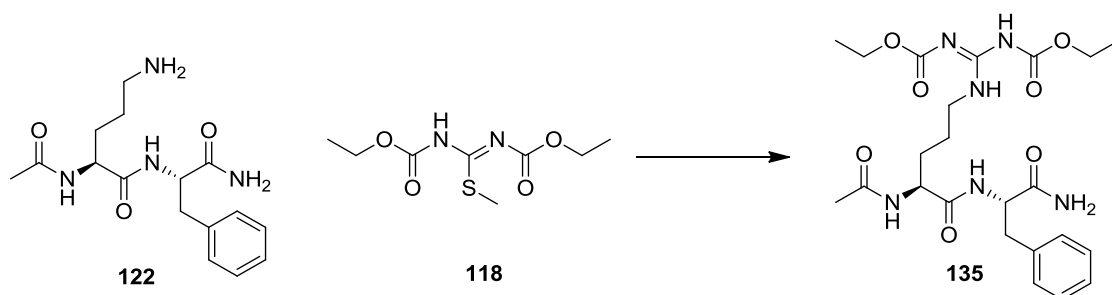
Scheme 4-24: Synthesis of *N*-acetyl ornithyl phenylalanine amide **122**.



In the final step, **134** was Boc deprotected by acidolysis using a 50% solution of TFA in DCM for 3 h at rt. Trituration of the resulting residue with diethyl ether afforded *N*-acetyl ornithyl phenylalanine amide **122** in a yield of 97% (Scheme 4-24, ii). Successful synthesis of **122** was confirmed by ^1H NMR with a loss of a singlet at δ 1.42 and 3.69 ppm being observed, which corresponded to the Boc and methyl ester protons, respectively. Further confirmation was provided by TOF MS (ES^+) revealing a base peak at m/z 321.1889, which was assigned as the $[\text{M}+\text{H}]^+$ species.

The successful synthesis of **122** using established chemistry supplied a compound that could then be used for the synthesis of AM and AO protected arginyl derivatives. The model reaction shown in Scheme 4-25 was investigated to determine the optimum condition for the guanidinylation of **122**. The guanidinating agent **118** was used as it was predicted that the AO protecting groups would be more stable than the AM groups, thus being more suitable for initial reactions investigating different conditions.

Scheme 4-25: Synthesis of AO protected *N*-acetyl arginyl phenylalanine amide derivative **135**.



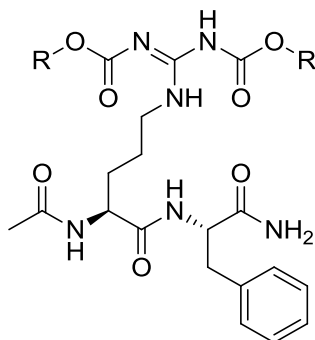
Initial attempts focused on using sulfonyl chloride to activate the guanidylating agent **118** as previously described. However, this proved unsuccessful, thus several alternative conditions were investigated. Table 4-5 outlines the conditions used for the synthesis of **135**.

Table 4-5: Conditions investigated for the synthesis of **135**.

Solvent	Base	Reagent	Temperature	Result
DCM	DIPEA	SO ₂ Cl ₂	rt	122 insoluble
DCM	DIPEA	SO ₂ Cl ₂	40 °C	122 insoluble
DMF	DIPEA	SO ₂ Cl ₂	rt, 1 h	No reaction
DMF	DIPEA	HgCl ₂	rt, 6 h	Product formation
MeCN/H ₂ O (1:1)	DIPEA	HgCl ₂	rt, 6 h	Product formation

The pre-activation of **118** with sulfonyl chloride was not successful in DCM or DMF. Alternatively, isothiourea **118** was dissolved in DMF followed by the addition of a stoichiometric amount of mercuric chloride and DIPEA. The dipeptide **122** was then added to this solution followed by stirring of the reaction mixture for 6 h. Subsequent analysis of the crude reaction mixture by TOF MS (ES⁺) detected a peak at *m/z* 535.2875 that corresponded to the calculated value for the [M+H]⁺ species of **135**.

Thus, activation of **118** with mercuric chloride proved successful. The synthesis of **135** was carried out on a larger scale using DMF as a reaction solvent. Preparative HPLC of the crude reaction mixture allowed for isolation of **135** in a yield of 45%. These conditions were then applied to the synthesis of several *N*^G-protected *N*-acetyl arginyl phenylalanine analogues using the previously prepared AM and AO protected isothioureas. Table 4-6 shows the synthesised analogues and their corresponding yields.



	R protecting group	Yield	TOF MS (ES ⁺), <i>m/z</i> [M+H] ⁺
136	CH ₂ OCOCH(CH ₃) ₂	22%	651.2841
137	CH ₂ OCOC(CH ₃) ₃	23%	679.3285
135	CH ₂ CH ₃	45%	507.2562
138	CH(CH ₃) ₃	29%	535.2875
139	C(CH ₃) ₃	70%	563.3188

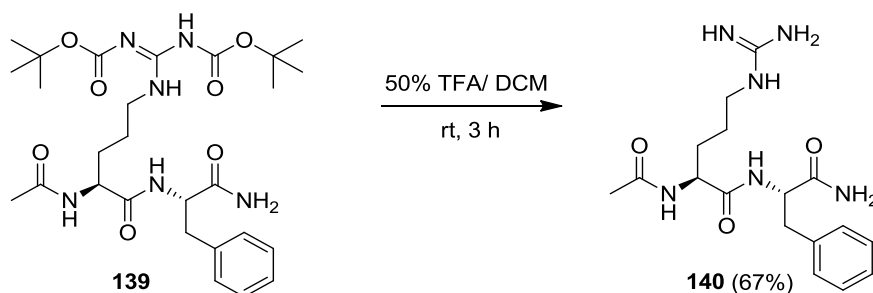
Table 4-6: The synthesised protected *N*-acetyl arginyl phenylalanine derivatives.

The *N,N'*-bis(acyloxymethoxycarbonyl)-*S*-methylisothioureas **116** and **117** were successfully activated using mercuric chloride and used to guanidylate the ornithine side-chain of **122**. Notably, this activation method did not result in breakdown of the AM protecting groups.

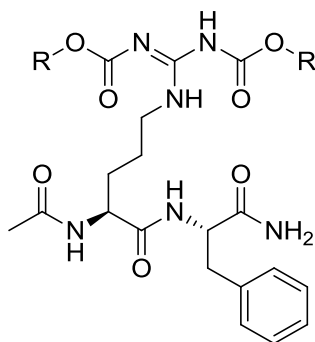
4.2.2.1 Hydrolytic stability of the AM and AO protecting groups

The prepared AM and AO protected dipeptides were used in a HPLC based assay to assess the hydrolytic stability of the AM and AO protecting groups. It was predicted that the AM protecting groups may break down to give the unprotected arginine residue in aqueous buffers. Thus, to provide a positive control for the HPLC assay, the *N*^G-Boc protected *N*-acetyl arginyl phenylalanine amide **139** was deprotected by acidolysis using TFA to afford **140** (Scheme 4-26).

Scheme 4-26: Synthesis of *N*-acetyl arginine phenylalanine amide **140**.



Analytical HPLC of the AM and AO protected *N*-acetyl arginyl phenylalanine amide analogues showed one major peak before being used in the stability assay. Table 4-7 shows the retention times for the unprotected dipeptide **140** and the AO (**135** and **138**) and AM (**136** and **137**) protected dipeptides.



	R group	t_R / min*
140	-	3.10
136	CH ₂ OCOCH(CH ₃) ₂	6.34
137	CH ₂ OCOC(CH ₃) ₃	6.97
135	CH ₂ CH ₃	4.85
138	CH(CH ₃) ₃	5.41

Table 4-7: Analytical HPLC chromatograms for the AO and AM protected dipeptides before use in the stability assays. *1-90% B over 10 min, 3 ml/min (Onyx Monolithic C₁₈, 100 x 4.6 mm).

The stability of the protected dipeptides was assessed at pH 5.0, 7.4 and 9.0. Using a Britton–Robinson buffer ²⁴¹, a 0.2 mM solution of the protected dipeptides was prepared with a pH of 5.0 and 9.0, a PBS buffer was used to prepare the pH 7.4 sample. Each sample was then incubated at 37 °C and at specific time points an aliquot was removed and analysed by analytical HPLC. Further analysis of the major peaks using TOF MS (ES⁺) confirmed the identity of the deprotected dipeptide species. Figure 4-9 and Figure 4-10 show the HPLC traces of the AM protected

dipeptides **136** and **137** after incubation for 1 h and 12 h at 37 °C at pH 5.0, 7.4 and 9.0.

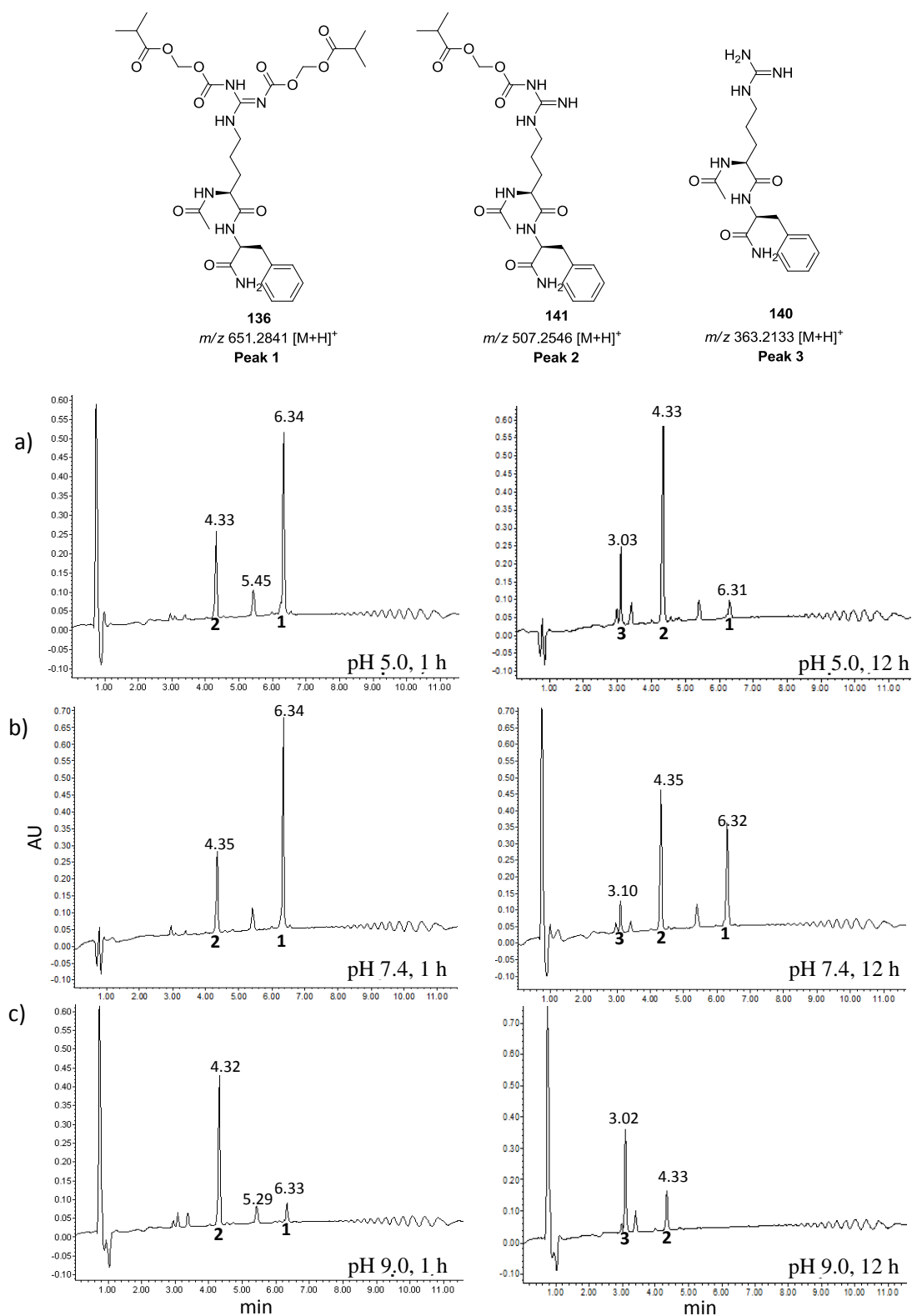


Figure 4-9: HPLC chromatograms of the AM protected dipeptide **136** after incubation at 37 °C in aqueous buffer with a) pH 5.0, b) pH 7.4 and c) pH 9.0 over 12 h. Peaks 1, 2 and 3 were identified using HRMS TOF MS (ES⁺). The HPLC method used was 1-90% B over 10 min, 3 ml/min (Onyx Monolithic C₁₈, 100 x 4.6 mm).

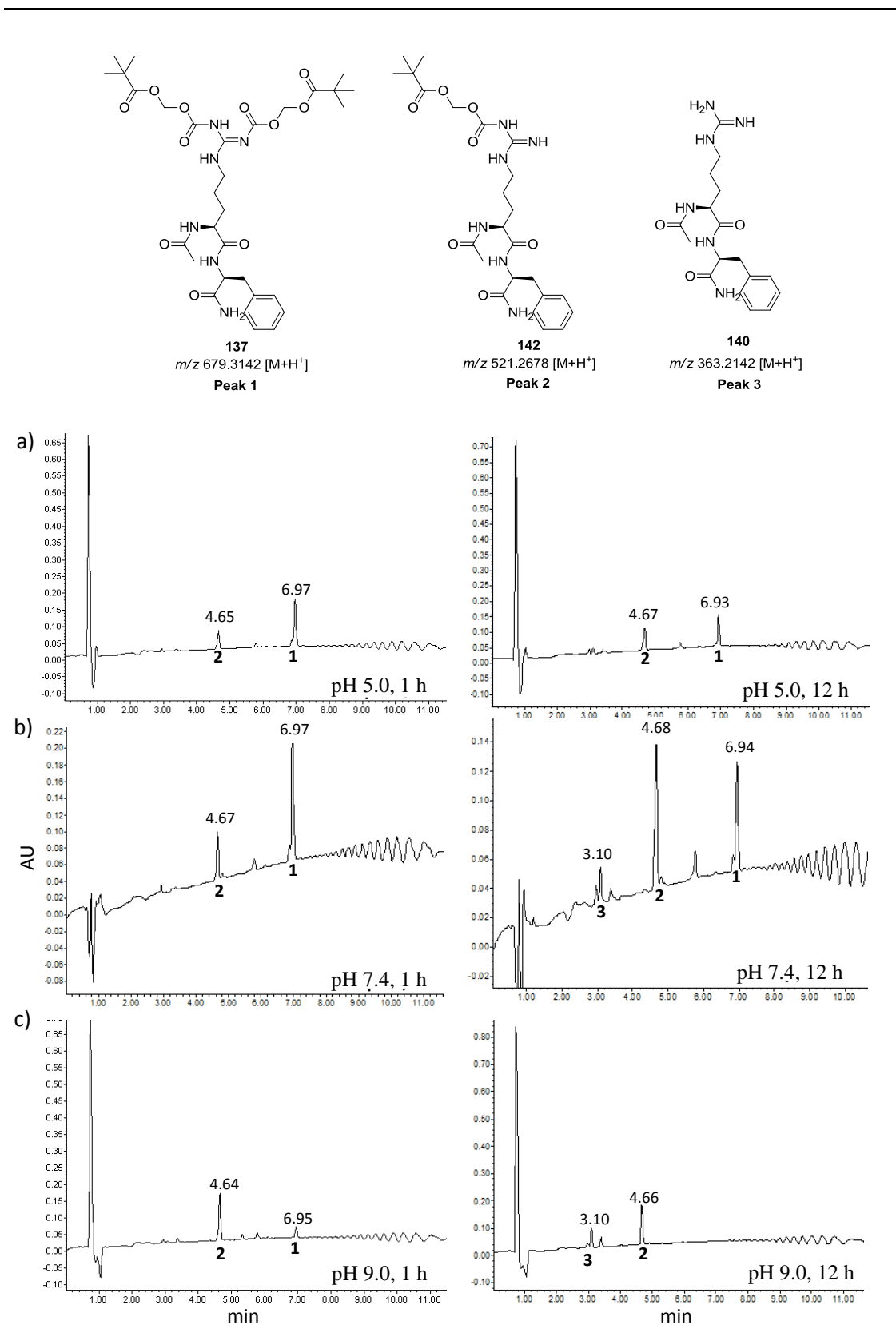


Figure 4-10: HPLC chromatograms of the AM protected dipeptide **137** after incubation at 37 °C in aqueous buffer with a) pH 5.0, b) pH 7.4 and c) pH 9.0 over 12 h. Peaks 1, 2 and 3 were identified using HRMS TOF MS (ES^+). The HPLC method used was 1-90% B over 10 min, 3 ml/min (Onyx Monolithic C_{18} , 100 x 4.6 mm).

A summary of the stability of the AM and AO protected dipeptides after incubation in an aqueous buffer at either pH 5.0, 7.4 or 9.0 at 37 °C is summarised in Table 4-8.

Table 4-8: The time range of AM and AO deprotection from the AM and AO protected dipeptides after incubation at 37 °C in aqueous buffer at pH 5.0, 7.4 and 9.0.

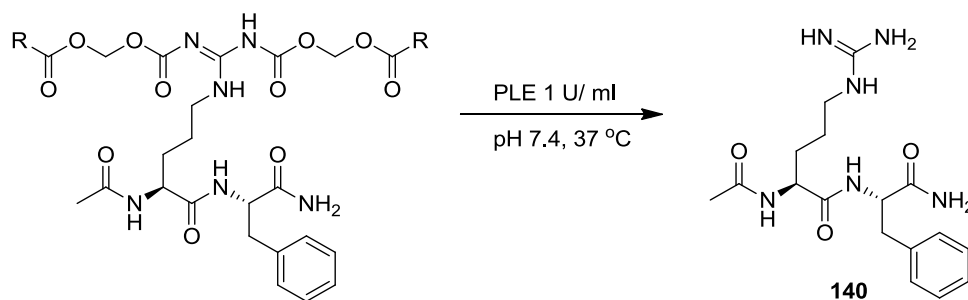
#	R protecting group	Stability		
		pH 5.0	pH 7.4	pH 9.0
136	COCH ₂ OCH(CH ₃) ₂	< 12 h	> 12 h	< 1 h
137	COCH ₂ OC(CH ₃) ₃	> 12 h	> 12 h	< 1 h
135	CH ₂ CH ₃		> 24 h	
138	CH(CH ₃) ₂			

The two AM protected dipeptides **136** and **137** are deprotected over 12 h in aqueous buffer to initially give the mono-protected dipeptide and then finally the unprotected arginine residue **140**. At pH 5.0, 7.4 and 9.0 the isobutanoyloxymethyl carbonyl protected dipeptide **137** (Figure 4-9) is deprotected to **140** to a greater extent than the pivaloyloxymethyl carbonyl protected dipeptide **131** (Figure 4-10). Moreover, **136** is deprotected to a greater extent at pH 9.0 and pH 5.0 compared to at pH 7.4. In contrast, the AO protected dipeptides **136** and **137** showed no detectable deprotection over 24 h at pH 5.0, 7.4 and 9.0 at 37 °C.

4.2.2.2 Esterase-mediated deprotection of the protected arginine derivatives

The esterase-mediated deprotection of the AO and AM protecting groups was also investigated. Previous studies by Gogate *et al.* (1987) and Saulnier *et al.* (1994) have focussed on the kinetics of AM breakdown using pig liver esterase (PLE, *E.C.3.1.1.1*), human blood plasma and in aqueous buffers.^{147, 234-235} Scheme 4-27 shows the esterase-mediated deprotection of an AM protected *N*-acetyl arginyl phenylalanine amide derivative to afford the unprotected arginine residue **140**.

Scheme 4-27: Deprotection of AM protected *N*-acetyl arginyl phenylalanine amide derivative by pig liver esterase (PLE).



The stability of the AO and AM protected dipeptides in the presence of PLE was investigated. Thus, 0.2 mM solutions of the protected dipeptides in PBS (pH 7.4) were treated with PLE to give final concentration of 1 U/ml followed by incubation at 37 °C. At specified time points an aliquot was removed and added to an equal volume of MeCN to stop the reaction. Each time point was then analysed using analytical HPLC and each peak identified by TOF MS (ES^+). The chromatograms for the AM protected analogues **136** and **137** are shown in Figure 4-11.

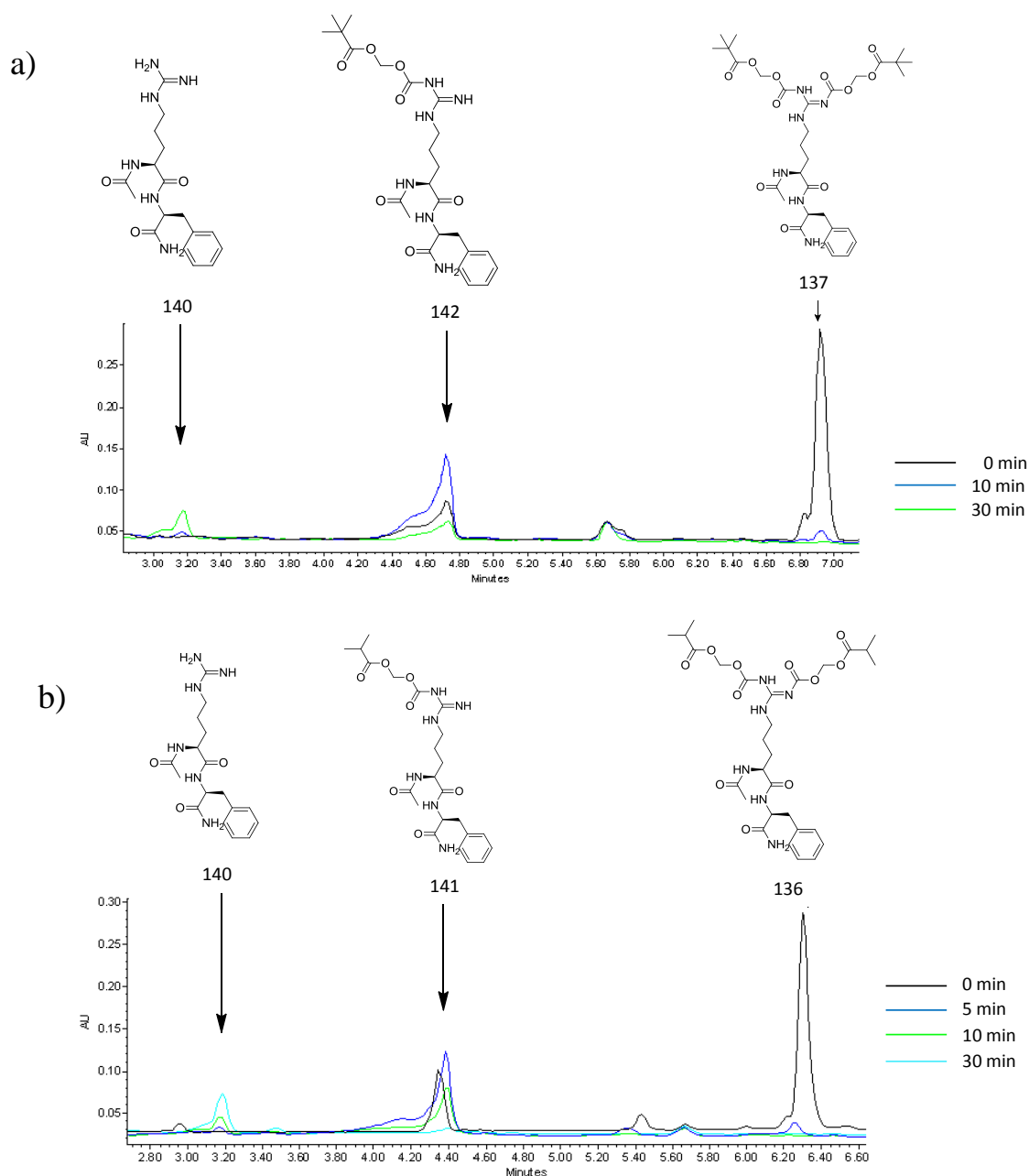


Figure 4-11: HPLC trace of AM protected dipeptides a) **137** and b) **136**. Samples were incubated at 0.2 mM in PBS (pH 7.4) with 1 U/ ml porcine liver esterase (PLE) at 37 °C. Aliquots were taken at certain time points and analysed using 1-90% B over 10 min, 3 ml/min (Onyx monolithic C₁₈ column 100 x 4.6 mm). Analysis of each peak using TOF MS (ES⁺) allowed for the identification of each dipeptide species.

Both the isobutoxymethyl carbonyl and the pivolyloxymethyl carbonyl protected dipeptides are deprotected by PLE. The starting molecule is deprotected to give the mono-acetylated product within the first 5 min of incubation. Over the next 30 min the mono-acylated product is further deprotected to the *N*-acetyl arginyl phenylalanine amide **140**. The stability of **136** and **137** at pH 7.4 in PBS has previously been shown (Figure 4-9 and Figure 4-10) confirming that the AM deprotection observed is esterase

driven. The AO protected dipeptides **135** and **138** showed no significant deprotection after incubation with PLE at for 24 h at 37 °C. Table 4-9 summarises the qualitative data for the AM and AO protected dipeptides incubated with 1 U/ml of PLE.

Table 4-9: The time range of AM and AO deprotection from the AM and AO protected dipeptides after incubation at 37 °C with PLE (1 U/ml) in PBS (pH 7.4).

#	R protecting group	Stability, $t_{1/2}$ (1 U PLE/ml)
136	COCH ₂ OCH(CH ₃) ₂	< 0.5 h
137	COCH ₂ OC(CH ₃) ₃	< 0.5 h
135	CH ₂ CH ₃	> 24 h
138	CH(CH ₃) ₂	> 24 h

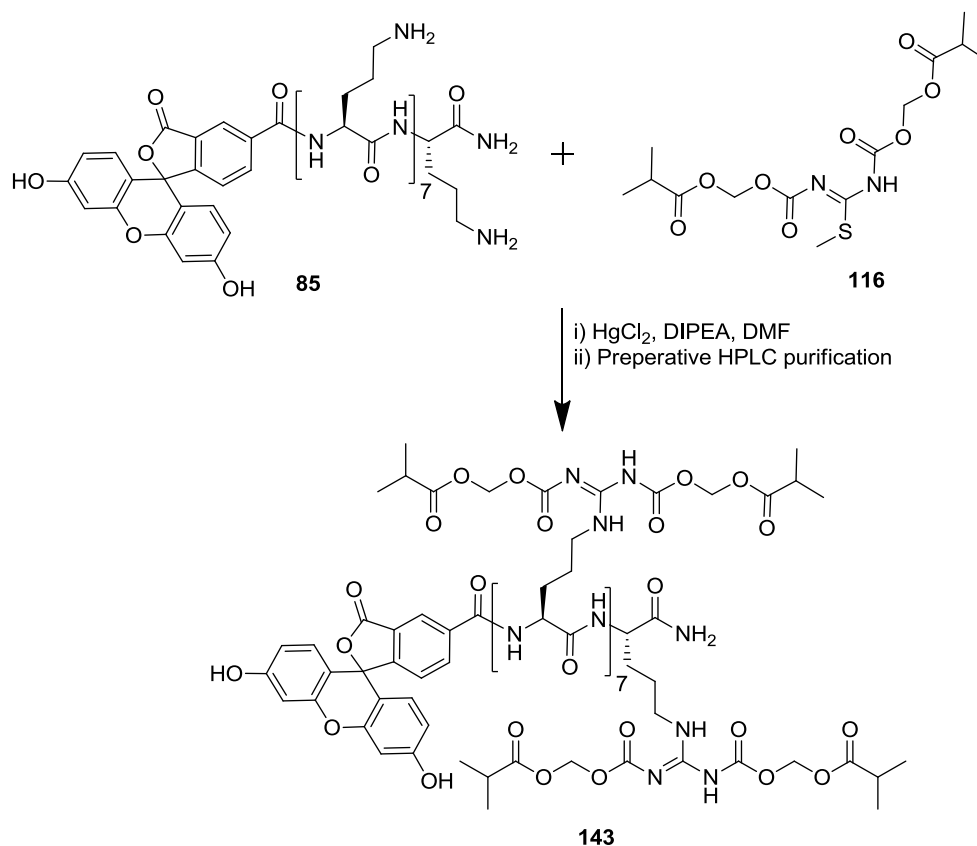
Based on the esterase and hydrolytic stability assays it is clear that the AO protected arginine residues **135** and **138** are not deprotected in the presence of PLE or in an aqueous buffer at pH 5.0, 7.4 or 9.0. Thus, these protecting groups are not suitable for the labile protection of the guanidine functionality of an octa-arginine derivative. However, the AM protected arginine residues of **136** and **137** were deprotected to afford the desired unprotected arginine residue upon treatment with 1 U/ml of PLE (<0.5 h) and also deprotected at pH 5.0 and pH 9.0, and to a lesser extent at pH 7.4. Thus, the AM protecting groups were deemed suitable for the N^G-protection of an octa-arginine derivative.

4.2.3 Synthesis of an acyloxymethyl carbonyl protected octa-arginine derivative

The guanidinylation of octa-ornithine derivatives **85** and **86** using the AM protected isothiurea *N,N'*-bis-((isobutanoyloxy)methyloxycarbonyl)-*S*-methylthiurea **116** was investigated using the same method as described for the synthesis of the N^G-Boc protected FAM-(R(di-Boc)-Ahx)₈-[NH₂] **98**.

The first step was the pre-activation of isothiurea **116** (10 eq.) with HgCl₂ (10 eq.) in DMF. A solution of **85** (1 eq.) and DIPEA (10 eq.) in H₂O (1 ml) was then added dropwise to the activated isothiurea, followed by stirring at rt (Scheme 4-28).

Scheme 4-28: Synthesis of AM protected octa-arginine derivative **143**.



After stirring of the reaction mixture at rt for 2 h, the solvent was removed *in vacuo*. The resulting orange residue was suspended in MeCN and centrifuged at 13000 g for 20 min. The supernatant was analysed by HPLC, which revealed a major product at t_R 8.85 min (Figure 4-12).

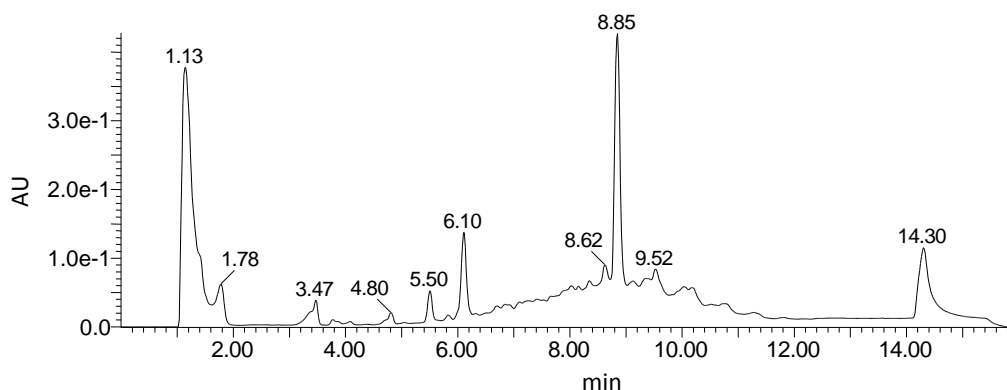


Figure 4-1210: Analytical HPLC chromatogram for the crude reaction mixture for synthesis of the AM protected octa-arginine derivative **143**. The HPLC method used was 1-90% B over 10 min, 3 ml/min (Chromolith Semi-prep C_{18} , 100 x 10 mm).

The major peak at 8.85 min was isolated and analysed by TOF MS (ES^+). The fragmentation pattern of this HPLC fraction is shown in Figure 4-13 with the corresponding structures.

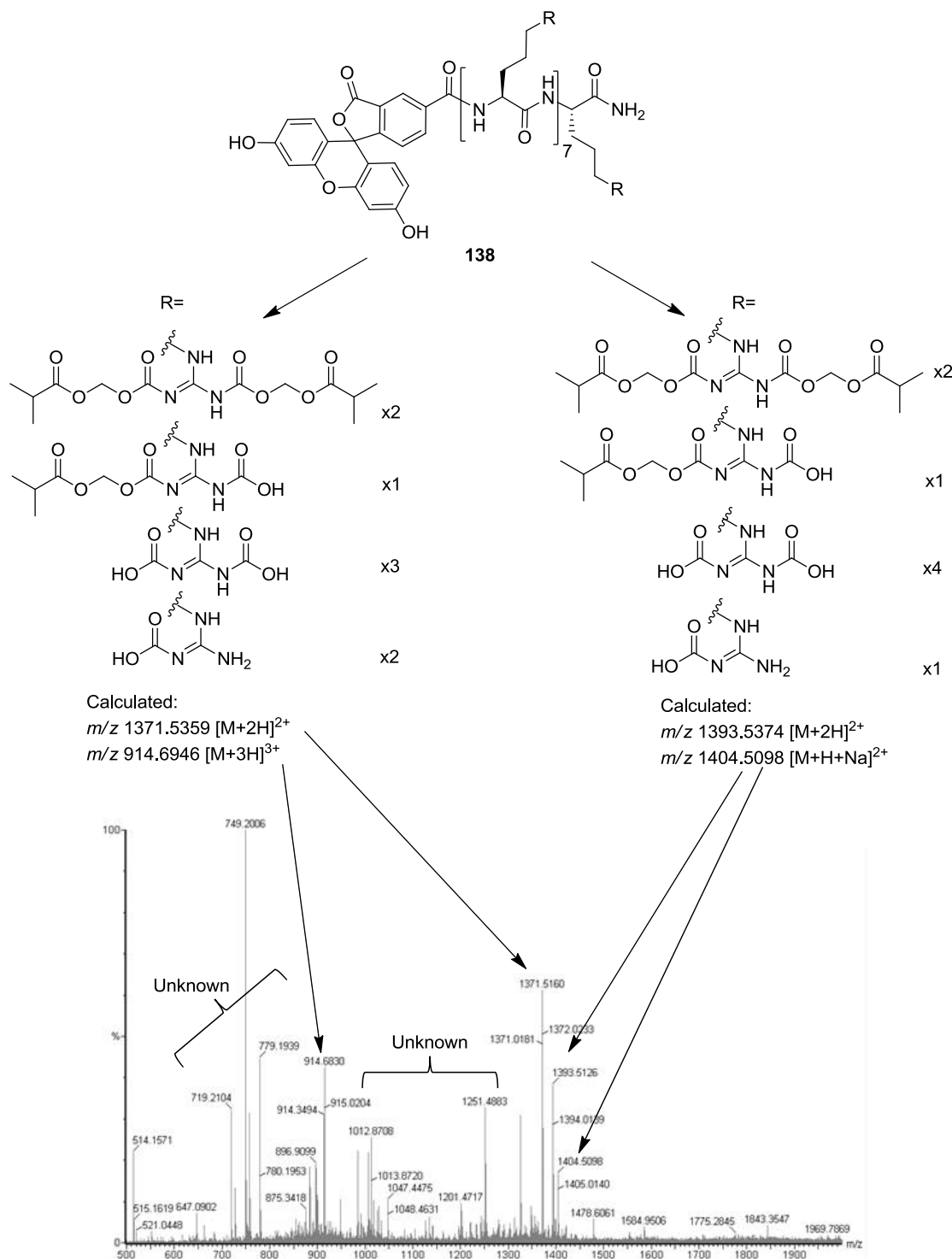
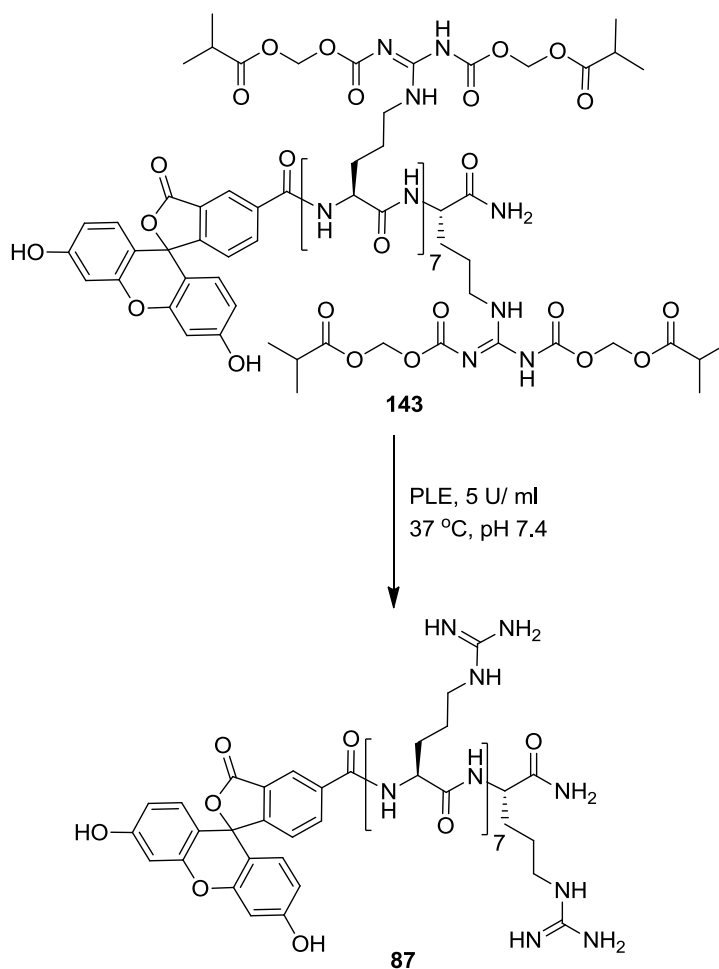


Figure 4-123: HRMS TOF MS (ES^+) spectra of the 8.85 min peak from the HPLC analysis of the reaction mixture of the AM protected octa-arginine derivative **143**. The corresponding peptide fragments and calculated masses are also shown.

Isolation of the peak at 8.85 min using preparative HPLC afforded **143** in a yield of 33%. However, further analysis of the isolated sample using TOF MS (ES^+) at a lower mass range revealed a peak at m/z 379.1175 corresponding to the $[\text{M}+\text{H}]^+$ species of isothiurea **116** (see Scheme 4-28). This suggests that the isolated material is a mixture of both protected peptide **143** and isothiurea **116**. Further purification using a number of RP-HPLC methods could not resolve this mixture.

Nevertheless, preliminary studies investigating the stability of the protected peptide **143** were performed using the peptide **143**/isothiurea **116** mixture. Hence, a 0.1 mM solution of the peptide reagent **143** in PBS (pH 7.4) was treated with 5 U/ml of PLE at 37 °C (Scheme 4-29).

Scheme 4-29: Deprotection of AM protected octa-arginine derivative **143** by pig liver esterase (PLE).



At specified time points, an aliquot from the reaction mixture was removed and added to an equal volume of MeCN. This sample was then analysed using analytical HPLC.

Figure 4-14 shows the HPLC chromatograms for the AM protected octa-arginine **143** after incubation for 15 min and 30 min with PLE (10 U/ml).

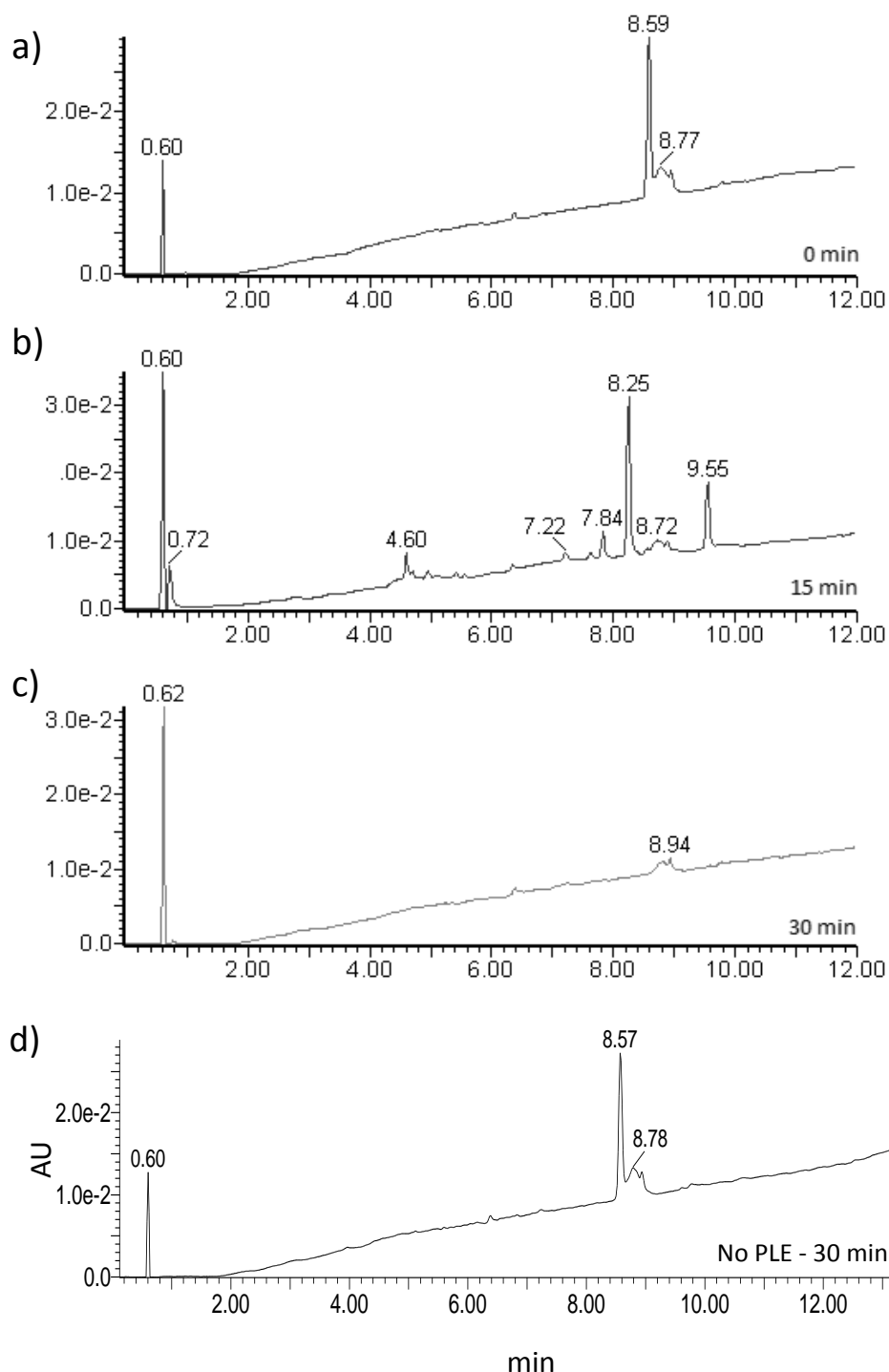


Figure 4-14: HPLC chromatograms of a 0.1 mM solution of the AM protected octa-arginine **143** after incubation at 37 °C with PLE (5 U/ ml) for a) 0 min, b) 15 min, c) 30 min and d) incubation at 37 °C without PLE for 30 min. The HPLC method used was 1-90% B over 10 min, 1.2 ml/min (Onyx Monolithic C₁₈, 100 x 3.00 mm).

After 15 min (Figure 4-14, b) there are a number of species detected, suggesting that PLE is removing the AM protecting groups of **143**. Interestingly, after 30 min there are no detectable species and no peak corresponding to **143** (t_R 8.59 min) (Figure 4-14, c).

To confirm that the deprotection of **143** was esterase catalysed, **143** was also incubated at 37 °C in PBS (pH 7.4) for 30 min in the absence of PLE (Figure 4-13, d). In the absence of PLE it is clear that there is no detectable deprotection of **143**, suggesting that the fragmentation pattern seen in Figure 4-14, b) is due to the activity of PLE. Two further controls were also performed, Figure 4-15 a) shows the HPLC chromatogram for the unprotected octa-arginine **87**. Figure 4-15 b) shows the chromatogram of a 0.2 mM solution of isothioureia **116**, after treatment with PLE (1 U/ml) for 2 min. As mentioned earlier, analysis of **143** using TOF MS (ES^+) detected remaining isothioureia **116** in the sample. The identity of each peak in Figure 4-15, b) was determined using TOF MS (ES^+).

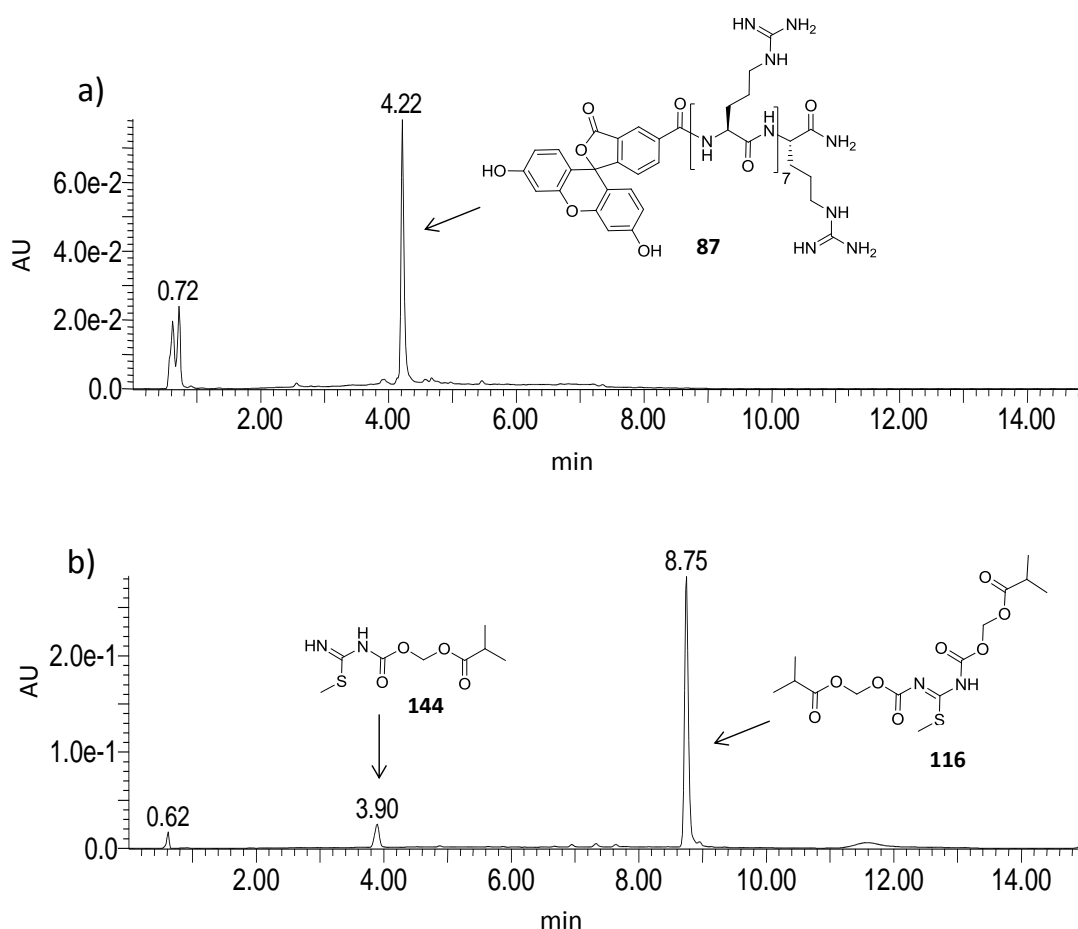


Figure 4-15: HPLC chromatograms of a) the unprotected octa-arginine **87** (t_R 4.22 min) and b) the isothioureia **116** (t_R 8.75 min) after incubation at 37 °C with PLE (1 U/ ml) for 5 min. The HPLC method used was 1-90% B over 10 min, 1.2 ml/min (Onyx Monolithic C₁₈, 100 x 3.00 mm).

Importantly, Figure 4-15 b) shows the PLE-mediated deprotection of isothioureia **116** to form the mono-protected isothioureia **144** at t_R 3.90 min. Comparing this to the chromatogram of the AM protected octa-arginine **143** after incubation with PLE for 15 min (Figure 4-14 b) it is clear that the fragmentation patterns are significantly different. However, Figure 4-15 a) shows the chromatogram for the unprotected octa-arginine derivative **87**. This single peak at 4.22 min is not seen in the chromatograms of **143** after incubation with PLE for 15 or 30 min (Figure 4-14, b and c). Thus, suggesting that **143** is either completely digested by PLE or partially deprotected to form many different deprotected peptide species. If the number of deprotected species is vast then it is possible that they would not be detected by absorbance using HPLC.

It was predicted that the octa-arginine species observed after incubation of **143** with PLE may internalise into cells. Thus, in a preliminary experiment, a 10 μ M solution of **143** was treated with PLE (1 U/ml) at 37 °C. After 2.5 min and 15 min aliquots were removed and added to an equal volume of MeCN to stop the reaction. Samples were then lyophilised, reconstituted into RPMI-1640 media and then added to HeLa cells. Cells were incubated with the samples for 30 min at 37 °C, followed by removal of the media, washing of the cells with PBS and finally imaging using CLSM. Figure 4-16 shows the z-sectioning of HeLa cells incubated with 10 μ M of **143** (green) after incubation with PLE (1 U/ml). Cells were also incubated with the nuclear stain Draq5 (purple).

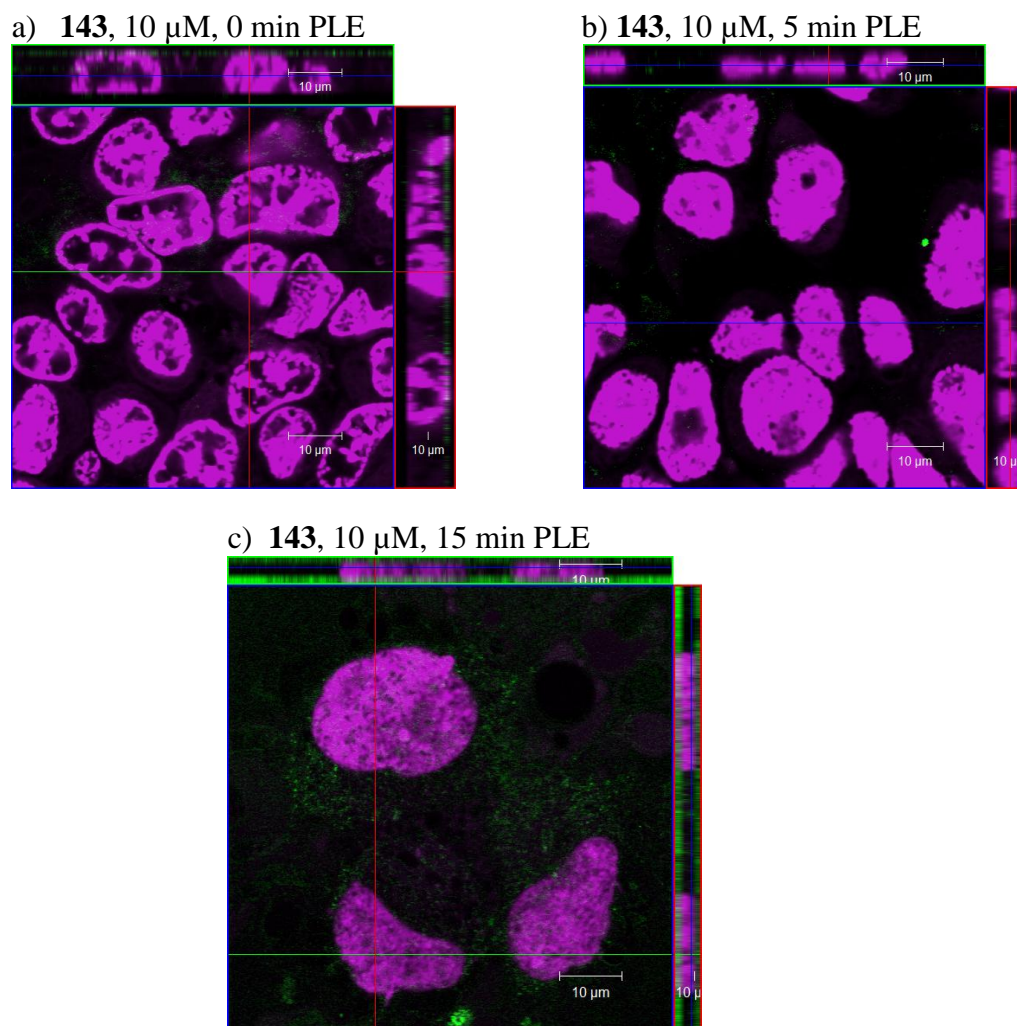


Figure 4-16: Cell internalisation of the AM protected octa-arginine derivative **143**. HeLa cells treated with 10 µM of **135** that had been pre-incubated with PLE (1 U/ml) at 37 °C for a) 0 min b) 5 min and c) 15 min. After incubation of HeLa cells with the PLE treated PLE for 30 min at 37 °C the cells were then washed with PBS and incubated with the nuclear stain Dra5 (purple) followed by z-sectioning using CLSM with an inverted x63 oil immersion lens.

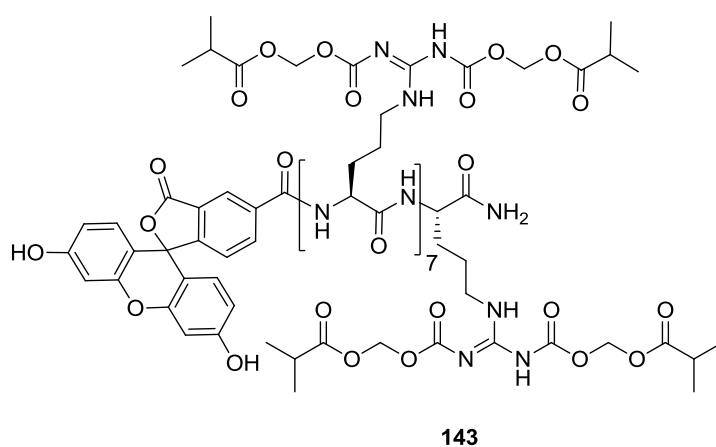
Figure 4-16 a) shows HeLa cells after incubation with octa-arginine **143**, before incubation with PLE. It is clear that the AM protecting groups inhibit internalisation of the octa-arginine, as no cell associated green fluorescence is observed (Figure 4-16, a). After 2.5 min incubation of **143** with PLE (1 U/ml) there is still no internalisation into HeLa cells detected (Figure 4-16, b). Interestingly, cell associated fluorescence is seen for HeLa cells incubated with **143** after incubation of the peptide with PLE (1 U/ml) for 15 min. This suggests that the AM protected octa-arginine **143** is deprotected by PLE enabling cellular internalisation. However, the green fluorescence seen in Figure 4-16 c) is only minimal, suggesting that only a small amount of the

peptide is able to internalise into HeLa cells and that **143** may not be significantly deprotected by PLE after 15 min incubation.

4.1 Conclusions

The major aim of this chapter was to develop a novel method to mask the cationic charge and control the cell penetrating capabilities of the CPP octa-arginine. In the initial phase of the study it was demonstrated that N^G -Boc protection of an octa-arginine derivative successfully inhibited its cell entry capabilities. Thus, further investigations focussed on the protection of the guanidine functionality of octa-arginine using the esterase-sensitive acyloxymethyl carbonyl (AM) protecting groups.

The synthesis of the AM protected octa-arginine derivative **143** was deemed successful and confirmed by TOF MS (ES^+) with a number of fragments corresponding to **143** being detected (see Figure 4-13).



Incubation of **143** with PLE showed a complex deprotection pattern, however, no fully unprotected octa-arginine **87** species was detected. This suggests that a large number of deprotected species are formed after incubation with PLE. Incubation of PLE treated **143** with HeLa cells allowed for detection of cell associated fluorescence using CLSM, thus suggesting that the AM protected octa-arginine **143** is deprotected sufficiently to enable internalisation of the peptide into the HeLa cells.

Further CLSM studies investigating the cell penetration capabilities of the AM protected octa-arginine after PLE treatment are required. Studies using a panel of cell

lines together with treatment of the **143** with PLE over a longer time course will provide greater insight into the effectiveness of this approach for the controlled activation of octa-arginine's cell penetrating capabilities. The quantification of internalised AM octa-arginine after PLE treatment will be important for detailed assessment of the octa-arginine deprotection and subsequent cell internalisation. Robust quantification of the internalised octa-arginine could be achieved using MALDI-TOF MS using a modified method based on that described by Burlina *et al.* (2005).²⁴² A schematic for this proposed approach is outlined in Figure 4-17.

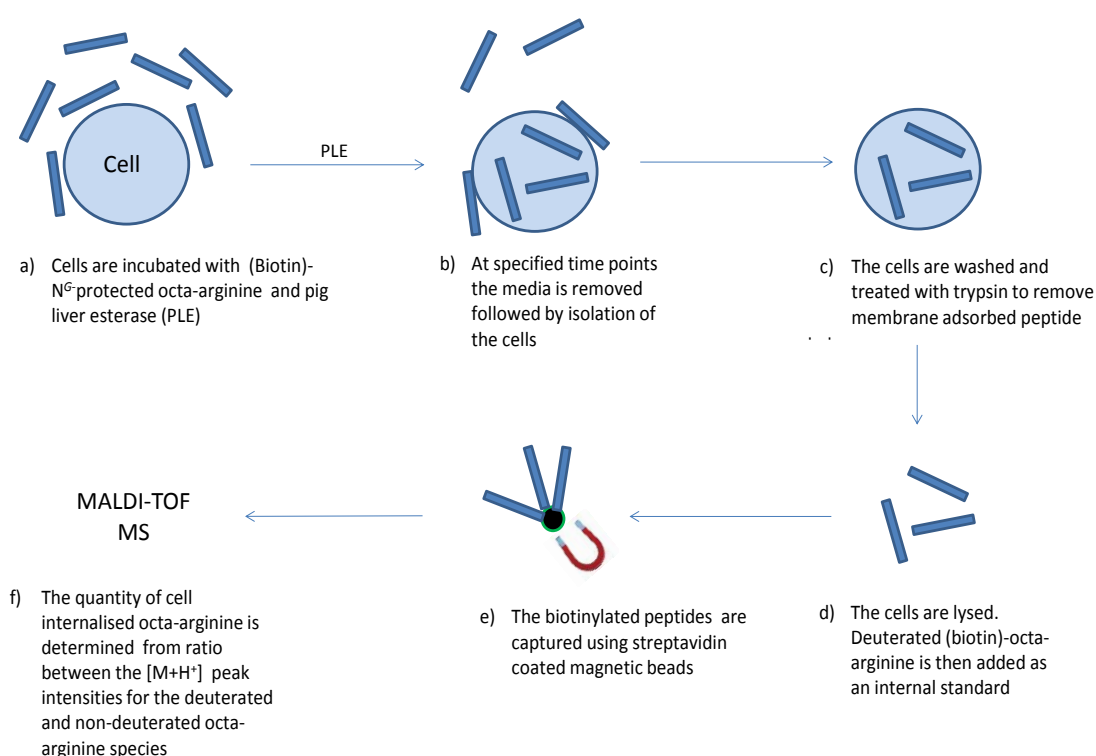


Figure 4-17: Quantification of internalised octa-arginine using MALDI-TOF MS using the method described by Burlina *et al.* (2005).²⁴²

The application of a biotinylated AM protected octa-arginine would enable isolation of internalised octa-arginine using streptavidin coated beads. Subsequent elution of the peptide from the beads will then allow for analysis of the peptide using MALDI-TOF MS. This method could be used to quantitatively monitor the amount of AM protected octa-arginine that is internalised into cells in the presence of PLE.

Overall, this proof-of-principle study has provided compelling evidence that the cell penetrating properties of the CPP octa-arginine can be inhibited through carbamate

protection of the guanidine functionality. The study also presents preliminary data on the protection of an octa-arginine derivative with esterase and hydrolytically labile protecting groups. These results suggest that the esterase-sensitive AM protecting groups are suitable for the inhibition of octa-arginine cellular internalisation. Further studies to confirm the exact deprotection and activation mechanism of an AM protected octa-arginine derivative are required. However, the data presented in this chapter suggests that this is a promising approach to controlling the cell penetrating activity and masking the cationic charge of octa-arginine.

4.2 Materials and methods

The HPLC stability assays were performed using a Waters 2525 pump, Waters 2487 Detector, Waters 2767 Fraction collector and autosampler. An Onyx Monolithic C₁₈, (100 x 4.00 mm) analytical column was used for all experiments using the following solvents: solvent A – H₂O, 0.06% TFA and solvent B – 90% MeCN, 10% H₂O, 0.06% TFA. The standard method used for all assays was a linear gradient of 1-90% B over 10 min, 3 ml/min. The injection volume for each run was 100 µl. This was achieved by using a 100 µl injection loop. To ensure reproducibility between runs, 120 µl of sample was injected into the injection loop for each run. The detector was set-up to record the absorbance of the effluent at 214 nm.

4.2.1 Hydrolytic stability assay

Test compounds were dissolved in methanol followed by addition to a Britton-Robinson buffer (0.04 M H₃BO₃, 0.04 M H₃PO₄ and 0.04 M CH₃COOH)²⁴¹ prepared at either pH 5.0 or 9.0 to give a 2% methanol/buffer solution and a final dipeptide concentration of 0.2 mM. For samples tested at pH 7.4 a PBS buffer was used. The samples were then incubated at for 24 h at 37 °C and at specified time points (0, 1, 12 and 24 h) a 120 µl aliquot was removed for analytical HPLC analysis using the standard method previously described.

4.2.2 Esterase assay

Pig liver esterase (PLE, 165 U/mg, Sigma-Aldrich) was used for all of the esterase assays. Test compounds were dissolved in methanol followed by addition of 1x PBS (pH 7.4) to give a final 2% methanol/PBS solution and a final dipeptide concentration of 0.2 mM. Enzyme reactions were initiated by addition of PLE to give a final concentration of 1 U PLE/ml unless otherwise stated. Reactions were incubated at 37 °C and at specified time points a 60 µl aliquot was removed and added to an equal volume of ice cold MeCN. Samples were then analysed using the standard HPLC previously described.

4.2.3 Confocal scanning laser microscopy

All CLSM was carried out using the same instrument and general method described in Section 3.8.9. HeLa cells were seeded at 1×10^5 cells/well in 6-well plates containing glass coverslips, and allowed to adhere for 24 h at 37 °C. 5-FAM labelled peptides dissolved in DMSO at 40-100 µg/ml were added to RPMI-1640 media to give a final peptide concentration of 10 µM (>1% total DMSO content). 2 ml/well of the peptide solution was then added to the cells, followed by incubation for 30 min at 37 °C. After incubation, the media was removed and the coverslips were washed 3x with 2 ml of PBS followed by incubation of the cells with 500 µl of the nuclear stain Draq5[®] (5 µM, New England Biolabs) for 5 min at rt. The coverslips were then washed 3x with 2 ml of PBS. The coverslips were then removed and placed onto a cover slide. To prevent the cells from drying out, 50 µl of HBSS buffer was applied onto glass slides prior to placing coverslip cells down. The coverslip was then held in place by applying nail varnish around the edges. Cells were then imaged and z-sections taken using the Zeiss LSM510 operating software.

Conclusions and future directions

A systematic approach to modifying antibody fragments with CPPs to enable cellular penetration has been developed, together with a novel method to control the *in vivo* properties of a CPP. This methodology will allow for optimisation of the cell penetrating capabilities and *in vivo* properties of a transbody (i.e. an antibody delivered into a cell), thus providing a gateway to unlocking the immense potential of therapeutic transbodies.

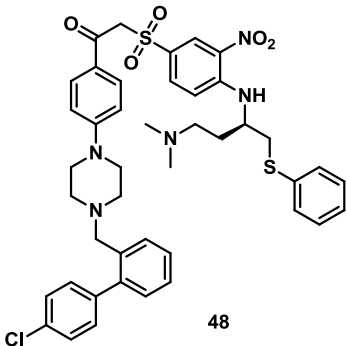
In the initial phase of the project, specific scFv towards the anti-apoptotic proteins Bcl-2 and Bcl-xL were isolated from naïve scFv phage display libraries. This was achieved by high-throughput screening of enriched scFv libraries selected against Bcl-2 and Bcl-xL using an *in vitro* competition assay for the interaction of Bcl-2 and Bcl-xL with BID BH3. Table 5-1 shows the IC₅₀ values of the most potent neutralising anti-Bcl-2/xL scFv isolated from the scFv libraries.

Table 5-1: A selection of IC₅₀ values determined for the isolated anti-Bcl-2/xL scFv for the inhibition of the Bcl-2/ xL interaction with BID BH3 in an Alpha screen assay

scFv #	IC ₅₀ , nM		V _H CDR3 amino acid sequence
	Bcl-xL	Bcl-2	
44	-	2	DLWELLLADAFDI
45	-	6	SKFLWFGGRNYFDP
22	21	-	TGEYSGYDTSGVEL
24	6 ± 2	-	DATTAPFYYYMDV
61	2	18	ALSQTYWGFFPTYFDS
67	22	14	SGSSSWYRPDDAFDI

The isolated scFv showed IC₅₀ values in the low nanomolar range. Moreover, scFv that specifically inhibit either Bcl-2 or Bcl-xL, or cross inhibitors of both proteins were isolated. In future studies, it will be important to verify the specificity of the lead scFv for other Bcl-2 family members. This will be possible by using a binding ELISA and a panel of Bcl-2 family members such as, Mcl-1, A1 and Bcl-w. Nonetheless, the scFv isolated in this project are significantly more potent inhibitors of Bcl-2 and Bcl-xL than the previously reported anti-Bcl-2/xL scFv (scFv84)⁶³ and the small molecule Bcl-2/ xL inhibitor ABT-737 **48** (Table 5-2).²²⁷

Table 5-2: IC₅₀ values determined for scFv84 and ABT-737 **48** for the inhibition of the Bcl-2/xL interaction with BID BH3 in an Alpha screen assay.

scFv #	IC ₅₀ , μM		V _H CDR3 amino acid sequence
	Bcl-xL	Bcl-2	
scFv84	0.152 ± 0.002	> 4	YGYTFDY
 48	1.2 ± 0.3	0.5 ± 0.2	

The next stage of the project was to modify the lead scFv with a CPP to enable cell penetration. A systematic approach to modifying the isolated scFv with CPPs was developed to enable cell penetration. The CPP construct design is shown in Figure 5-1.

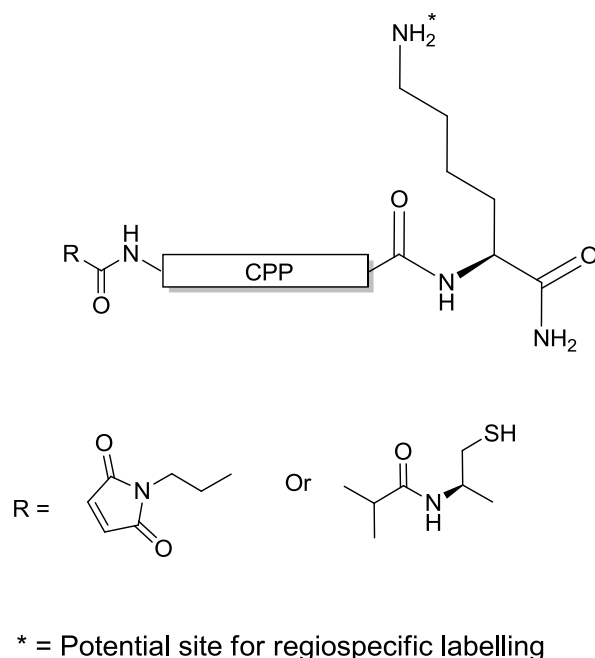
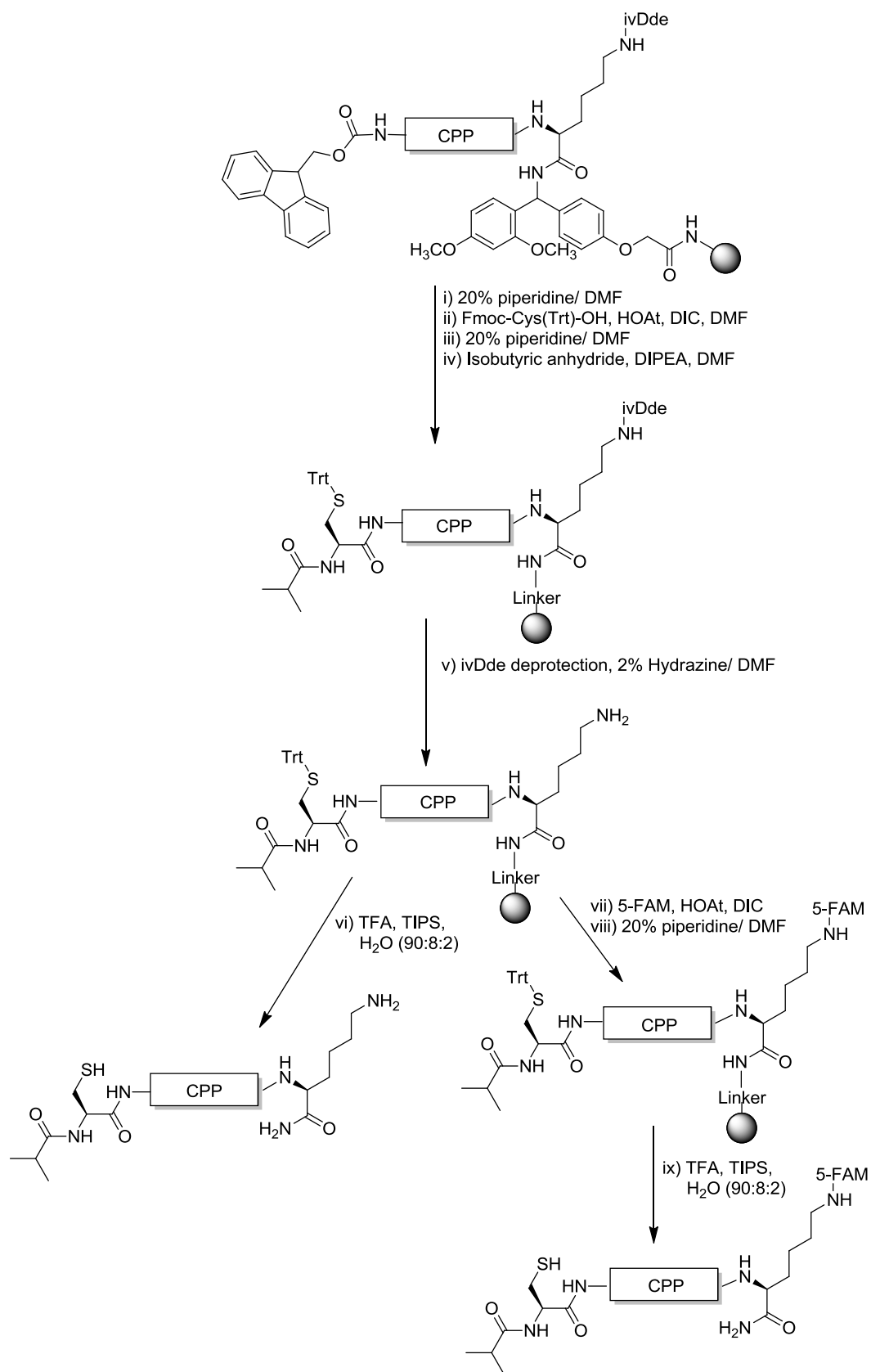


Figure 5-1: The general design of CPP derivatives, a C-terminal lysine residue will allow for fluorescent labelling of the peptide, The free N-terminus will allow for coupling of either a maleimidopropionyl or isobutyryl cysteine moiety for site-specific conjugation to scFv-Cys.

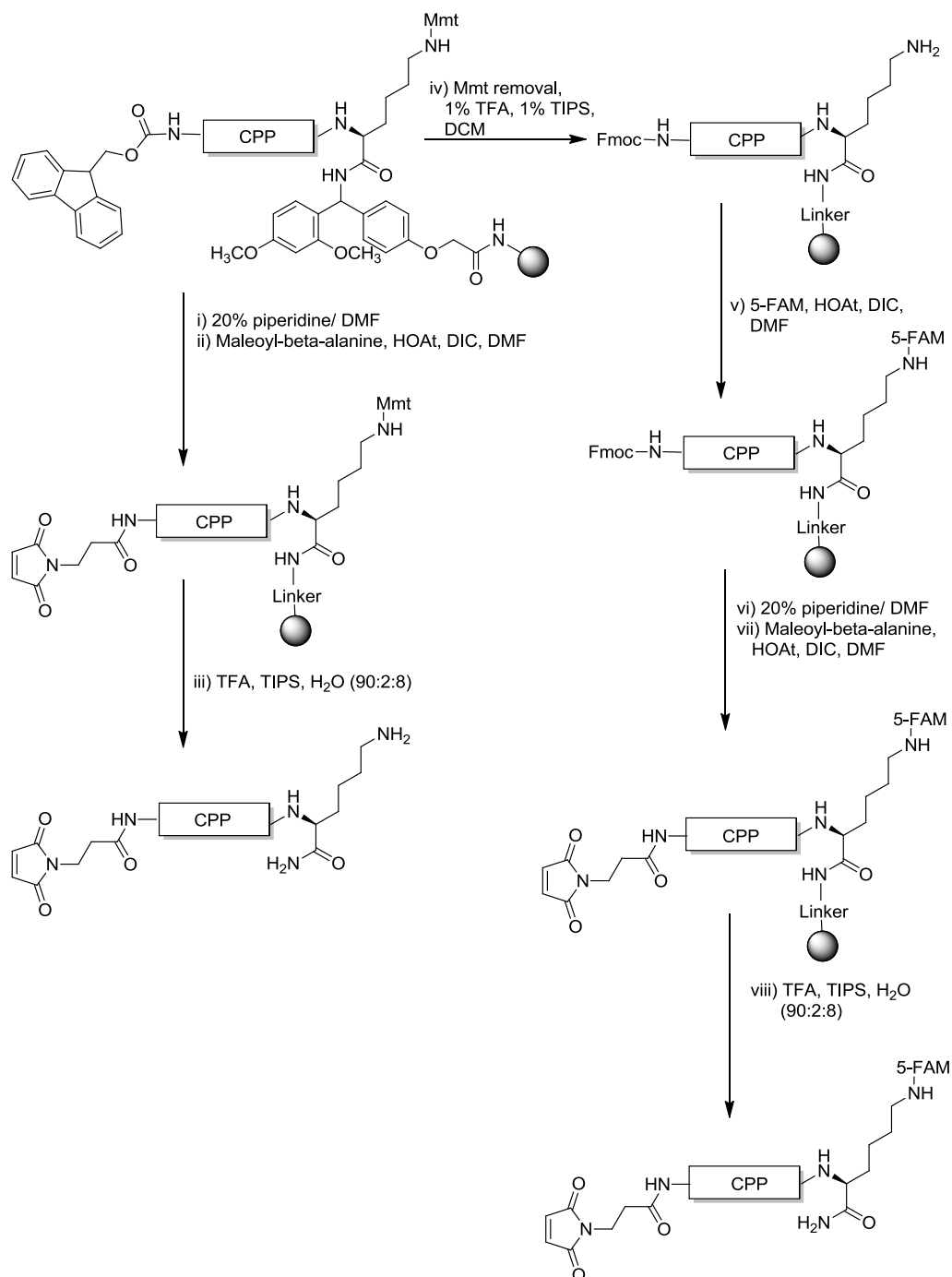
This CPP construct allowed for regioselective labelling with 5-carboxyfluorescein (5-FAM) to the C-terminal lysine residue. Additionally, the introduction of either N-maleimidopropionyl or N-isobutyryl cysteinyl moieties allowed for the site-specific conjugation of the CPP to lead scFv *via* a C-terminally located cysteine residue in the protein.

CPP derivatives possessing the aforementioned functionality were successfully synthesised using standard Fmoc solid-phase peptide synthesis (Fmoc SPPS). Regioselective labelling of the C-terminal lysine residue was achieved by introducing an orthogonally protected lysine residue to the peptidyl resin. Subsequent deprotection of the orthogonal protecting group from the peptidyl resin then allowed for regioselective introduction of 5-FAM to the CPP. Scheme 5-1 and Scheme 5-2 show the synthetic procedures for the synthesis of N-maleimidopropionyl and N-isobutyryl cysteinyl CPPs.

Scheme 5-1: Synthesis of the *N*-isobutyryl Cys CPP derivatives



Scheme 5-2: Synthesis of *N*-maleimidopropionyl CPP derivatives.



This strategy provided a robust method for the synthesis of a panel of CPP derivatives. Four different 5-FAM labelled CPP derivatives were then conjugated to scFv24 and the cell penetrating capabilities of these conjugates were determined using Confocal Laser Scanning Microscopy (CLSM) (Table 5-3).

Table 5-3: scFv-CPP(FAM) internalisation and localisation; summary of CLSM and Fluorescence microscopy.

scFv-CPP	CPP	Sequence	Localisation of scFv-CPP conjugate	
			HeLa	RBL-2H3
scfv24-77	octa-arginine	Mal-(R) ₈ -K(FAM)-[NH ₂]	cellular vesicles	cytoplasm
scfv24-79	Tat ₄₉₋₅₇	Mal-RKKRRQRRR-K(FAM)-[NH ₂]	Minimal internalisation, cellular vesicles	
scFv24-74	Antp ₅₂₋₅₈	Mal-RRMKKWKK-K(FAM)-[NH ₂]	Minimal cell internalisation	n.d
scFv24-81	Pro ₁₄	<i>i</i> Butyl-C-(P) ₁₄ -K(FAM)-[NH ₂]	extracellular	n.d

Based on the CLSM studies it was clear that **scFv24-77** possessed the most efficient cellular penetration capabilities. A summary of the preparation of **scFv24-77** and subsequent cellular internalisation is shown in Figure 5-2.

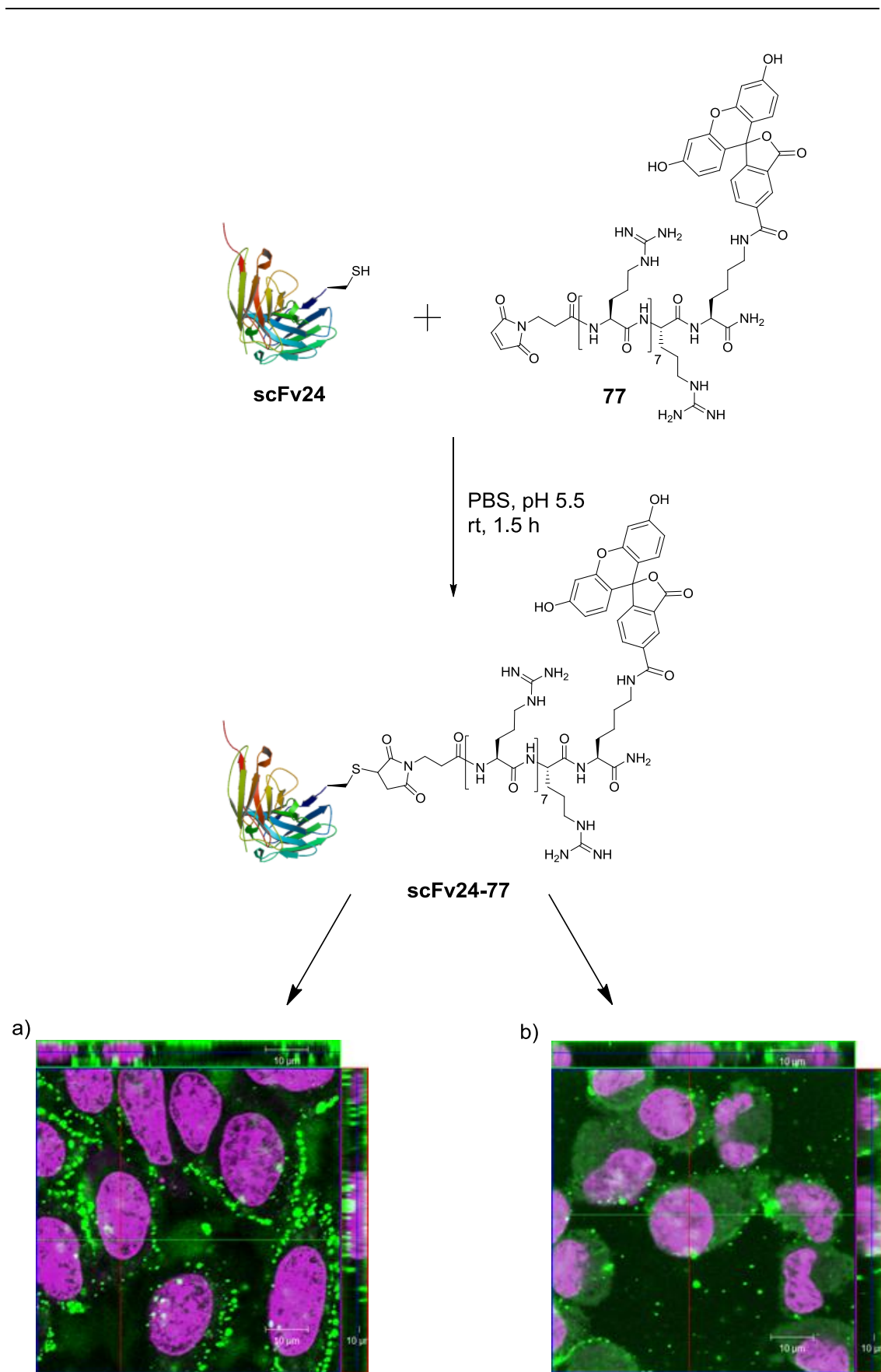
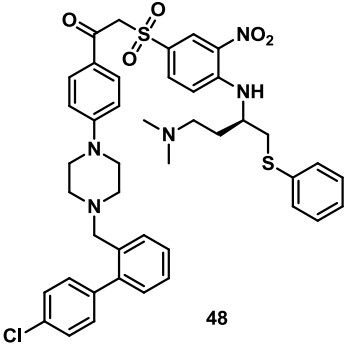


Figure 5-2: Z-sectioning using confocal microscopy of a) HeLa cells and b) RBL-2H3 cells treated with **scFv24-77** (Green) for 30 min at 37 °C, 10 μM and 90 min at 37 °C, 10 μM . Draq5 was used to stain cell nuclei (Purple).

Investigation into the biological effect of **scFv24-77** was achieved using a cell viability assay. Table 5-4 shows the EC₅₀ for the positive control ABT-737 **48** for the two cell lines used in the study.

Table 5-4: EC₅₀ value of ABT-737 for RBL-2H3 and Jurkat cells.

	Cell line	EC ₅₀ , μ M
 48	RBL-2H3	12 \pm 2
	Jurkat	14.0 \pm 0.6

Unfortunately, treatment of both cell lines with 40 μ M of **scFv24-77** did not affect cell viability. This is likely due to insufficient quantities of scFv being delivered into the cytoplasm of the cells to induce a biological effect. There are many studies that demonstrate CPP-cargo conjugates being retained in cellular vesicles.^{99, 73} Thus, it is possible that entrapment of the scFv-CPP in cellular vesicles is an influential factor in this study. Of equal importance is that scFv24 is specific to Bcl-xL only, thus the sensitivity of the RBL-2H3 and Jurkat cells to Bcl-xL inhibition has to be considered. For this reason, screening of a wider range of cell lines with scFv that are specific to Bcl-2 and Bcl-xL only and also cross-selective should be performed. The use of cell lines that have been tested with ABT-737 will give guidance to the sensitivity of the cell to Bcl-2/xL inhibition. Table 5-5 shows a selection of cell lines and the EC₅₀ values for ABT-737 reported in the literature.

Table 5-5: EC₅₀ of cell lines to ABT-737 treatment

Cell Line	EC ₅₀ , μM		Reference
	Culture conditions		
	10% FBS	Reduced FBS (%)	
HL-60	>10	-	High <i>et al.</i> (2010) ²²⁵
K562	>10	-	
Nalm6	>10	-	
Jurkat	5.00	-	
Molt4	0.92	-	
REH	0.68	-	
CEM	0.30	-	
Hal-01	0.19	-	
DoHH2	0.13	0.001 (3%)	Bruncko <i>et al.</i> (2007) ²²⁶
RS11380	0.15	0.014 (3%)	
SUDHL-4	0.85	0.220 (3%)	
NCI-H146	0.09	0.015 (0%)	Shoemaker <i>et al.</i> (2006) ²²⁷
A549	22.3	5.200 (0%)	

In addition to screening a wider panel of cell lines, it is also proposed that by introducing endosomolytic peptides to the CPP construct the quantity of scFv in the cytoplasm could be increased, thus increasing the quantity of scFv available to inhibit Bcl-2 and Bcl-xL. Table 5-6 shows a selection of peptides that have been reported to promote endosomal escape of an attached cargo.

Table 5-6: A selection of endosomolytic peptides

#	Endosomolytic Peptides	Reference
18	HA2; GLFGAIAAGFIEGGWTGNIDGWYG	Wadia <i>et al.</i> (2004) ¹¹¹
19	H5WYG; GLFHAIHFIHGGWHGLIGGWGYG	Pichon <i>et al.</i> (2001) ¹¹²
20	10HIS; HHHHHHHHHH	Lo <i>et al.</i> (2008) ¹¹³
21	4 ₃ E; LAELLAELLAEL	Ohmori <i>et al.</i> (1997) ¹¹⁴

The screening of a panel of scFv conjugated to different CPPs and endosomolytic peptides will allow for determination of the most effective peptides for efficient cytoplasmic delivery.

Nevertheless, we have successfully developed methodology for the systematic modification of a scFv to enable cellular internalisation. The optimisation of CPP conjugation to lead scFv *via* a C-terminal cysteine allowed for efficient preparation of scFv-CPP conjugates. This will allow for future screening of a wider panel of scFv

and CPP combinations to determine the most suitable CPP for intracellular delivery. Further screening of the neutralising scFv specific for Bcl-2 and Bcl-xL scFv in a wider range of cell lines together with comparison with the small molecule Bcl-2/xL inhibitor ABT-737 will allow for rational optimisation of the scFv-CPP conjugate.

Complementary to the preparation of scFv-CPP conjugates, a novel method for controlling the *in vivo* properties of the CPP octa-arginine has been developed. In the first stage of this proof-of-principle study, it was demonstrated that masking the guanidine functionality of octa-arginine inhibits its cellular internalisation (Figure 5-3).

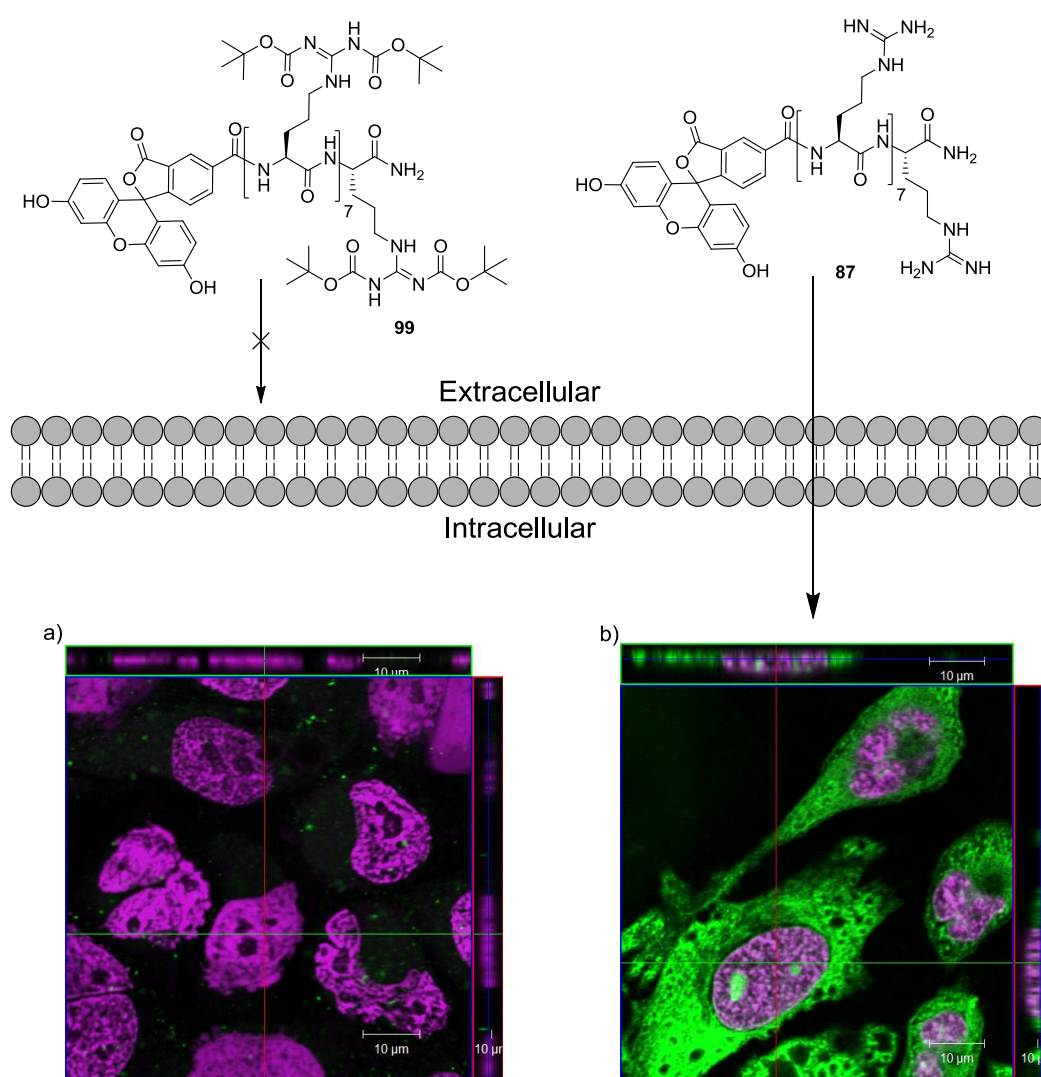
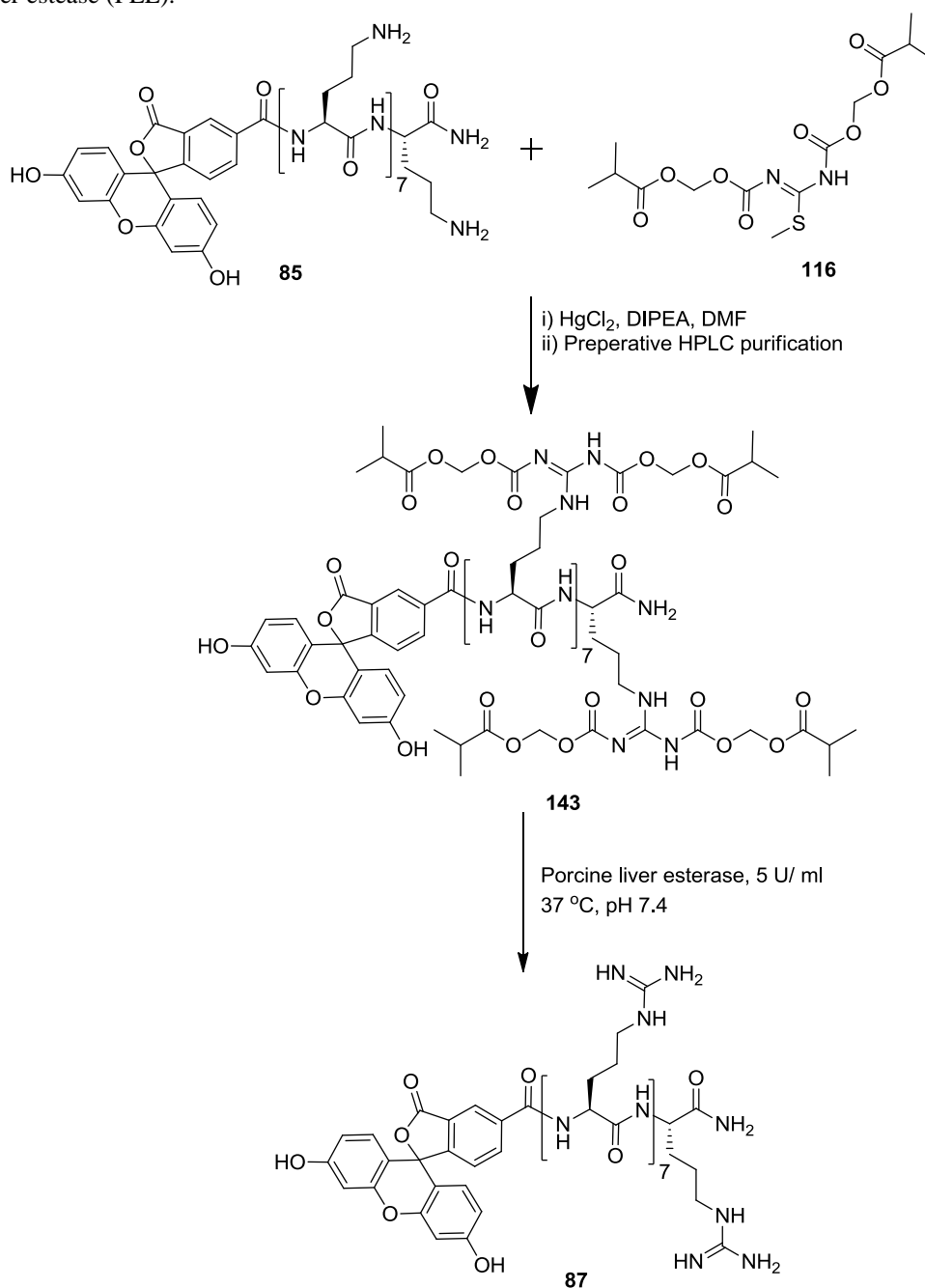


Figure 5-3: HeLa cells treated with 10 μM of 5-FAM labelled peptide (green), for 30 min at 37 °C. Cells were then washed and incubated with the nuclear stain Draq5 (purple) and Z-sections of the cells were taken using CLSM with an inverted x63 oil immersion lens **a)** FAM-(R(di-Boc))₈-[NH₂] **99** and **b)** FAM-(R)₈-[NH₂] **87**.

The inhibition of octa-arginine is most likely a result of masking the positive charge of the peptide, similar studies by Jiang *et al.* (2004) support this inference. In this study, the authors completely inhibit the cellular penetration of nona-arginine by masking the cationic charge with the anionic nona-glutamate.¹³⁸

This principle was then expanded to using the esterase and hydrolytically sensitive acyloxymethyl carbonyl (AM) protecting groups to mask octa-arginine. A preliminary study investigating the masking of the guanidine functionality of an octa-arginine derivative with AM protecting groups was deemed successful. Scheme 5-3 illustrates the approach taken to introduce AM protected guanidine moieties to the octa-ornithine derivative **85** affording the AM protected octa-arginine derivative **143**.

Scheme 5-3: : Synthesis of AM protected octa-arginine derivative **143** and subsequent deprotection with pig liver esterase (PLE).



Studies using analytical HPLC confirmed that the AM protected octa-arginine was deprotected by pig liver esterase (PLE). Further CLSM studies investigating the cell penetrating capabilities of the AM protected octa-arginine **143** after treatment with PLE, incubation in aqueous buffers and most importantly in blood plasma are required. Additionally, robust quantification of octa-arginine internalisation would provide insight into the effectiveness of the controlled unmasking of the AM protected octa-arginine **143** and subsequent cellular internalisation. Quantification of

internalised octa-arginine after treatment with PLE could be achieved using MALDI-TOF MS using a modified method based on that described by Burlina *et al.* (2005).²⁴²

This proof-of-concept study afforded compelling evidence that esterase-labile AM protecting groups could be used to mask the cationic charge of octa-arginine. The potential of the N^G-masking approach to modulate the cell penetrating capabilities of a CPP are numerous. For example, this approach is predicted to increase the circulation time of the CPP and reduce widespread non-specific tissue uptake. Moreover, the activation of the CPP is reliant on hydrolytic and/or esterase unmasking of the cationic charge. This separation between the tissue targeting and CPP activation mechanism is in contrast to the other approaches described for modulating the activity of a CPP.^{138,137} Therefore, this approach could be used in conjunction with different tissue targeting molecules and different macromolecular cargo.

The major goal of this project was to define rules for the modification of antibody reagents to possess cell penetrating capabilities whilst retaining suitable *in vivo* properties. This thesis aimed to achieve this by taking a systematic approach to modifying scFv with CPPs. The development of efficient methodology to produce scFv-CPP conjugates has been achieved and will allow for rapid screening of a panel of scFv-CPP conjugates in future studies. Moreover, the design of the CPP construct and development of a novel guanidino-masking technique to controlling the cell penetrating capabilities of a CPP will allow for optimisation of the *in vivo* properties of a scFv-CPP conjugate.

Experimental

6.1 Materials and Instrumentation

All solvents used of were high grade and purchased from Fischer Scientific (Loughborough, UK) and used as received. All amino acids were purchased from Novabiochem (Nottingham, UK) and all other commercial reagents were purchased from Sigma-Aldrich and were used as received without further purification. Analytical thin-layer chromatography (TLC) was performed on Merck silica gel 0.25 mm silica gel 60 F₂₅₄ plates. TLC plates were visualised using UV absorbance at 254 nm, or by staining with potassium permanganate dip. Flash chromatography was performed using Merck silica gel (200-400 mesh).

Analytical RP-HPLC was carried out using a Waters setup, comprised of two 510 pumps, a 486 detector and MilleniumTM software. The detector was set-up to record the absorbance of the effluent at 214 nm. The systems used were;

- System 1: 1-90% B over 10 min, 3 ml/ml, Onyx analytical C₁₈ (100 x 4.6 mm)
- System 2: 1-90% B over 10 min, 1 ml/min, Ace analytical C₈ (5 µm, 50 x 3 mm)
- System 3: 1-100% B over 10 min, 3 ml/min, Onyx analytical C₁₈ (100 x 4.6 mm)
- System 4: 1-90% B over 10 min, 1.2 ml/min, Onyx analytical C₁₈ (100 x 3.00 mm)

Preparative RP-HPLC was performed on a Waters Setup comprising of two Waters 2525 pumps, a Waters 2487 Detector and a Waters 2767 Fraction collector. The detector was set-up to record the absorbance of the effluent at 214 nm. Standard solvents used for both analytical and preparative HPLC were: 100% H₂O, 0.06% TFA (Solvent A) and 90% MeCN, 10% H₂O and 0.06% TFA (Solvent B).

¹H and ¹³C NMR spectra were acquired on a Bruker-AV 400 spectrometer operating at 400 and 100 MHz respectively and processed using Bruker TopSpin NMR 3.0 software. Deuterated solvents used were CDCl₃ (Cambridge Isotope Laboratories Inc.) and CD₃OD (Sigma-Aldrich). Chemical shifts (δ) are recorded in ppm relative to TMS and coupling constants (*J*) recorded in Hz. Abbreviations used in the description of spectra are; s (singlet), br s (broad singlet), d (doublet), dd (doublet of doublet), t (triplet), q (quartet) and m (multiplet).

Mass spectra were recorded on a High Resolution Time of Flight (TOF) electrospray ionisation (ES) system comprising of a Waters 2795 Separations module and Micromass LCT, data was processed using MassLynx™ software. Alternatively, spectra were recorded by Matrix Assisted Laser Desorption Ionisation TOF MS (MALDI-TOF MS) using a Bruker Daltonics Ultraflex instrument. The data was processed using Bruker Daltonics Flexanalysis™ software.

FTIR spectra were recorded using a Pierce ThermoScientific Nicolet IR200 FTIR and the data processed using OMNIC™ software. Samples were prepared using either KBr powder or NaCl plates. Melting points were recorded on a Gallenkamp melting point apparatus.

Confocal imaging of live cells was performed using a Zeiss LSM510 META Confocal Imaging System and Zeiss LSM510 operating software. Cells were imaged using an inverted 63x oil objective and Argon (458, 477, 488, 504 nm) and He-Ne 633 nm lasers.

6.1.1 General method for Fmoc solid-phase peptide synthesis of CPPs

All solvents used were of HPLC grade and purchased from Fischer Scientific unless otherwise stated. DMF was of peptide synthesis grade, purchased from Rathburn

Chemicals Ltd. All peptides were chemically synthesized by 9-fluorenylmethoxycarbonyl (Fmoc) solid-phase synthesis on a Rink Amide NovaGel™ resin (Novabiochem, Prod# 855031, 0.67 mmol/g⁻¹) on a 0.1 (150 mg resin) or 0.2 mmol (300 mg resin) scale, unless otherwise stated. The coupling reagent HATU; 2-(7-aza-1H-benzotriazole-1-yl)-1,1,3,3-tetramethyluronium hexafluorophosphate was purchased from Fluorochem Ltd and Pyoxim®; *O*-[(1-cyano-2-ethoxy-2-oxoethylidene)amino]-oxytri(pyrrolidin-1-yl) phosphonium hexafluorophosphate²¹³ were purchased from Novabiochem. All amino acid residues introduced to the peptidyl resin were standard *N*^α-Fmoc protected derivatives with acid-labile side-chain protecting groups, unless otherwise stated. Table 6-1 shows the *N*^α-Fmoc-amino acids used for each peptide synthesis.

Table 6-1: Standard *N*^α-Fmoc amino acids with acid-labile side-chain protecting groups used in Fmoc SPPS

	Mw
Fmoc-Arg(Pbf)-OH	648.8
Fmoc-Asn(Trt)-OH	596.7
Fmoc-Cys(Trt)-OH	585.7
Fmoc-Gln(Trt)-OH	610.7
Fmoc-Ile-OH	353.4
Fmoc-Lys(Boc)-OH	468.5
Fmoc-Met-OH	371.5
Fmoc-Orn(Boc)-OH	454.5
Fmoc-Phe-OH	387.4
Fmoc-Pro-OH	337.4
Fmoc-Trp(Boc)-OH	526.6

All acylations were carried out in an Omnifit™ continuous flow glass column (150 x 10 mm), and all wash steps were performed using a NOVASYN® GEM manual peptide synthesiser, unless otherwise stated. The UV absorbance of the effluent was measured at 290 nm using a LKB Biochrom Ultrospec II spectrometer, and recorded using a LKB Bromma 2210 recorder.

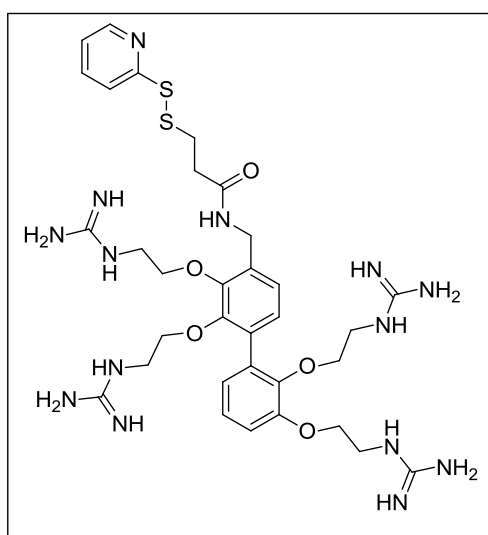
All amino acid residues, for a 0.2 and 0.1 mmol scale synthesis, were introduced to the peptidyl resin using the following reaction mixture unless otherwise stated; Fmoc-amino acids (4 equivalents), HATU (3.9 equivalents), DIPEA (8 equivalents) in DMF (~1.5 ml). This reaction mixture was added to the resin, followed by intermittent stirring for 3 h at rt.

After 3 h the peptidyl resin was washed with DMF to remove excess amino acid and coupling reagents, followed by Fmoc deprotection using 20% piperidine/DMF (2.8 ml/min, 10 min). The Fmoc deprotection was monitored by UV absorbance of the effluent at 290 nm. Finally, peptidyl resins were washed with DMF (2.8 ml/min, 10 min) to remove remaining piperidine before the next amino acid coupling.

After the introduction of the required amino acid residues to the peptidyl resin the peptidic material was cleaved from the resin and universally deprotected by suspending the peptidyl resin in a solution of trifluoroacetic acid (TFA, 9 ml), triisopropylsilane (TIPS, 0.2 ml) and H₂O (0.8 ml) for 3-5 h at rt. The suspension was filtered and the filtrate evaporated to dryness *in vacuo*. The resulting residue was triturated with cold diethyl ether (3 x 10 ml) to afford the crude peptidic material. Preparative HPLC was used to isolate the desired peptide followed by lyophilisation. The peptide purity was then determined by analytical HPLC.

6.2 Experimental for Chapter 3

***N*-[2, 3, 2', 3'-tetra(2-guanidino-ethyloxy)-biphenyl-4-ylmethyl]-3-[2-pyridyl)dithio]propionamide trifluoroacetate salt, (14)**⁹⁷⁻⁹⁸

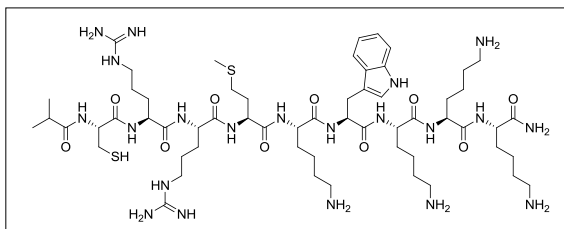


N'-Bis(*tert*butoxycarbonyl) guanidino]-ethyloxy]-biphenyl-4-ylmethyl]-3-[2-pyridyl)dithio]-propionamide **84** (106 mg, 0.067 mmol) was Boc deprotected by acidolysis using 50% TFA/DCM (10 ml). The reaction was stirred for 2 h at rt followed by removal of reaction solvent *in vacuo*. The resulting residue was triturated with cold diethyl ether to afford the title compound as a clear solid (80 mg, 97%) that was spectroscopically identical to the literature

precedent.⁹⁸ ¹H NMR (400 MHz, CDCl₃): δ/ppm; 2.74 (2H, t, *J*= 6.8 Hz), 3.11 (2H, t, *J*= 6.8 Hz), 3.23-3.30 (4H, m), 3.60-3.71 (4H, m), 3.89 (2H, m), 3.97 (2H, m), 4.22 (4H, m), 4.48 (2H, s), 6.87 (1H, m), 7.02 (1H, d, *J*= 7.8 Hz), 7.10-7.20 (4H, m), 7.22

(2H, m), 7.80-7.87 (2H, m). **HRMS TOF (ES⁺):** m/z calcd. for C₃₃H₅₀N₁₄O₅S₂²⁺ [M+2H]²⁺ 393.1760 found 393.1749.

***N*-Isobutyryl cysteinyl arginyl arginyl methionyl lysyl lysyl tryptophyl lysyl lysyl lysyl amide; Antp₅₂₋₅₇ derivative, (61)**



Rink Amide NovaGelTM resin (300 mg, 0.2 mmol) was swollen using DMF (1.5 ml) at rt for 1 h. The resin was then washed using a NOVASYN[®] GEM manual peptide synthesiser with 20%

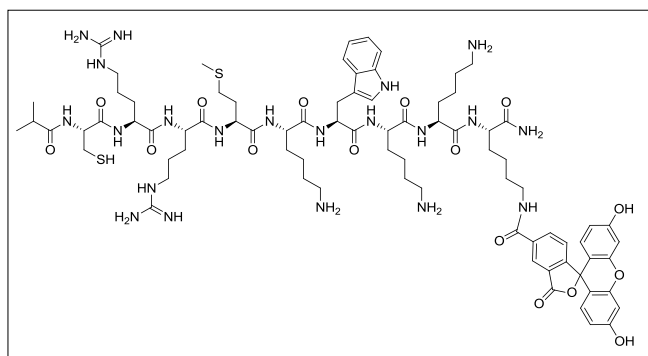
piperidine/DMF (2.8 ml/min, 10 min), followed by DMF (2.8 ml/min, 10 min). Fmoc-Lys(ivDde)-OH (460 mg, 0.8 mmol) was pre-activated using HATU (297 mg, 0.79 mmol) and DIPEA (207 mg, 278.7 μ l, 1.6 mmol) in DMF (~ 1.5 ml). This coupling mixture was added to the resin and stirred intermittently for 6 h at rt. The peptidyl resin was then washed with DMF (2.8 ml/min, 5 min) to remove excess reagents, followed by treatment with 20% piperidine/DMF (2.8 ml/min, 10 min) and finally washed with DMF (2.8 ml/min, 10 min). All subsequent Fmoc-amino acids (0.8 mmol) were pre-activated using HATU (297 mg, 0.79 mmol), DIPEA (207 mg, 279 μ l, 1.6 mmol) in DMF (~ 1.5 ml) for 3 h at rt with intermittent stirring before Fmoc deprotection. All amino acids were coupled by repeated cycles of coupling and deprotection to yield peptidyl resin **58**.

Fmoc deprotection of **58** was achieved as previously described. Fmoc-Cys(Trt)-OH (469 mg, 0.8 mmol) was pre-activated using HOAt (109 mg, 0.8 mmol) and DIC (100 mg, 124 μ l, 0.8 mmol) in DMF (~ 1 ml) and added to the peptidyl resin for 3 h with intermittent stirring. This was followed by washing with DMF and Fmoc deprotection as described. The peptidyl resin was then treated with isobutyric anhydride (126.5 mg, 133 μ l, 0.8 mmol) and DIPEA (207 mg, 279 μ l, 1.6 mmol) for 1 h followed by washing of resin with DMF (2.8 ml/min, 10 min) to afford peptidyl resin **59**.

Peptidyl resin **59** was treated with 2% Hydrazine/DMF (2.8 ml/min, 15 min) with monitoring of the reaction by absorbance of the effluent at 290 nm. Upon reaction completion the resin was washed with DMF (2.8 ml/min, 10 min).

The peptidyl resin was then transferred to a Buchner funnel and washed with DMF (20 ml), DCM (20 ml), hexane (20 ml), and dried *in vacuo* for 3 h to afford peptidyl resin **60** (623 mg, 77%). Approximately 1/3 of peptidyl resin **60** (0.07 mmol) was suspended in trifluoroacetic acid (TFA, 9 ml), triisopropylsilane (TIPS, 0.2 ml) and H₂O (0.8 ml) for 4 h. The suspension was filtered and the filtrate evaporated to dryness *in vacuo*. The resulting residue was triturated with cold diethyl ether (3 x 10 ml) to afford an off white residue (34 mg, 50%). The residue was dissolved in H₂O and lyophilised to afford Antp₅₂₋₅₇ derivative **61**. Preparative HPLC (Onyx Semi-prep Monolith C₁₈ column, 100 mm x 10 mm, 10-40% B over 10 min, *t*_R; 3.12 min) of 20 mg crude peptide **61** gave 10 mg (51%) of the title compound as a white solid. **HPLC**: system 1; *t*_R 1.38 min (purity >85%); **HRMS TOF (ES⁺)**: *m/z* calcd. for C₅₉H₁₀₇N₂₁O₁₀S₂²⁺ [M+2H]²⁺ 666.8970 found 666.7127, calcd. for C₅₉H₁₀₈N₂₁O₁₀S₂³⁺ [M+3H]³⁺ 444.9338 found 444.9823.

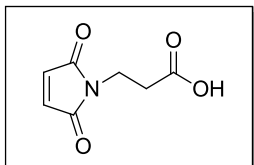
***N*-isobutyryl cysteinyl arginyl arginyl methionyl lysyl lysyl tryptophyl lysyl lysyl (*N*'-fluorescein-5-carbonyl) lysyl amide, Antp₅₂₋₅₇ derivative, (**63**)**



The title compound was synthesised using approximately 1/3 (0.07 mmol) of the ivDde deprotected resin **60**. 5-FAM (75 mg, 0.2 mmol) was pre-activated using HOAt (27 mg, 0.2 mmol) and DIC (25 mg, 31 μ l, 0.2 mmol) in DMF (1 ml) and added to the peptidyl resin, followed by intermittent stirring for 16 h at rt. The resin was then washed with DMF (2.8 ml/min, 10 min), followed by treatment with 20% piperidine/ DMF (2.8 ml/min, 20 min) and finally DMF (2.8 ml/min). The peptidyl resin was then collected and washed with DMF, DCM and hexane, and dried *in vacuo* (208 mg, 72%). The peptide was cleaved from the resin and deprotected as previously described using TFA-TIPS-H₂O (90:2:8) for 3 h at rt followed by removal of the TFA *in vacuo*. Subsequent trituration of the remaining residue using diethyl ether afforded an orange residue (52 mg, 89%). Preparative HPLC (Chromolith Semi-prep C₁₈ column, 100 mm x 10 mm, 10-40% B over 8 min,

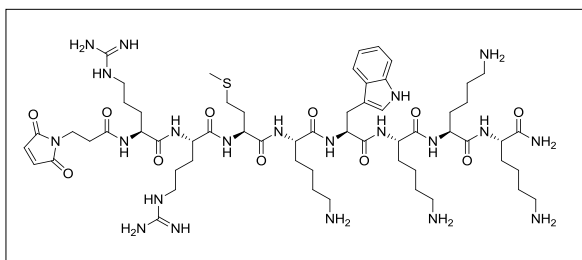
t_R 4.52 min) of 23.1 mg of crude peptide afforded 11 mg (46%) of the title compound as an orange solid. **HPLC:** system 1; t_R 3.96 min (purity >85%). **HRMS TOF (ES⁺):** m/z calcd. for $C_{80}H_{117}N_{21}O_{16}S_2^{2+}$ [M+2H]²⁺ 845.9209 found 845.5109, calcd. for $C_{80}H_{118}N_{21}O_{16}S_2^{3+}$ [M+3H]³⁺ 546.2830 found 546.2165, calcd. for $C_{80}H_{119}N_{21}O_{16}S_2^{4+}$ [M+4H]⁴⁺ 423.4641 found 423.5317.

***N*-Maleoyl- β -alanine, (64)²¹²**



Maleic anhydride (1.53 g, 15.6 mmol) and β -alanine (1.35 g, 1.2 mmol) were dissolved in 25 ml glacial acetic acid (AcOH) at rt. The reaction mixture was then refluxed for 16 h with stirring. AcOH was removed *in vacuo* giving a light brown residue. The residue was dissolved in toluene (25 ml) and the solution evaporated to dryness *in vacuo*. This process was repeated three times. *N*-Maleoyl- β -alanine was isolated using silica chromatography (SiO₂, 10% MeOH/ DCM R_f: 0.34) as a white solid (1.28 g, 50%). **¹H NMR (400 MHz, DMSO-*d*₆):** δ /ppm; 2.49 (2H, t, J = 7.3 Hz, CH₂CH₂), 3.61 (2H, t, J = 7.3 Hz, CH₂CH₂), 7.01 (2H, s), 12.35 (1H, s). **¹³C NMR (100 MHz, DMSO-*d*₆):** δ /ppm; 32.86 (CH₂), 33.76 (CH₂), 134.56 (CH), 172.00 (C=O), 170.69 (C=O). **HRMS TOF (ES⁻):** m/z calcd. for C₇H₆NO₄⁻ [M-H]⁻ 168.0302 found 168.0191. **FTIR (KBr):** 3458 (CH₂), 3093 (CH₂), 2633 (CH), 1704 (C=O). **M.pt:** 95-97 °C (lit.²¹² 92-94°C)

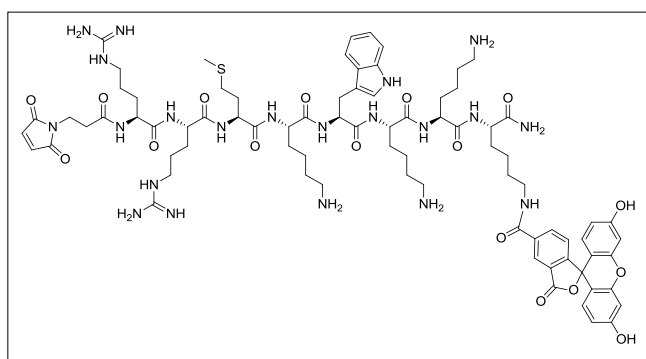
***N*-maleimidopropionyl arginyl arginyl methionyl lysyl lysyl tryptophyl lysyl lysyl lysyl amide, Antp₅₂₋₅₇ derivative, (70)**



Fmoc-Lys(Mmt)-OH (513 mg, 0.8 mmol) was pre-activated using HATU (297 mg, 0.79 mmol) and DIPEA (207 mg, 279 μ l, 1.6 mmol, DIPEA) in DMF (~1.5 ml) and added to the NovaGelTM Rink Amide resin (300 mg, 0.2 mmol) for 6 h with intermittent stirring at rt. All subsequent amino acids were coupled and deprotected as previously described to afford peptidyl resin **68**. Approximately 1/2 of peptidyl resin **68** (0.1 mmol) was Fmoc deprotected as previously described using 20% piperidine/DMF. *N*-maleoyl- β -alanine (67 mg, 0.4 mmol) was pre-activated with HOAt (109 mg, 0.4 mmol) and DIC

(25 mg, 30 μ l, 0.4 mmol) in DMF (~1.5 ml) and added to the resin followed by intermittent stirring of the resin for 3 h at rt followed by washing of the resin with DMF (2.8 ml/min, 10 min). The peptidyl resin was then collected and washed with DMF, DCM and hexane, and dried *in vacuo* (345 mg, 90%). The peptide was cleaved from the resin and deprotected as previously described for **61** using TFA-TIPS-H₂O (90:2:8) for 3 h at rt followed by removal of the TFA *in vacuo*. Subsequent trituration of the remaining residue using diethyl ether afforded an off white residue (98 mg, 90%). Preparative HPLC (Phenomenex Luna C₁₈ column, 5 μ m, 50 x 21.2 mm, 20-27% B over 8 min, 20.41 ml/min, t_R 4.06 min) of 22 mg crude peptide gave 15 mg (69%) of the title compound as a white solid. **HPLC:** system 1; t_R 3.00 min (purity >90 %). **HRMS TOF (ES⁺):** m/z calcd. for C₅₉H₁₀₁N₂₁O₁₁S²⁺ [M+2H]²⁺ 655.8850 found 655.8702, calcd. for C₅₉H₁₀₂N₂₁O₁₁S³⁺ [M+3H]³⁺ 437.5924 found 437.5938.

***N*-maleimidopropionyl arginyl arginyl methionyl lysyl lysyl tryptophyl lysyl lysyl (*N'*-fluorescein-5-carbonyl) lysyl amide, Antp₅₂₋₅₇ derivative, (74)**



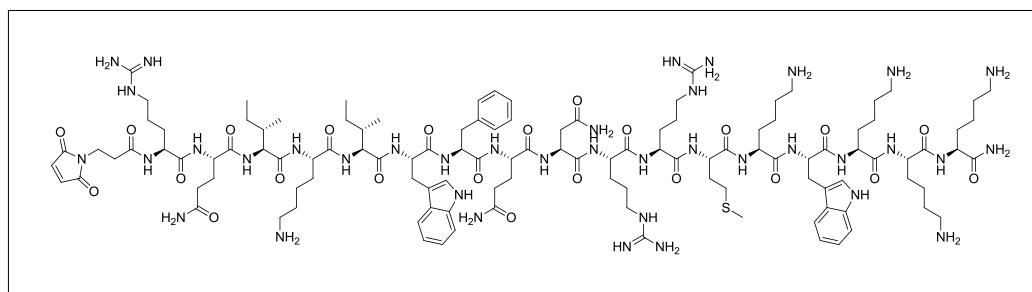
The Mmt protecting group of peptidyl resin **68** (~0.1 mmol) was removed using 1% TFA/1% TIPS/DCM.²⁰⁸ This was carried out using an Omnifit™ continuous flow glass column (150 x 10 mm). Firstly, the resin

was washed with DCM (20 ml) to remove any residue DMF, the resin was then treated with the 1% TFA/1% TIPS/DCM (~100 ml) by allowing the cleavage mixture to slowly flow through the column, this was continued until no orange eluent was observed. To remove remaining TFA, the resin was washed with DCM (25 ml) followed by DMF (25 ml).

5-FAM was then coupled to the deprotected Lys by pre-activation of 5-FAM (75 mg, 0.2 mmol) using HOAt (27 mg, 0.2 mmol) and DIC (25 mg, 31 μ l, 0.2 mmol) in DMF (1 ml). This mixture was then added to the peptidyl resin, followed by intermittent stirring for 16 h at rt. The resin was then washed with DMF (2.8 ml/min, 10 min), followed by treatment with 20% piperidine/DMF (2.8 ml/min, 20 min) and finally

DMF (2.8 ml/min). *N*-maleoyl- β -alanine (67 mg, 0.4 mmol) was then pre-activated with HOAt (109 mg, 0.4 mmol) and DIC (25 mg, 30 μ l, 0.4 mmol) in DMF (~ 1.5 ml) and added to the resin followed by intermittent stirring of the resin for 3 h at rt followed by washing of the resin with DMF (2.8 ml/min, 10 min). The peptidyl resin was collected and washed with DMF, DCM and hexane, and dried *in vacuo* (293.3 mg, 74%). The peptide was cleaved from the resin and deprotected as previously described using TFA-TIPS-H₂O (90:2:8) for 3 h at rt followed by removal of the TFA *in vacuo*, subsequent trituration of the remaining residue using diethyl ether afforded an orange residue (102 mg, 83%). Preparative HPLC (Hichrom semi-prep C₁₈, 50 x 21.2 mm, 25-40% B over 20 min, 4.0 ml/min, *t*_R 9.74 min) of 6 mg crude peptide gave 2.6 mg (43%) of the title compound as an orange solid. **HPLC**: system 1; *t*_R 4.30 min (purity >85%), system 2; *t*_R 5.47 min (purity >85%) **HRMS TOF (ES⁺)**; *m/z* calcd. for C₈₀H₁₁₁N₂₁O₁₇S²⁺ [M+2H]²⁺ 834.9089 found 835.0024, calcd. for C₈₀H₁₁₁N₂₁O₁₇S³⁺ [M+3H]³⁺ 556.9417 found 556.8813.

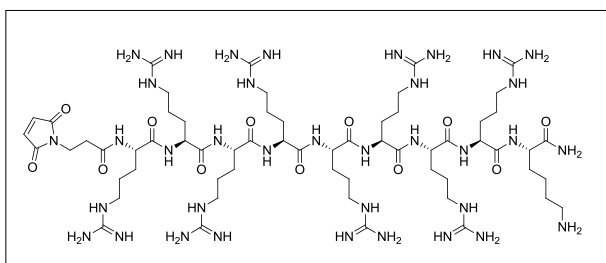
***N*-maleimidopropionyl arginyl glutaminyl isoleucyl lysyl isoleucyl tryptophyl phenylalanyl glutaminyl arginyl arginyl methionyl lysyl tryptophyl lysyl lysyl lysyl amide, Antp₅₂₋₅₇ derivative, (75)**



The synthesis of the title compound was achieved as described for peptide **70** on a 0.1 mmol scale (152 mg, 0.1 mmol). However, all amino acids after residue eight were coupled for 6 h with each coupling step being repeated before Fmoc deprotection and introduction of the next amino acid residue. Following addition of all of the residues, *N*-maleoyl- β -alanine was introduced to approximately 1/2 of the resin (~0.05 mmol) as previously described for **70**. The resin was then collected and washed with DMF, DCM and hexane, and dried *in vacuo* (279 mg, 67%). The peptidyl resin was cleaved and deprotected as previously described using TFA-TIPS-H₂O (90:2:8) for 5 h at rt, followed by removal of the TFA *in vacuo*. Subsequent trituration of the remaining

residue using diethyl ether afforded a white residue (84 mg, 105%). Preparative HPLC (Chromolith Semi-prep C₁₈ column, 100 mm x 10 mm, 20-50% B over 10 min, 7.0 ml/min, *t_R* 4.09 min) of 25.6 mg crude peptide gave 5.1 mg (20%) of the title compound as a white solid. **HPLC:** system 1; *t_R* 4.60 min (purity >85%) **HRMS TOF (ES⁺);** *m/z* calcd. for C₁₁₇H₁₈₈N₃₈O₂₃S²⁺ [M+2H]²⁺ 1263.2227 found 1263.2030, calcd. for C₁₁₇H₁₈₉N₃₈O₂₃S³⁺ [M+3H]³⁺ 842.4842 found 842.4617, calcd. for C₁₁₇H₁₉₀N₃₈O₂₃S⁴⁺ [M+4H]⁴⁺ 632.1150 found 632.0976.

***N*-maleimidopropionyl (arginyl)₈-lysyl amide, octa-arginine derivative, (76)**

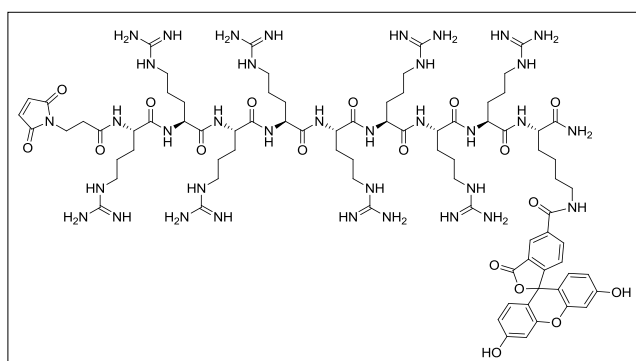


Synthesis of the title compound was performed on a 0.2 mmol scale (300 mg of resin) and achieved following the method described for peptide **70** with slight modification. In the first step, Fmoc-Lys(Mmt)-OH (513 mg,

0.8 mmol) was pre-activated using HATU (297 mg, 0.79 mmol) and DIPEA (207 mg, 279 μ l, 1.6 mmol, DIPEA) in DMF (~ 1.5 ml) and added to the NovaGelTM Rink Amide resin (300 mg, 0.2 mmol) for 6 h with intermittent stirring at rt. Each subsequent coupling of Fmoc-Arg(Pbf)-OH (230 mg, 0.4 mmol) was achieved by pre-activation using O-[(1-cyano-2-ethoxy-2-oxoethylidene)amino]-oxytri(pyrrolidin-1-yl) phosphonium hexafluorophosphate, PyOxim[®] 213 (211 mg, 0.4 mmol) and DIPEA (103 mg, 139 μ l, 0.8 mmol) in DMF (~1 ml). This mixture was then added to the resin followed by intermittent stirring for 1 h at rt. Each amino acid coupling was carried out twice before Fmoc deprotection. Approximately 1/2 (~0.1 mmol) of the resin was Fmoc deprotected followed by coupling of *N*-maleoyl- β -alanine (67 mg, 0.4 mmol) using HOAt (109 mg, 0.4 mmol) and DIC (25 mg, 30 μ l, 0.4 mmol) in DMF (~1.5 ml). This mixture was added to the resin and stirred intermittently for 3 h at rt. The peptidyl resin was then collected and washed with DMF, DCM and hexane, and dried *in vacuo* (391 mg, 77%). The peptide was then cleaved and deprotected as previously described using TFA-TIPS-H₂O (90:2:8) for 5 h at rt followed by removal of the TFA *in vacuo*. Subsequent trituration of the remaining residue using diethyl ether afforded a white residue (64 mg, 53%). Preparative HPLC (Chromolith Semi-prep C₁₈ column,

100 mm x 10 mm, 1-25% B over 6 min, t_R 4.43 min) of 32 mg crude peptide gave 5 mg (15%) of the title compound as a white solid. **HPLC:** system 1; t_R 2.72 min (purity >85%), system 2; t_R 4.14 min (purity >85 %). **HRMS TOF (ES⁺):** m/z calcd. for $C_{61}H_{119}N_{36}O_{12}^{3+}$ [M+3H]³⁺ 515.9931 found 515.9893, calcd. for $C_{61}H_{119}N_{36}O_{12}^{4+}$ [M+4H]⁴⁺ 387.2466 found 387.2472.

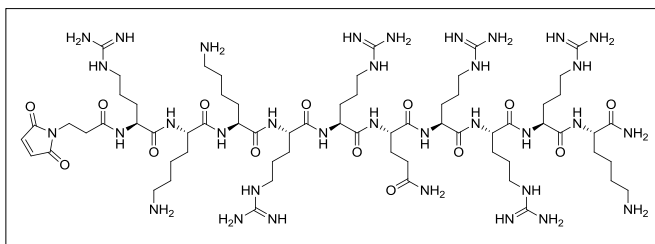
***N*-maleimidopropionyl (arginyl)₈ -(*N'*-fluorescein-5-carbonyl) lysyl amide, octa-arginine derivative, (77)**



Approximately ½ of the Fmoc protected resin from **76** (~0.1 mmol) was treated with 1% TFA/1% TIPS/DCM (100 ml) to remove the Mmt protecting group as described for **74**. To remove remaining TFA, the resin was

washed with DCM (25 ml) followed by DMF (25 ml). 5-FAM was then coupled to peptidyl resin as previously described for **74**, followed by washing of the resin with 20% piperidine/DMF. *N*-maleoyl-β-alanine was then introduced to the peptidyl resin as previously described for **74**. The peptidyl resin was then collected and washed with DMF, DCM and hexane, and dried *in vacuo* (332 mg, 61%). The peptide was cleaved from the resin and deprotected as previously described using TFA-TIPS-H₂O (90:2:8) for 5 h at rt, followed by removal of the TFA *in vacuo*. Subsequent trituration of the remaining residue using diethyl ether afforded an orange residue (61 mg, 52%). Preparative HPLC (Chromolith Semi-prep C₁₈ column, 100 mm x 10 mm, 1-50% B over 10 min, t_R 5.95 min) of 37 mg crude peptide gave 11 mg (30%) of the title compound as an orange solid. **HPLC:** system 1; t_R 3.85 min (purity >95 %), system 2; t_R 5.30 min (purity >95%). **HRMS TOF (ES⁺):** m/z calcd. for $C_{82}H_{129}N_{36}O_{18}^{3+}$ [M+3H]³⁺ 635.3423 found 635.6711, calcd. for $C_{82}H_{130}N_{36}O_{18}^{4+}$ [M+4H]⁴⁺ 476.7586 found 477.0062.

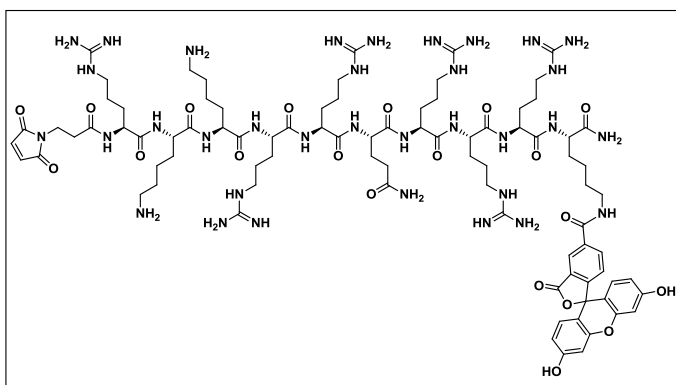
***N*-maleimidopropionyl arginyl lysyl lysyl arginyl arginyl glutaminyl arginyl arginyl arginyl lysyl amide, Tat₄₉₋₅₈ derivatives, (78)**



Synthesis of the title compound was achieved following the same method as described for **76** on a 0.2 mmol scale (300 mg of resin). After coupling of all of

the amino acids, approximately ¼ of the resin (~0.05 mmol) was Fmoc deprotected. *N*-Maleoyl-β-alanine was then introduced to the peptidyl resin as previously described. The peptidyl resin was then collected and washed with DMF, DCM and hexane, and dried *in vacuo* (165 mg, 62%). The peptide was cleaved from the resin and deprotected as previously described using TFA-TIPS-H₂O (90:2:8) for 5 h at rt followed by removal of the TFA *in vacuo*. Subsequent trituration of remaining residue using diethyl ether afforded a white residue (33 mg, 66%). Preparative HPLC (Chromolith Semi-prep C₁₈ column, 100 mm x 10 mm, 1-50 B over 10 min, *t_R* 3.64 min) of 8.6 mg crude peptide gave 1.6 mg (19%) of the title compound as a white solid. **HPLC**: system 1; *t_R* 2.55 min (purity >90%). **HRMS TOF (ES⁺)**: *m/z* calcd. for C₆₆H₁₂₇N₃₄O₁₄³⁺ [M+3H]³⁺ 540.3430 found 540.0051, calcd. for C₆₆H₁₂₈N₃₄O₁₄⁴⁺ [M+4H]⁴⁺ 405.2582 found 405.2563.

***N*-maleimidopropionyl arginyl lysyl lysyl arginyl arginyl glutaminyl arginyl arginyl arginyl (*N'*-fluorescein-5-carbonyl) lysyl amide, Tat₄₉₋₅₈ derivatives, (79)**

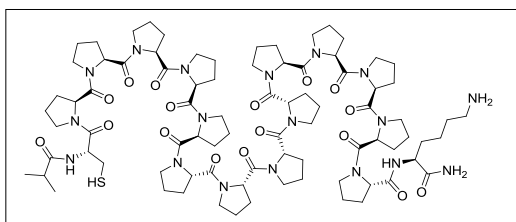


Approximately 0.07 mmol of Fmoc protected resin from the synthesis of **78** was Mmt deprotected using 1% TFA/1% TIPS/DCM (100 ml) as described for **74**. To remove remaining TFA, the resin was washed with DCM (25 ml)

followed by DMF (25 ml). 5-FAM was then coupled to peptidyl resin as previously

described for **74**, followed by washing of the resin with 20% piperidine/DMF. *N*-Maleoyl- β -alanine was then introduced to the peptidyl resin as previously described. The peptidyl resin was then collected and washed with DMF, DCM and hexane, and dried *in vacuo* (315 mg, 86%). The peptide was cleaved from the resin and deprotected as previously described using TFA-TIPS-H₂O (90:2:8) for 5 h at rt, followed by removal of the TFA *in vacuo*. Subsequent trituration of the remaining residue using diethyl ether afforded an orange residue (114 mg, 68%). Preparative HPLC (Chromolith Semi-prep C₁₈ column, 100 mm x 10 mm, 15-50 B over 10 min, *t*_R 3.72 min) of 23 mg crude peptide gave 8 mg (36%) of the title compound as an orange solid. **HPLC**: system 1; *t*_R 3.80 min (purity >95 %), system 2; *t*_R 5.63 min (purity >95 %). **HRMS TOF (ES⁺)**: *m/z* calcd. for C₈₇H₁₃₇N₃₄O₂₀³⁺ [M+3H]³⁺ 659.3577 found 659.6850, calcd. for C₈₇H₁₃₈N₃₄O₂₀⁴⁺ [M+4H]⁴⁺ 494.7701 found 495.0150.

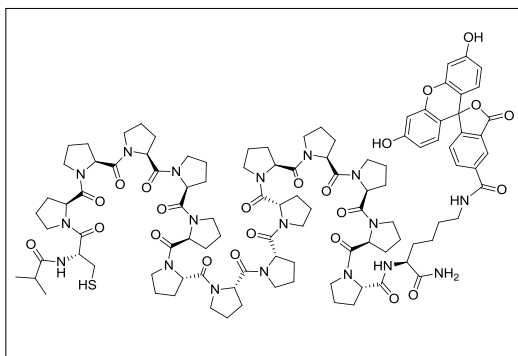
***N*-isobutyryl cysteinyl (prolyl)₁₄ lysyl amide, Pro₁₄ derivative, (**80**)**



Synthesis of **80** was achieved following the same method as described for **61** a 0.2 mmol scale (300 mg of resin). Proline residues were introduced to the peptidyl resin using Fmoc-Pro-OH (270 mg, 0.8 mmol), HATU (297 mg, 0.79 mmol) and DIPEA (207 mg, 279 μ l, 1.6 mmol) in DMF (~ 1.5 ml). This reaction mixture was added to the peptidyl resin as stirred intermittently for 3 h. Approximately 1/2 of the peptidyl resin (0.1 mmol) was collected and then cleaved from the resin as previously described using TFA-TIPS-H₂O (90:2:8) for 3 h at rt followed by removal of the TFA *in vacuo*. Subsequent trituration of remaining residue using diethyl ether afforded a white residue (64 mg, 88%).

Preparative HPLC (Onyx Semi-prep Monolith C₁₈ column, 100 mm x 10 mm, 10-35% B over 10 min, *t*_R 5.00 min) of 25.3 mg crude peptide gave 10.9 mg (43%) of the title compound as a white solid. **HPLC**: system 1; *t*_R 4.72 min (purity >80%). **HRMS TOF (ES⁺)**: *m/z* calcd. for C₈₃H₁₂₅N₁₈O₁₇S⁺ [M+H]⁺ 1678.9196 found 1678.8091, calcd. for C₈₃H₁₂₅N₁₈O₁₇S²⁺ [M+2H]²⁺ 839.4629 found 839.3392.

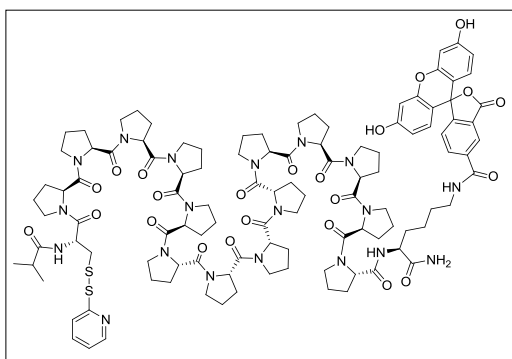
***N*-isobutyryl cysteinyl (prolyl)₁₄ -(*N'*-fluorescein-5-carbonyl) lysyl amide, Pro₁₄ derivative, (81)**



Synthesis of **81** was achieved following the same general method as described for **63**. Approximately ½ of the peptidyl resin from **80** (~0.1 mmol) was labelled with 5-FAM as described for **63**. The peptide was then cleaved from the resin as previously described using TFA-TIPS-H₂O (90:2:8)

for 3 h at rt followed by removal of the TFA *in vacuo*. Subsequent trituration of remaining residue using diethyl ether afforded an orange residue (61 mg, 93%). Preparative HPLC (Onyx Semi-prep Monolith C₁₈ column, 100 mm x 10 mm, 10-60% B over 10 min, *t_R* 7.50 min) of 52 mg crude peptide gave 14 mg (28%) of the title compound as an orange solid. **HPLC**: system 1; *t_R* 5.39 min (purity >90%), system 2; *t_R* 6.24 min (purity >90%). **HRMS TOF (ES⁺)**: *m/z* calcd. for C₁₀₄H₁₃₆N₁₈O₂₃S²⁺ [M+2H]²⁺ 1018.9885 found 1018.9812, calcd. for C₁₀₄H₁₃₇N₁₈O₂₃S³⁺ [M+3H]³⁺ 679.6614 found 679.6570.

***N*-isobutyryl-*S*-2-pyridylthio-cysteinyl-(prolyl)₁₄-(*N'*-fluorescein-5-carbonyl) lysyl amide, Pro₁₄ derivative, (83)**



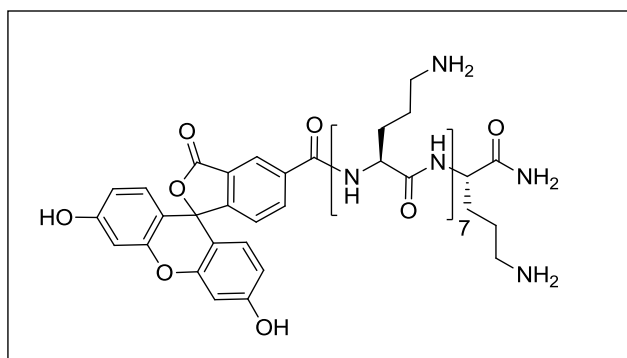
To a stirred solution of **81** (3 mg, 1.79 μmol) in AcOH:H₂O (2 ml, 3:1 v/v) was added 2,2'-dithiodipyridine (2 mg, 8.95 μmol). After stirring for 3 h at rt the solvent was evaporated to dryness *in vacuo*. The orange residue was dissolved in H₂O (2 ml) followed by washing with diethyl ether (3x

2 ml) to remove all unreacted 2,2'-dithiodipyridine and the by-product 2-mercaptopyridine to afford the title compound as an orange solid (2.5 mg, 65%).

HPLC: system 1; *t_R* 5.80 min (purity >75%); **HRMS TOF (ES⁺)**: *m/z* calcd. for C₁₀₉H₁₃₉N₁₉O₂₃S₂²⁺ [M+2H]²⁺ 1073.4716 found 1073.4878, calcd. for C₁₀₉H₁₄₀N₁₉O₂₃S₂³⁺ [M+3H]³⁺ 715.9842 found 715.9943.

6.3 Experimental for Chapter 4

FAM-(Orn)₈-[NH₂], (85)



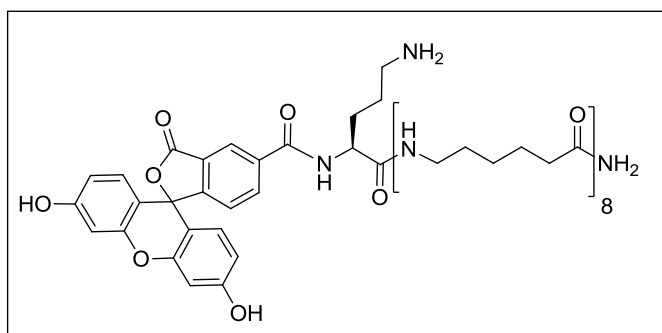
Rink amide NovaGelTM resin (300 mg, 0.2 mmol) was swollen using DMF (1.5 ml) at rt for 1 h. The resin was then washed using a NOVASYN[®] GEM manual peptide synthesiser with 20% piperidine/ DMF (2.8 ml/min, 10 min), followed by DMF (2.8 ml/min, 10 min). Fmoc-Orn(Boc)-OH (364 mg, 0.8 mmol) was pre-activated using *O*-(1-cyano-2-ethoxy-2-oxoethylidene)amino]-oxytri(pyrrolidin-1-yl) phosphonium hexafluorophosphate, PyOxim[®] 213 (422 mg, 0.8 mmol) and DIPEA (207 mg, 279 μ l, 1.6 mmol) in DMF (~ 1.5 ml). The coupling mixture was added to the resin and stirred intermittently for 6 h at rt. The peptidyl resin was then washed with DMF (2.8 ml/min, 5 min) to remove excess reagents, followed by treatment with 20% piperidine/ DMF (2.8 ml/min, 10 min) and finally washed with DMF (2.8 ml/min, 10 min). This is repeated eight times to afford peptidyl resin **89**.

Fmoc deprotection of **89** was achieved using 20% piperidine/ DMF (2.8 ml/min, 10 min) followed by washing the peptidyl resin with DMF (2.8 ml/min, 10 min). The next step involved the pre-activation of 5-FAM (150 mg, 0.4 mmol) using HOAt (54 mg, 0.4 mmol) and DIC (50 mg, 62 μ l, 0.4 mmol) in DMF (1 ml) this mixture was then added to the peptidyl resin and stirred intermittently at rt for 16 h. The peptidyl resin was then washed with DMF (2.8 ml/min, 10 min), followed by treatment with 20% piperidine/ DMF (2.8 ml/min, 20 min) and finally DMF (2.8 ml/min) to afford peptidyl resin **90**.

Peptidyl resin **90** was transferred to a Buchner funnel and washed with DMF (20 ml), DCM (20 ml), hexane (20 ml), and dried *in vacuo* for 3 h. The resin was then suspended in TFA (9 ml), TIPS (0.2 ml) and H₂O (0.8 ml) for 4 h at rt. The suspension was filtered and the filtrate evaporated to dryness *in vacuo*. The resulting residue was triturated with cold diethyl ether (3 x 10 ml) to afford the title compound as an orange solid (182.2 mg, 71%). Analytical RP-HPLC of the lyophilised peptide

showed a crude peptide of good purity (>80%), thus peptide **85** was used without further purification. **HPLC**; system 1: t_R 3.12 min (purity >80%), system 2: t_R 5.55 min (purity >80%), **HRMS TOF (ES⁺)**; m/z calcd. for C₆₁H₉₅N₁₇O₁₄²⁺ [M+2H]²⁺ 644.8617 found 644.8573.

FAM-(Orn-Ahx)₈-[NH₂], (**86**)



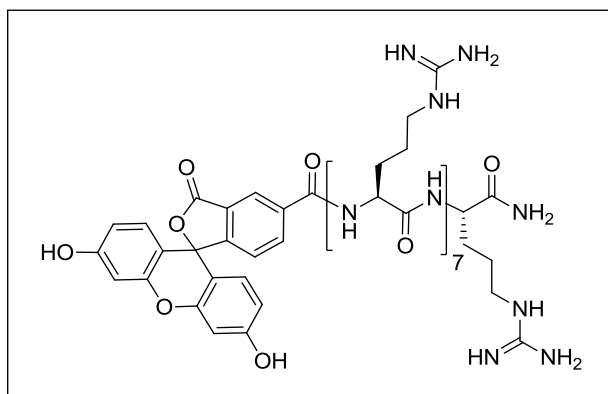
Rink amide NovaGel™ resin (151 mg, 0.1 mmol) was swollen using DMF (1.5 ml) at rt for 1 h. The resin was then washed using a NOVASYN® GEM manual peptide synthesiser with 20%

piperidine/ DMF (2.8 ml/min, 10 min), followed by DMF (2.8 ml/min, 10 min). Fmoc-6-aminohexanoic acid (141 mg, 0.4 mmol) was pre-activated using HATU (148 mg, 0.39 mmol) and DIPEA (104 mg, 140 µl, 0.8 mmol) in DMF (~ 1.5 ml). The coupling mixture was added to the resin and stirred intermittently for 6 h at rt. The peptidyl resin was then washed with DMF (2.8 ml/min, 5 min) to remove excess reagents, followed by treatment with 20% piperidine/ DMF (2.8 ml/min, 10 min) and finally washed with DMF (2.8 ml/min, 10 min). The second amino acid to introduced to the peptidyl resin was Fmoc-Orn(Boc)-OH (182 mg, 0.4 mmol) was pre-activated using HATU (148 mg, 0.39 mmol) and DIPEA (104 mg, 140 µl, 0.8 mmol) in DMF (~ 1.5 ml). Again the activated amino acid was added to the resin a stirred for 3 h at rt. The aforementioned couplings were repeated until a total of eight ornithine residues had been added to the resin to afford peptidyl resin **91**.

Fmoc deprotection of **91** was achieved using 20% piperidine/DMF (2.8 ml/min, 10 min) followed by washing the peptidyl resin with DMF (2.8 ml/min, 10 min). The next step involved the pre-activation of 5-FAM (75 mg, 0.4 mmol) using HOAt (27 mg, 0.2 mmol) and DIC (25 mg, 31 µl, 0.2 mmol) in DMF (1 ml) this mixture was then added to the peptidyl resin and stirred intermittently at rt for 16 h. The peptidyl resin was then washed with DMF (2.8 ml/min, 10 min), followed by treatment with 20% piperidine/DMF (2.8 ml/min, 20 min) and finally DMF (2.8 ml/min) to afford peptidyl resin **92**.

Peptidyl resin **92** was transferred to a Buchner funnel and washed with DMF (20 ml), DCM (20 ml), hexane (20 ml), and dried *in vacuo* for 3 h. The resin was then suspended in TFA (9 ml), TIPS (0.2 ml) and H₂O (0.8 ml) for 4 h at rt. The suspension was filtered and the filtrate evaporated to dryness *in vacuo*. The resulting residue was triturated with diethyl ether as previously described followed by lyophilisation of the remaining residue to afford the title compound as an orange solid (227 mg, 111%). The crude peptide was purified using preparative HPLC (Chromolith semi-prep C₁₈ column, 100 mm x 10 mm, 15-25% B over 15 min, 7 ml/min, *t_R* 3.42 min) 22 mg of crude peptide gave 10 mg (46 %) of the title compound as an orange solid. **HPLC**: system 1; *t_R* 3.45 min (purity >95 %). **HRMS TOF (ES⁺)**: *m/z* calcd. for C₁₀₉H₁₈₃N₂₅O₂₂²⁺ [M+2H]²⁺ 1097.6996 found 1097.6907, calcd. for C₁₀₉H₁₈₄N₂₅O₂₂³⁺ [M+3H]³⁺ 732.1355 found 732.1321, calcd. for C₁₀₉H₁₈₅N₂₅O₂₂⁴⁺ [M+4H]⁴⁺ 549.3535 found 549.3470.

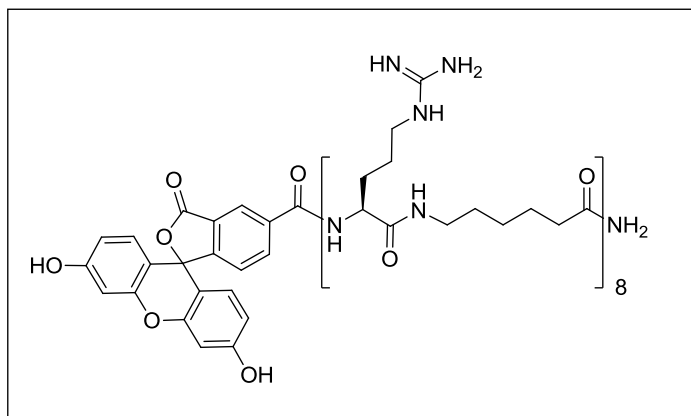
FAM-(Arg)₈-[NH₂], (**87**)



To FAM-(Arg(di-Boc))₈-[NH₂] **15** (2 mg, 0.62 mmol) was added TFA (1.3 ml), TIPS (50 µl) and H₂O (160 µl). The reaction mixture was stirred for 2 h at rt. The TFA was removed *in vacuo* to give an orange residue. The residue was triturated with cold diethyl ether followed by

purification using preparative HPLC (Chromolith Semi-prep C₁₈ column, 100 mm x 10 mm, 1-50% B over 10 min, *t_R*; 5.17 min) to yield an orange solid (401 µg, 40%). **HPLC**; system 1: *t_R* 3.47 min (purity >90 %), system 2: *t_R* 4.85 (purity >90 %). **MALDI-TOF MS (sinapic acid)**: *m/z* calcd. for C₆₉H₁₁₀N₃₃O₁₄⁺ 1624.89 [M+H]⁺ found 1625.86.

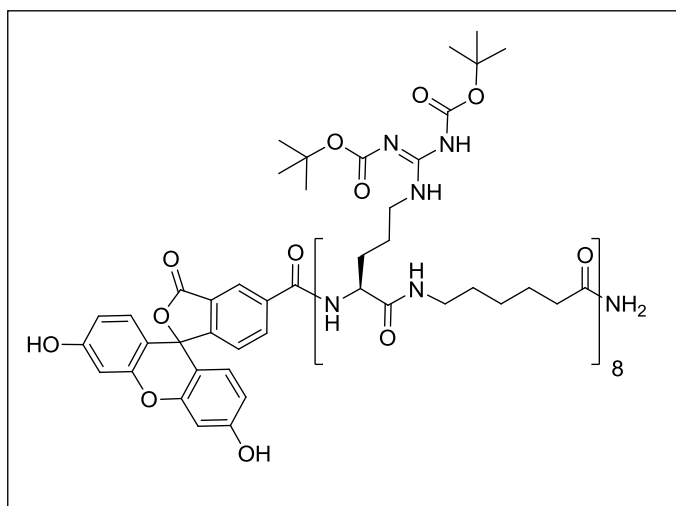
FAM-(Arg-Ahx)₈-[NH₂], (88)



To FAM-(Arg(di-Boc)-Ahx)₈-[NH₂] **98** (1 mg, 0.242 mmol) was added TFA (1.3 ml), triisopropylsilane (50 μ l) and water (160 μ l). The reaction mixture was stirred for 4 h at rt. The TFA was removed *in vacuo* to give an orange residue. The residue

was triturated with cold diethyl ether followed by purification using preparative HPLC (Chromolith Semi-prep C₁₈ column, 100 mm x 10 mm, 5-70% B over, 7 ml/min, *t_R*: 4.49 min) to afford the title compound as an orange residue (390 μ g, 56%). **HPLC:** System 1: *t_R* 3.88 min (purity >70 %), **MALDI-TOF MS (sinapic acid);** *m/z* calcd. for C₁₁₇H₁₉₈N₄₁O₂₂⁺ [M+H]⁺ 2530.57 found 2531.30.

FAM-(Arg(Di-Boc)-Ahx)₈-[NH₂], (98)

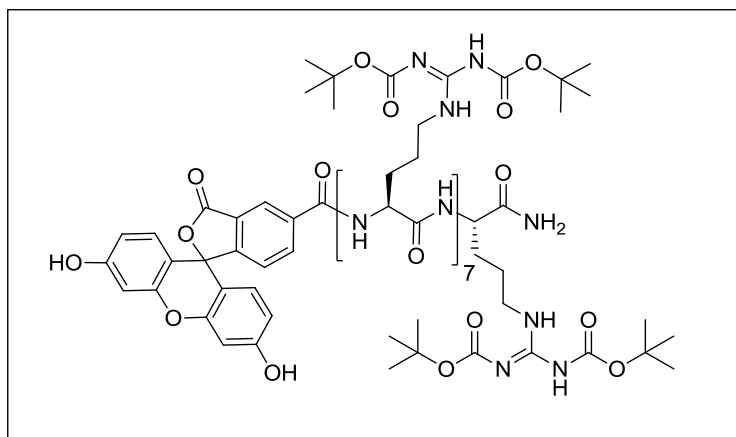


N,N'-bis(*tert*-butoxycarbonyl)-*S*-methylthiourea **96** (5.08 mg, 17.48 μ mol) was pre-activated with HgCl₂ (4.8 mg, 17.48 μ mol) in MeCN (1 ml). A solution of DIPEA (7.6 μ l, 43.7 μ mol) and FAM-(Orn-Ahx)₈-[NH₂] **86** (4 mg, 1.82 μ mol) in 1 ml H₂O was added dropwise to this solution

followed by stirring at rt for 2 h. The reaction solvents were evaporated to dryness *in vacuo* to afford an orange residue. This residue was dissolved into MeCN (2 ml) and centrifuged at 13000 g for 20 min to give a white pellet and orange supernatant. The title compound was isolated from the supernatant using preparative HPLC (Chromolith Semi-prep C₁₈ column, 100 mm x 10 mm, 50-90% B over 10 min, 7 ml/min, *t_R* 5.99 min) and lyophilised to afford the title compound as an orange residue

(4.3 mg, 57%). **HPLC**; System 3: t_R 6.76, 7.09, 7.42, 7.76 min (purity n.d.), **HRMS TOF (ES⁺)**; m/z calcd. for $C_{197}H_{328}N_{41}O_{54}^{3+}$ [M+3H]³⁺ 1378.1024 found 1378.1410, calcd. for $C_{197}H_{329}N_{41}O_{54}^{4+}$ [M+4H]⁴⁺ 1033.8576 found 1033.8420, calcd. for $C_{197}H_{330}N_{41}O_{54}^{5+}$ [M+5H]⁵⁺ 827.2875 found 827.2668, calcd. for $C_{192}H_{322}N_{41}O_{52}^{5+}$ [M+5H-Boc]⁵⁺ 807.2771 found 807.2635, calcd. for $C_{187}H_{314}N_{41}O_{50}^{5+}$ [M+5H-2Boc]⁵⁺ 787.2666 found 787.2573, calcd. for $C_{182}H_{306}N_{41}O_{48}^{5+}$ [M+5H-3Boc]⁵⁺ 767.0554 found 767.0530.

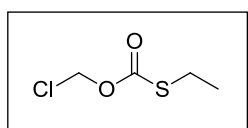
FAM-(Arg(di-Boc))₈-[NH₂], (99)



N,N'-bis(*tert*-butoxycarbonyl)-*S*-methylthiourea **96** (25.3 mg, 87.2 μmol) was pre-activated by the addition of HgCl₂ (23.7 mg, 17.48 μmol) in MeCN (5 ml). A solution of DIPEA (30.4 μl, 174.4 μmol) and

FAM-(Orn)₈-[NH₂] **88** (12.0 mg, 9.10 μmol) in 5 ml H₂O was added dropwise to the pre-activated isothiourea, followed by stirring at 50 °C for 2 h. The reaction mixture was then evaporated to dryness *in vacuo* to afford an orange residue. This residue was dissolved in MeCN (3 ml) and centrifuged at 13000 g for 20 min. The supernatant was then purified using preparative HPLC (Chromolith Semi-prep C₁₈ column, 100 mm x 10 mm, 50-100% over 10 min, 7 ml/min, t_R 8.92 min) to afford the title compound as an orange residue (6.8 mg, 23%). **HPLC**: system 2: t_R 8.95 min (purity >70 %), system 3: t_R 9.29 min (purity >70%). **HRMS TOF (ES⁺)**; m/z calcd. for $C_{149}H_{241}N_{33}O_{46}^{4+}$ [M+4H]⁴⁺ 807.4386 found 807.4263.

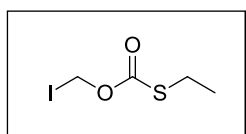
O-(Chloromethyl)-*S*-ethyl ester, (109) ²³⁸



A solution of ethanethiol (5.45 ml, 4.7 g, 78 mmol) and DIPEA (13.7 ml, 9.05 g, 78 mmol) in diethyl ether (20 ml) was added dropwise to an ethereal solution (60 ml) of chloromethyl chloroformate (3.6 ml, 40 mmol) at 0-4 °C with stirring. The reaction was then

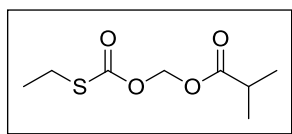
allowed to warm to rt and stirred for 16 h. The reaction mixture was firstly filtered and the filtrate evaporated to dryness *in vacuo*. The crude oil was then purified by passage through a silica plug (SiO₂, 50% petroleum ether/ 50% ethyl acetate, R_f; 0.63) to afford the title compound as a clear colourless oil (11.8g, 98%), which was spectroscopically identical to that described in the literature.^{238,243} **¹H NMR (400 MHz, CDCl₃):** δ/ppm; 1.35 (3H, t, CH₂CH₃, *J* = 7.5 Hz), 2.93 (q, 2H, CH₂CH₃ *J* = 7.3 Hz), 5.77 (s, 2H, CH₂Cl); **¹³C NMR (100 MHz, CDCl₃):** δ/ppm; 14.82 (CH₃), 25.71 (CH₂), 70.25 (ClCH₂), 170.38 (C=O). **FTIR (NaCl disc);** 2976 (CH), 1723 (C=O) cm⁻¹.

***O*-(Iodomethyl)-*S*-ethyl carbonothioate (110)²³⁸**



A solution of *O*-(chloromethyl)-*S*-ethyl ester **109** (11 g, 71 mmol) in acetone (50 ml) was added dropwise to a solution of sodium iodide (21.14 g, 142 mmol) and sodium bicarbonate (613 mg, 7.1 mmol) in acetone (150 ml) with stirring at rt. The reaction mixture was then heated to 40 °C and stirred for 4 h. The reaction mixture was filtered and the precipitated sodium chloride was washed with acetone (2 x 10 ml). The filtrate was evaporated to dryness *in vacuo*. The resulting deep purple oil was dissolved in H₂O (50 ml) and extracted with hexane (4 x 50 ml). The organic phase was then washed with 5% NaHCO₃ (1 x 50 ml), 1% Na₂S₂O₃ (2 x 50 ml) and dried over NaSO₄. Finally, the solvent was evaporated to dryness *in vacuo* to yield the title compound as a colourless, clear liquid (14.98 g, 88%), which was spectroscopically identical to that described in the literature.^{238,243} **¹H NMR (400 MHz, CDCl₃):** δ/ppm; 1.33 (3H, t, CH₂CH₃, *J* = 7.5 Hz), 2.92 (2H, q, CH₂CH₃ *J* = 7.5 Hz), 5.98 (2H, s, CH₂I); **¹³C NMR (100 MHz, CDCl₃):** δ/ppm; 14.68 (CH₃), 25.55 (CH₂), 31.46 (CH₂I) 169.90 (C=O). **FTIR (NaCl disc);** 2976 (CH), 1721 (C=O) cm⁻¹.

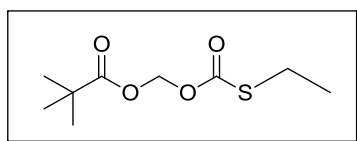
Isobutanoyloxymethyl-*S*-ethyl carbonothioate, (111)²³⁸



To a solution of sodium isobutyrate (4.01 g, 36 mmol) in dry DMF (50 ml), was added dropwise a solution of iodomethyl-*S*-ethyl carbonothioate **110** (7.00 g, 28 mmol) in dry DMF (10 ml) at -20 °C with stirring. The reaction mixture was allowed to warm to rt and stirred for 16 h. The reaction mixture was then filtered to remove precipitated sodium

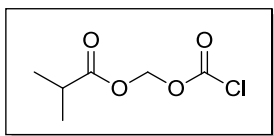
chloride. The precipitate was washed with DMF (10 ml) and diethyl ether (100 ml). H₂O (60 ml) was added to the filtrate, followed by extraction of the title compound with diethyl ether (4 x 40 ml). The organic layer was isolated and washed with 5% NaHCO₃ (50 ml), H₂O (50 ml), 0.1 M HCl (50 ml), brine (50 ml) and finally dried over Na₂SO₄. The solvent was evaporated to dryness *in vacuo* to afford the title compound as a colourless clear oil (4.57 g, 79%), which was spectroscopically identical to that described in the literature.²⁴³ **¹H NMR (400 MHz, CDCl₃):** δ/ppm; 1.17 (6H, d, *J*= 7.0 Hz, CH(CH₃)₂), 1.31 (3H, t, *J*= 7.3 Hz, CH₂CH₃), 2.59 (1H, sept, *J*= 7.0 Hz, CH(CH₃)₂), 2.88 (2H, q, *J*= 7.3 Hz, CH₂CH₃), 5.79 (2H, s, OCH₂O); **¹³C NMR (100 MHz, CDCl₃):** δ/ppm; 14.70 (CH₃CH₂), 18.54 (CH(CH₃)₂), 25.33 (CH₃CH₂), 33.67 (CH(CH₃)₂), 80.27 (OCH₂O), 170.60 (C=O), 175.41 (C=O). **FTIR (NaCl disc):** 2976 (CH), 1760 (C=O), 1722 (C=O) cm⁻¹.

Pivaloyloxymethyl-*S*-ethyl carbonothioate, (112)²³⁸



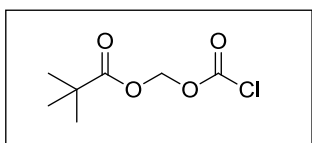
To a solution of sodium pivaloate (9.68 g, 78 mmol) in dry DMF (80 ml) was added a solution of iodomethyl-*S*-ethyl carbonothioate **110** (14.7 g, 60 mmol) in dry DMF (10 ml) was dropwise at -20 °C. The reaction was allowed to warm to rt and stirred for 16 h. The reaction mixture was then filtered to remove precipitated sodium chloride. The precipitate was washed with DMF (20 ml) and diethyl ether (100 ml). H₂O (60 ml) was added to the filtrate, followed by extraction of the title compound with diethyl ether (4 x 40 ml). The organic layer was isolated and washed with 5% NaHCO₃ (50 ml), H₂O (50 ml), 0.1 M HCl (50 ml), brine (50 ml) and finally dried over Na₂SO₄. The solvent was evaporated to dryness *in vacuo* to give the title compound as a clear, colourless oil (10.7 g, 82%), which was spectroscopically identical to that described in the literature.^{238,243} **¹H NMR (400 MHz, CDCl₃):** δ/ppm; 1.20 (9H, s, C(CH₃)₃), 1.31 (3H, t, *J*= 7.4 Hz, CH₂CH₃), 2.88 (q, 2H, *J*= 7.4 Hz, CH₂CH₃), 5.79 (2H, s, OCH₂O); **¹³C NMR (100 MHz, CDCl₃):** δ/ppm; 14.73 (CH₃CH₂), 25.33 (CH₃CH₂), 26.75 (C(CH₃)₃), 38.73 (C(CH₃)₃), 80.50 (OCH₂O), 170.55 (C=O), 176.84 (C=O). **FTIR (NaCl disc):** 2975 (CH), 1757 (C=O), 1724 (C=O) cm⁻¹.

Isobutanoyloxymethyl carbonochloridate, (113) ²³⁸



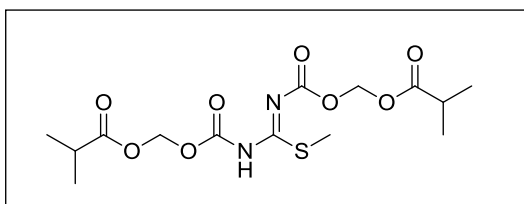
Sulfuryl chloride (337 μ l, 628 mg, 4.7 mmol) was added dropwise to *O*-(isobutanoyloxy)methyl-*S*-ethyl carbonothioate **111** (770 mg, 3.9 mmol) at 0 °C with stirring. The reaction mixture was then allowed to warm to room temperature with stirring for 1 h. Unreacted sulfuryl chloride and the by-product sulfenyl chloride were removed *in vacuo*. The crude liquid was purified using a Kugelrohr distillation apparatus. The title compound was isolated at approximately 75-80 °C and 15 mbar as a light yellow oil with a pungent odour (190 mg, 27%), which was spectroscopically identical to that described in the literature.²⁴³ **¹H NMR (400 MHz, CDCl₃):** δ /ppm; 1.22 (6H, d, J = 7.0 Hz, CH(CH₃)₂), 2.60 (1H, sept, J = 7.0 Hz, CH(CH₃)₂), 5.82 (2H, s, OCH₂O); **¹³C NMR (100 MHz, CDCl₃):** δ /ppm; 18.74 (CH(CH₃)₂), 33.84 (CH(CH₃)₂), 80.76 (OCH₂O), 174.50 (C=O), 175.62 (C=O). **FTIR (NaCl disc):** 2980 (CH), 1789 (C=O), 1762 (C=O) cm⁻¹.

Pivaloyloxymethyl carbonochloridate, (114) ²³⁸



Sulfuryl chloride (6.83 g, 4.1 ml, 50 mmol) was added to *O*-(pivaloyloxy)methyl-*S*-ethyl carbonothioate **112** (10.2 g, 0.46 mol) at 0 °C. The reaction was then allowed to warm to room temperature with stirring for 1 h. The by-products were removed *in vacuo*. The crude liquid was then purified by Kugelrohr distillation. The title compound was isolated at approximately 85-90 °C at 15 mbar as a clear yellow liquid with a pungent odour (5.34 g, 60%), which was spectroscopically identical to that described in the literature.^{238,243} **¹H NMR (400 MHz, CDCl₃):** δ /ppm; 1.23 (s, 9H, C(CH₃)₃), 5.81 (s, 2H, CH₂). **FTIR (NaCl disc):** 2978 (CH), 1791 (C=O), 1761 (C=O) cm⁻¹.

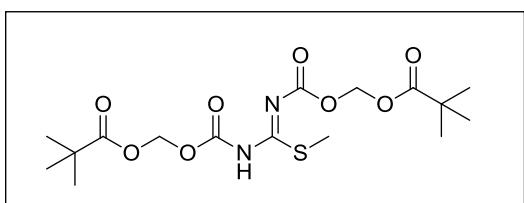
***N,N'*-bis-((isobutanoyloxy)methyloxycarbonyl)-*S*-methylthiourea, (116)**¹⁴⁷



To a vigorously stirred solution of 2-methyl-2-thiopseudourea hemisulfate (70 mg, 0.5 mmol) in saturated NaHCO₃ (10 ml) was added isobutanoyloxymethyl carbonochloridate **111** (180 mg, 1 mmol)

in DCM (10 ml). After stirring at rt for 24 h the organic phase was evaporated to dryness *in vacuo*. The crude reaction mixture was then purified by silica chromatography (SiO₂, 30% ethyl acetate/petroleum ether, R_f; 0.30) to afford the title compound as a colourless clear oil (80 mg, 23%). **¹H NMR (400 MHz, CDCl₃):** δ/ppm; 1.19 (12H, d, *J*= 7.1 Hz, CH(CH₃)₂), 2.44 (3H, s, SCH₃), 2.61 (2H, m, CH(CH₃)₂), 5.82 (4H, s, OCH₂O), 11.73 (1H, br s, NH); **¹³C NMR (100 MHz, CDCl₃):** δ/ppm; 14.89 (SCH₃), 18.76 (CH(CH₃)₂), 33.88 (CH(CH₃)₂), 80.72 (OCH₂O), 81.30 (OCH₂O), 150.33 (CSCH₃), 159.69 (C=O), 159.78 (C=O), 174.47 (C=O), 175.59 (C=O). **HRMS TOF (ES⁺):** *m/z* calcd. for C₁₄H₂₃N₂O₈S⁺ [M+H]⁺ 379.1170 found 379.119. **FTIR (KBr):** 3425 (CH), 3188 (CH), 2977 (CH), 2935 (CH), 1759 (C=O), 1661 (C=O), 1573 (C=O) cm⁻¹.

***N,N'*-bis-((pivaloyloxy)methyloxycarbonyl)-*S*-methylthiourea, (117)**¹⁴⁷

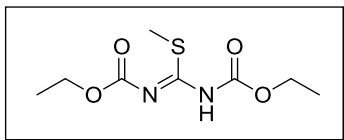


To a vigorously stirred solution of 2-methyl-2-thiopseudourea hemisulfate (1.81 g, 13 mmol) in saturated NaHCO₃ (30 ml) was added pivaloxymethyl

carbonochloridate **114** (5 g, 26 mmol) in DCM (20 ml). After stirring at rt for 24 h the organic phase was evaporated to dryness *in vacuo*. The crude reaction mixture was purified by silica chromatography (SiO₂, 20% ethyl acetate/ petroleum ether, R_f; 0.35) to afford the title compound as an oil that solidified on standing to give a white solid (2.9 g, 55%). **¹H NMR (400 MHz, CDCl₃):** δ/ppm; 1.13 (s, 18H, C(CH₃)₃), 2.45 (s, 3H, SCH₃), 5.82 (s, 4H, OCH₂O), 11.73 (br s, 1H, NH). **¹³C NMR (100 MHz, CDCl₃):** δ/ppm; 14.94 (SCH₃), 27.02 (C(CH₃)₃), 38.98 (C(CH₃)₃), 81.17 (OCH₂O), 174.41 (C=O), 177.08 (C=O). **HRMS TOF (ES⁺):** *m/z* calcd. for C₁₆H₂₇N₂O₈S⁺

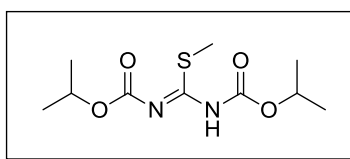
[M+H]⁺ 407.1483 found 407.1324. **FTIR (KBr):** 3178 (CH), 2977 (CH), 2935 (CH), 2875 (CH), 1770 (C=O), 1752 (C=O), 1733 (C=O), 1678 (C=O) cm⁻¹.

***N,N'*-bis-(ethyloxycarbonyl)-*S*-methylthiourea, (118)**²³⁹



To a solution of 2-methyl-2-pseudothiourea hemisulfate (5.89 g, 43 mmol) in dry dichloromethane (40 ml) and DIPEA (16.67 g, 22.46 ml, 130 mmol) was added ethyl chloroformate (14 g, 12.29 ml, 130 mmol) dropwise with stirring at 0 °C. The reaction mixture was then allowed to warm to rt and stirred for 16 h. The reaction solvent was evaporation to dryness *in vacuo* to afford a yellow oil. This crude oil was dissolved in DCM (50 ml) and washed with saturated NaHCO₃ (3 x 50 ml), water (3 x 50 ml), brine (3 x 50 ml) and the dried over MgSO₄. The title compound was purified by silica chromatography (SiO₂, 20% ethyl acetate/petroleum ether, R_f; 0.39) to afford a colourless clear oil (7.62 g, 76%). **¹H NMR (400 MHz, CDCl₃):** δ/ppm; 1.31 (6H, t, *J*= 7.3 Hz, CH₂CH₃), 2.88 (3H, s, SCH₃), 5.78 (4H, q, *J*= 7.3 Hz, CH₂CH₃); **¹³C NMR (100 MHz, CDCl₃):** δ/ppm; 14.80 (SCH₃), 18.62 (CH₂CH₃), 80.33 (CH₂CH₃), 170.66 (C=O), 175.52 (CSCH₃). **HRMS TOF (ES⁺):** *m/z* calcd. for C₈H₁₅N₂O₄S⁺ [M+H]⁺ 235.0748 found 235.0838. **FTIR (NaCl disc):** 3132 (CH), 2987 (CH), 2931 (CH), 1752 (C=O), 1649 (C=O) cm⁻¹.

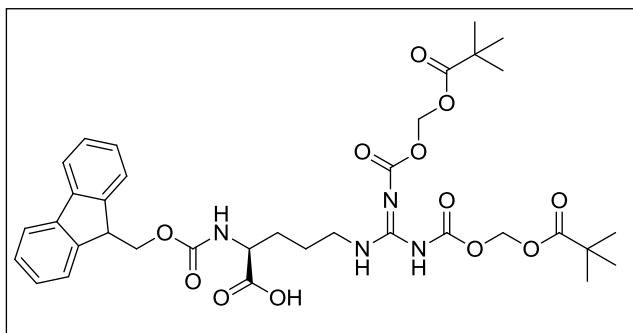
***N,N'*-bis-(isopropyloxycarbonyl)-*S*-methylthiourea, (119)**



To a solution of 2-methyl-2-pseudothiourea hemisulfate (2.65 g, 19 mmol) in dry dichloromethane (50 ml) and DIPEA (7.37 g, 9.9 ml, 130 mmol) was added a solution of 1 M isopropyl chloroformate in toluene (57 ml, 57 mmol) at 0 °C with stirring over 30 min. The reaction mixture was then allowed to warm to rt and stirred for 16 h. The reaction solvent was evaporation to dryness *in vacuo* to afford yellow oil. This crude oil was dissolved in DCM (50 ml) and washed with saturated NaHCO₃ (3x 50 ml), water (3x 50 ml), brine (3x 50 ml) and the dried over MgSO₄. The title compound was purified by silica chromatography (SiO₂, 0.5% MeOH/ DCM, R_f; 0.74) to afford a white solid (2.2 g, 44%). **¹H NMR (400 MHz, CDCl₃):** δ/ppm; 1.28 (6H, d, *J*= 6.4 Hz, CH(CH₃)₂), 1.32 (6H, d, *J*= 6.4 Hz, CH(CH₃)₂), 2.41 (3H, s, SCH₃), 4.97 (2H, m, CH(CH₃)₂), 11.79 (1H, br s, NH); **¹³C**

NMR (100 MHz, CDCl₃): δ /ppm; 14.72 (SCH₃), 22.15 (CH(CH₃)₂), 31.01 (CH(CH₃)₂), 70.05 (CH(CH₃)₂), 71.10 (CH(CH₃)₂), 151.50 (C=O), 161.11 (C=O), 172.53 (CSCH₃). **HRMS TOF (ES⁺):** m/z calcd. for C₁₀H₁₉N₂O₄S⁺ [M+H]⁺ 263.1061 found 263.1097. **FTIR (KBr):** 3145 (CH), 2981 (CH), 2933 (CH), 1746 (C=O), 1644 (C=O) cm⁻¹. **M.pt:** 45-47 °C.

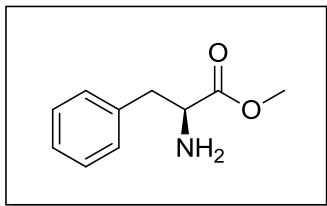
***N*-Fmoc-*N',N''*-bis((pivaloyloxy)methyloxycarbonyl)arginine, (124)**



To a solution of isothiurea **117** (104 mg, 0.26 mmol) in DCM (1 ml) was added sulfonyl chloride (52 mg, 50 μ l) dropwise at 0 °C with stirring. The reaction mixture was warmed to rt and stirred for 1 h. The reaction

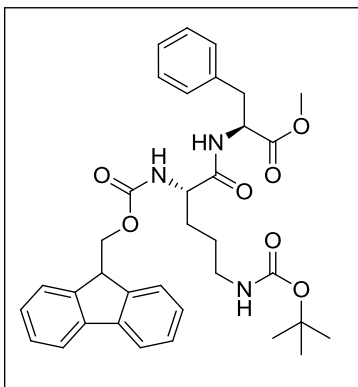
solvent was then evaporated to dryness *in vacuo*. The crude residue (102 mg) was then dissolved into DCM (0.5 ml) and added dropwise to a solution of Fmoc-Orn-OH (78 mg, 0.22 mmol), DIPEA (74 mg, 100 μ l, 0.57 mmol) in DCM (1 ml) at 0-4 °C with stirring. The reaction mixture was then warmed to rt and stirred for 16 h. The reaction solvent was evaporated to dryness *in vacuo* followed by purification of the crude residue by silica chromatography (SiO₂, 5% MeOH/DCM, R_f: 0.33) to afford the title compound as an off white solid (120.7 mg, 77%). **¹H NMR (400 MHz, CDCl₃):** δ /ppm; 1.18 (9H, s, C(CH₃)₃), 1.67 (9H, s, C(CH₃)₃), 1.42-1.86 (4H, m, CH₂CH₂), 3.25-3.50 (2H, m, CH₂NH), 4.16 (1H, t, J = 6.9, CH Fmoc), 4.36 (2H, d, J = 6.9 Hz, CH₂ Fmoc), 4.64 (1H, br s, CH^u), 5.46 (4H, s, OCH₂O), 7.24-7.76 (8H, m, Fmoc), 7.87 (1H, br s, NH), 8.45 (1H, br s, NH). **¹³C NMR (100 MHz, CDCl₃):** δ /ppm; 25.90 (CH₂), 26.82 (C(CH₃)₃), 27.08 (C(CH₃)₃), 29.68 (CH₂), 38.80 (CH₂), 47.10 (CH₂CH Fmoc), 53.79 (^uCH), 67.18 (CH₂CH Fmoc), 80.48 (OCH₂O), 119.98 (CH Fmoc), 120.33 (CH Fmoc), 125.09 (CH Fmoc), 127.09 (CH Fmoc), 127.74 (CH Fmoc), 141.30 (quaternary C), 143.62 (quaternary C), 149.58 (quaternary C), 152.86 (quaternary C), 156.56 (quaternary C), 177.06 (C=O), 177.51 (C=O). **HRMS TOF (ES⁺):** m/z calcd. for C₃₅H₄₅N₄O₁₂⁺ [M+H]⁺ 713.3029 found 713.2852. **FTIR (KBr):** 3359 (CH), 2974 (CH), 1752 (C=O), 1710 (C=O). **M.pt:** 79-82°C.

Phenylalanine methyl ester hydrochloride salt, (**127**)²⁴⁰



Thionyl chloride (3.87 g, 2.34 ml, 32.5 mmol) was added drop wise to a solution of phenylalanine (4.13 g, 25.0 mmol) in methanol (30 ml) at 0-4 °C. Once the addition was complete, the reaction was refluxed for 1 h with stirring. All solvent was then removed and the product recrystallized from methanol/diethyl ether (2:1) to afford the title compound as white crystals (4.78 g, 89%). **¹H NMR (400 MHz, CDOD₃):** δ/ppm ; 3.16-3.03 (2H, m, CH₂ benzyl), 3.78 (3H, s, OCH₃), 4.33 (1H, m, CH^α), 7.25-7.40 (5H, m, phenyl), **¹³C NMR (100 MHz, CDOD₃):** δ/ppm; 37.31 (CH₂ benzyl), 53.53 (OCH₃), 55.16 (CH^α), 128.89 (CH Phenyl), 130.10 (CH Phenyl), 130.40 (CH Phenyl), 135.26 (*ipso*C Phenyl), 170.35 (C=O). **HRMS TOF (ES⁺):** *m/z* calcd. for C₁₀H₁₄NO₂⁺ [M+H]⁺ 180.1019 found 180.0858. **FTIR (KBr):** 3405.95 (CH), 2855.77 (CH), 1746.91 (C=O). **M.pt:** 156-158 °C (lit.²⁴⁴ 158-162 °C).

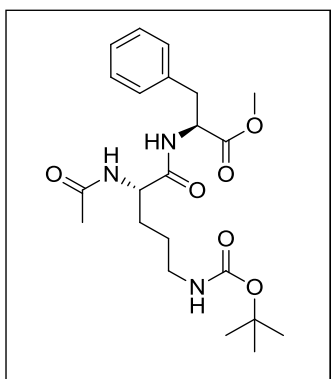
N-Fmoc(*N'*-(*tert*-butoxycarbonyl)ornithyl)phenylalanine methyl ester, (**129**)



Phenylalanine methyl ester **127** (460 mg, 2.13 mmol) in DMF was added dropwise to a solution of Fmoc-Orn(Boc)-OH (1.46 g, 3.2 mmol), HATU (1.21 g, 3.2 mmol) and DIPEA (1.13 ml, 6.39 mmol) in DMF. The reaction was stirred vigorously at rt for 16 h. DMF was removed *in vacuo* followed by precipitation of the desired dipeptide using ethyl acetate (30 ml). The precipitate was isolated by filtration and washed with ethyl acetate followed by drying *in vacuo* to afford the title compound as a white solid (1.02 g, 78%). **¹H NMR (400 MHz, CDCl₃):** δ/ppm; 1.44 (9H, s, C(CH₃)₃), 1.47-1.93 (4H, m, CH₂CH₂), 2.97-3.35 (4H, m, CH₂NH, CH₂ benzyl), 3.69 (3H, s, CH₃O), 4.19 (1H, m, CH₂CH Fmoc), 4.25-4.44 (3H, m, CH₂CH Fmoc, CH^α Orn), 4.39 (1H, m, CH^α Orn), 4.72 (1H, br s, NH), 4.80 (1H, m, CH^α Phe), 5.60 (1H, br s, NH), 6.81 (1H, br s, NH), 7.08-7.80 (13H, m, phenyl, Fmoc). **¹³C NMR (100 MHz, CDCl₃):** δ/ppm; 26.29 (CH₂), 28.41 (C(CH₃)₃), 30.00 (CH₂), 37.70 (CH₂), 47.09 (CH₂), 52.29, 53.35 (CH), 53.70 (CH), 67.02 (CH₂CO), 79.30 (C(CH₃)₃), 119.94 (CH), 125.09 (CH), 125.97

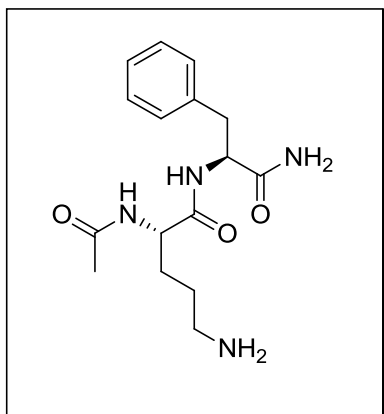
(CH), 127.07 (CH), 127.69 (CH), 128.66 (CH), 129.19 (CH), 135.78 (*ipso*C phenyl), 141.27 (quaternary C), 143.81 (quaternary C), 156.13 (C=O), 156.46 (C=O), 171.54 (C=O), 171.69 (C=O). **HRMS (TOF ES⁺):** *m/z* calcd. for C₃₅H₄₂N₃O₇⁺ [M+H]⁺ 616.3018 found 616.2902. **FTIR (KBr):** 3342 (CH), 3062 (CH), 2970 (CH), 1740 (C=O), 1684 (C=O), 1650 (C=O) cm⁻¹. **M.pt:** 180-182 °C.

***N*-Acetyl(*N'*-(*tert*-butoxycarbonyl)ornithyl)phenylalanine methyl ester, (130)**



To a solution of **129** (914 mg, 1.5 mmol) in 10 ml DCM was added diethylamine (2 ml, 19 mmol) followed by stirring at rt for 3 h. The reaction solvent and DEA were then evaporated to dryness *in vacuo*. The crude residue was then dissolved into DCM (50 ml) and filtered. To the filtrate was added DIPEA (10 ml, 58 mmol) and acetic anhydride (2.8 ml, 30 mmol), followed by stirring at rt for 3h. Again the reaction solvent was evaporated to dryness *in vacuo*. The crude residue was dissolved into DCM and washed with Sat. NaHCO₃ (3 x 25 ml), 0.01 M HCl (3 x 25 ml), brine (3 x 25 ml) and dried over MgSO₄. The desired compound was purified by silica chromatography (SiO₂, 3% MeOH/DCM, R_f: 0.3) to afford the title compound as an off white solid (348 mg, 54%). **¹H NMR (400 MHz, CDCl₃):** δ/ppm; 1.36 (9H, s, C(CH₃)₃), 1.39-1.56 (2H, m, CH₂CH₂), 1.71-1.81 (2H, m, CH₂CH₂), 1.96 (3H, s, COCH₃), 2.92-3.25 (4H, m, CH₂NH, CH₂ benzyl), 3.71 (3H, s, CH₃O), 4.45 (1H, m, CH^α Orn), 4.72 (1H, m, NH), 4.73 (1H, m, CH^α Phe), 6.38 (1H, br m, NH), 6.87 (1H, br s, NH), 7.04-7.25 (5H, m, Phenyl). **¹³C NMR (100 MHz, CDCl₃):** δ/ppm; 23.13 (COOCH₃), 26.39 (CH₂), 28.40 (C(CH₃)₃), 29.62 (CH₂), 37.68 (CH₂ phenyl), 39.47 (CH₂), 52.08 (COOCH₃), 52.37 (^αCH), 53.46 (^αCH), 79.47 (C(CH₃)₃), 127.77 (CH phenyl), 128.58 (CH phenyl), 129.20 (CH phenyl), 136.83 (*ipso*C phenyl), 156.62 (C=O), 170.17 (C=O), 171.633 (C=O), 171.74 (C=O). **HRMS TOF (ES⁺):** *m/z* calcd. for C₂₂H₃₃N₃NaO₆⁺ [M+Na]⁺ 458.2267 found 458.2262. **FTIR (KBr):** 3344 (CH), 2983 (CH), 1740 (C=O), 1684 (C=O), 1650 (C=O) cm⁻¹. **M.pt:** 162-164 °C.

***N*-acetyl ornithyl phenylalanine amide trifluoroacetate salt, (122)**



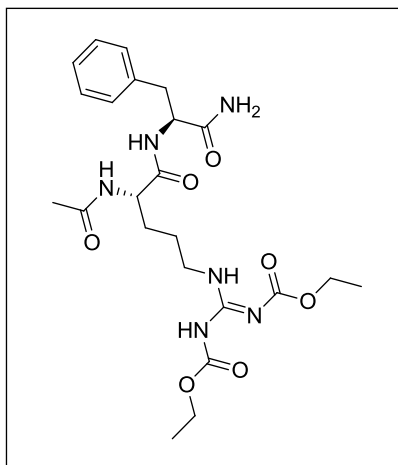
N-Acetyl-Orn(Boc)-Phe methyl ester **130** (340 mg, 0.78 mmol) was dissolved into a 7 N ammonia in methanol (10 ml) and stirred for 16 h at rt. The ammonia was then removed by blowing nitrogen onto the reaction mixture. The reaction solvent was then evaporated to dryness *in vacuo*. The crude residue was then Boc deprotected using 50% TFA in DCM (10 ml) with stirring at rt for 3 h. The TFA and solvent were then evaporated to dryness *in vacuo*.

The resulting residue was triturated with diethyl ether (3 x 10 ml) and the resulting residue lyophilised to afford the title compound as an off white residue (327 mg, 97%). **¹H NMR (400 MHz, CD₃OD):** δ/ppm; 1.59-1.79 (4H, m, CH₂CH₂), 1.96 (3H, s, COCH₃), 2.84-2.97 (3H, m, CH₂NH, CHH benzyl), 3.16 (1H, dd, *J*= 5.6, 13.9 Hz, CHH benzyl), 4.30 (1H, m, CH^α Orn), 4.62 (1H, dd, *J*= 5.6, 8.7 Hz, CH^α Phe), 7.16-7.32 (5H, m, phenyl); **¹³C NMR (100 MHz, CD₃OD):** δ/ppm; 21.07 (CH₃CO), 23.39 (CH₂), 28.20 (CH₂), 37.40 (CH₂), 38.72 (CH₂), 52.62 (CH), 54.15 (CH), 126.39 (CH phenyl), 128.05 (CH phenyl), 128.96 (CH phenyl), 138.352 (*ipso*C phenyl), 173.424 (C=O), 173.607 (C=O), 175.992 (C=O). **HRMS TOF (ES⁺):** *m/z* calcd. for C₁₆H₂₅N₄O₃⁺ [M+H]⁺ 321.1922 found 321.1732. **FTIR (KBr):** 3275 (CH), 1681 (C=O), 1640 (C=O), 1543 (C=O) cm⁻¹.

General Procedure for synthesis of N^G-protected *N*-acetyl ornithyl phenylalanine amide (135-139)

The isothiourrea (0.07 mmol) was pre-activated with HgCl₂ (16 mg, 0.06 mmol) in DMF (2 ml). A solution of DIPEA (40 μl, 0.24 mmol) and *N*-acetyl ornithyl phenylalanine amide **122** (25 mg, 0.06 mmol) in 1 ml of H₂O was added dropwise to this solution followed by stirring for 2h at rt. The reaction solvents were then evaporated to dryness *in vacuo* to afford a white residue. This residue was dissolved into MeCN:H₂O (1:1, 2 ml) and centrifuged at 13000 g for 20 min to give a white pellet and clear supernatant. The title compound was isolated from the supernatant using preparative HPLC unless otherwise stated.

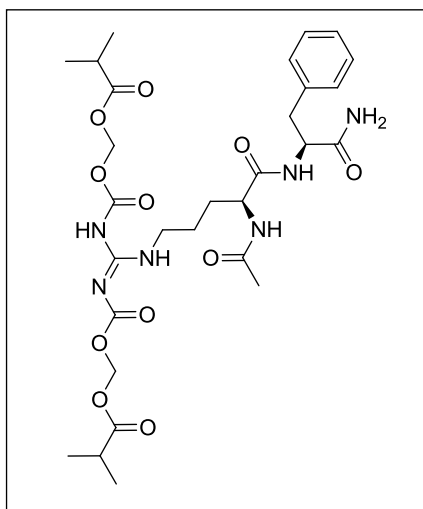
***N*-Acetyl(*N*',*N*''-bis-(ethyloxycarbonyl)arginyl)phenylalanine amide, (135)**



The title compound was prepared according to the above procedure using *N*-acetyl-ornithyl phenylalanine amide **122** (25 mg, 0.06 mmol) and *N,N'*-bis-(ethyloxycarbonyl)-*S*-methylthiourea **118** (14 mg, 0.06 mmol) in 3 ml DMF/H₂O (3:1, v/v). The crude residue was purified by preparative HPLC (40-75%B over 10 min, 7 ml/min, Chromolith Semi-prep C₁₈ column, 100 mm x 10 mm, *t_R* 5.47 min) to afford a white residue (13 mg, 45%). **¹H NMR (400**

MHz, CD₃OD): δ/ppm; 1.27 (3H, t, *J*= 7.3 Hz, CH₃CH₂), 1.33 (3H, t, *J*= 7.3 Hz, CH₃CH₂), 1.41-1.70 (4H, m, CH₂CH₂), 1.97 (3H, s, CH₃CO), 2.94 (1H, dd, *J*= 9.3, 13.9 Hz, CHH benzyl), 3.20 (1H, dd, *J*= 5.1, 13.9 Hz, CHH benzyl), 3.33 (2H, m, CH₂NH), 4.12 (2H, q, *J*= 7.1 Hz, CH₃CH₂), 4.19 (1H, dd, *J*= 5.3, 7.5 Hz, CH^α Orn), 4.27 (2H, q, *J*= 7.1 Hz, CH₃CH₂), 4.61 (1H, m, CH^α Phe), 7.15-7.29 (5H, m). **HRMS TOF (ES⁺):** *m/z* calcd. for C₂₃H₃₅N₆O₇⁺ [M+H]⁺ 507.2562 found 507.2606. **HPLC:** system 1; *t_R* 4.85 min.

***N*-acetyl-(*N*',*N*''-bis-((isobutanoyloxy)methyloxycarbonyl)-arginyl)-phenylalanine amide, (136)**

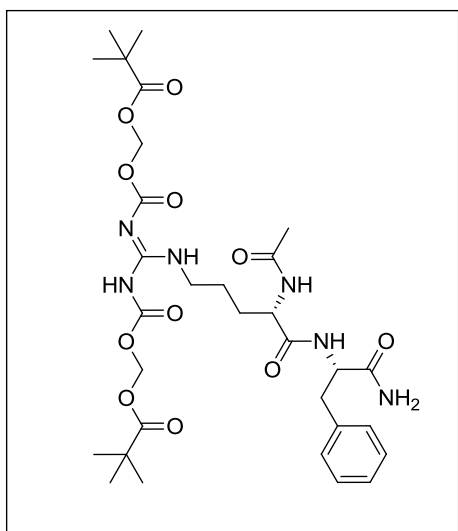


The title compound was prepared according to the above procedure using *N*-acetyl-ornithyl phenylalanine amide **122** (25 mg, 0.06 mmol) and *N,N'*-bis-((isobutanoyloxy)methyloxycarbonyl)-*S*-methylthiourea **116** (22 mg, 0.06 mmol) in 3 ml DMF/ H₂O (3:1, v/v). The crude residue was purified by preparative HPLC (40-56% B over 5 min, 7 ml/min, Chromolith Semi-prep C₁₈ column, 100 mm x 10 mm, *t_R* 7.22 min) to afford the title compound as a white residue (9 mg, 22%). **¹H**

NMR (400 MHz, CD₃OD): δ/ppm; 1.20 (12H, d, CH(CH₂)₃), 1.48 (2H, m, CH₂CH₂),

1.53-1.70 (2H, m, CH₂CH₂), 1.96 (3H, s, CH₃CO), 2.54-2.67 (2H, m, 2x CH(CH₂)₃), 2.93 (1H, dd, *J* = 9.2, 13.9 Hz, CHH benzyl), 3.23 (1H, dd, *J* = 5.6, 13.9 Hz, CHH benzyl), 3.37 (2H, t, *J* = 7.0 Hz, CH₂NH), 4.20 (1H, dd, *J* = 5.9, 8.0 Hz, CH^α Orn), 4.62 (1H, m, CH^α Phe), 5.76 (2H, s, OCH₂O), 5.85 (2H, s, OCH₂O), 7.16-7.30 (5H, m, phenyl). **HRMS TOF (ES⁺):** *m/z* calcd. for C₂₉H₄₃N₆O₁₁⁺ [M+H]⁺ 651.2752 found 651.2841. **HPLC:** system 1; *t*_R 6.34 min.

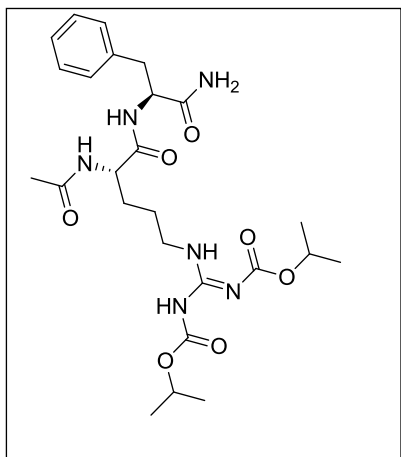
***N*-Acetyl-(*N'*,*N''*-bis-((pivaloyloxy)methyloxycarbonyl)-arginyl)-phenylalanine amide, (137)**



The title compound was prepared according to the above procedure using *N*-acetyl-ornithyl phenylalanine amide **122** (25 mg, 0.06 mmol) and *N,N'*-bis-((pivaloyloxy)methyloxycarbonyl)-*S*-methylthiourea **117** (24 mg, 0.06 mmol) in 3 ml DMF/ H₂O (3:1, v/v). The crude residue was purified by preparative HPLC (40-64%B over 8 min, 7 ml/min, Chromolith Semi-prep C₁₈ column, 100 mm x 10 mm, *t*_R 5.52 min) to afford the title compound as a white residue (10 mg, 23%). ¹H

NMR (400 MHz, CD₃OD): δ/ppm; 1.20 (9H, s, C(CH₃)₃), 1.22 (9H, s, C(CH₃)₃), 1.49 (2H, m, CH₂CH₂), 1.59 (2H, m, CH₂CH₂), 2.73 (3H, s, CH₃CO), 2.94 (1H, dd, *J* = 9.3, 13.8 Hz, CHH benzyl), 3.20 (1H, dd, *J* = 5.5, 13.8 Hz, CHH benzyl), 3.36 (2H, t, *J* = 7.29 Hz, NHCH₂), 4.20 (1H, dd, *J* = 5.3, 8.6 Hz, CH^α Orn), 4.64 (1H, m, CH^α Phe), 5.77 (2H, s, OCH₂O), 5.86 (2H, s, OCH₂O), 7.16-7.29 (5H, m, phenyl). **HRMS TOF (ES⁺):** *m/z* calcd. for C₃₁H₄₇N₆O₁₁⁺ [M+H]⁺ 679.3298 found 679.3285. **HPLC:** system 1; *t*_R 6.97 min

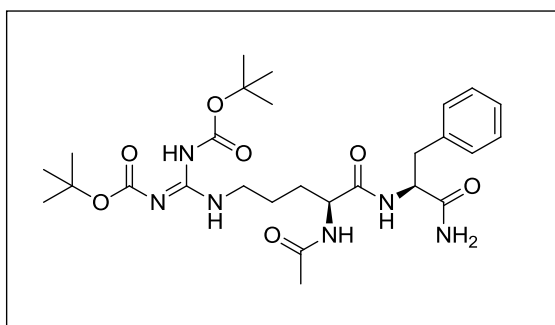
***N*-acetyl-(*N'*,*N''*-bis-(isopropoxyloxycarbonyl)-arginyl)phenylalanine amide, (138)**



The title compound was prepared according to the above procedure using *N*-acetyl-ornithyl phenylalanine amide **122** (25 mg, 0.06 mmol) and *N,N'*-bis-(isopropoxyloxycarbonyl)-*S*-methylthiourea **119** (19 mg, 0.06 mmol) in 3 ml DMF/H₂O (3:1, v/v). The crude residue was purified by preparative HPLC (40-90%B over 10 min, 7 ml/min, Chromolith Semi-prep C₁₈ column, 100 mm x 10 mm, *t*_R 6.24 min) to afford the title compound as a

white residue (11 mg, 29%). **¹H NMR (400 MHz, CD₃OD):** δ/ppm; 1.29 (6H, d, *J*= 6.7 Hz, CH(CH₃)₂), 1.33 (6H, d, *J*= 6.7 Hz, CH(CH₃)₂), 1.44-1.54 (2H, m, CH₂CH₂), 1.55-1.70 (2H, m, CH₂CH₂), 1.97 (3H, s, SCH₃), 2.94 (1H, dd, *J*= 9.3, 13.9 Hz, CHH benzyl), 3.20 (1H, dd, *J*= 5.4, 13.9 Hz, CHH benzyl), 3.36 (2H, t, *J*= 7.2 Hz, NHCH₂), 4.21 (1H, dd, *J*= 5.9, 7.9 Hz CH^α Orn), 4.62 (1H, m, CH^α Phe), 4.93-5.05 (2H, m, CH(CH₃)₂, CH(CH₃)₂), 7.16-7.30 (5H, m, phenyl). **HRMS TOF (ES⁺):** *m/z* calcd. for C₂₅H₃₉N₆O₇⁺ [M+H]⁺ 535.2875 found 535.2783. **HPLC;** system 1: 5.41 min

***N*-Acetyl-(*N'*,*N''*-bis(*tert*-butoxycarbonyl)arginyl)phenylalanine amide, (139)**

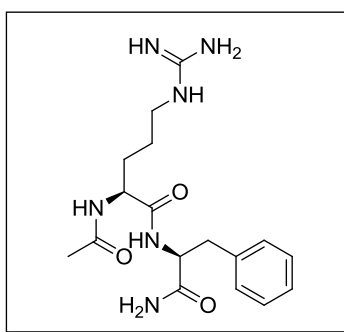


The title compound was prepared according to the above procedure using *N*-acetyl-ornithyl phenylalanine amide **122** (100 mg, 0.23 mmol) and *N,N'*-bis(*tert*-butoxycarbonyl)-*S*-methylthiourea **96** (70 mg, 0.24 mmol) in MeCN/H₂O (1:1, v/v). The crude

residue was purified by silica chromatography (SiO₂, 3% MeOH/DCM, R_f: 0.1 used to elute non-polar impurities, followed by elution of compound using 10% MeOH/DCM) to afford the title compound as a white residue (104 mg, 70%). **¹H NMR (400 MHz, CD₃OD):** δ/ppm; 1.42 (2H, m, CH₂CH₂), 1.48 (2H, m, CH₂CH₂), 1.54 (9H, s,

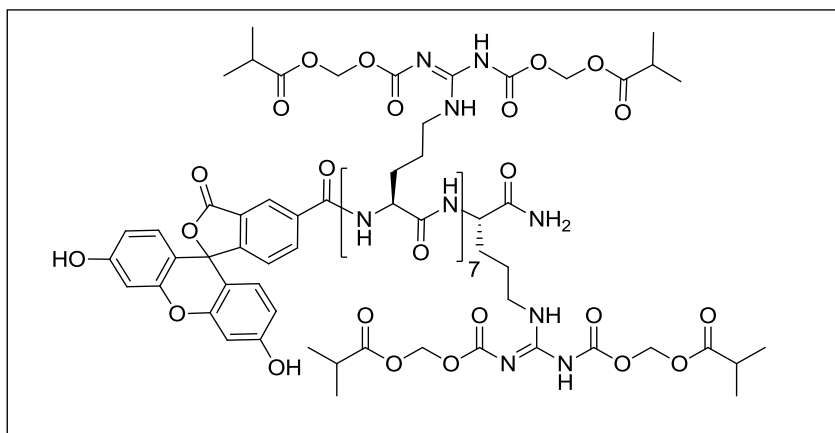
C(CH₃)₃), 1.69 (9H, s, C(CH₃)₃), 1.97 (3H, s, COCH₃), 2.94 (1H, dd, *J* = 9.1, 13.8 Hz, CHH benzyl), 3.16-3.31 (3H, m, CHH benzyl, NHCH₂CH₂), 4.18 (1H, dd, *J* = 5.8, 7.8 Hz, CH^α Orn), 4.60 (1H, dd, *J* = 5.2, 8.9 Hz, CH^α Phe), 7.16-7.29 (5H, m, phenyl); ¹³C NMR (100 MHz, CD₃OD): δ/ppm; 22.51 (CH₃CO), 26.43 (CH₂), 28.27 (C(CH₃)₃), 28.40 (CH₂ benzyl), 28.58 (C(CH₃)₃), 29.59 (CH₂), 41.28 (CH₂), 55.27 (^αCH) 55.50 (^αCH), 80.43 (C(CH₃)₃), 84.52 (C(CH₃)₃), 127.74 (CH phenyl), 129.45 (CH phenyl), 130.34 (CH phenyl), 138.60 (CH phenyl), 154.17 (C=O), 157.64 (C=O), 164.57 (NHCNH₂N), 173.99 (C=O), 175.93 (C=O). HRMS TOF (ES⁺): *m/z* calcd. for C₂₇H₄₃N₆O₇⁺ [M+H]⁺ 563.3188 found 563.2790. FTIR (KBr): 3321 (CH), 1672 (C=O), 1544.

***N*-acetyl arginyl phenylalanine amide trifluoroacetate salt, (140)**



N-Acetyl-(*N'*,*N''*-bis(*tert*-butoxycarbonyl)arginyl) phenylalanine amide **139** (20 mg, 0.036 mmol) was Boc deprotected by acidolysis using 50% TFA in DCM. The reaction was stirred for 6 h at rt. TFA and solvent were removed *in vacuo*, the resulting residue was then triturated with cold diethyl ether (3 x 10 ml) followed by lyophilisation of the remaining residue to afford the title compound as a white solid (10 mg, 67%). ¹H NMR (400 MHz, CD₃OD): δ/ppm; 1.50 (2H, m, CH₂CH₂), 1.54-1.76 (2H, m, CH₂CH₂), 1.97 (3H, s, COCH₃), 2.93 (1H, dd, *J* = 9.0, 14.2 Hz, CHH benzyl), 3.13 (2H, t, *J* = 7.4 Hz, NHCH₂), 3.18 (1H, dd, *J* = 5.3, 14.2 Hz, CHH benzyl), 4.26 (1H, m, CH^α Orn), 4.60-4.67 (1H, m, CH^α Phe), 7.17-7.38 (5H, m, phenyl). ¹³C NMR (100 MHz, CD₃OD): δ/ppm; 22.49 (CH₃CO), 25.99 (CH₂), 29.84 (CH₂), 38.87 (CH₂ benzyl), 41.88 (NHCH₂), 54.52 (^αCH), 55.43 (^αCH), 127.81 (CH Phenyl), 129.45 (CH Phenyl), 130.33 (CH Phenyl), 138.43 (*ipso*C Phenyl), 145.47 (NHCNH₂N), 173.63 (C=O), 176.02 (C=O). HRMS TOF (ES⁺): *m/z* calcd. for C₁₇H₂₇N₆O₃⁺ [M+H]⁺ 363.2140 found 363.2146. FTIR (KBr): 2977 (CH), 1770 (C=O), 1752 (C=O), 1733 (C=O), 1539, 1431 cm⁻¹. HPLC: system 1: *t*_R 3.10 min.

***N*-FAM-((*N*',*N*''-bis-((isobutanoyloxy)methyloxycarbonyl)-arginyl)₈ amide, (143)**



N,N'-bis-((isobutanoyloxy)methyloxycarbonyl)-*S*-methylthiourea **116** (10 mg, 26.21 μ mol) was pre-activated with HgCl_2 (7 mg, 26 μ mol) in DMF (3 ml). To this solution was added a mixture of FAM-(Orn)₈-[NH₂] **87** (6 mg, 2.73 μ mol) and DIPEA (24 μ l, 32.3 μ mol) dropwise, followed by stirring of the reaction mixture at rt for 2 h. The reaction solvent was then evaporated to dryness *in vacuo* to afford an orange residue. This residue was then dissolved into MeCN (2 ml) and centrifuged at 13000 g for 20 min to give a white pellet and orange supernatant. The title compound was isolated from the supernatant using preparative HPLC (Onyx Semi-prep Monolith C₁₈ column, 100 mm x 10 mm, 50-80% B over 6 min, 7 ml/min, t_R 4.07 min) and the collected HPLC fraction lyophilised to afford an orange residue (3.5 mg, 33%). **HPLC**: system 1: t_R 7.85 min (>85%), system 2: t_R 8.97 min (>85%), **HRMS TOF (ES⁺)**; m/z (%); 719.2104 (33), 749.2119 (100), 779.1939 (47), 914.6830 (43), 1012.8709 (27), 1251.4883 (33), 1371.5160 (63), 1393.5126 (40), 1404.5098 (20).

References

1. Hanahan, D.; Weinberg, R. A., The Hallmarks of Cancer. *Cell* **2000**, *100* (1), 57-70.
2. Vaux, D. L.; Cory, S.; Adams, J. M., Bcl-2 gene promotes haemopoietic cell survival and cooperates with c-myc to immortalize pre-B cells. *Nature* **1988**, *335* (6189), 440-442.
3. Dippold, W. G.; Jay, G.; Deleo, A. B.; Khoury, G.; Old, L. J., P53 Transformation-related protein – detection by monoclonal-antibody in mouse and human cells. *Proceedings of the National Academy of Sciences of the United States of America-Biological Sciences* **1981**, *78* (3), 1695-1699.
4. Loregian, A.; Marsden, H. S.; Palù, G., Protein–protein interactions as targets for antiviral chemotherapy. *Reviews in Medical Virology* **2002**, *12* (4), 239-262.
5. Wells, J. A.; McClendon, C. L., Reaching for high-hanging fruit in drug discovery at protein-protein interfaces. *Nature* **2007**, *450* (7172), 1001-1009
6. Walters, W. P.; Murcko, A. A.; Murcko, M. A., Recognizing molecules with drug-like properties. *Current Opinion in Chemical Biology* **1999**, *3* (4), 384-387.
7. Gonzalez-Ruiz, D.; Gohlke, H., Targeting protein-protein interactions with small molecules: Challenges and perspectives for computational binding epitope detection and ligand finding. *Current Medicinal Chemistry* **2006**, *13* (22), 2607-2625.
8. Meister, G.; Tuschl, T., Mechanisms of gene silencing by double-stranded RNA. *Nature* **2004**, *431*, 343-349.
9. Cao, T.; Heng, B. C., Intracellular Antibodies (Intrabodies) versus RNA Interference for Therapeutic Applications. *Annals of Clinical and Laboratory Science* **2005**, *35* (3), 227-229.
10. Paddison, P. J.; Caudy, A. A.; Bernstein, E.; Hannon, G. J.; Conklin, D. S., Short hairpin RNAs (shRNAs) induce sequence-specific silencing in mammalian cells. *Genes & Development* **2002**, *16* (8), 948-958.

-
11. Silva, J.; Chang, K.; Hannon, G. J.; Rivas, F. V., RNA-interference-based functional genomics in mammalian cells: reverse genetics coming of age. *Oncogene* **2000**, *23* (51), 8401-8409.
 12. Tiemann, K.; Rossi, J. J., RNAi-based therapeutics—current status, challenges and prospects. *EMBO Molecular Medicine* **2009**, *1* (3), 142-151.
 13. Persengiev, S. P.; Zhu, X.; Green, M. R., Nonspecific, concentration-dependent stimulation and repression of mammalian gene expression by small interfering RNAs (siRNAs). *RNA* **2004**, *10* (1), 12-18.
 14. Oh, Y.-K.; Park, T. G., siRNA delivery systems for cancer treatment. *Advanced Drug Delivery Reviews* **2009**, *61* (10), 850-862.
 15. Zhao, L.; Chmielewski, J., Inhibiting protein-protein interactions using designed molecules. *Current Opinion in Structural Biology* **2005**, *15* (1), 31-34.
 16. Chames, P.; Van Regenmortel, M.; Weiss, E.; Baty, D., Therapeutic antibodies: successes, limitations and hopes for the future. *British Journal of Pharmacology* **2009**, *157* (2), 220-233.
 17. Nizak, C.; Monier, S.; del Nery, E.; Moutel, S.; Goud, B.; Perez, F., Recombinant Antibodies to the Small GTPase Rab6 as Conformation Sensors. *Science* **2003**, *300* (5621), 984-987.
 18. Meli, G.; Visintin, M.; Cannistraci, I.; Cattaneo, A., Direct in Vivo Intracellular Selection of Conformation-sensitive Antibody Domains Targeting Alzheimer's Amyloid-[beta] Oligomers. *Journal of Molecular Biology* **2009**, *387* (3), 584-606.
 19. Kehoe, J. W.; Velappan, N.; Walbolt, M.; Rasmussen, J.; King, D.; Lou, J.; Knopp, K.; Pavlik, P.; Marks, J. D.; Bertozzi, C. R.; Bradbury, A. R. M., Using Phage Display to Select Antibodies Recognizing Post-translational Modifications Independently of Sequence Context. *Molecular & Cellular Proteomics* **2006**, *5* (12), 2350-2363.
 20. Lodish, H.; Berk, A.; Kaiser, C.; Krieger, M.; Scott, M.; Bretscher, A.; Ploegh, H.; Matsudaira, P., *Molecular Cell Biology (Lodish, Molecular Cell Biology)*. W. H. Freeman: 2007.
 21. *Monoclonal antibodies : the second generation / [edited by] Hedy Zola*. BIOS Scientific Pub: Oxford :, 1995.
 22. Charles A Janeway, J., Paul Travers, Mark Walport, Mark J Shlomchik, The structure of a typical antibody molecule. In *Immunobiology: The Immune System in Health and Disease. 5th edition.*, Garland Science: New York, 2001.
 23. Porter, R. R., Hydrolysis of rabbit gamma-globulin and antibodies with crystalline papain. *Biochem. J.* **1959**, *73*, 119-126.
 24. Breedveld, F. C., Therapeutic monoclonal antibodies. *The Lancet* **2000**, *355* (9205), 735-740.

-
25. Kohler, G.; Milstein, C., Continuous cultures of fused cells secreting antibody of predefined specificity. *Nature* **1975**, *256* (5517), 495-497.
26. Schroff, R. W.; Foon, K. A.; Beatty, S. M.; Oldham, R. K.; Morgan, A. C., Human Anti-Murine Immunoglobulin Responses in Patients Receiving Monoclonal Antibody Therapy. *Cancer Research* **1985**, *45* (2), 879-885.
27. Neuberger, M. S.; Williams, G. T.; Mitchell, E. B.; Jouhal, S. S.; Flanagan, J. G.; Rabbitts, T. H., A hapten-specific chimaeric IgE antibody with human physiological effector function. *Nature* **1985**, *314* (6008), 268-270.
28. Jones, P. T.; Dear, P. H.; Foote, J.; Neuberger, M. S.; Winter, G., Replacing the complementarity-determining regions in a human antibody with those from a mouse. *Nature* **1986**, *321* (6069), 522-525.
29. McCafferty, J.; Fitzgerald, K.; Earnshaw, J.; Chiswell, D.; Link, J.; Smith, R.; Kenten, J., Selection and rapid purification of murine antibody fragments that bind a transition-state analog by phage display. *Applied Biochemistry and Biotechnology* **1994**, *47* (2), 157-173.
30. Carmen, S.; Jermutus, L., Concepts in antibody phage display. *Briefings in Functional Genomic and Proteomics* **2002**, *1* (2), 189-203.
31. Vaughan, T. J.; Williams, A. J.; Pritchard, K.; Osbourn, J. K.; Pope, A. R.; Earnshaw, J. C.; McCafferty, J.; Hodits, R. A.; Wilton, J.; Johnson, K. S., Human Antibodies with Sub-nanomolar Affinities Isolated from a Large Non-immunized Phage Display Library. *Nature Biotechnology* **1996**, *14* (3), 309-314.
32. Bradbury, A. R. M.; Sidhu, S.; Dubel, S.; McCafferty, J., Beyond natural antibodies: the power of in vitro display technologies. *Nature Biotechnology* **2011**, *29* (3), 245-254.
33. Glockshuber, R.; Malia, M.; Pfitzinger, I.; Plueckthun, A., A comparison of strategies to stabilize immunoglobulin Fv-fragments. *Biochemistry* **1990**, *29* (6), 1362-1367.
34. Holliger, P.; Brissinck, J.; Williams, R. L.; Thielemans, K.; Winter, G., Specific killing of lymphoma cells by cytotoxic T-cells mediated by a bispecific diabody. *Protein Engineering* **1996**, *9* (3), 299-305.
35. Kortt, A. A.; Lah, M.; Oddie, G. W.; Gruen, C. L.; Burns, J. E.; Pearce, L. A.; Atwell, J. L.; McCoy, A. J.; Howlett, G. J.; Metzger, D. W.; Webster, R. G.; Hudson, P. J., Single-chain Fv fragments of anti-neuraminidase antibody NC10 containing five- and ten-residue linkers form dimers and with zero-residue linker a trimer. *Protein Engineering* **1997**, *10* (4), 423-433.
36. Le Gall, F.; Kipriyanov, S. M.; Moldenhauer, G.; Little, M., Di-, tri- and tetrameric single chain Fv antibody fragments against human CD19: effect of valency on cell binding. *FEBS Letters* **1999**, *453* (1-2), 164-168.
37. Todorovska, A.; Roovers, R. C.; Dolezal, O.; Kortt, A. A.; Hoogenboom, H. R.; Hudson, P. J., Design and application of diabodies, triabodies and tetrabodies for cancer targeting. *Journal of Immunological Methods* **2001**, *248* (1-2), 47-66.

-
38. Holliger, P.; Hudson, P. J., Engineered antibody fragments and the rise of single domains. *Nature Biotechnology* **2005**, 23 (9), 1126-1136.
39. Adams, G. P.; Schier, R.; McCall, A. M.; Crawford, R. S.; Wolf, E. J.; Weiner, L. M.; Marks, J. D., Prolonged in vivo tumour retention of a human diabody targeting the extracellular domain of human HER2/neu. *British Journal of Cancer* **1998**, 77 (9), 1405-1412.
40. Wittel, U. A.; Jain, M.; Goel, A.; Chauhan, S. C.; Colcher, D.; Batra, S. K., The in vivo characteristics of genetically engineered divalent and tetravalent single-chain antibody constructs. *Nuclear Medicine and Biology* **2005**, 32 (2), 157-164.
41. Yang, W.-P.; Green, K.; Pinz-Sweeney, S.; Briones, A. T.; Burton, D. R.; Barbas Iii, C. F., CDR Walking Mutagenesis for the Affinity Maturation of a Potent Human Anti-HIV-1 Antibody into the Picomolar Range. *Journal of Molecular Biology* **1995**, 254 (3), 392-403.
42. Boder, E. T.; Midelfort, K. S.; Wittrup, K. D., Directed evolution of antibody fragments with monovalent femtomolar antigen-binding affinity. *Proceedings of the National Academy of Sciences* **2000**, 97 (20), 10701-10705.
43. Heng, B. C.; Cao, T., Making cell-permeable antibodies (Transbody) through fusion of protein transduction domains (PTD) with single chain variable fragment (scFv) antibodies: Potential advantages over antibodies expressed within the intracellular environment (Intrabody). *Medical Hypotheses* **2005**, 64 (6), 1105-1108.
44. Carlson, J. R., A new means of inducibly inactivating a cellular protein. *Molecular Cell Biology* **1988**, 8 (6), 2638-2646.
45. Marasco, W. A.; Haseltine, W. A.; Chen, S. Y., Design, intracellular expression, and activity of a human anti-human immunodeficiency virus type 1 gp120 single-chain antibody. *Proceedings of the National Academy of Sciences* **1993**, 90 (16), 7889-7893.
46. Glockshuber, R.; Schmidt, T.; Plueckthun, A., The disulfide bonds in antibody variable domains: effects on stability, folding in vitro, and functional expression in *Escherichia coli*. *Biochemistry* **1992**, 31 (5), 1270-1279.
47. Biocca, S.; Ruberti, F.; Tafani, M.; Pierandrel-Amaldi, P.; Cattaneo, A., Redox State of Single Chain Fv Fragments Targeted to the Endoplasmic Reticulum, Cytosol and Mitochondria. *Nature Biotechnology* **1995**, 13 (10), 1110-1115.
48. Wörn, A.; Plückthun, A., An intrinsically stable antibody scFv fragment can tolerate the loss of both disulfide bonds and fold correctly. *FEBS Letters* **1998**, 427 (3), 357-361.
49. Visintin, M.; Tse, E.; Axelson, H.; Rabbitts, T.; Cattaneo, A., Selection of antibodies for intracellular function using a two-hybrid in vivo system. *Proceedings of the National Academy of Sciences* **1999**, 96, 11723-11728.
50. Visintin, M.; Settanni, G.; Maritan, A.; Graziosi, S.; Marks, J. D.; Cattaneo, A., The intracellular antibody capture technology (IACT): towards a consensus sequence for intracellular antibodies. *Journal of Molecular Biology* **2002**, 317 (1), 73-83.

-
51. Tanaka, T.; Lobato, M. N.; Rabbitts, T. H., Single Domain Intracellular Antibodies: A Minimal Fragment For Direct In Vivo Selection of Antigen-specific Intrabodies. *Journal of Molecular Biology* **2003**, *331* (5), 1109-1120.
52. Tanaka, T.; Rabbitts, T. H., Protocol for the selection of single-domain antibody fragments by third generation intracellular antibody capture. *Nature Protocols* **2010**, *5* (1), 67-92.
53. Philibert, P.; Stoessel, A.; Wang, W.; Sibler, A.-P.; Bec, N.; Larroque, C.; Saven, J.; Courtete, J.; Weiss, E.; Martineau, P., A focused antibody library for selecting scFvs expressed at high levels in the cytoplasm. *BMC Biotechnology* **2007**, *7* (1), 81.
54. Takeda, K., Delivery of magic bullets: on the still rocky road to gene therapy. *British Journal of Pharmacology* **2009**, *157* (2), 151-152.
55. Thomas, C. E.; Ehrhardt, A.; Kay, M. A., Progress and problems with the use of viral vectors for gene therapy. *Nature Reviews Genetics* **2003**, *4* (5), 346-358.
56. Takeda, K., Delivery of magic bullets: on the still rocky road to gene therapy. *British Journal of Pharmacology* **2009**, *157* (2), 151-152.
57. Hacein-Bey-Abina, S.; Von Kalle, C.; Schmidt, M.; McCormack, M. P.; Wulffraat, N.; Leboulch, P.; Lim, A.; Osborne, C. S.; Pawliuk, R.; Morillon, E.; Sorensen, R.; Forster, A.; Fraser, P.; Cohen, J. I.; de Saint Basile, G.; Alexander, I.; Wintergerst, U.; Frebourg, T.; Aurias, A.; Stoppa-Lyonnet, D.; Romana, S.; Radford-Weiss, I.; Gross, F.; Valensi, F.; Delabesse, E.; Macintyre, E.; Sigaux, F.; Soulier, J.; Leiva, L. E.; Wissler, M.; Prinz, C.; Rabbitts, T. H.; Le Deist, F.; Fischer, A.; Cavazzana-Calvo, M., LMO2-Associated Clonal T Cell Proliferation in Two Patients after Gene Therapy for SCID-X1. *Science* **2003**, *302* (5644), 415-419.
58. Kikuchi, H.; Goto, Y.; Hamaguchi, K., Reduction of the buried intrachain disulfide bond of the constant fragment of the immunoglobulin light chain: global unfolding under physiological conditions. *Biochemistry* **1986**, *25* (8), 2009-2013.
59. Hennig, I. M.; Laissue, J. A.; Horisberger, U.; Reubi, J.-C., Substance-P receptors in human primary neoplasms: Tumoral and vascular localization. *International Journal of Cancer* **1995**, *61* (6), 786-792.
60. Rizk, S. S.; Luchniak, A.; Uysal, S.; Brawley, C. M.; Rock, R. S.; Kosiakoff, A. A., An engineered substance P variant for receptor-mediated delivery of synthetic antibodies into tumor cells. *Proceedings of the National Academy of Sciences* **2009**, *106* (27), 11011-11015.
61. Fawell, S.; Seery, J.; Daikh, Y.; Moore, C.; Chen, L. L.; Pepinsky, B.; Barsom, J., Tat-mediated delivery of heterologous proteins into cells. *Proceedings of the National Academy of Sciences* **1994**, *91* (2), 664-668.
62. Niesner, U.; Halin, C.; Lozzi, L.; Gunthert, M.; Neri, P.; Wunderli-Allenspach, H.; Zardi, L.; Neri, D., Quantitation of the Tumor-Targeting Properties of Antibody Fragments Conjugated to Cell-Permeating HIV-1 TAT Peptides. *Bioconjugate Chemistry* **2002**, *13* (4), 729-736.

-
63. Cohen-Saidon, C.; Nechushtan, H.; Kahlon, S.; Livni, N.; Nissim, A.; Razin, E., A novel strategy using single-chain antibody to show the importance of Bcl-2 in mast cell survival. *Blood* **2003**, *102* (7), 2506-2512.
64. Nakajima, O.; Hachisuka, A.; Okunuki, H.; Takagi, K.; Teshima, R.; Sawada, J. I., Method for delivering radiolabeled single-chain Fv antibody to the brain. *Journal of Health Science* **2004**, *50* (2), 159-163.
65. Avignolo, C.; Bagnasco, L.; Biasotti, B.; Melchiori, A.; Tomati, V.; Bauer, I.; Salis, A.; Chiossone, L.; Mingari, M. C.; Orecchia, P.; Carnemolla, B.; Neri, D.; Zardi, L.; Parodi, S., Internalisation via Antennapedia protein transduction domain of an scFv antibody toward c-Myc protein. *The FASEB Journal* **2008**, *22* (4), 1237-1245.
66. Pongpair, O.; Pootong, A.; Maneewatch, S.; Srimanote, P.; Tongtawe, P.; Songserm, T.; Tapchaisri, P.; Chaicumpa, W., A Human Single Chain Transbody Specific to Matrix Protein (M1) Interferes with the Replication of Influenza A Virus. *Bioconjugate Chemistry* **2010**, *21* (7), 1134-1141.
67. Shin, I.; Edl, J.; Biswas, S.; Lin, P. C.; Mernaugh, R.; Arteaga, C. L., Proapoptotic Activity of Cell-Permeable Anti-Akt Single-Chain Antibodies. *Cancer Research* **2005**, *65* (7), 2815-2824.
68. Wu, F.; Fan, S.; Martiniuk, F.; Pincus, S.; Muller, S.; Kohler, H.; Tchou-Wong, K.-M., Protective effects of anti-ricin A-chain antibodies delivered intracellularly against ricin-induced cytotoxicity. *World journal of biological chemistry* **2010**, *1* (5), 188-95.
69. Kameyama, S.; Horie, M.; Kikuchi, T.; Omura, T.; Takeuchi, T.; Nakase, I.; Sugiura, Y.; Futaki, S., Effects of Cell-Permeating Peptide Binding on the Distribution of 125I-Labeled Fab Fragment in Rats. *Bioconjugate Chemistry* **2006**, *17* (3), 597-602.
70. Stein, S.; Weiss, A.; Adermann, K.; Lazarovici, P.; Hochman, J.; Wellhöner, H., A disulfide conjugate between anti-tetanus antibodies and HIV (37-72)Tat neutralizes tetanus toxin inside chromaffin cells. *FEBS Letters* **1999**, *458* (3), 383-386.
71. Chen, B.-X.; Erlanger, B. F., Cell cycle inhibition by an anti-cyclin D1 antibody chemically modified for intracellular delivery. *Cancer Letters* **2006**, *244* (1), 71-75.
72. Hu, M.; Chen, P.; Wang, J.; Scollard, D.; Vallis, K.; Reilly, R., 123I-labeled HIV-1 tat peptide radioimmunoconjugates are imported into the nucleus of human breast cancer cells and functionally interact in vitro and in vivo with the cyclin-dependent kinase inhibitor, p21WAF-1/Cip-1. *European Journal of Nuclear Medicine and Molecular Imaging* **2007**, *34* (3), 368-377.
73. Tünnemann, G.; Martin, R. M.; Haupt, S.; Patsch, C.; Edenhofer, F.; Cardoso, M. C., Cargo-dependent mode of uptake and bioavailability of TAT-containing proteins and peptides in living cells. *The FASEB Journal* **2006**, *20* (11), 1775-1784.
74. Marschall, A.; Frenzel, A.; Schirrmann, T.; Schüngel, M.; Dübel, S., Targeting antibodies to the cytoplasm. *mAb* **2011**, *3* (1), 3-16.
75. Frankel, A. D.; Pabo, C. O., Cellular uptake of the tat protein from human immunodeficiency virus. *Cell* **1988**, *55* (6), 1189-1193.

-
76. Joliot, A.; Pernelle, C.; Deagostini-Bazin, H.; Prochiantz, A., Antennapedia homeobox peptide regulates neural morphogenesis. *Proceedings of the National Academy of Sciences* **1991**, 88 (5), 1864-1868.
77. Vives, E.; Charneau, P.; van Rietschoten, J.; Rochat, H.; Bahraoui, E., Effects of the Tat basic domain on human immunodeficiency virus type 1 transactivation, using chemically synthesized Tat protein and Tat peptides. *Journal of Virology* **1994**, 68 (5), 3343-3353.
78. Derossi, D.; Joliot, A. H.; Chassaing, G.; Prochiantz, A., The third helix of the Antennapedia homeodomain translocates through biological membranes. *Journal of Biological Chemistry* **1994**, 269 (14), 10444-10450.
79. Derossi, D.; Calvet, S.; Trembleau, A.; Brunissen, A.; Chassaing, G.; Prochiantz, A., Cell Internalisation of the Third Helix of the Antennapedia Homeodomain Is Receptor-independent. *Journal of Biological Chemistry* **1996**, 271 (30), 18188-18193.
80. Lindgren, M.; Langel, Ü., Classes and Prediction of Cell-Penetrating Peptides. In *Cell-Penetrating Peptides*, Langel, Ü., Ed. Humana Press: 2011; Vol. 683, pp 3-19.
81. Fischer, M., P, Cellular uptake mechanisms and potential therapeutic utility of peptidic cell delivery vectors: Progress 2001-2006. *Medicinal Research Reviews* **2007**, 27 (6), 755-795.
82. Madani, F.; Lindberg, S.; Langel, Ü.; Futaki, S.; Gr, A., Mechanisms of Cellular Uptake of Cell-Penetrating Peptides. *Journal of Biophysics* **2011**, 2011.
83. Ziegler, A., Thermodynamic studies and binding mechanisms of cell-penetrating peptides with lipids and glycosaminoglycans. *Advanced Drug Delivery Reviews* **2008**, 60 (4-5), 580-597.
84. Pooga, M.; Hällbrink, M.; Zorko, M.; Langel, Ü., Cell penetration by transportan. *The FASEB Journal* **1998**, 12 (1), 67-77.
85. Morris, M. C.; Depollier, J.; Mery, J.; Heitz, F.; Divita, G., A peptide carrier for the delivery of biologically active proteins into mammalian cells. *Nature Biotechnology* **2001**, 19 (12), 1173-1176.
86. Morris, M. C.; Chaloin, L.; Méry, J.; Heitz, F.; Divita, G., A novel potent strategy for gene delivery using a single peptide vector as a carrier. *Nucleic Acids Research* **1999**, 27 (17), 3510-3517.
87. Oehlke, J.; Scheller, A.; Wiesner, B.; Krause, E.; Beyermann, M.; Klauschenz, E.; Melzig, M.; Bienert, M., Cellular uptake of an [alpha]-helical amphipathic model peptide with the potential to deliver polar compounds into the cell interior non-endocytically. *Biochimica et Biophysica Acta (BBA) - Biomembranes* **1998**, 1414 (1-2), 127-139.
88. Elmquist, A.; Lindgren, M.; Bartfai, T.; Langel, Ü., VE-Cadherin-Derived Cell-Penetrating Peptide, pVEC, with Carrier Functions. *Experimental Cell Research* **2001**, 269 (2), 237-244.

-
89. Wender, P. A.; Mitchell, D. J.; Pattabiraman, K.; Pelkey, E. T.; Steinman, L.; Rothbard, J. B., The design, synthesis, and evaluation of molecules that enable or enhance cellular uptake: Peptoid molecular transporters. *Proceedings of the National Academy of Sciences* **2000**, 97, 13003-13008.
90. Vives, E.; Brodin, P.; Lebleu, B., A Truncated HIV-1 Tat Protein Basic Domain Rapidly Translocates through the Plasma Membrane and Accumulates in the Cell Nucleus. *Journal of Biological Chemistry* **1997**, 272 (25), 16010-16017.
91. Balayssac, S.; Burlina, F.; Convert, O.; Bolbach, G.; Chassaing, G.; Lequin, O., Comparison of Penetratin and Other Homeodomain-Derived Cell-Penetrating Peptides: Interaction in a Membrane-Mimicking Environment and Cellular Uptake Efficiency. *Biochemistry* **2006**, 45 (5), 1408-1420.
92. Mitchell, D. J.; Steinman, L.; Kim, D. T.; Fathman, C. G.; Rothbard, J. B., Polyarginine enters cells more efficiently than other polycationic homopolymers. *The Journal of Peptide Research* **2000**, 56 (5), 318-325.
93. Futaki, S.; Suzuki, T.; Ohashi, W.; Yagami, T.; Tanaka, S.; Ueda, K.; Sugiura, Y., Arginine-rich Peptides. *Journal of Biological Chemistry* **2001**, 276 (8), 5836-5840.
94. Taylor, B. N.; Mehta, R. R.; Yamada, T.; Lekmine, F.; Christov, K.; Chakrabarty, A. M.; Green, A.; Bratescu, L.; Shilkaitis, A.; Beattie, C. W.; Das Gupta, T. K., Noncationic Peptides Obtained From Azurin Preferentially Enter Cancer Cells. *Cancer Research* **2009**, 69 (2), 537-546.
95. Crespo, L.; Sanclimens, G.; Montaner, B.; Perez-Tomas, R.; Royo, M.; Pons, M.; Albericio, F.; Giralt, E., Peptide Dendrimers Based on Polyproline Helices. *Journal of the American Chemical Society* **2002**, 124 (30), 8876-8883.
96. Martín, I.; Teixidó, M.; Giralt, E., Design, Synthesis and Characterization of a New Anionic Cell-Penetrating Peptide: SAP(E). *ChemBioChem* **2011**, 12 (6), 896-903.
97. Okuyama, M.; Laman, H.; Kingsbury, S. R.; Visintin, C.; Leo, E.; Eward, K. L.; Stoeber, K.; Boshoff, C.; Williams, G. H.; Selwood, D. L., Small-molecule mimics of an $[\alpha]$ -helix for efficient transport of proteins into cells. *Nature Methods* **2007**, 4 (2), 153-159.
98. Rebstock, A.-S.; Visintin, C.; Leo, E.; Garcia Posada, C.; Kingsbury, S. R.; Williams, G. H.; Stoeber, K.; Selwood, D. L., Modular Assembly Using Sequential Palladium Coupling Gives Easy Access to the SMoC Class of Cellular Transporters. *ChemBioChem* **2008**, 9 (11), 1787-1796.
99. Richard, J. P.; Melikov, K.; Vives, E.; Ramos, C.; Verbeure, B.; Gait, M. J.; Chernomordik, L. V.; Lebleu, B., Cell-penetrating Peptides. *Journal of Biological Chemistry* **2003**, 278 (1), 585-590.
100. Fischer, R.; Fotin-Mleczek, M.; Hufnagel, H.; Brock, R., Break on through to the Other Side - Biophysics and Cell Biology Shed Light on Cell-Penetrating Peptides. *ChemBioChem* **2005**, 6 (12), 2126-2142.
101. Kosuge, M.; Takeuchi, T.; Nakase, I.; Jones, A.; Futaki, S., Cellular Internalisation and Distribution of Arginine-Rich Peptides as a Function of

Extracellular Peptide Concentration, Serum, and Plasma Membrane Associated Proteoglycans *Bioconjugate Chem* **2008**, *19*, 656-664.

102. Nakase, I.; Tadokoro, A.; Kawabata, N.; Takeuchi, T.; Katoh, H.; Hiramoto, K.; Negishi, M.; Nomizu, M.; Sugiura, Y.; Futaki, S., Interaction of Arginine-Rich Peptides with Membrane-Associated Proteoglycans Is Crucial for Induction of Actin Organization and Macropinocytosis. *Biochemistry* **2007**, *46* (2), 492-501.

103. Jones, A. T., Macropinocytosis: searching for an endocytic identity and role in the uptake of cell penetrating peptides. *Journal of Cellular and Molecular Medicine* **2007**, *11* (4), 670-684.

104. Richard, J. P.; Melikov, K.; Brooks, H.; Prevot, P.; Lebleu, B.; Chernomordik, L. V., Cellular Uptake of Unconjugated TAT Peptide Involves Clathrin-dependent Endocytosis and Heparan Sulfate Receptors. *Journal of Bioorganic Chemistry* **2005**, *280* (15), 15300-15306.

105. Fittipaldi, A.; Ferrari, A.; Zoppe, M.; Arcangeli, C.; Pellegrini, V.; Beltram, F.; Giacca, M., Cell Membrane Lipid Rafts Mediate Caveolar Endocytosis of HIV-1 Tat Fusion Proteins. *Journal of Bioorganic Chemistry* **2003**, *278* (36), 34141-34149.

106. Nakase, I.; Niwa, M.; Takeuchi, T.; Sonomura, K.; Kawabata, N.; Koike, Y.; Takehashi, M.; Tanaka, S.; Ueda, K.; Simpson, J. C.; Jones, A. T.; Sugiura, Y.; Futaki, S., Cellular Uptake of Arginine-Rich Peptides: Roles for Macropinocytosis and Actin Rearrangement. *Molecular Therapy* **2004**, *10* (6), 1011-1022.

107. Ter-Avetisyan, G.; Tünnemann, G.; Nowak, D.; Nitschke, M.; Herrmann, A.; Drab, M.; Cardoso, M. C., Cell Entry of Arginine-rich Peptides Is Independent of Endocytosis. *Journal of Biological Chemistry* **2009**, *284* (6), 3370-3378.

108. Ikuhiko Nakase; Akiko Tadokoro; Noriko Kawabata; Toshihide Takeuchi; Hironori Katoh; Kiyo Hiramoto; Manabu Negishi; Motoyoshi Nomizu; Yukio Sugiura; Futaki, S., Interaction of Arginine-Rich Peptides with Membrane-Associated Proteoglycans Is Crucial for Induction of Actin Organization and Macropinocytosis. *Biochemistry* **2007**, *46*, 492-501.

109. Cheung, C. Y.; Murthy, N.; Stayton, P. S.; Hoffman, A. S., A pH-Sensitive Polymer That Enhances Cationic Lipid-Mediated Gene Transfer. *Bioconjugate Chemistry* **2001**, *12* (6), 906-910.

110. Philippova, O. E.; Hourdet, D.; Audebert, R.; Khokhlov, A. R., pH-Responsive Gels of Hydrophobically Modified Poly(acrylic acid). *Macromolecules* **1997**, *30* (26), 8278-8285.

111. Wadia, J. S.; Stan, R. V.; Dowdy, S. F., Transducible TAT-HA fusogenic peptide enhances escape of TAT-fusion proteins after lipid raft macropinocytosis. *Nature Medicine* **2004**, *10* (3), 310-315.

112. Pichon, C.; Gonçalves, C.; Midoux, P., Histidine-rich peptides and polymers for nucleic acids delivery. *Advanced Drug Delivery Reviews* **2001**, *53* (1), 75-94.

113. Lo, S. L.; Wang, S., An endosomolytic Tat peptide produced by incorporation of histidine and cysteine residues as a nonviral vector for DNA transfection. *Biomaterials* **2008**, *29* (15), 2408-2414.

-
114. Ohmori, N.; Niidome, T.; Wada, A.; Hirayama, T.; Hatakeyama, T.; Aoyagi, H., The Enhancing Effect of Anionic [α]-Helical Peptide on Cationic Peptide-Mediating Transfection Systems. *Biochemical and Biophysical Research Communications* **1997**, 235 (3), 726-729.
115. Han, X.; Bushweller, J. H.; Cafiso, D. S.; Tamm, L. K., Membrane structure and fusion-triggering conformational change of the fusion domain from influenza hemagglutinin. *Nature Structural Biology* **2001**, 8 (8), 715-720.
116. El-Sayed, A.; Futaki, S.; Harashima, H., Delivery of Macromolecules Using Arginine-Rich Cell-Penetrating Peptides: Ways to Overcome Endosomal Entrapment. *The AAPS Journal* **2009**, 11 (1), 13-22.
117. Chen, L.; Wright, L. R.; Chen, C.-H.; Oliver, S. F.; Wender, P. A.; Mochly-Rosen, D., Molecular transporters for peptides: delivery of a cardioprotective ε -PKC agonist peptide into cells and intact ischemic heart using a transport system, R7. *Chemistry & Biology* **2001**, 8 (12), 1123-1129.
118. Murriel, C. L.; Dowdy, S. F., Influence of protein transduction domains on intracellular delivery of macromolecules. *Expert Opinion on Drug Delivery* **2006**, 3 (6), 739-746.
119. Lee, H. J.; Pardridge, W. M., Pharmacokinetics and Delivery of Tat and Tat-Protein Conjugates to Tissues in Vivo. *Bioconjugate Chemistry* **2001**, 12 (6), 995-999.
120. Schwarze, S. R.; Ho, A.; Vocero-Akbani, A.; Dowdy, S. F., In Vivo Protein Transduction: Delivery of a Biologically Active Protein into the Mouse. *Science* **1999**, 285 (5433), 1569-1572.
121. Carnemolla, B.; Balza, E.; Siri, A.; Zardi, L.; Nicotra, M. R.; Bigotti, A.; Natali, P. G., A tumor-associated fibronectin isoform generated by alternative splicing of messenger RNA precursors. *The Journal of Cell Biology* **1989**, 108 (3), 1139-1148.
122. Sarko, D.; Beijer, B.; Boy, R. G.; Nothelfer, E.-M.; Leotta, K.; Eisenhut, M.; Altmann, A.; Haberkorn, U.; Mier, W., The Pharmacokinetics of Cell-Penetrating Peptides. *Molecular Pharmaceutics* **2010**, 7 (6), 2224-2231.
123. Kloß, A.; Henklein, P.; Siele, D.; Schmolke, M.; Apcher, S.; Kuehn, L.; Sheppard, P. W.; Dahlmann, B., The cell-penetrating peptide octa-arginine is a potent inhibitor of proteasome activities. *European Journal of Pharmaceutics and Biopharmaceutics* **2009**, 72 (1), 219-225.
124. Cameron, A.; Appel, J.; Houghten, R. A.; Lindberg, I., Polyarginines Are Potent Furin Inhibitors. *Journal of Biological Chemistry* **2000**, 275 (47), 36741-36749.
125. El-Andaloussi, S.; Jarver, P.; Johansson, H. J.; Langel, U., Cargo-dependent cytotoxicity and delivery efficacy of cell-penetrating peptides: a comparative study. *Biochemical Journal* **2007**, 407, 285-292.
126. Holm, T.; Räägel, H.; Andaloussi, S. E. L.; Hein, M.; Mäe, M.; Pooga, M.; Langel, Ü., Retro-inversion of certain cell-penetrating peptides causes severe cellular toxicity. *Biochimica et Biophysica Acta (BBA) - Biomembranes* **2011**, 1808 (6), 1544-1551.

-
127. Cardozo, A. K.; Buchillier, V.; Mathieu, M.; Chen, J.; Ortis, F.; Ladrière, L.; Allaman-Pillet, N.; Poirot, O.; Kellenberger, S.; Beckmann, J. S.; Eizirik, D. L.; Bonny, C.; Maurer, F., Cell-permeable peptides induce dose- and length-dependent cytotoxic effects. *Biochimica et Biophysica Acta (BBA) - Biomembranes* **2007**, 1768 (9), 2222-2234.
128. Rothbard, J. B.; Garlington, S.; Lin, Q.; Kirschberg, T.; Kreider, E.; McGrane, P. L.; Wender, P. A.; Khavari, P. A., Conjugation of arginine oligomers to cyclosporin A facilitates topical delivery and inhibition of inflammation. *Nature Medicine* **2000**, 6 (11), 1253-1257.
129. Chen, L.; Hahn, H.; Wu, G.; Chen, C.-H.; Liron, T.; Schechtman, D.; Cavallaro, G.; Banci, L.; Guo, Y.; Bolli, R.; Dorn, G. W.; Mochly-Rosen, D., Opposing cardioprotective actions and parallel hypertrophic effects of δ PKC and ϵ PKC. *Proceedings of the National Academy of Sciences* **2001**, 98 (20), 11114-11119.
130. Ikeno, F.; Inagaki, K.; Rezaee, M.; Mochly-Rosen, D., Impaired perfusion after myocardial infarction is due to reperfusion-induced 1 PKC-mediated myocardial damage. *Cardiovascular Research* **2007**, 73 (4), 699-709.
131. Inagaki, K.; Chen, L.; Ikeno, F.; Lee, F. H.; Imahashi, K.-i.; Bouley, D. M.; Rezaee, M.; Yock, P. G.; Murphy, E.; Mochly-Rosen, D., Inhibition of Protein Kinase C Protects Against Reperfusion Injury of the Ischemic Heart In Vivo. *Circulation* **2003**, 108 (19), 2304-2307.
132. ClinicalTrials.gov, <http://clinicaltrials.gov/ct2/results?term=KAI-9803>, accessed on Aug'11.
133. Johnson, R. M.; Harrison, S. D.; Maclean, D., Therapeutic Applications of Cell-Penetrating Peptides. In *Cell-Penetrating Peptides*, Vol. 683, pp 535-551.
134. Tan, M.; Lan, K.-H.; Yao, J.; Lu, C.-H.; Sun, M.; Neal, C. L.; Lu, J.; Yu, D., Selective Inhibition of ErbB2-Overexpressing Breast Cancer In vivo by a Novel TAT-Based ErbB2-Targeting Signal Transducers and Activators of Transcription 3–Blocking Peptide. *Cancer Research* **2006**, 66 (7), 3764-3772.
135. Myrberg, H.; Zhang, L.; Mäe, M.; Langel, U., Design of a tumor-homing cell-penetrating peptide. *Bioconjugate Chemistry* **2008**, 19 (1), 70-75.
136. Mäe, M.; Myrberg, H.; El-Andaloussi, S.; Langel, Ü., Design of a Tumor Homing Cell-Penetrating Peptide for Drug Delivery. *International Journal of Peptide Research and Therapeutics* **2009**, 15 (1), 11-15.
137. Zhang, W.; Song, J.; Zhang, B.; Liu, L.; Wang, K.; Wang, R., Design of Acid-Activated Cell Penetrating Peptide for Delivery of Active Molecules into Cancer Cells. *Bioconjugate Chemistry* **2011**, 22 (7), 1410-1415.
138. Jiang, T.; Olson, E. S.; Nguyen, Q. T.; Roy, M.; Jennings, P. A.; Tsien, R. Y., Tumor imaging by means of proteolytic activation of cell-penetrating peptides. *Proceedings of the National Academy of Sciences* **2004**, 101 (51), 17867-17872.
139. Bremer, C.; Tung, C.-H.; Weissleder, R., In vivo molecular target assessment of matrix metalloproteinase inhibition. *Nature Medicine* **2001**, 7 (6), 743-748.

-
140. Aguilera, T. A.; Olson, E. S.; Timmers, M. M.; Jiang, T.; Tsien, R. Y., Systemic in vivo distribution of activatable cell penetrating peptides is superior to that of cell penetrating peptides. *Integrative Biology* **2009**, *1* (5-6), 371-381.
141. Amersdorfer, P.; Wong, C.; Smith, T.; Chen, S.; Deshpande, S.; Sheridan, R.; Marks, J. D., Genetic and immunological comparison of anti-botulinum type A antibodies from immune and non-immune human phage libraries. *Vaccine* **2002**, *20* (11-12), 1640-1648.
142. Liang, J. F.; Park, Y. J.; Song, H.; Li, Y. T.; Yang, V. C.-M., ATTEMPTS: A heparin/protamine-based prodrug approach for delivery of thrombolytic drugs. *Journal of Controlled Release* **2001**, *72* (1-3), 145-156.
143. Huang, Y.; Park, Y. S.; Wang, J.; Moon, C.; Kwon, Y. M.; Chung, H. S.; Park, Y. J.; Yang, V. C., ATTEMPTS System: A Macromolecular Prodrug Strategy for Cancer Drug Delivery. *Current Pharmaceutical Design* **2010**, *16* (21), 2369-2376.
144. Kwon, Y. M.; Li, Y. T.; Liang, J. F.; Park, Y. J.; Chang, L.-C.; Yang, V. C., PTD-modified ATTEMPTS system for enhanced asparaginase therapy: A proof-of-concept investigation. *Journal of Controlled Release* **2008**, *130* (3), 252-258.
145. Li, Y. T.; Kwon, Y. M.; Spangrude, G. J.; Liang, J. F.; Chung, H. S.; Park, Y. J.; Yang, V. C., Preliminary in vivo evaluation of the protein transduction domain-modified ATTEMPTS approach in enhancing asparaginase therapy. *Journal of Biomedical Materials Research Part A* **2009**, *91A* (1), 209-220.
146. Simplicio, A.; Clancy, J.; Gilmer, J., Prodrugs for Amines. *Molecules* **2008**, *13* (3), 519-547.
147. Saulnier, M. G.; Frennesson, D. B.; Deshpande, M. S.; Hansel, S. B.; Vyas, D. M., An efficient method for the synthesis of guanidino prodrugs. *Bioorganic & Medicinal Chemistry Letters* **1994**, *4* (16), 1985-1990.
148. Chadd, H. E.; Chamow, S. M., Therapeutic antibody expression technology. *Current Opinion in Biotechnology* **2001**, *12* (2), 188-194.
149. Tsumoto, K.; Shinoki, K.; Kondo, H.; Uchikawa, M.; Juji, T.; Kumagai, I., Highly efficient recovery of functional single-chain Fv fragments from inclusion bodies overexpressed in *Escherichia coli* by controlled introduction of oxidizing reagent--application to a human single-chain Fv fragment. *Journal of Immunological Methods* **1998**, *219* (1-2), 119-129.
150. Jurado, P.; Ritz, D.; Beckwith, J.; de Lorenzo, V.; Fernández, L. A., Production of Functional Single-Chain Fv Antibodies in the Cytoplasm of *Escherichia coli*. *Journal of Molecular Biology* **2002**, *320* (1), 1-10.
151. Kipriyanov, S. M.; Moldenhauer, G.; Little, M., High level production of soluble single chain antibodies in small-scale *Escherichia coli* cultures. *Journal of Immunological Methods* **1997**, *200* (1-2), 69-77.
152. Schmiedl, A.; Breitling, F.; Winter, C. H.; Queitsch, I.; Dübel, S., Effects of unpaired cysteines on yield, solubility and activity of different recombinant antibody constructs expressed in *E. coli*. *Journal of Immunological Methods* **2000**, *242* (1-2), 101-114.

-
153. Kipriyanov, S. M.; Moldenhauer, G.; Martin, A. C.; Kupriyanova, O. A.; Little, M., Two amino acid mutations in an anti-human CD3 single chain Fv antibody fragment that affect the yield on bacterial secretion but not the affinity. *Protein Engineering* **1997**, *10* (4), 445-453.
154. Koutsokeras, A.; Kabouridis, P. S., Secretion and uptake of TAT-fusion proteins produced by engineered mammalian cells. *Biochimica et Biophysica Acta (BBA) - General Subjects* **2009**, *1790* (2), 147-153.
155. Shaw, P. A.; Catchpole, I. R.; Goddard, C. A.; Colledge, W. H., Comparison of Protein Transduction Domains in Mediating Cell Delivery of a Secreted CRE Protein†. *Biochemistry* **2008**, *47* (4), 1157-1166.
156. Brinkley, M., A brief survey of methods for preparing protein conjugates with dyes, haptens and crosslinking reagents. *Bioconjugate Chemistry* **1992**, *3* (1), 2-13.
157. Mao, H.; Hart, S. A.; Schink, A.; Pollok, B. A., Sortase-Mediated Protein Ligation: A New Method for Protein Engineering. *Journal of the American Chemical Society* **2004**, *126* (9), 2670-2671.
158. Hao, Z.; Hong, S.; Chen, X.; Chen, P. R., Introducing Bioorthogonal Functionalities into Proteins in Living Cells. *Accounts of Chemical Research* **2011**, *44* (9), 742-751.
159. van Hest, J. C. M.; Kiick, K. L.; Tirrell, D. A., Efficient Incorporation of Unsaturated Methionine Analogues into Proteins in Vivo. *Journal of the American Chemical Society* **2000**, *122* (7), 1282-1288.
160. van Hest, J. C. M.; van Delft, F. L., Protein Modification by Strain-Promoted Alkyne–Azide Cycloaddition. *ChemBioChem* **2011**, *12* (9), 1309-1312.
161. Hermanson, G. T., The Chemistry of Reactive Groups. In *Bioconjugate Techniques (Second Edition)*, Academic Press: New York, 2008; pp 169-212.
162. Rusiecki, V. K.; Warne, S. A., Synthesis of N α -Fmoc-N ϵ -Nvoc-Lysine and use in the preparation of selectively functionalized peptides. *Bioorganic & Medicinal Chemistry Letters* **1993**, *3* (4), 707-710.
163. Hansen, P. R.; Olsen, C. E.; Holm, A., A New Method for the Synthesis of Neoglycopeptides. *Bioconjugate Chemistry* **1998**, *9* (1), 126-131.
164. Marburg, S.; Neckers, A. C.; Griffin, P. R., Introduction of the Maleimide Function onto Resin-Bound Peptides: A Simple, High-Yield Process Useful for Discriminating among Several Lysines. *Bioconjugate Chemistry* **1996**, *7* (5), 612-616.
165. Tedaldi, L. M.; Smith, M. E. B.; Nathani, R. I.; Baker, J. R., Bromomaleimides: new reagents for the selective and reversible modification of cysteine. *Chemical Communications* **2009**, (43), 6583-6585.
166. Smith, M. E. B.; Schumacher, F. F.; Ryan, C. P.; Tedaldi, L. M.; Papaioannou, D.; Waksman, G.; Caddick, S.; Baker, J. R., Protein Modification, Bioconjugation, and Disulfide Bridging Using Bromomaleimides. *Journal of the American Chemical Society* **2010**, *132* (6), 1960-1965.

-
167. West, K. R.; Otto, S., Reversible covalent chemistry in drug delivery. *Current drug discovery technologies* **2005**, 2 (3), 123-60.
168. Thorpe, P. E.; Wallace, P. M.; Knowles, P. P.; Relf, M. G.; Brown, A. N. F.; Watson, G. J.; Knyba, R. E.; Wawrzynczak, E. J.; Blakey, D. C., New Coupling Agents for the Synthesis of Immunotoxins Containing a Hindered Disulfide Bond with Improved Stability in Vivo. *Cancer Research* **1987**, 47 (22), 5924-5931.
169. Adams, J. M.; Cory, S., The Bcl-2 apoptotic switch in cancer development and therapy. *Oncogene* 26 (9), 1324-1337.
170. Youle, R. J.; Strasser, A., The BCL-2 protein family: opposing activities that mediate cell death. *Nature Reviews Molecular Cell Biology* **2008**, 9 (1), 47-59.
171. Sattler, M.; Liang, H.; Nettesheim, D.; Meadows, R. P.; Harlan, J. E.; Eberstadt, M.; Yoon, H. S.; Shuker, S. B.; Chang, B. S.; Minn, A. J.; Thompson, C. B.; Fesik, S. W., Structure of Bcl-xL-Bak peptide complex: recognition between regulators of apoptosis. *Science* **1997**, 275 (5302), 983-6.
172. Ji, H.; Shekhtman, A.; Ghose, R.; McDonnell, J. M.; Cowburn, D., NMR determination that an extended BH3 motif of pro-apoptotic BID is specifically bound to BCL-XL. *Magnetic Resonance in Chemistry* **2006**, 44 Spec No, S101-7.
173. Wang, J.-L.; Liu, D.; Zhang, Z.-J.; Shan, S.; Han, X.; Srinivasula, S. M.; Croce, C. M.; Alnemri, E. S.; Huang, Z., Structure-based discovery of an organic compound that binds Bcl-2 protein and induces apoptosis of tumor cells. *Proceedings of the National Academy of Sciences* **2000**, 97 (13), 7124-7129.
174. Wang, G.; Nikolovska-Coleska, Z.; Yang, C.-Y.; Wang, R.; Tang, G.; Guo, J.; Shangary, S.; Qiu, S.; Gao, W.; Yang, D.; Meagher, J.; Stuckey, J.; Krajewski, K.; Jiang, S.; Roller, P. P.; Abaan, H. O.; Tomita, Y.; Wang, S., Structure-Based Design of Potent Small-Molecule Inhibitors of Anti-Apoptotic Bcl-2 Proteins. *Journal of Medicinal Chemistry* **2006**, 49 (21), 6139-6142.
175. Degterev, A.; Lugovskoy, A.; Cardone, M.; Mulley, B.; Wagner, G.; Mitchison, T.; Yuan, J., Identification of small-molecule inhibitors of interaction between the BH3 domain and Bcl-xL. *Nature Cell Biology* **2001**, 3 (2), 173-182.
176. Tse, C.; Shoemaker, A. R.; Adickes, J.; Anderson, M. G.; Chen, J.; Jin, S.; Johnson, E. F.; Marsh, K. C.; Mitten, M. J.; Nimmer, P.; Roberts, L.; Tahir, S. K.; Xiao, Y.; Yang, X.; Zhang, H.; Fesik, S.; Rosenberg, S. H.; Elmore, S. W., ABT-263: A Potent and Orally Bioavailable Bcl-2 Family Inhibitor. *Cancer Research* **2008**, 68 (9), 3421-3428.
177. Oltersdorf, T.; Elmore, S. W.; Shoemaker, A. R.; Armstrong, R. C.; Augeri, D. J.; Belli, B. A.; Bruncko, M.; Deckwerth, T. L.; Dinges, J.; Hajduk, P. J.; Joseph, M. K.; Kitada, S.; Korsmeyer, S. J.; Kunzer, A. R.; Letai, A.; Li, C.; Mitten, M. J.; Nettesheim, D. G.; Ng, S.; Nimmer, P. M.; O'Connor, J. M.; Oleksijew, A.; Petros, A. M.; Reed, J. C.; Shen, W.; Tahir, S. K.; Thompson, C. B.; Tomaselli, K. J.; Wang, B.; Wendt, M. D.; Zhang, H.; Fesik, S. W.; Rosenberg, S. H., An inhibitor of Bcl-2 family proteins induces regression of solid tumours. *Nature* **2005**, 435 (7042), 677-681.

-
178. Walensky, L. D.; Kung, A. L.; Escher, I.; Malia, T. J.; Barbuto, S.; Wright, R. D.; Wagner, G.; Verdine, G. L.; Korsmeyer, S. J., Activation of apoptosis in vivo by a hydrocarbon-stapled BH3 helix. *Science* **2004**, *305* (5689), 1466-70.
179. Walensky, L. D.; Pitter, K.; Morash, J.; Oh, K. J.; Barbuto, S.; Fisher, J.; Smith, E.; Verdine, G. L.; Korsmeyer, S. J., A stapled BID BH3 helix directly binds and activates BAX. *Molecular Cell* **2006**, *24* (2), 199-210.
180. Goldsmith, K. C.; Liu, X.; Dam, V.; Morgan, B. T.; Shabbout, M.; Cnaan, A.; Letai, A.; Korsmeyer, S. J.; Hogarty, M. D., BH3 peptidomimetics potently activate apoptosis and demonstrate single agent efficacy in neuroblastoma. *Oncogene* **2006**, *25* (33), 4525-4533.
181. Wang, J.-L.; Zhang, Z.-J.; Choksi, S.; Shan, S.; Lu, Z.; Croce, C. M.; Alnemri, E. S.; Korngold, R.; Huang, Z., Cell Permeable Bcl-2 Binding Peptides: A Chemical Approach to Apoptosis Induction in Tumor Cells. *Cancer Research* **2000**, *60* (6), 1498-1502.
182. McCafferty, J.; Griffiths, A. D.; Winter, G.; Chiswell, D. J., Phage antibodies: filamentous phage displaying antibody variable domains. *Nature* **1990**, *348* (6301), 552-554.
183. Griffiths, A. D.; Williams, S. C.; Hartley, O.; Tomlinson, I. M.; Waterhouse, P.; Crosby, W. L.; Kontermann, R. E.; Jones, P. T.; Low, N. M.; Allison, T. J.; Prospero, T. D.; Hoogenboom, H. R.; Nissim, A.; Cox, J. P. L.; Harrison, J. L.; Zaccolo, M.; Gherardi, E.; Winter, G., Isolation of high-affinity human-antibodies directly from large synthetic repertoires. *The EMBO Journal*. **1994**, *13* (14), 3245-3260.
184. Hoogenboom, H. R.; Griffiths, A. D.; Johnson, K. S.; Chiswell, D. J.; Hudson, P.; Winter, G., Multi-subunit proteins on the surface of filamentous phage: methodologies for displaying antibody (Fab) heavy and light chains. *Nucleic Acids Research* **1991**, *19* (15), 4133-4137.
185. McCafferty, J., Fitzgerald, K., Earnshaw, J., Chiswell, D., Link, J., Smith, R., Kenten, J. , Selection and rapid purification of murine antibody fragments that bind a transition-state analog by phage display. *Applied Biochemistry and Biotechnology* **1994**, *47*.
186. Kabat, E. A.; Wu, T. T., Identical V region amino acid sequences and segments of sequences in antibodies of different specificities. Relative contributions of VH and VL genes, minigenes, and complementarity-determining regions to binding of antibody-combining sites. *Journal of Immunology* **1991**, *147* (5), 1709-1719.
187. Griffiths, A. D.; Malmqvist, M.; Marks, J. D.; Bye, J. M.; Embleton, M. J.; McCafferty, J.; Baier, M.; Holliger, K. P.; Gorick, B. D.; Hughes-Jones, N. C., Human anti-self antibodies with high specificity from phage display libraries. *The EMBO journal* **1993**, *12* (2), 725-34.
188. Ullman, E. F.; Kirakossian, H.; Singh, S.; Wu, Z. P.; Irvin, B. R.; Pease, J. S.; Switchenko, A. C.; Irvine, J. D.; Dafforn, A.; Skold, C. N., Luminescent oxygen channeling immunoassay: measurement of particle binding kinetics by

chemiluminescence. *Proceedings of the National Academy of Sciences of the United States of America* **1994**, 91 (12), 5426-5430.

189. Certo, M.; Moore, V. D. G.; Nishino, M.; Wei, G.; Korsmeyer, S.; Armstrong, S. A.; Letai, A., Mitochondria primed by death signals determine cellular addiction to antiapoptotic BCL-2 family members. *Cancer cell* **2006**, 9 (5), 351-365.

190. Letai, A.; Bassik, M. C.; Walensky, L. D.; Sorcinelli, M. D.; Weiler, S.; Korsmeyer, S. J., Distinct BH3 domains either sensitize or activate mitochondrial apoptosis, serving as prototype cancer therapeutics. *Cancer Cell* **2002**, 2 (3), 183-92.

191. Rega, M. F.; Reed, J. C.; Pellecchia, M., Robust lanthanide-based assays for the detection of anti-apoptotic Bcl-2-family protein antagonists. *Bioorganic Chemistry* **2007**, 35 (2), 113-120.

192. Kosower, N. S.; Kosower, E. M., The Glutathione Status of Cells. In *International Review of Cytology*, G.H. Bourne, J. F. D.; Jeon, K. W., Eds. Academic Press: 1978; Vol. Volume 54, pp 109-160.

193. Brockmann, E.-C.; Cooper, M.; Strömsten, N.; Vehniäinen, M.; Saviranta, P., Selecting for antibody scFv fragments with improved stability using phage display with denaturation under reducing conditions. *Journal of Immunological Methods* **2005**, 296 (1-2), 159-170.

194. Lloyd, C.; Lowe, D.; Edwards, B.; Welsh, F.; Dilks, T.; Hardman, C.; Vaughan, T., Modelling the human immune response: performance of a 1011 human antibody repertoire against a broad panel of therapeutically relevant antigens. *Protein Engineering Design and Selection* **2009**, 22 (3), 159-168.

195. Sanger, F., Nicklen, S., Coulson, A, DNA sequencing with chain-terminating inhibitors. *Proceedings of the National Academy of Sciences* **1977**, 74, 5463-5467.

196. Stewart, K. M.; Horton, K. L.; Kelley, S. O., Cell-penetrating peptides as delivery vehicles for biology and medicine. *Organic & Biomolecular Chemistry* **2008**, 6 (13), 2242-2255.

197. Sawant, R.; Torchilin, V., Intracellular transduction using cell-penetrating peptides. *Molecular BioSystems* **2010**, 6 (4), 628-640.

198. Leong, S. S. J.; Chen, W. N., Preparing recombinant single chain antibodies. *Chemical Engineering Science* **2008**, 63 (6), 1401-1414.

199. Baneyx, F., Recombinant protein expression in *Escherichia coli*. *Current Opinion in Biotechnology* **1999**, 10 (5), 411-421.

200. Blom, N.; Sicheritz-Pontén, T.; Gupta, R.; Gammeltoft, S.; Brunak, S., Prediction of post-translational glycosylation and phosphorylation of proteins from the amino acid sequence. *Proteomics* **2004**, 4 (6), 1633-1649.

201. Gupta, R. NetNGlyc 1.0 Server. <http://www.cbs.dtu.dk/services/NetNGlyc/>. accessed on June'11.

202. Fischer, P. M., Zhelev, N. Z., Wang, S., Melville, J E., Fåhræus R., Lane, D P., Structure-activity relationship of truncated and substituted analogues of the

intracellular delivery vector Penetratin. *The Journal of Peptide Research* **2000**, 55 (2), 163-172.

203. Atherton, E.; Fox, H.; Harkiss, D.; Sheppard, R. C., Application of polyamide resins to polypeptide synthesis: an improved synthesis of [small beta]-endorphin using fluorenylmethoxycarbonylamino-acids. *Journal of the Chemical Society, Chemical Communications* **1978**, (13), 539-540.

204. Chan, W. C.; Bycroft, B. W.; Evans, D. J.; White, P. D., A novel 4-aminobenzyl ester-based carboxy-protecting group for synthesis of atypical peptides by Fmoc-But solid-phase chemistry. *Journal of the Chemical Society, Chemical Communications* **1995**, (21), 2209-2210.

205. Chan, W. C.; White, P. D., *Fmoc solid-phase peptide synthesis: a practical approach*. Oxford University Press: 2000.

206. Carpino, L. A., 1-Hydroxy-7-azabenzotriazole. An efficient peptide coupling additive. *Journal of the American Chemical Society* **1993**, 115 (10), 4397-4398.

207. Chhabra, S. R.; Hothi, B.; Evans, D. J.; White, P. D.; Bycroft, B. W.; Chan, W. C., An appraisal of new variants of Dde amine protecting group for solid-phase peptide synthesis. *Tetrahedron Letters* **1998**, 39 (12), 1603-1606.

208. Aletras, A.; Barlos, K.; Gatos, D.; Koutsogianni, S.; Mamos, P., Preparation of the very acid-sensitive Fmoc-Lys(Mtt)-OH Application in the synthesis of side-chain to side-chain cyclic peptides and oligolysine cores suitable for the solid-phase assembly of MAPs and TASP. *International Journal of Peptide and Protein Research* **1995**, 45 (5), 488-496.

209. Weber, P. J. A.; Bader, J. E.; Folkers, G.; Beck-Sickinger, A. G., A fast and inexpensive method for N-terminal fluorescein-labeling of peptides. *Bioorganic & Medicinal Chemistry Letters* **1998**, 8 (6), 597-600.

210. Parkhouse, S. M.; Garnett, M. C.; Chan, W. C., Targeting of polyamidoamine-DNA nanoparticles using the Staudinger ligation: Attachment of an RGD motif either before or after complexation. *Bioorganic & Medicinal Chemistry* **2008**, 16 (13), 6641-6650.

211. Angell, Y. M.; Alsina, J.; Barany, G.; Albericio, F., Practical protocols for stepwise solid-phase synthesis of cysteine-containing peptides. *The Journal of Peptide Research* **2002**, 60 (5), 292-299.

212. Kassianidis, E.; Pearson, R. J.; Philp, D., Probing Structural Effects on Replication Efficiency through Comparative Analyses of Families of Potential Self-Replicators. *Chemistry – A European Journal* **2006**, 12 (34), 8798-8812.

213. Subiros-Funosas, R.; El-Faham, A.; Albericio, F., PyOxP and PyOxB: the Oxyma-based novel family of phosphonium salts. *Organic & Biomolecular Chemistry* **2010**, 8 (16), 3665-3673.

214. Shafer, D. E.; Inman, J. K.; Lees, A., Reaction of Tris(2-carboxyethyl)phosphine (TCEP) with Maleimide and [alpha]-Haloacyl Groups: Anomalous Elution of TCEP by Gel Filtration. *Analytical Biochemistry* **2000**, 282 (1), 161-164.

-
215. Getz, E. B.; Xiao, M.; Chakrabarty, T.; Cooke, R.; Selvin, P. R., A Comparison between the Sulfhydryl Reductants Tris(2-carboxyethyl)phosphine and Dithiothreitol for Use in Protein Biochemistry. *Analytical Biochemistry* **1999**, 273 (1), 73-80.
216. Saito, G.; Swanson, J. A.; Lee, K.-D., Drug delivery strategy utilizing conjugation via reversible disulfide linkages: role and site of cellular reducing activities. *Advanced Drug Delivery Reviews* **2003**, 55 (2), 199-215.
217. Rabanal, F.; DeGrado, W. F.; Dutton, P. L., Use of 2,2'-dithiobis(5-nitropyridine) for the heterodimerization of cysteine containing peptides. Introduction of the 5-nitro-2-pyridinesulfenyl group. *Tetrahedron Letters* **1996**, 37 (9), 1347-1350.
218. Rothbard, J. B.; Kreider, E.; VanDeusen, C. L.; Wright, L.; Wylie, B. L.; Wender, P. A., Arginine-Rich Molecular Transporters for Drug Delivery: Role of Backbone Spacing in Cellular Uptake. *Journal of Medicinal Chemistry* **2002**, 45 (17), 3612-3618.
219. Kameyama, S.; Horie, M.; Kikuchi, T.; Omura, T.; Tadokoro, A.; Takeuchi, T.; Nakase, I.; Sugiura, Y.; Futaki, S., Acid wash in determining cellular uptake of Fab/cell-permeating peptide conjugates. *Peptide Science* **2007**, 88 (2), 98-107.
220. Prasad, V.; et al., Confocal microscopy of colloids. *Journal of Physics: Condensed Matter* **2007**, 19 (11), 113102.
221. Jiao, C.-Y.; Delaroche, D.; Burlina, F.; Alves, I. D.; Chassaing, G.; Sagan, S., Translocation and Endocytosis for Cell-penetrating Peptide Internalisation. *Journal of Biological Chemistry* **2009**, 284 (49), 33957-33965.
222. Moosmeier, M. A.; Bulkescher, J.; Reed, J.; Schnölzer, M.; Heid, H.; Hoppe-Seyler, K.; Hoppe-Seyler, F., Transtactin: a universal transmembrane delivery system for Strep-tag II-fused cargos. *Journal of Cellular and Molecular Medicine* **2010**, 14 (7), 1935-1945.
223. Crouch, S. P. M.; Kozlowski, R.; Slater, K. J.; Fletcher, J., The use of ATP bioluminescence as a measure of cell proliferation and cytotoxicity. *Journal of Immunological Methods* **1993**, 160 (1), 81-88.
224. Chen, S.; Dai, Y.; Harada, H.; Dent, P.; Grant, S., Mcl-1 Down-regulation Potentiates ABT-737 Lethality by Cooperatively Inducing Bak Activation and Bax Translocation. *Cancer Research* **2007**, 67 (2), 782-791.
225. High, L. M.; Szymanska, B.; Wilczynska-Kalak, U.; Barber, N.; O'Brien, R.; Khaw, S. L.; Vikstrom, I. B.; Roberts, A. W.; Lock, R. B., The Bcl-2 Homology Domain 3 Mimetic ABT-737 Targets the Apoptotic Machinery in Acute Lymphoblastic Leukemia Resulting in Synergistic in Vitro and in Vivo Interactions with Established Drugs. *Molecular Pharmacology* **2010**, 77 (3), 483-494.
226. Bruncko, M.; Oost, T. K.; Belli, B. A.; Ding, H.; Joseph, M. K.; Kunzer, A.; Martineau, D.; McClellan, W. J.; Mitten, M.; Ng, S.-C.; Nimmer, P. M.; Oltersdorf, T.; Park, C.-M.; Petros, A. M.; Shoemaker, A. R.; Song, X.; Wang, X.; Wendt, M. D.; Zhang, H.; Fesik, S. W.; Rosenberg, S. H.; Elmore, S. W., Studies Leading to Potent, Dual Inhibitors of Bcl-2 and Bcl-xL. *Journal of Medicinal Chemistry* **2007**, 50 (4), 641-662.

-
227. Shoemaker, A. R.; Oleksijew, A.; Bauch, J.; Belli, B. A.; Borre, T.; Bruncko, M.; Deckwirth, T.; Frost, D. J.; Jarvis, K.; Joseph, M. K.; Marsh, K.; McClellan, W.; Nellans, H.; Ng, S.; Nimmer, P.; O'Connor, J. M.; Oltersdorf, T.; Qing, W.; Shen, W.; Stavropoulos, J.; Tahir, S. K.; Wang, B.; Warner, R.; Zhang, H.; Fesik, S. W.; Rosenberg, S. H.; Elmore, S. W., A Small-Molecule Inhibitor of Bcl-XL Potentiates the Activity of Cytotoxic Drugs In vitro and In vivo. *Cancer Research* **2006**, *66* (17), 8731-9.
228. Qiagen, The QIAexpressionist. **2003**.
229. Chazotte, B., Mounting Live Cells onto Microscope Slides. *Cold Spring Harbor Protocols* **2011**, *2011* (1), pdb.prot5554.
230. Wender, P. A.; Jessop, T. C.; Pattabiraman, K.; Pelkey, E. T.; VanDeusen, C. L., An Efficient, Scalable Synthesis of the Molecular Transporter Octaarginine via a Segment Doubling Strategy. *Organic Letters* **2001**, *3* (21), 3229-3232.
231. Katritzky, A. R.; Rogovoy, B. V., Recent Developments in Guanylation Agents. *ChemInform* **2005**, *36* (30),
232. Kent, D. R.; Cody, W. L.; Doherty, A. M., Two new reagents for the guanylation of primary, secondary and aryl amines. *Tetrahedron Letters* **1996**, *37* (48), 8711-8714.
233. Levallet, C.; Lerpiniere, J.; Ko, S. Y., The HgCl₂-promoted guanylation reaction: The scope and limitations. *Tetrahedron* **1997**, *53* (14), 5291-5304.
234. Gogate, U. S.; Repta, A. J.; Alexander, J., N-(Acyloxyalkoxycarbonyl) derivatives as potential prodrugs of amines. I. kinetics and mechanism of degradation in aqueous solutions. *International Journal of Pharmaceutics* **1987**, *40* (3), 235-248.
235. Gogate, U. S.; Repta, A. J., N-(Acyloxyalkoxycarbonyl) derivatives as potential prodrugs of amines. II. esterase-catalysed release of parent amines from model prodrugs. *International Journal of Pharmaceutics* **1987**, *40* (3), 249-255.
236. Cundy, K. C.; Annamalai, T.; Bu, L.; De Vera, J.; Estrela, J.; Luo, W.; Shirsat, P.; Torneros, A.; Yao, F.; Zou, J.; Barrett, R. W.; Gallop, M. A., XP13512 [(±)-1-[(α-Isobutanoyloxyethoxy)carbonyl] aminomethyl)-1-cyclohexane Acetic Acid], A Novel Gabapentin Prodrug: II. Improved Oral Bioavailability, Dose Proportionality, and Colonic Absorption Compared with Gabapentin in Rats and Monkeys. *Journal of Pharmacology and Experimental Therapeutics* **2004**, *311* (1), 324-333.
237. Gangwar, S.; Pauletti, G. M.; Siahaan, T. J.; Stella, V. J.; Borchardt, R. T., Synthesis of a Novel Esterase-Sensitive Cyclic Prodrug of a Hexapeptide Using an (Acyloxy)alkoxy Promoiety. *The Journal of Organic Chemistry* **1997**, *62* (5), 1356-1362.
238. Folkmann, M.; Lund, F. J., Acyloxymethyl carbonodchloridates – new intermediates in prodrug synthesis. *Synthesis* **1990**, (12), 1159-1166.
239. Gyrase inhibitors and uses thereof. US2005/0038247, 2005.

-
240. Xu, B.; Huang, Z.; Liu, C.; Cai, Z.; Pan, W.; Cao, P.; Hao, X.; Liang, G., Synthesis and anti-hepatitis B virus activities of Matijing-Su derivatives. *Bioorganic & Medicinal Chemistry* **2009**, *17* (8), 3118-3125.
241. Britton, H. T. S.; Robinson, R. A., CXCVIII.-Universal buffer solutions and the dissociation constant of veronal. *Journal of the Chemical Society* **1931**, 1456-1462.
242. Burlina, F.; Sagan, S.; Bolbach, G.; Chassaing, G., Quantification of the Cellular Uptake of Cell-Penetrating Peptides by MALDI-TOF Mass Spectrometry. *Angewandte Chemie International Edition* **2005**, *44* (27), 4244-4247.
243. Josyula, V. P. V. N.; Gadwood, R. C.; Thomasco, L. M.; Kim, J.-Y.; Choy, A. L.; Boyer, F. E. Acyloxymethylcarbamate prodrugs of oxazolidinones. US 07265140, Sep 4 2007, 2007.
244. Rivero, I. A.; Heredia, S.; Ochoa, A., Esterification of amino acids and mono acids using triphosgene. *Synthetic Communications* **2001**, *31* (14), 2169-2175.
245. Tomlinson, I. M.; Walter, G.; Marks, J. D.; Llewelyn, M. B.; Winter, G., The repertoire of human germline vH sequences reveals about fifty groups of VH segments with different hypervariable loops. *Journal of Molecular Biology* **1992**, *227* (3), 776-798.

Appendix I

The integrity of biotinylated human Bcl-2 (rhBcl-2) and human and mouse Bcl-xL (rhBcl-xL and rmBcl-xL) was determined using a standard binding ELISA and anti-Bcl-2 and anti-Bcl-xL mAbs. Additionally, the ability of Bcl-2 and Bcl-xL to bind to BID BH3 was determined using the standard phage ELISA protocol using phage displaying BID BH3. The results of the binding ELISA are shown below.

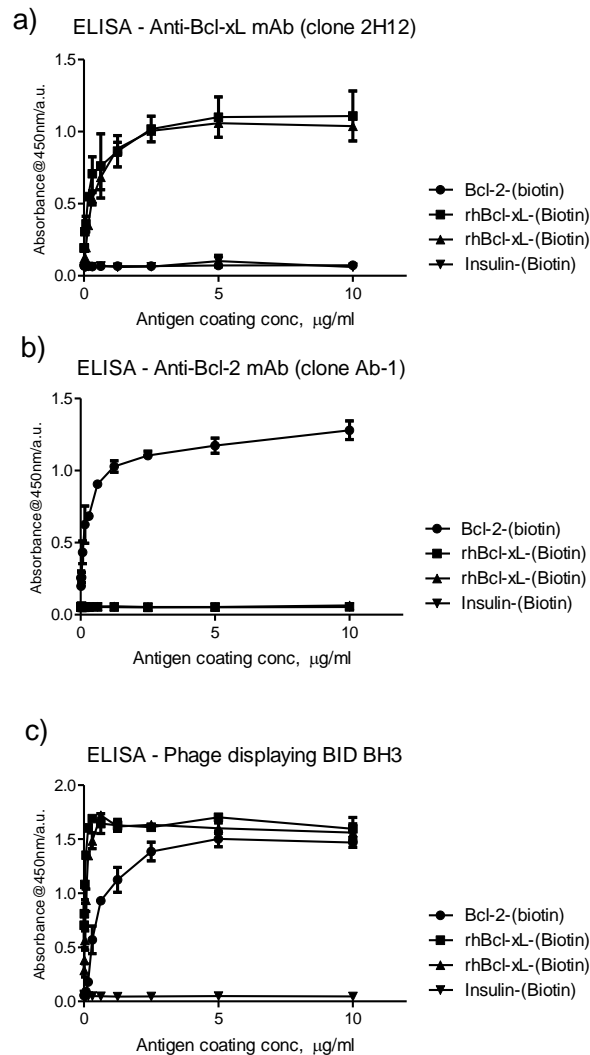


Figure 2 15: Calibration curve for Biotinylated human Bcl-2, human Bcl-xL and mouse Bcl-xL. ELISAs carried out on 96 Costar 200 µl streptavidin coated plate. a) incubation with anti-Bcl-2, b) incubation with anti-Bcl-xL and c) incubation with phagemid BH3pC6.

Appendix II

The primers used in this thesis were synthesised by the DNA sequencing team at MedImmune (Cambridge, U.K).

Primers:

MYC: 5' CAAAACTCATCTCAGAAGAG'3

PUV_R: 5'AGCGGATAATTTCACACAGG'3

T7 Forward: 5'TAATACGACTCACTATAGGG'3

AR138: 5'GCCGCCACCATGCTCTGG'3

AR142: 5'GGCCGGGGCCATCCAGACATG'3

Appendix III

The amino acid sequences of the isolated anti-Bcl-2 and anti-Bcl-xL scFv:

Cea6

QVQLVQSGAEVKKPGSSVKVSCKASGGTFSNSPINWLRQAPGQGLEWMGSIIP
SFGTANYAQKFQGRLTITADESTSTAYMELSSLRSEDTAVYYCAGRSHNYELY
YYYMDVWGQGTMTVTVSGGGGSGGGGSGGGGSDIQMTQSPSTLSASIGDRVT
ITCRASEGIYHWLAWYQQKPGKAPKLLIYKASSLASGAPSRFSGSGSGTDFTLT
ISSLPDDFATYYCQQYSNYPLTFGGGGTKLEIKRAAA

ScFv19

EVQLVQSGAEARRPGSSVKVSCKASGGALRGFAINWVRQAPGQGLEYLGGIIP
LFGTTKLAQKFQDRVTVAADESTNTAYMELTGLTSEDTAVYYCARDGLQFDI
DAFDMWGRGTLVTVSGGGGSGGGGSGGGGSQSVLTQPPSVSAAPGQKVTISC
SGSSSNIGNNYVSWYQQLPGTAPKLLIYDNNKRPSGIPDRFSGSKSGTSATLGI
TGLQTGDEADYYCAAWDDSLNGWVFGGGTKLTV

ScFv20

EVQLVQSGAEVKKPGSSVKVSCKASGGTFSSYAISWVRQAPGQGLEWMGGII
PIFGTGNYAQKFQGRVTITADESTSTAYMELSSLRSEDTAAYYCARENSNYDA
FDIWGQGTLVTVSGGGGSGGGGSGGGGSQSVLTQPPSASGTPGQRVTISCSGS
SSNIGSNTVNWYQRLPGAAPQLLIYNNDQRPSGIPDRFSGSKSGTSGSLVISGL
QSEDEADYYCASWDDSLNGRVFGGGTKLTV

ScFv21

EVQLVQSGGDVKKPGSSVTVSCTASGVAFSSYGISWVRQAPGQRLEWMGWII
RICSTGNYAQKLQGRVTITADESTSTAYMDMSSLTSEDTAAYYCARENSKYD
ACICGAEGQWSGGGGSGGGGSGGGGSPQJLLNQPPSPSGTPAQRVTIWSSGSS
SNIGSNTANWYQRLPGAAPQLVIYNNDQRPSGIPDRFSGSKSGTSGSLVISGLQ
SEDEADYYCASWDDSGNRGVFGGGTKLTVLEIKRAAA

ScFv23

QVQLVQSGGGVVQPGRSLRLSCAASGFTFSNYGMNWVRQAPGKGLEWVAVI
SYNGETKYYADSVQGRFTVSRDNSKNTLYLQMNSLRTEDTAMYYCAKVAGD
TPIDYWGRGTLTVSGGGGSGGGGSGGGGSYELTQPPSASGTPGQRTISCSG
SSSNIGSNTVNWYQQLPGTAPKLLIYSNNQRPSGVPDRFSGSRSGTSASLAISG
LQSEDEADYYCATWDDSLNTWPFGGGTKLTVLEIKRAAA

ScFv24

EVQLLESGGGLVQPGGSLRLSCAASGFTFSSYAMSWVRQAPGKGLEWVSAIS
GSGGSTYYADSVKGRFTISRDNSKNTLYLQMNSLRAEDTAVYYCARDATTAP
FYYYMDVWGQGTMTVSGGGGSGGGGSGGGGSAQAVLTQPSSASGTPGQR
VAISCFGSSSNIETNSVSWFQQFPGTAPKLLIYNNNQRPSGVPDRFSGSKSGTSA
SLAIRGLQSDDEADYYCAAWDDSLSGWVFGGGTKLTVLGAAA

ScFv25

EVQLLESGGGLVQPGGSLRLSCAASGFTFSSYAMSWVRQAPGKGLEWVSAIS
GSGGSTYYADSVKGRFTISRDNSKNTLYLQMNSLRAEDTAVYYCARATGDPS
GYNWFDPWGRGTLTVSGGGGSGGGGSGGGGSQSVLTQPPSASGTPGQRTI
SCSGSRFNIGSNTVHWYQHLPGMAPKLLIYSNNQRPSGVPDRFSGSKSGTSAS
LAISGLQSEDEADYYCAVWDDILNSWLFGGGTKLTV

ScFv26

EVQLLESGGGLVQPGGSLRLSCAASGFTFSSYAMSWVRQAPGKGLEWVSAIS
GSGGSTYYADSVKGRFTISRDN SKNTLYLQMNSLRAEDTAVYYCVRDCSSVG
CYTSLDYWGQGTMTVTVSGGGGSGGGGSGGGGSQSVLTQPPSVSGAPGQRVTI
SCTGTTSNIGAGYDVHWYQHLPGAAPKLLIYDSTNRPSGVPDRFSGSKSGTSA
SLAITGLQAEDEADYYCQSYDTRLAYVFGTGTKLTV

ScFv28

EVQLLESGGGLVQPGGSLRLSCAASGFTFSSYAMSWVRQAPGKGLEWVSAIS
GSGGSTYYADSVKGRFTISRDN SKNTLYLQMNSLRAEDTAVYYCARDMIRLD
WGDLSIDNWFDPWGQGTMTVTVSGGGGSGGGGSGGGGSQSVLTQPPSASGTP
GQRVTISCSGGSSNIGSNTVNWYQQLPGTAPKLLIYSNNLRPSGVPDRFSGSKS
GTSASLALSELQSEDETDYYCAAWDDSLNAYVFGTGTKVTV

ScFv29

EVQLLESGGGLVQPGGSLRLSCAASGFTFSSYAMSWVRQAPGKGLEWVSAIS
GSGGSTYYADSVKGRFTISRDN SKNTLYLQMNGSLRAEDTAVYYCARDFGNW
NYYYYYYYGMDVWGKGTMTVTVSGGGGSGGGGSGGGGSLPVLTPPPSASGT
PGQRVTISCSGSSNIGSNTVNWYQQLPGTAPKLLIYSNNQRPSGVPDRFSGSK
SGTSASLAISGLQSEHEADYFCAAWDDTLDGWVFGGGTKVTV

ScFv30

EVQLLESGGGLVQPGGSLRLSCAASGFTFSSYAMSWVRQAPGKGLEWVSAIS
GSGGSTYYADSVKGRFTISRDN SKNTLYLQMNSLRAEDTAVYYCARDSWGA
GGVDAFDVWGRGTLTVTVSGGGGSGGGGSGGGGSQAVLTQPSSVSGAPGQRV
TISCTGSSSNIGAGYDVHWYQQLPGSAPKLLIFGNNNRPSGVPDRFSGSKSGTS
VSLAITGLQAEDEADYYCQSYDNSLRGSVFGGGTKLTV

ScFv31

EQQLMEYVRGLDQRGGSRRRLSCSAJVFTASSOATSSIIYQTTGMGQEPVSGINGI
JGSTYYADSAKGGFSMSRDNSMNRENLNNSDRQEDTARYDYARQDRYGSG
TSCYYEQYFDVGGGRATVTVSGGGGSGGGGSGGGGSQSFLKQPPSPSRTPGQ
RVTIQSSGNRVNIGSNNAHWYQHHPGKAPNLLIYSNNQRPSGVPDRFSGSKSD
ASASLTISGVQSEDEADYYCTVWEDIENSWLFGGGTKVTV

ScFv32

EVQLLES GGGLVQPGGSLRLSCAASGFTFSSYAMSWVRQAPGKGLEWVSAIS
GSGGSTYYADSVKGRFTISRDN SKNTLYLQMNSLRAEDTAVYYCARDRLWL
GINYYYGMDVWGKGTMTVSGGGGSGGGGSGGGGSQAVLTQPSSVSVAPG
KTARITCGGTDIGSKSVHWYQQKPGQAPVLV VYYDRDRPSGIPERFSGSNSGN
TATLTISRVEAEDEADYYCQVWHTVDDFRCLRRKGPKLTV

ScFv42

GVQLVQSGAEVKKPGSSVKV SCKSSGGSLRQYDISWLRQAPGQGPEWMGGIS
PSLG PANYAQKFQGRITITADEATTTVYMQLD SLTSED TAVYFCARDPLSLYP
YFDSWGQGTMTVSGGGGSGGGGSGGGGSQSVLTQPASVSGSPGQSITISCTG
TSSDVGGYNYVSWYQQHPGKAPKLMIYEGSKRPSGIPDRFSGSSSGNTASLTIT
GAQAEDEADYYCHSRDSSGNHVLFGGGTKLTVEIKRAAA

ScFv43

QVQLVQSGGGLVKPGGSLRLSCAACGFTFSDYYMSWIRQAPGKGLEWVSYIS
SSSSYTNYADSVKGRFTISRDN AKNSLYLQMNSVRAEDTAVYYCASWDYSSA
FDIWGRGTLVTVSGGGGSGGGGSGGGGSQSVLTQPPSVSAAPGQKVTISCSGS
TSNIGNNYVSWYQQHPGKAPKLMIYDVSKRPSGVPDRFSGSKSGNSASLDISG
LQYEEEDDYYCAAWDDSMSEFLFGTGTKLTV

ScFv44

QVQLLQSAAEVKKPGSSVKVSCKASGGTFSSYAINWVRQAPGQGLEWMGGII
PIFGTANYAQKFQGRVTITADGSTSTAYMELSSLRSEDNAVYYCARDLWELLL
ADAFDIWGRGTLVTVSSSSGGGGSGGGGSGGGGSQSVLTQPPSASGTPGQRV
TISCSGSSSNIGSNTVNWYQRLPGAAPQLLIYNNDQRPSGIPDRFSGSKSGTSGS
LVISGLQSEDEADYYCASWDDSLNGRVFGGGGTKLTV

ScFv45

QVQLQQSGAEVKKPGASVKVSCKVSGYTLTELSMHWVRQAPGKGLEWMGG
FDPEDGQTTYAQKFQGRVIMTEDTSTDAYMELSRLRSEDNAVYYCATSKFL
WFGERNYFDPWGRGTLVTVSGGGGSGGGGSGGGGSSSELTQDPAVSVALGR
TVRITCQGDSLRSYYASWYQQKPGQAPVLVIYGKNNRPSGIPDRFSGSSSGNT
ASLTITGAQAEDEADYYCNSRDSSGNHVVFGGGGTKLTV

ScFv46

EVQLVQSGAEVKKSGESLKISCSGSGYSFATHWIGWARQLPGKGLEWVGIVFP
GDADTKYSPSFEGQVTISVDKISGTAYLQWRSLKASDSAKYFCARLGTSGWPF
YYHYYYMDVWGRGTTVTVSGGGGSGGGGSGGGGSSSELTQDLAVSVALGQ
TVRITCQGDSLRSYYASWYQQKPGQAPVLVIYGKNNRPSGIPDRFSGSSSGNT
ASLTITGAQAEDEADYYCNSRDSSGNHVVFGGGGTKLTV

ScFv49

EVQLVQSGAEVKKPGSSVRVSCKASGGSLTTFPISWVRQAPGQGLEWMGRIV
PLLDITNYAQKFRGRVTLTADKSTNTVYMDVNSLTSEDNAVYYCARPSYDYW
SAYPQRNYFYHGMDVWGQGTLVTVSGGGGSGGGGSGGGGSALSSELTQDPA
VSVALGQTVRITCQGDSLRSDSANWFQQKPGQAPVLVIYGKDRRPSGIPDRIS
GSSSGNTASLTITGAHAEDEADYYCNSRDSSDTHLELFGGGGTKLTVLCAAA

ScFv53

EVQLLES GGGLVQP GGS LRLSCAASGFTFSSYAMSWVRQAPGKGLEWVSAIS
GSGGSTYYADSVKGRFTISRDN SKNTLYLQMNSLRAEDTAVYYCAKSRHMSD
FWGSYLLPSGFFDVWGQGTMTVSGGGGSGGGGSGGGGSELTQDPAVSVAL
GQTVRITCQGDSLRSYYVSWYQQKPGQAPVVVIYDKNIRPSGIPDRFSGSRSG
NTASLTITGAQAEDEADYYCSSRDSSGNFVVFGGG TKLTVEIKRAAA

ScFv54

EVQLLES GGGLVQP GGS LRLSCAASGFTFSSYAMSWVRQAPGKGLEWVSAIS
GSGGSTYYADSVKGRFTISRDN SKNTLYLQMNSLRAEDTAVYYCAKIDCIGDF
CDSGSSSF DYWGRGTLVTVSGGGGSGGGGSGGGGSQSVLTQPPSASGTPGQR
VTISCSGSYSNIGSNYVYWYQQLPGTAPKLLIYTNNQRPSGVPDRFSGSKSGTS
ASLAITGLQAEDEADYYCQSYDSGLWVFGGGT KLTV

ScFv55

EVQLLES GGGLVQP GGS LRLSCAASGFTFSSYAMSWVRQAPGKGLEWVSAIS
GSGGSTYYADSVKGRFTISRDN SKNTLYLQMNSLRAEDTAVYYCAREDCGGT
TCLGADSWGQGTMTVSGGGGSGGGGSGGGGSQSVLTQPPSASGTPGQRVTI
SCSGSSSNIGDNFVYWYQHLPGTAPKLLIYRDDQRPSGVPDRFSGSKSGTSVSL
AVSGLRSEDEADYYCATWDDSVRGYVFGTG TKLTV

ScFv56

EVQLLES GGGLVQP GGS LRLSCAASGFTFSSYAMSWVRQAPGKGLEWVSAIS
GSGGSTYYADSVKGRFTISRDN SKNTLYLQMNSLRAEDTAVYYCARES QHIV
GAAYLDYWGRGTMVTVSGGGGSGGGGSGGGGSELTQDPAVSVALGQTVRIT
CQGDSLRRYYARWYQQKPGQAPVVVMYGEKNRPSGIPDRFSGSSSGNTASLT
ITGAQADDEADYYCNSRGSSGNLVFGGGT KLTV

ScFv57

EVQLLES GGGLVQP GGS LRLSCAASGFTFSSYAMSWVRQAPGKGLEWVSAIS
GSGGSTYYADSVKGRFTISRDN SKNTLYLQMNSLRAEDTAVYYCAKDQWLA
PFDYWGKGTTVTVS GGGGSGGGGSGGGGSYVLTQPPSASGTPGQRVTISCSG
SRSHIAGNFVYWYQHLP GTAPKLLIYQNDRRPSGVPDRFSGSQSGTSASLVISG
LRSEDEGDYYCAA WDDSLDGPVFGGGTKVTV

ScFv59

EVQLLES GGGLVQP GGS LRLSCAASGFTFSSYAMSWVRQAPGKGLEWVSAIS
GSGGSTYYADSVKGRFTISRDN SKNTLYLQMNSLRAEDTAVYYCAGHSGSG
WYWDHYFDHWGRGTLVTVS GGGGSGGGGSGGGGSQSVLTQPPSASGTPGQ
RVTISCSGGGSNIGRNSVSWYQQLPGTAPKLILYSNDQRPSGVPDRFSGSKSGT
SASLAISGLRSEDEALYYCAA WDDSLTGLCLRRGTKLTV

ScFv60

EVQLLES GGGLVQP GGS LRLSCAASGFTFSSYAMSWVRQAPGKGLEWVSAIS
GSGGSTYYADSVKGRFTISRDN SKNTLYLQMNSLRAEDTAVYYCARGVSATY
YEPYYFDFWGRGTLVTVS GGGGSGGGGSGGGGSQAVLTQPSSVSGAPGQRV
TISCTGNISNIGAGYDVHWYQQLPGTAPKLLIFGYNNRPSGVPDRFSGSKSGTS
ASLAITGLHPED EADYYCQSF DSSVSGSWVFGGGTKVTV

ScFv61

EVQLLES GGGLVQP GGS LRLSCAASGFTFSSYAMSWVRQAPGKGLEWVSAIS
GSGGSTYYADSVKGRFTISRDN SKNTLYLQMNSLRAEDTAVYYCARALSQYT
YWTGFFPTYFDSWGRGTMVTVS GGGGSGGGGSGGGGSDIQLTQSPSSLASV
GDRVTTICRASQVIGSYLAWYQQKAGLAPKLLIYRASTLQSGVPSRFSGSGSG
TDFTLTISSLQPEDFGTYYCQQVNSYPITFGQGTRLEI

ScFv65

QVQLLQSEAEVKKPGASVTVSCKASGYSGSYAIHWLRQAPGQRLEQMGWID
VGDGSTKYSQKFQGRVTITRDTSAATTAYMDLSRMRSDDTAIYYCARDSNTFW
RGFWGYFFNVWGQGTLVTVSGGGGSGGGGSGGGGSHVILTQPPSVSGAPGQ
KVTISCTGSSSNIGAGYDVHWYQQLPGTAPKLLIYGNSNRPSGVPDRFSGSKS
GTSASVAITGLQADDEDDYYCQSYDSSMSGVVFGGGTKLTVEIKRAAA

ScFv67

QVQLVQSGGGLVKPGGSLRLSCAASGFTFSSYSMNWVRQAPGKGLEWVSSIS
SSSSYTTYADSVKGRFTISRDNANKNSLYLQMNNLRAEDTAVYYCARSGSSSW
YRPDDAFDIWGQGTMTVTVSGGGGSGGGGSGGGGSQPVLTPPPSASGTPGQR
VIISCSGSGFNIGRNSVNWYQQLPGTAPKLLVYSDKYRPSGVPDRFSGSKSGTS
ASLAISGLQSEDEADYYCATWDDSVNAWVFGKRDP AHP

ScFv68

EVQLLES GGGLVQPGGSLRLSCAASGFTFSSYAMSWVRQAPGKGLEWVSAIS
GSGGSTYYADSVKGRSTISRDN SKNTLYLQMNSLRAEDTAVYYCARGVSGFT
LPFDSWGRGTLVTVSGGGGSGGGGSGGGGSELTQDPAVSVALGQTVRITCQG
DSLRSYYASWYQQKPGQAPVLVIYGKNNRPSGIPDRFSGSSSGNTASLAITGA
QAEDEADYYCNSRDSSGNHVVFGGGTKVTVEIKRAAA

ScFv69

GVQLVQSGGGLVRPGESLTLSTASGFIFNTYSMNWVRQAPGKGLEWVASAS
SSGSFKYYGDSVEDRFTISRDNANKNALFLHMNGLTAEDTAMYYCVRASYQHF
DWSPLGVDSKGTMTVTVSGGGGSGGGGSGGGGSELTQDPAVSVALGQTVRIT
CQGDSLRSYYASWYQQKPGQAPVLVIYGKNNRPSGIPDRFSGSSSGNTASLTIT
GAQAEDEADYYCSSTGQPVVTVVFGGGTKLTV

ScFv70

QVQLQQSGAEVKKPGSSVKVSCKASGGTFSSYAISWVRQAPGQGLEWMGGII
PIFGTANYAQKFQGRVTITADESTSTAYMELSSLRSEDNAVYYCARETGYYDA
FDLWGRGTMVTVSGGGGSGGGGSGGGGSQSVLTQPPSASGTPGQRVTISCSG
SSSNIGSNTVNWYQRLPGAAPQLLIYNNDQRPSGIPDRFSGSKSGTSGSLVISGL
QSEDEADYYCASWDDSLNGRVFGGGTKLTV

ScFv73

GAQMVQCGAEVKKPGSSVKVSFKNFGGAFSRYGINQVRQAHGQGIEWMGGII
TIYVTGNYEQKIQDRVTMTTEESANSASMELSSVRCGDTGGYCCVRENSEYD
SVDMWGRGSLVSVSGGGGSGGGGSGGGGSLCMTQPPSAFGAPGQRVTIFCFG
RRSNLGSNNVNWYQRLPGGAPQLLFYQKINNGPQGCPCGGFFCSNQGTSGSLVI
RGVQLOEEGDYYCATSEDSMNSRVFGGGNKMTV

ScFv74

AEQLVQSGGVVVQPGGSLRLSCAASGFTFDDYAMHWVRQAPGKGLEWVSLI
SWDGGSPYYADSVKGRFTISRDN SKNSLYLQMNSLRAEDTALYYCAKDLNY
DFWSGTGMDVWGKGLTVTVSGGGGSGGGGSGGGGSQSVLTQPASVSGSPGQ
SITISCTGTSSDVGGYNYVSWYQQHPGKAPKLMIYEGSKRPSGVSNRFSGSKS
GNTASLTISGLQAEDEADYYCSSYTTRSTRVFGGGTKLTV

ScFv77

QVQLVQSGGEVKRPGASVKVSCKASGYTFTTYDITWVRQAPGRGLEWMGWI
NTYNGNTKYAQTVQGRVTMSTDSTGTAYLDLTSLRPDDTAVYYCARVSKW
DRPGYLDYWGGQGLTVTVSGGGGSGGGGSGGGGSQAVLTQPSSVSGAPGQRV
TISCTGSSSNIGAGYDVQWYQQIPGTAPKVLIIYNNNNRPSGVPDRFSGSKSGTT
GSLAITGLQTEDEAVYYCQSFDRLNTMSSQSGTQLTK

scFv84

EVQLLESGGGLVQPGGSLRLSCAASGFTFSSYAMSWVRQAPGKGLEWVSAIS
ASGTSTSYADSVKGRFTISRDN SKNTLYLQMNSLRAEDTAVYYCAKYGYTFD
YWGQGTLLTVSGGGGSGGGGSGGGGSTD IQMTQSPSSLSASVGDRVITTCRA
SQSISSYLNWYQQKPGKAPKLIYSASALQSGVPSRFSGSGSGTDFTLTISSLQPE
DFATYYCQQYSNYPLTFGGGGTKLEIKRAAA